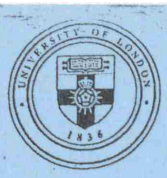

REFERENCE ONLY

UNIVERSITY OF LONDON THESIS

Degree PhD Year 2006 Name of Author VENDON-NOE G.M.

This thesis comes within category D.

☑ This copy has been deposited in the Library of UCL

☐ This copy has been deposited in the Senate House Library, Senate House, Malet Street, London WC1E 7HU.

DEVELOPMENT OF A MULTI-LOCATION MOTION DISPLACEMENT TEST FOR DETECTION OF EARLY GLAUCOMA

GAY MARY VERDON-ROE

DEPARTMENT OF VISUAL SCIENCE
INSTITUTE OF OPHTHALMOLOGY
UNIVERSITY COLLEGE LONDON

DOCTOR OF PHILOSOPHY (PHD)
OPHTHALMOLOGY
MAY 2006

ProQuest LLC
789 East Eisenhower Parkway
P.O. Box 1346
Ann Arbor, MI 48106-1346

DECLARATION

I declare that this thesis submitted for the degree of Doctor of Philosophy, conducted at University College London, is my own composition and the data presented herein is my own original work, unless otherwise stated.

Gay Mary Verdon-Roe MSc

ABSTRACT

This thesis describes the development of a multi-location motion displacement test (MDT) for the early detection of glaucoma. The test uses line displacement stimuli, which are orientated with the retinal nerve fibre layer (RNFL) and scaled with ganglion cell density. Psychophysical properties of hyperacuity motion displacement were explored and results applied to optimize the stimulus presentation and test format. Investigations included the following:

(i) Optical blur: MDT was found to be robust to peripheral astigmatism. The effect of spherical blur was quantified and the implication for discrimination between glaucoma and normal discussed.

(ii) Spatial summation properties: equivalent MDT thresholds were demonstrated for equivalent length of single and multi-line stimuli. Equivalent MDT thresholds were also found for stimuli of equivalent energy ([stimulus area] * [stimulus luminance – background luminance]), in accordance with Ricco's Law. A linear relationship (slope 0.5) was found between log MDT threshold and log relative stimulus energy. A new law is proposed to apply to MDT summation properties, giving the relationship $T = K\sqrt{E}$ [T = MDT threshold; K = constant; E = stimulus energy]. This may be used to predict MDT threshold for different configurations of stimuli.

(iii) Shortening of response time was observed as stimulus duration is reduced and explained by altered temporal summation properties. The results were applied to modify the subject response window, with benefit of reduced test duration.

(iv) Selection of stimulus number and position was made by study of attention, together with application of the anatomical relationship of the RNFL with the optic nerve head.

(v) A staircase strategy was developed. Parameters were selected by analysis of results gained within the PhD and earlier studies.

Results were pooled to accomplish an operational test. Preliminary assessment indicates that focal glaucomatous defects detected by standard automated perimetry are replicated by the new MDT.

TABLE OF CONTENTS

LIST OF FIGURES

LIST OF TABLES

SUPERVISORS

F.W. Fitzke PhD
Professor of Visual Optics and Psychophysics, Department of Visual Science,
Institute of Ophthalmology, London EC1V 9EL

D.F. Garway-Heath MD FRCOphth
Research Lead, Glaucoma Research Unit, Moorfields Eye Hospital,
London EC1V 2PD

* * * * * * * * * * * * * * *

ETHICAL APPROVAL

THIS PROJECT WAS APPROVED BY THE
ETHICAL COMMITTEEE OF MOORFIELDS EYE HOSPITAL

PROJECT REFERENCE
WESM1001 (previously LORS 605)

ACKNOWLEDGEMENTS

It has been a privilege to work under the direction of my two supervisors, Professor Fitzke PhD and Mr Garway-Heath MD FRCOphth, for the duration of this study. Initial thanks must go to Professor Fitzke for conceiving the idea of the original motion displacement test (MDT), without which this study would not have transpired. Both supervisors have been an inspiration in their different fields of interest. This has added breadth and challenge to the study and strengthened the development of the new test.

Secondly, I must thank Mr Viswanathan MD FRCOphth for the excellent design of the computer software, which enabled absolute flexibility in varying the many parameters of the stimulus presentation for the purpose of this study.

Mr Viswanathan MD FRCOphth and Mr Westcott MD FRCOphth have each been of great assistance in their advice on the test development, drawing from their wide experience in psychophysical testing for glaucoma, both in standard automated perimetry and the original MDT.

Two research fellows from Moorfields Eye Hospital, Stefano de Cilla MD and Patricio Schlottmann MD, acted as second subjects for the psychophysical investigations. I owe a debt of gratitude to each for their time commitment and good humour in conducting numerous, repetitive tests.

I am appreciative of the constructive comments given by Bill Swanson PhD on an early version of the IOVS manuscript, which relates to chapters 5 and 6 of this PhD. My thanks also extend to Mr Andrew Milliken, Senior Optometrist to Moorfields Eye Hospital, for performing the peripheral refraction and to Mr Vy Luong, for IT assistance.

This study would not have been possible without the sponsorships of The Friends of Moorfields (Sponsors 2000-1) and Pfizer [previously Pharmacia] (Sponsors 2001-4), for which I am extremely grateful.

GMVR May 2006

GLOSSARY OF ABBREVIATIONS AND TERMS

AGIS: Advanced Glaucoma Intervention Study

ASB: Apostilb

BP: Blood pressure

BS: Blind spot

CCT: Central corneal thickness

Cd: Candela (10 cd = 31.3 asb)

CFF: Critical flicker fusion (highest resolvable flicker frequency)

CI: Confidence interval

COR: Cytochrome oxidase reactivity

CRF: Classical Receptive Field

DALY: Disability adjusted life year

dB: Decibel

DCyl: Dioptre cylinder

DLS: Differential light sensitivity

Dmax: Maximum displacement for motion detection using RDK

Dmin: Minimum displacement for motion detection using RDK

DSph: Dioptre sphere

ECRF: Extraclassical Receptive Field

FDP: Frequency doubling perimetry

FDT: Frequency doubling technology

FDT-1: Original FDP

FDT-2: The Matrix

FMM: Fine matrix mapping

FOS: Frequency of seeing

GCD: Ganglion cell density

GMVR: Gay Mary Verdon-Roe

GNP: Gross National Production

GON: Glaucomatous optic neuropathy

HPRP: High Pass Resolution Perimetry

HSRP: High Spatial Resolution Perimetry

HTG: High tension glaucoma

IAPB: International Agency for the Prevention of Blindness

IOP: Intraocular pressure

IPL: Inner plexiform layer

IPS: International Perimetric Society

IQR: Interquartile range

K: Konicellular

LDMAX: Largest magnitude of MDT coincident with optimal response

LGN: Lateral geniculate nucleus

M: Magnocellular

MAP: Motion Automated Perimetry

MD: Mean defect

MDT: Motion Displacement Test

MOBS: Modified binary search

NPV: Negative predictive value

NTG: Normal tension glaucoma

OHT: Ocular hypertension

OHTS: Ocular Hypertension Treatment Study

ONH: Optic nerve head

OPL: Outer plexiform layer

P: Parvocellular

PACG: Primary angle closure glaucoma

PD: Pattern deviation

PDP: Pattern discrimination perimetry

POAG: Primary open angle glaucoma

PPV: Positive predictive value

PSD: Pattern standard deviation

PxF: Pseudoexfoliation glaucoma

QALY: Quality adjusted life year

RDK: Random dot kinetogram

RF: Receptive field (the area of visual space to which a neuron responds)

rgb: red green blue

RGC: Retinal ganglion cell

RNFL: Retinal nerve fiber layer

SAP: Standard automated perimetry

SWAP: Short wave automated perimetry

TCS: Temporal contrast sensitivity

TD: Total deviation

TED: Threshold-energy-displacement law

TIGR: Trabecular meshwork inducible glucocorticoid response

TMP: Temporal modulation perimetry

WHO: World Health Organization

ZEST: Zippy estimation of sequential testing

PSYCHOPHYSICAL LAWS (LACHENMAYR AND VIVELL 1993)

Weber's Law:

The just-perceptible increment of stimulus intensity is a constant fraction of the stimulus intensity.

$\Delta I/I$ = constant where ΔI = incremental threshold; I = background intensity

Ricco's Law: (complete summation)

At threshold: A x I = Constant where A = stimulus area; I = stimulus intensity

Piper's Law (incomplete summation)

At threshold: $\sqrt{A}$ x I = constant where A = stimulus area; I = stimulus intensity

Bloch's Law (the temporal analogue of Ricco's law) Applicable for $T \leq 100$msec

At threshold T x I = constant where T = stimulus duration and I = stimulus intensity

Contrast:

(a) Simple Contrast

Contrast = Lmax/Lmin

(b) Michelson's Contrast

Contrast = % (Lmax –Lmin/Lmax+Lmin) where L =Luminance

(c) Weber's law

Contrast = (Lmax-Lmin)/Lmin where L = Luminance

STANDARD TESTING PROCEDURES

SELECTION OF PATIENT AND CONTROLS: ref WESM1001

Exclusion Criteria for both control and patient groups

History of diabetes; previous ocular history such as trauma; secondary glaucoma; amblyopia; refractive error > +/- 6.0 DSph; non-glaucomatous visual field loss e.g. neurological or retinal cause.

Control Inclusion Criteria

Normal optic disc by clinical analysis and normal SAP determined by glaucoma hemifield test. The field test must be valid, as defined by fixation losses and false negative rate each of 20% or less, and a false positive rate of 15% or less.

Control Exclusion Criteria

IOP > 21 mm Hg; Family history of glaucoma.

Patient Inclusion Criteria:

Glaucomatous optic disc by clinical analysis.

Visual field selection criteria for early to moderate glaucomatous field defect

Early loss: MD better than, or equal to, – 4dB

Moderate loss: MD between – 4dB and – 8 dB

A defect consists of at least two of the following:

1. A Pattern Standard Deviation (PSD) significant at $p < 5\%$ level.
2. Abnormal Glaucoma Hemifield Test (GHT) result.
3. A cluster of 3 or more non-edge points depressed at $p < 5\%$ level, and one of those points depressed at $p < 1\%$ level, or a cluster of 2 or more points both depressed at $p < 1\%$ level. The probability is defined according to the pattern deviation (PD) Humphrey plot. The points within a cluster should be contiguous (horizontally, vertically or obliquely) and the cluster should be sited within a single hemifield (superior or inferior).

A defect should be reproducible, i.e. the field should be abnormal by the above criteria on at least two consecutive tests and, within a cluster, at least 1 point should be repeated with $p < 5\%$ in the same location.

The test must be valid, as defined by a false positive response of 15% or less, a false negative response of 20% or less and fixation losses of 20% or less.

Patients were recruited from the outpatient glaucoma clinics of Mr M. Miller and Mr A C Viswanathan.

Controls were spouses and friends accompanying patients attending these outpatient clinics.

COMPUTER:

(a) Viglen Genie ATX Intel Pentium 200 MHzMMX processor 32 MB RAM

Used for First Multi-location Study.

(b) Dell Dimension 8100 Intel Pentium 4 1.3 GHz; 128 RAM

Used for all tests following first multi-location study.

MONITOR:

(a) Hitachi CM2198ME 21-inch screen

Screen resolution: 1280 x 1024 pixels; 0.28 dot pitch.

Used for all investigations excluding pilot study 2004.

(b) Dell UltraSharp 20-inch flat screen

Screen resolution: 1600 x 1200 pixels @ 60 Hz; 0.255 dot pitch.

Used for development of post doctorate work (chapter 12).

COMPUTER SOFTWARE:

Developed by Ananth Viswanathan using C++

LUMINANCE: (measured using Minolta Chroma Meter CS-100)

(a) Hitachi CM2198ME

CONTRAST: 84%

BACKGROUND: rgb: 65, 65, 65; luminance: 10 cd/m^2

STIMULUS: rgb: 255, 255, 255; luminance: 112 cd/m^2

(b) Dell UltraSharp

CONTRAST: 85%

BACKGROUND: rgb: 68, 68, 68; luminance: 10 cd/m^2

STIMULUS: rgb: 210, 210, 210; luminance: 124 cd/m^2

STIMULUS PRESENTATION (refer Chapter 7, figure 7-3; figure 7-4b)

3 oscillations per presentation

Stimulus Duration: 200 msec per cycle

Adaptation period at start of test: 5000 msec

Fixed pre-displacement: 1500 msec (*1000 msec)

Random pre-displacement: 500 msec (*750 msec)

Listening window: 1500 msec (*1000 msec)

Post response wait: 1500 msec (*1000 msec)

* Modification following Chapter 7 (refer figure 7-6; figure 7-10)

TEST DISTANCE: 30 cm

ROOM ILLUMINATION: Mesopic

MDT METHOD:

Subject fixes central fixation target on computer monitor and presses left mouse button when line stimulus is seen to move.

NOTE: CHAPTERS 3-6

Detailed investigation of summation, optical blur and contrast were all performed using a single location. Nasal location –27,3 was selected because it is a common site for early glaucoma loss. Also, the stimulus is horizontal, making it straightforward to examine in terms of contrast in that no "feathering" (chapter 2) is required. The displacement range was 0-24 min arc, frequency-of-seeing curves were generated and the threshold taken as the displacement corresponding to 50% of the probit-fitted curve.

STATISTICAL ANALYSIS: SPSS for Windows versions10.1 and 11.5

Chapter 1

INTRODUCTION

1.1 BACKGROUND

This thesis describes the development of a multi-location motion displacement test (MDT) for the early diagnosis of glaucoma. The new test uses the principles of a single-location MDT, which was pioneered by Professor Fitzke at the Institute of Ophthalmology and run on a BBC computer (Fitzke et al. 1987). The original version has been shown by several published studies to offer greater sensitivity to detect early glaucoma than standard automated perimetry (SAP), (Fitzke et al. 1987; Fitzke et al. 1989; Poinoosawmy et al. 1992; Ruben and Fitzke 1994; Baez et al. 1995).

The PhD represents an interim phase in a six-year program, which is summarized by figure 1-1. The doctorate author, Gay Mary Verdon-Roe (GMVR), has taken part in all stages of this development.

The pre-doctorate period was spent adapting the BBC MDT to a modern PC format. Mr Ananth Viswanathan programmed the computer software and GMVR conducted all clinical investigation and statistical analysis under the supervision of Professor Fitzke and Mr Mark Westcott. The stimulus timings were investigated to shorten the test duration.

The aim of the PhD was to develop a multi-location MDT through applied scientific study. The protocol included exploration of the psychophysical properties of the MDT stimulus. The knowledge gained was used to optimize stimulus parameters to ensure maximum test sensitivity (proportion of diseased individuals correctly identified as diseased) and specificity (proportion of non-diseased individuals

Figure 1-1. Summary of the multi-location MDT six-year development program. Presentations and publications are shown in parentheses.

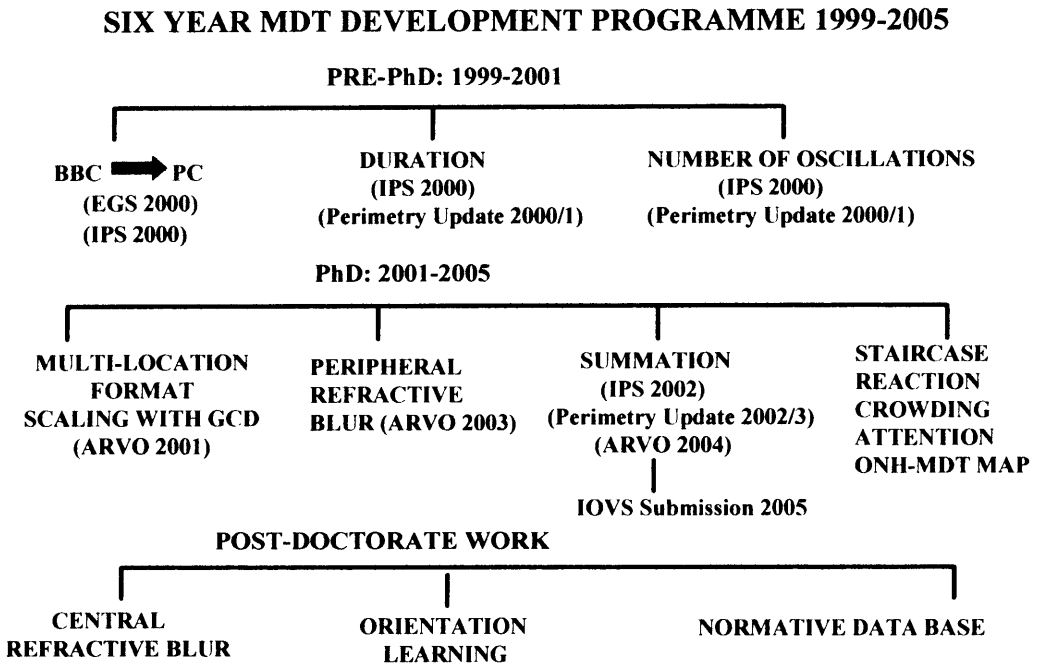

correctly identified as non-diseased), (Harper et al. 2000). A staircase strategy was developed and responses times studied to improve test efficiency and give an index of reliability.

Post-doctorate studies have been initiated as a continuum to the PhD to prepare the new test for release as a high quality, well-researched tool for the early diagnosis of glaucoma.

Our understanding of the disease process of glaucoma and its implications for global blindness has changed profoundly over the last thirty years. This introductory chapter will discuss these aspects and consider the need for new screening tests and the rational for further development of the original MDT. A summary of the objectives and accomplishments of the PhD is given, in order to provide a general perspective to the detailed descriptions of the subsequent chapters.

1.2 CLASSIFICATION OF GLAUCOMA

Glaucoma is a collective term for a complex group of conditions that have a common end point of progressive optic neuropathy. Glaucomatous optic neuropathy (GON) is characterized by distinctive patterns of structural changes at the optic nerve head (ONH) and retinal nerve fiber layer (RNFL) with associated loss of visual field function.

The conventional classification of primary glaucoma is by the anatomical configuration of the drainage system of the eye: primary open angle glaucoma (POAG), where the drainage angle is non-occludable, and primary angle closure (PACG), where the drainage angle is occludable. Secondary glaucoma may be due to a variety of processes, which include, for example, steroid induction, pseudoexfoliation, pigment dispersion or trauma.

The modern concept of POAG is that it is a primary neurogenerative disease of the optic nerve, with complex local ocular and systemic contributions, which may be influenced by genetic and environmental factors.

1.3 EPIDEMIOLOGY AND SOCIO-ECONOMIC CONSEQUENCES OF GLAUCOMA

Glaucoma is a leading cause of irreversible blindness worldwide (Thylefors and Negrel 1994). The estimated world figure for primary glaucoma for the year 2000 was 66.8 million, with 6.7 million suffering bilateral blindness (Quigley 1996). Fewer than 50% of those with glaucoma in the developed world are aware of their condition, with this figure being even higher in the developing world (Tielsch et al. 1991b; Coffey et al. 1993; Leske et al. 1995; Mitchell et al. 1996; Dandona et al. 2000a; Dandona et al. 2000b; Bourne et al. 2003; Nizankowska and Kaczmarek 2004).

The risk of glaucoma increases with age (Tielsch et al. 1991b; Klein et al. 1992; Mitchell et al. 1996; Dandona et al. 2000b; Quigley et al. 2001; Bourne et al. 2003). Increasing life expectancy predicts that these global estimates are set to rise with profound socio-economic consequences. Modern health care economic analysis quantifies the burden of a disease to society in terms of direct costs (e.g. diagnosis and treatment) and indirect costs [e.g. social service provision and inability to work, with consequent effect on Gross National Production (GNP)]. Resources are targeted according to cost-benefit and cost-effectiveness analyses. Cost-utility analysis provides a numerical formula for assessing the price of intervention whilst taking into account patient perceived values of treatment [£/QALY: Expenditure per quality adjusted life years] and time lost due to disability [£/DALY: Expenditure per disability adjusted life years], (Brown et al. 2003).

Glaucoma currently affects an estimated 2.2 million in the UK (Reidy et al. 1998; Langley-Hawthorne 2003). The annual total cost to the British economy is calculated between £16-38 Billion, with the vast majority of expenditure being directed to social support and the far-reaching consequences of loss of sight (Langley-Hawthorne 2003). An example of this is given by a recent study, which shows that visual field loss due to glaucoma is associated with a high rate of fall and consequent hip fracture. This is associated not only with the stress and cost of hospitalization and disability, but high morbidity (Yu F, et al. *IOVS* 2004; 45: ARVO E-Abstract 1124).

Economic models for the management of glaucoma have traditionally been limited by lack of evidence-based outcome measures. Studies are now being directed to address this omission and evidence is emerging that glaucoma treatment can effectively slow the disease progression (Leske et al. 1999; Heijl et al. 2002; Kass et al. 2002; Miglior et al. 2002).

It is suggested that a government saving of up to £1 Billion would be achieved if 10% of glaucoma patients received earlier treatment which arrested the disease process (Reidy et al. 1998; Langley-Hawthorne 2003).

In 1999 the World Health Organization (WHO) and the International Agency for the prevention of blindness (IAPB) set up an initiative "Vision 2020 "The Right to Sight" with the aim to eliminate preventable blindness by the year 2020 (Pararajasegaram 1999; WHO 1999). The conditions nominated include cataract, trachoma, onchocerciasis, childhood blindness and refractive error. There is a notable absence of glaucoma despite it being the second commonest cause of preventable blindness. The background reasons behind this include lack of perceived significance of the condition and the relative high cost of diagnosis and treatment, with the requirement for long-term care. Also, at the time, there was lack of evidence for successful outcome of treatment. Additionally, screening tools are expensive, lack adequate sensitivity and specificity, and have poor portability to remote areas.

1.4 RISK FACTORS FOR THE DEVELOPMENT OF GLAUCOMA

Epidemiology studies conducted over the last thirty years show that there is a wide variation of estimated glaucoma prevalence between populations. Each study needs to be evaluated with caution due to lack of consensus in diagnostic criterion and un-standardized methods of investigation (Wormald 1995; Harper et al. 2000; Foster et al. 2002). Change in investigative techniques over time make it difficult to make accurate calculations of glaucoma incidence (number of new cases reported per annum).

POAG is estimated to occur in 1-2% of Caucasians between the age of 40-60, increasing to 3-5% at 70 years (Tielsch et al. 1991b; Klein et al. 1992; Coffey et al. 1993). Estimates for those over the age of 80 are found to vary: in the Roscommon and Baltimore studies prevalence is found to level off or fall away respectively. By contrast, in the Blue Mountain trial, an exponential increase up to 11% is reported (Mitchell et al. 1996). A study of the Hispanic population in Arizona, USA, found the prevalence of POAG to be between that of the American White and Black but with an increased risk with age (12.6% over 80 years), (Quigley et al. 2001). These discrepancies of risk with age may be explained by sampling error due to the reduced number of subjects in the upper age limit.

The risk of POAG increases for those of Afro-Caribbean origin (Ntim-Amponsah et al. 2004), with an earlier presentation, more rapid progression and reduced responsiveness to current glaucoma treatment (Racette et al. 2003). A four-fold greater risk is estimated for the black population living in the USA (Tielsch et al. 1991b) and London (Wormald et al. 1994).

A cross-sectional study of ten thousand individuals of all ages from the Indian state of Andhra Pradesh found a glaucoma prevalence of 11%, with the risk increasing for those of lower socio-economic status (Dandona et al. 2002).

The prevalence of PACG is greater amongst Asian groups (Foster et al. 1996; Seah et al. 1997; Dandona et al. 2000a; Bourne et al. 2003) due to ethnic anatomical features, including shallowing of the anterior chamber. Acute PACG is less common than chronic/latent ("creeping") PACG (Lachkar 2003). Chinese Singaporeans are at higher risk than the island's other ethnic groups (Malay and Indian), (Seah et al. 1997). Isolated Inuit communities also have a higher prevalence of PACG (Bourne et al. 2001). All these studies report lower mean intraocular pressure (IOP) than for white populations.

On the assumption that the Singaporean Chinese represent urban China and that Mongolia represents rural China, it is estimated that 9.4 million Chinese have GON. Of this figure, 5.2 million (55%) are estimated to be blind in one eye and 1.7 million (18.1%) to suffer bilateral blindness (Foster and Johnson 2001).

A greater than expected effect of age was found in a study of 790 individuals over the age of 50 years in Bangkok (Bourne et al. 2003), relative to calculations used to predict prevalence of glaucoma (Quigley 1996; Quigley and Vitale 1997). This suggests that current world estimates may be conservative.

The epidemiology studies cited above show that glaucoma presents a global challenge with a clear need to raise public awareness and provide improved methods of early diagnosis and long term care.

Raised IOP of > 21 mm Hg is regarded as a risk factor for the development of glaucoma but is not in itself diagnostic of glaucoma (Sommer 1989; Sommer et al. 1991; Sommer and Tielsch 1996). A single gene may account for 18% of the population variance of IOP (Viswanathan et al. 2004). POAG may occur in the presence of high IOP or "normal" IOP (Normal tension glaucoma [NTG], where IOP is < 20 mm Hg). Ocular hypertension (OHT) describes a condition where the optic nerve head and psychophysical function are normal, but the IOP is higher than 21 mm mercury.

The recent introduction of calibrating IOP according central corneal thickness (CCT) provides a means for adjustment of measurement error. The traditional gold standard test for measuring IOP is Goldmann applanation tonometry, which assumes CCT of approximately 520 micron. If no allowance is made for CCT, subjects with thick CCT (> 600 micron) may falsely be identified with raised IOP and be diagnosed with OHT. In reverse, subjects with thin CCT may falsely be identified with normal or low IOP and be wrongly classified as NTG (Copt et al. 1999; Shah et al. 1999; Brusini et al. 2000; Brandt et al. 2001). Where there is inter-eye variation of CCT, the eye with the thinner cornea is at greater risk of developing glaucoma (Soans et al. 2004).

Study of biomechanical effects indicate that the diameter, thickness and rigidity/elasticity of the scleral shell each have significant effect on the ocular response to stress induced by raised IOP, with wide inter-subject variability (Ethier R, et al. *IOVS* 2005; 46:ARVO E-Abstract 2370; Sigal et al. *IOVS* 2005; 46:ARVO E-Abstract 1268).

Family history is a widely accepted risk factor for the development of glaucoma. However, family history was not found to be a risk factor in the presence of raised IOP in the Ocular Hypertension Treatment Study (OHTS), (Lee and Wilson 2003). Assessment of family history is subject to error where reliance on patient self-reporting leads to false positive and false negative diagnosis (Tielsch et al. 1994; Craig et al. 2001; Mitchell et al. 2002). The low prevalence of POAG in first-degree relatives contradicts a single-gene hypothesis (Garway-Heath 2000). A gene has been identified (TIGR: trabecular meshwork inducible glucocorticoid response), which is associated with aqueous outflow through the trabecular meshwork (Lutjen-Drecoll 1999) in POAG and Juvenile Glaucoma (Allingham et al. 1998). Polymorphism in the gene locus for optic atrophy (OPA1) has been shown to be a marker for NTG (Aung et al. 2002). Multiple mutations are predicted. Many diseases have glaucoma as a major feature for which different chromosome loci have been mapped e.g. Marfan's syndrome (Brdicka 1995) and Neurofibromatosis (Menon et al. 1990). Genetic profiling may be achieved by population phenotyping through

maximum likelihood estimation (Viswanathan et al. 2004) or by study of identical and non-identical twins. It is anticipated that this information will have profound effects in the management strategy of glaucoma screening in the future.

Currently unpublished twin studies conducted in Tasmania indicate that CCT and optic disc area are inherited features. It is possible that this may apply to other structural components of the eye and may assist in the identification and management of patients at risk of developing glaucoma in the future (A. Hewitt: Moorfields lecture. May 2005).

The role of the cardiovascular system in glaucoma is complex: systemic hypertension has been shown to be a risk factor for the development of glaucoma, particularly if uncontrolled (Mitchell et al. 2004). Paradoxically, it is suggested that, in the early stages, raised blood pressure (BP) is protective against the development of glaucoma due to increased ocular perfusion at the ONH. Over time, secondary vascular changes occur causing reduced ONH perfusion and consequent increased risk of POAG (Tielsch et al. 1995b).

Neuroretinal rim blood flow is inversely correlated with increased optic nerve cup disc ratio. In OHT larger cup disc ratios are associated with reduced rim blood flow. No association has been demonstrated between glaucoma and peripapillary retinal flow (Hafez et al. 2003). Nocturnal hypotension and high BP variability are suggested to be risk factors in functional progression (Graham et al. 1995; Graham and Drance 1999).

The association of glaucoma with diabetes is controversial: on the one hand it has been discounted on the grounds of selection bias (Tielsch et al. 1995a), on the other, a positive association is reported by epidemiological survey (Mitchell et al. 1997). Additional risk factors include pseudoexfoliation (Mitchell et al. 1999b; Allingham et al. 2001) and moderate-high myopia (Mitchell et al. 1999a; Nomura et

al. 2004). There is no clear gender significance in the epidemiology studies cited, although Levene reported increased risk of NTG in females (Levene 1980).

1.5 PRESENTATION OF GLAUCOMA

The onsets of POAG and latent PACG are each insidious and characterized by specific patterns of visual field loss of which the patient is frequently unaware until progressed to an advanced stage (Sheldrick et al. 1994).

Analysis of visual field loss is an essential part of the diagnosis and management of glaucoma and is conventionally performed by assessment of static differential light sensitivity (DLS), using automated field tests such as the Humphrey Field Analyzer 24-2 program. Different sub-groups of glaucoma may manifest specific patterns of visual field defect. A single study comparing POAG with chronic PACG, using standard automated perimetry (SAP), suggests that subjects with POAG have a greater tendency toward superior hemi-field defect and subjects with chronic PACG higher mean defect (MD), (Saw et al. 2003). Bourne reported that patients with chronic PACG are more likely to be referred to eye clinics than those with POAG (Bourne et al. 2003). A possible explanation may be different IOP levels.

1.6 DETECTION OF GLAUCOMA

POAG and latent PACG are generally unnoticed by the sufferer. Within the UK there is no systematic screening program, which means that detection of glaucoma depends on opportunistic case finding. This is almost entirely the responsibility of optometrists who initiate more than 96% of referrals to the hospital eye service (Sheldrick et al. 1994; Bell and O'Brien 1997). A high number (up to 68%) of hospital referrals are found to be false positive (Sheldrick et al. 1994), resulting in huge wastage of hospital resources and unnecessary anxiety and inconvenience to the patient.

The general household survey for 1990-1994 indicated that there is a wide difference in attendance for sight tests between socio-economic groups. Peak attendance concurs with the onset of presbyopia and the need for reading spectacles. Attendance declines in the seventh decade as presbyopia stabilizes. Ironically, this means that the age group most at risk of developing glaucoma is least likely to attend an optometrist (Wormald et al. 1997).

The recommended standard optometry examination for a subject thought to be at risk of glaucoma includes IOP, perimetry and subjective optic disc evaluation by ophthalmoscopy. Referral on SAP alone is found to account for high false positive rate (Newman et al. 1998). The positive predictive value [PPV: proportion of patients with positive screening test results who are found to have the disease, (Harper et al. 2000)] of glaucoma detection is improved by using supportive evidence from more than one of the standard tests (Tuck and Crick 1991; Crick and Tuck 1995; Tuck and Crick 1997). The number of false positive referrals may be reduced by "referral refinement" whereby initial referral is made to specially trained optometrists (Henson et al. 2003). The inherent variability of all tests used to diagnose glaucoma indicates that in early suspect glaucoma the examination is best repeated to avoid false positive and false negative diagnoses. This applies to both optometry and hospital services (Henson 1999).

Epidemiology studies suggest that at least 50% of glaucoma patients are undiagnosed, with this figure being much higher in the developing world (Tielsch et al. 1991b; Coffey et al. 1993; Leske et al. 1995; Mitchell et al. 1996; Dandona et al. 2000a; Dandona et al. 2000b; Bourne et al. 2003; Nizankowska and Kaczmarek 2004). It not known within developed countries whether failure to detect glaucoma may be explained by non-attendance to the optometry service or failure of current screening practices to diagnose glaucoma. In the third world there is a widespread lack of provision of eye services, with a clear need to provide financially affordable and portable screening devices.

Late detection may have profound consequences for visual outcome. Untreated glaucoma advances faster than treated glaucoma and the more advanced the glaucoma loss the more rapid the progression (Heijl et al. 2002). Late presentation relates to age, ethnicity, socio-economic group, access to services and awareness of condition (Tielsch et al. 1991a; Wilson 2002; Wilson et al. 2002). Zeyen followed optic disc and visual field deterioration in early glaucoma over a period of six years. There was an increased rate of change in subjects with an initially abnormal field compared with those with an initially normal field (Zeyen and Caprioli 1993).

A drive for improved glaucoma detection is therefore imperative. This may be achieved by a combination of public education about glaucoma and improved methods of early diagnosis. It is hoped that the new MDT may provide one such tool.

1.7 STRUCTURAL AND FUNCTIONAL RELATIONSHIPS IN GLAUCOMA

Diagnosis and monitoring of glaucoma is confounded by lack of concordance between structural measurements of the optic disc and psychophysical measurements of visual function (Henson D et al. IOVS 2004; 45: E-Abstract 5512). This may be explained by a number of factors. For example, there may be differences in the time course of structural and functional damage. It is possible that ganglion cell dysfunction may occur without evidence of structural change. Furthermore, structural change may relate to non-functional tissue e.g. bowing of laminar. Structural and functional measurements may thus give complementary but different information and this supports the testing of both modalities (Strouthidis NG et al. IOVS 2005; 46: ARVO E-Abstract 3636).

The logarithmic scaling of SAP in decibels (dB) may give the false impression of a ganglion cell functional reserve, with large changes in structure corresponding to small dB loss in early disease and small changes in structure corresponding to large dB loss in late disease. A continuous structural-functional relationship is found with SAP and neuroretinal rim area and pattern electroretinogram (PERG) when SAP

scaling is converted to a linear 1/Lambert scale. This is applicable when testing outside the central 15 degree field A non-linear relationship is predicted in the central field due to increased ganglion cell density (GCD) enhancing probability summation (Garway-Heath et al. 2002; Garway-Heath 2004).

Tests directed to both structure and function show large inter-subject variability (Garway-Heath 2004). Fluctuation is often marked early in the disease process, which hampers definitive diagnosis (Lan et al. 2003). Visual field variability increases as sensitivity decreases. This is evidenced in both normal and diseased eyes and thought to reflect difference in functional GCD (Henson et al. 2000).

Anatomical studies conducted from the early 1980s have suggested that a loss of 20-50% of ganglion cells may occur before a defect is detectable by SAP (Quigley et al. 1982; Quigley et al. 1988; Quigley et al. 1989; Harwerth et al. 1999). This knowledge prompted the quest for the development of more sensitive psychophysical tests for the early diagnosis of glaucoma.

The optic nerve is comprised of a complex of ganglion cell pathways, each of which is anatomically and functionally distinct. Dacey predicts the primate retina to contain as many as twenty cell types. Currently, five have been identified: the inner and outer parasol cells connecting to the dorsal magnocellular (M) pathway, the inner and outer midget cells to the ventral parvocellular (P) pathway and the small bistratified to the konicellular (K) pathway (Casagrande 1994; Martin et al. 1997).

Psychophysical investigations suggest that the properties of the M and P pathways of the optic nerve differ in four major ways: colour perception, receptive field size, speed and contrast sensitivity (Livingstone and Hubel 1988). The use of discrete chemical lesions at the lateral geniculate nucleus (LGN) in primates indicates that the P pathway is responsible for the processing of colour, texture, fine pattern and fine stereopsis and the M for fast flicker and motion (Schiller et al 1990). The P pathway has greater sensitivity relative to the M pathway for contrast detection at low

temporal and high spatial frequencies. The M pathway has greater sensitivity relative to the P pathway for stimuli of low contrast, high temporal and low spatial frequencies (Merigan, Katz et al 1991; Merigan, Byrne et al 1991).

Studies of human dendritic field size and cell density indicate that the midget cells increasingly out-number the parasol and bitstratified from peripheral to central retina (Dacey 1994). The midget cells are red-green opponent receiving antagonistic input from long and medium wave-length sensitive cones. The bistratified cells are "blue-on" receiving input from short sensitive cones. It was presumed that the "blue-on" were opposed by the combined long and medium input, but evidence has been presented to suggest the existence of "blue-off" (Vassilev et al. 2003). The parasol cells give a phasic non-opponent response. Dendritic connections to the inner plexiform layer (IPL) give an "on" response to luminance and those to the outer plexiform layer (OPL) an "off" response (Dacey and Lee 1994).

Histological studies (Quigley et al. 1987; Quigley et al. 1988; Glovinsky et al. 1993) suggest that in early glaucoma there may be preferential damage to the M pathway, both in experimentally induced glaucoma in primates (Weber et al. 2000) and humans with established glaucoma (Chaturvedi et al. 1993). Experimental glaucoma is induced by argon laser application to the trabecular meshwork (Quigley and Hohman 1983). It is questionable whether this methodology truly replicates human glaucoma, as the onset of high pressure is more acute.

Dandona found selective disruption of axoplasmic flow to the M cells in the dorsal LGN in experimentally induced chronic glaucoma in the Macaque. No difference was quantifiable in acute glaucoma (Dandona et al. 1991). It is possible that the relatively large surface-to-volume ratio of M cells make them more vulnerable to the effects of altered tissue perfusion that are secondary to raised IOP.

The concept of early M loss provided the original rational to develop a test more sensitive to early glaucoma based on motion/flicker perception. The subject of this

project, the MDT, pioneered by The Institute of Ophthalmology and Moorfields Eye Hospital since the mid 1980s, is one such test (Fitzke et al. 1987; Fitzke et al. 1989; Fitzke et al. 1992). Other tests include Displacement Threshold Perimetry (Johnson et al. 1995), Random Dot Kinetograms (RDK), (Silverman et al. 1990; Bullimore et al. 1993; Wall and Ketoff 1995; Bosworth et al. 1997a; Bosworth et al. 1997b; Joffe et al. 1997; Sample et al. 1997; Wall et al. 1997; Bosworth et al. 1998; Sample et al. 2000b) and Flicker Perimetry (Tyler 1981; Lachenmayr et al. 1988; Feghali et al. 1991; Lachenmayr et al. 1991; Austin et al. 1994; Horn et al. 1997; Yoshiyama and Johnson 1997; Gonzalez de la Rosa et al. 1998; Junemann et al. 2000; Langley-Hawthorne 2003). The Frequency Doubling Technology (FDT) test (Johnson and Samuels 1997) is suggested to be directed specifically to the Mγ cells which comprise 15-25% of a sub-population of the M pathway (Maddess and Henry 1992), although this has been disputed (White et al. 2002).

Several authors dispute the concept of specific M loss in glaucoma. Johnson suggests a theory of "reduced redundancy." The theory hypothesizes that early loss of M function may be explained by the relatively sparse population of M cells compared to P, giving less physiological capability for compensation through overlapping receptive fields (Johnson 1994). Morgan suggests errors may be made when assessing histological M cell density by neglecting cell shrinkage (Morgan 1994; Morgan et al. 2000; Morgan 2002).

Psychophysical evidence does not always support the theory of selective magnocellular loss in early glaucoma (Ansari et al. 2002a). Ansari found no statistical difference between early glaucoma and controls, when comparing contrast sensitivity of grating stimuli designed to preferentially isolate M cells (0.5 c/deg, 16 Hz), with grating stimuli designed to preferentially isolate the P pathway (8 c/deg, 0 Hz), (Ansari et al. 2002b). However, Anderson found increased separation of glaucoma from controls at 12 different retinal locations when using phase-reversed gratings compared to stationary gratings (Anderson and O'Brien 1997).

More recent study of neuronal metabolism by observation of cytochrome oxidase reactivity (COR) in experimental glaucoma in primates suggests that there is no preferential pathway loss at the level of the LGN. However, in the visual cortex at 4C, in direct contrast to the traditional view, parvocellular function (C4α) is found to be compromised compared with magnocellular (C4β), (Harwerth et al. 2002).

What is undeniably the case is that current psychophysical tests for the diagnosis of glaucoma lack adequate sensitivity to elicit functional loss in early disease.

Westcott found evidence of scotomata undetected by the standard 24-2 program by fine matrix mapping (FMM), also known as High Pass Resolution Perimetry (HPRP), of the Humphrey visual field (Westcott et al. 1997). In a second study, elevation of MDT was found in areas of normal Humphrey 24-2 field. In some, but not all patients, this was found to co-exist with fine matrix mapped scotoma (Westcott et al. 1998a).

Suspect glaucoma eyes with normal SAP may show abnormal visual function on a wide variety of tasks (Sample et al. 1994; Sample et al. 2000b). These include those processed through the M pathway mentioned above and Short-Wavelength Automated Perimetry (SWAP), (Sample and Weinreb 1992; Johnson et al. 1993; Sample et al. 1993; Johnson et al. 2003) mediated by the K pathway (Dacey and Lee 1994). This suggest that, even if there is no preferential damage to the M pathway, tests directed towards sampling a specific subset of ganglion cells may be more likely to be more sensitive to early damage than those that are non-specific. However, different psychophysical tests for glaucoma may yield different results, supporting the notion that more than one pathological mechanism may be involved in the disease process (Ruben et al. 1994). An alternative explanation could be variation of measurement of noise.

1.8 ALTERNATIVE PSYCHOPHYSICAL TESTS FOR THE DETECTION OF GLAUCOMA

Over the last twenty years, various attempts have been made to develop psychophysical tests for the early diagnosis of glaucoma as alternatives to SAP. The recent trend has been to target specific ganglion cell populations, on the basis of the theories of redundancy or early magnocellular loss as previously discussed. Reports in the literature on test sensitivity and specificity each need careful evaluation due to lack of consensus of methodological and reporting standards (Harper et al. 2000).

1.8.1 TESTS DIRECTED TO MAGNOCELLULAR PATHWAY

Tests directed towards M function fall into three categories: motion, the illusion of frequency doubling and flicker.

The psychophysical perception of motion is a response to the displacement of an object across space and time (figure 1-2).

Figure 1-2. Psychophysical Perception of Motion across time and space.

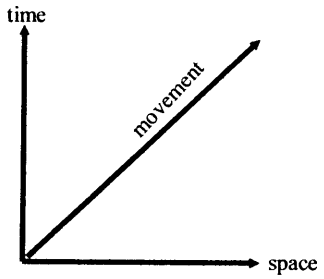

Motion in everyday life ("actual" motion) is perceived by a sequence of visual stimuli which track across retinal receptors. Experimental perception of motion ("apparent" motion) is based on models of "local" or "global" processing.

Local motion processing assumes the sampling of an image at two points in space at slightly different times by "bilocal" detectors. Each detector has an individual spatial span (ds). A time delay (dt) exists between detectors which is the difference in time that impulses are detected by a comparator unit if both detectors are stimulated simultaneously (Snowden and Braddick 1989).

"Global" motion processing requires the cooperation of a range of detectors and the combination of motion signals over time (Snowden and Braddick 1989). Barlow found the retinal ganglion cells in rabbits show directional selectivity and he suggested that this is achieved by inhibition of units in the non-preferred direction (Barlow et al. 1964; Barlow and Levick 1965).

Recent evidence shows that motion detection may begin early in the retina. Olveczky questioned how movement is distinguished from retinal drift. He used identical gratings for object and surround moving at different trajectories (figure 1-3) and found that ability to distinguish motion was blocked by Strychnine indicating mediation by retinal amacrine cells (Olveczky et al. 2003).

Figure 1-3. Investigation of early retinal processing of motion (from Olveczky et al., 2003).

Arrows indicate the different trajectory of motion used for the identical gratings of object and background.

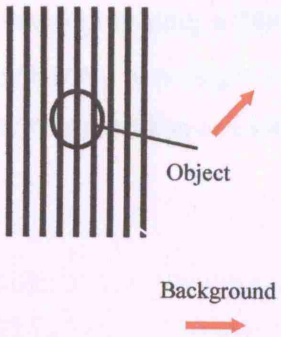

1.8.1.1 MOTION DISPLACEMENT TEST (MDT)

The MDT creates the illusion of apparent motion by fine positional displacement (< 30 min arc) of a line stimulus between computer frames and is therefore considered to be targeting "local" motion.

There remains a widespread general assumption that tests of motion displacement are directed to the M pathway, but review of the literature, which is covered in chapter 6, suggests this may be an over simplification.

Motion displacement acuity has long been recognised as a hyperacuity stimulus, offering directional sensitivity that is beyond what would be predicted from anatomical ganglion cell spacing (Scobey and Horowitz 1976). The MDT task is to discriminate the positional change between two lines and may thus be categorized as a temporal form of vernier acuity.

Electrophysiological studies of spot light displacement in primates indicate that all cells respond to movement displacement of < 10% the diameter of their receptive field. It is thought that intra receptive field directional sensitivity is achieved by pooling of the excitatory and inhibitory responses of overlapping on-off receptive fields (Scobey 1981).

BBC COMPUTER VERSION OF MDT (1987-1998)

The original MDT was developed using a BBC computer. A 2 degree x 2 min arc vertical line stimulus was presented at a single location, which was located above the blind spot in the supero-temporal meridian at 15,9, where 0,0 is fixation (figure 1-4).

Figure 1-4. Diagrammatic representation of the original MDT (Fitzke et al. 1987).

The white circle corresponds to central fixation (0,0) and the open circle the optic nerve head.

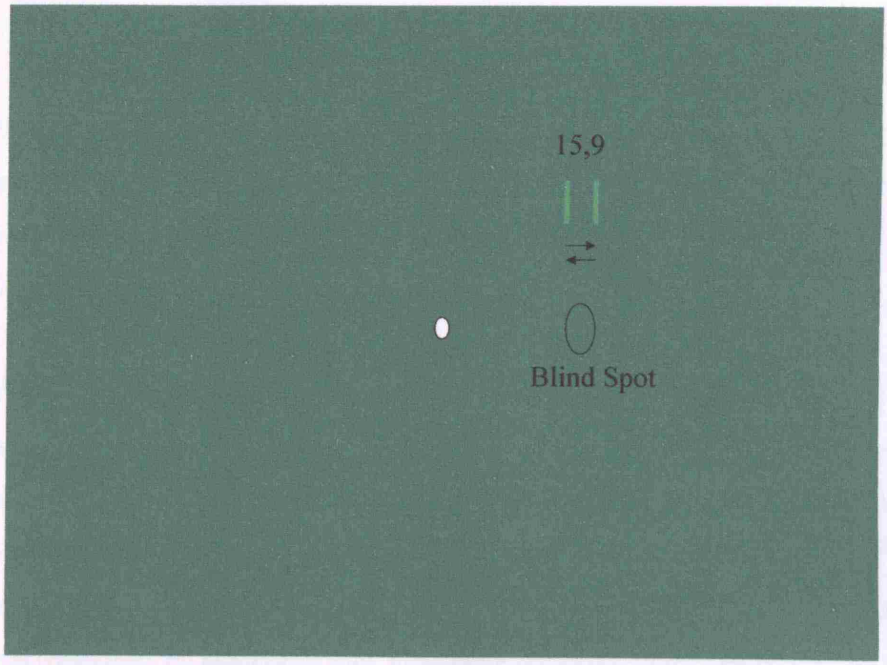

The stimulus was programmed to move through 5 oscillations per presentation at a speed of 400 msec per cycle for each of 10 presentations of 10 displacements, at 2 min arc intervals, from 0-18 min arc. Threshold was calculated by probit analysis and determined as 50% seen (Fitzke et al. 1987). Elevated MDT thresholds were found to be a predictor of future field loss (Fitzke et al. 1987; Fitzke et al. 1989; Poinoosawmy et al. 1992).

Ruben studied 50 eyes of 50 patients with OHT and normal Humphrey fields. He found significant correlation of MDT results with neuroretinal rim area (Ruben and Fitzke 1994).

Study of MDT frequency of seeing (FOS) curves gives information of the probability of seeing with variation of displacement distance (figure 1-5). FOS curves give indication of local variability and, as with Humphrey Field analysis (Chauhan et al. 1993b), different characteristics may be found in normal subjects and patients with glaucoma, even when thresholds are similar (Westcott et al. 1999).

Westcott also found the interquartile range (IQR), which corresponds to the difference between the 75% and 25% values of the MDT probit fitted curve, to be elevated in glaucoma and, when calculated together with the 50% threshold, gives improved separation from normal subjects (Westcott et al. 1999).

Westcott studied 29 control, 29 aged matched POAG patients and 28 aged-matched glaucoma suspects. The MDT 50% seen response, standard deviation and range was found to be 5.9 ± 1.7 (2.6 - 8.9) min arc in control, compared to 12.9 ± 5.8 (5.2 - 34.2) min arc in the POAG group and 8.7 ± 3.4 (5.0 - 17.6) min arc in the glaucoma suspect group. Analysis of the slope of the MDT FOS curves showed a shallower response in glaucoma and glaucoma suspects when compared to normal subjects.

In addition, Westcott observed that the largest magnitude of displacement coinciding with the optimal response (LDMax) was reduced (< 18 min arc) in 14 of the 29 POAG subjects, compared to only 1 of 29 controls (figure 1-5 d-g), (Westcott et al. 1998b).

LDMax should be distinguished from the D_{max} of short range apparent motion which applies to random dot kinetograms (Braddick 1974).

Further work by Westcott investigated the effect of changing the orientation of the line stimulus. Improved sensitivity to detect early RNFL defect was found by orientating the line in the same direction as the RNFL, with the vector of motion orthogonal to the stimulus (figure 1-6), (Westcott et al. 1996).

Figure 1-5. Examples of MDT frequency of seeing curves (from Westcott et al., 1999).

Black circles represent raw data with probit-fitted curve (solid black curve) and 95% confidence interval (dashed curve). Dashed black line indicates the 50% seen threshold.

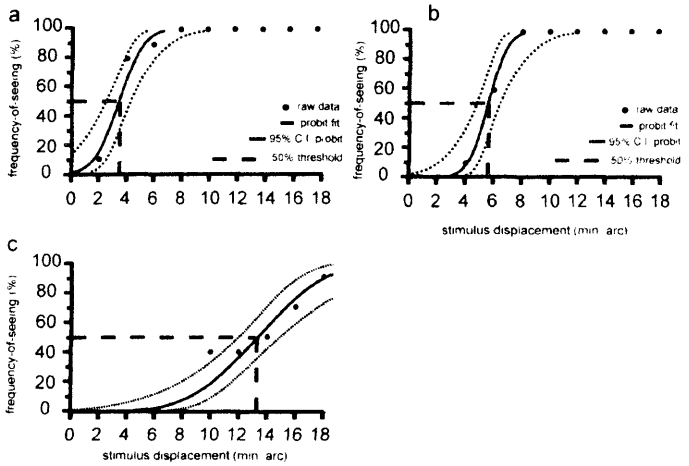

a and b: Normal frequency of seeing curves characterized by steep slopes and low MDT threshold (50% seen) of 3.4 and 5.5 min arc respectively. LDMax is coincident in each case with optimal response rate (18 min arc).
c: Frequency of seeing curve of glaucoma patient: note shallow slope with elevated MDT threshold (13.2 min arc) with normal LDMax (18 min arc).

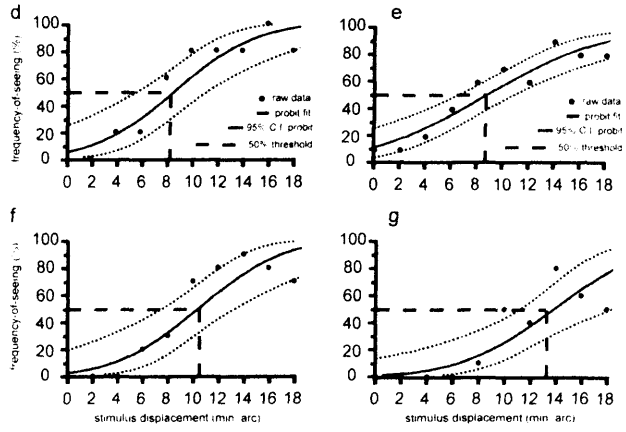

d and e: Frequency of seeing curves in a glaucoma suspect eye and a glaucomatous eye. Each shows an MDT threshold within the normal range (8.2 and 8.5 min arc respectively), but with a reduced LDMax (16 and 14 min arc respectively).
f and g: Frequency of seeing curves in glaucomatous eyes with elevated MDT thresholds (10.5 and 13.5 respectively) and reduced response rate at maximum displacements of 16 and 18 min arc giving an LDMax threshold of 14 min arc.

Figure 1-6. Illustration of an MDT stimulus orientated with retinal nerve fiber layer.

Photograph courtesy of Mark Westcott.

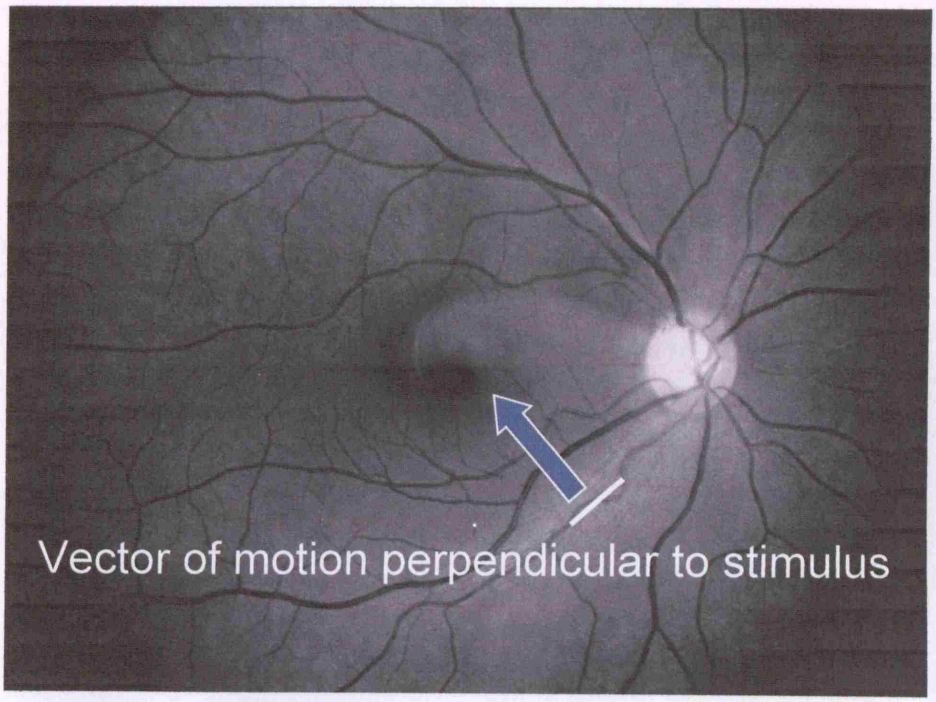

EARLY MULTI-LOCATION MDT

An early multi-location MDT was created on a 16 inch screen lap-top and shown to be a predictor of visual field loss (Wu et al. 1991; Wu et al. 1998). 48 vertical lines were depicted on the screen display six of which were test locations: four test locations were in the 15 degree quadrant positions, and two in the superior and inferior nasal field, 7 degrees from fixation (figure 1-7).

Figure 1-7. Early six-point motion and flicker multi-location test (from Wu 1993).

Double vertical lines denote test locations

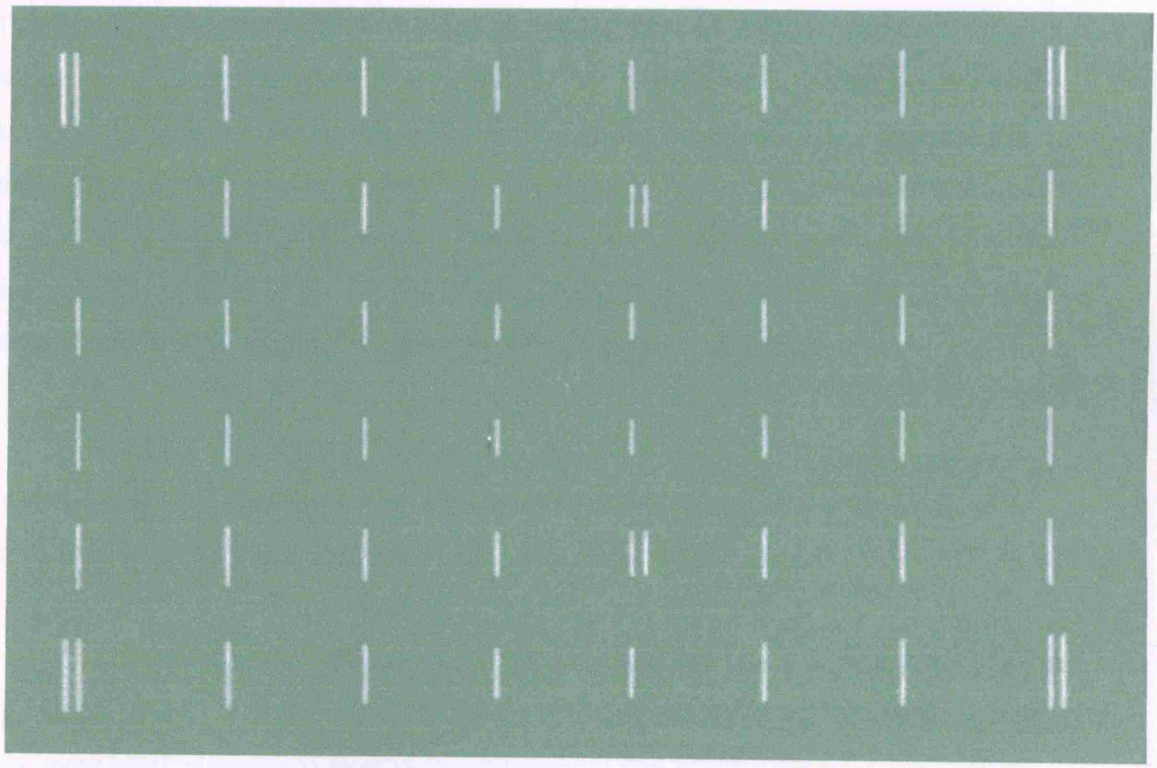

Each stimulus line was programmed to undergo 10 presentations each of three pixel displacements, corresponding to 4, 8 and 12 min arc. In addition, 10 trials of flicker were tested at each location using a speed of 40 Hz thus making a total of 240 presentations. The results were given as a percentage of the total seen at each location for each size of displacement (Wu 1993; Verdon Roe 1995). Drawbacks of the system included lack of normative threshold information, the long duration of the test (7-15 minutes) and the automatic shut down written into the program when < 50% of stimuli were detected in the first 18 presentations. The large number of locations present may introduce problems of visual attention. The test resistance to refractive artifact is unknown.

Johnson developed a unidirectional multi-location motion displacement test that was composed of 60 locations corresponding to the Humphrey 30-2 program. Presentation of a single target was found to cause confusion of target onset and target motion resulting in false positive response. All stimuli were therefore presented concurrently. The test was run on a Macintosh computer using a 21-inch monitor. The stimulus was a white square, subtending approximately 36 min arc at a test distance of 30 cm, with duration of 50 msec. Threshold was estimated by staircase with a displacement range of 3 min arc – 5 degrees. Stimulus luminance was 50 cd/m^2 and background 10 cd/m^2, giving a contrast of 66% (Johnson et al. 1995).

Preliminary findings indicated motion deficits equal to or larger than SAP. In some cases of OHT elevation of MDT was found, which followed the same pattern of nerve fiber bundle deficits associated with SAP (Johnson et al. 1995).

The disadvantage of this test is the large number of locations, which lengthen the test duration (12-15 minutes). The square stimulus may lack the sensitivity of the thin linear MDT stimulus to detect fine slit defects of the RNFL (Westcott et al. 1996). Analysis of oscillatory MDT stimulus FOS curves would suggest the displacement range used for the unidirectional stimulus is larger than one would predict necessary for a multi-location motion test based on the BBC MDT (Westcott et al. 1999). The

wide range may have been selected because a unidirectional stimulus will have reduced summation properties, with consequent higher motion thresholds, when compared to the MDT three oscillatory stimulus presentation (Verdon-Roe et al. 2000).

PC VERSION OF MDT (1998-2000)

Work conducted during 1999-2000 by Viswanathan, Westcott and Verdon-Roe demonstrated that a modern PC version of the single line BBC MDT is capable of producing equivalent results with the original, despite differences between the two systems (table 1-1), (Viswanathan et al. 2000).

The new test was designed by Ananth Viswanathan in C++. A white stimulus on a grey background was used in keeping with the previously reported lack of wavelength sensitivity of the M pathway. A high contrast system was selected, despite the M pathway being sensitive to low contrast, to ensure that the test remains robust to the effects of artifact such as cataract (Membrey and Fitzke 2000).

Table 1-1. Specifications of BBC and PC computer systems.

	BBC Microcomputer Model B	Viglen Genie ATX
Processing Speed		Intel Pentium 200 MHz
RAM		32 mb
Monitor	Green monochrome P31 Phosphor Video Display	32 Bit Colour 1280 x 1024 pixels 0.28 dot pitch
Stimulus	Bright Green	White (rgb 255,255,255)
Stimulus Luminance	27 cd m2	112 cd m2
Background	Green	Grey (rgb 65,65,65)
Background Luminance	7 cd m2	10 cd m2
Contrast	60%	84%

The standard BBC stimulus presentation was 5 oscillations with duration of 400 msec per cycle. The M system is tuned to short cycle times and higher frequencies of oscillation (Livingstone and Hubel 1987). Westcott and Verdon-Roe investigated the effect of reducing these parameters to make the test of shorter duration and more specifically M directed. A reduced test time has useful implications in terms of lessening patient fatigue and improving hospital efficiency, providing separation of glaucoma from control is maintained. MDT thresholds were compared for durations of 400 to 200 and 100 msec per cycle and oscillations of 5, 3 and 1 per stimulus presentation (figure 1-8).

Equivalent MDT thresholds were found for all durations tested (Westcott et al. 2000b) and for 3 and 5 oscillations per presentation (Verdon-Roe et al. 2000). However, MDT thresholds were markedly elevated when using a stimulus presentation of one oscillation (Verdon-Roe et al. 2000). This may be explained by altered properties of temporal summation.

The processing speed of the computer used will set the lower limit of stimulus duration that can be achieved. It is possible that the MS Windows environment may lead to disruption of the MDT stimulus timings due to conflict with tasks that are unrelated to the MDT and automated by the computer. Such conflicts need to be kept in mind and eliminated where possible in future versions of the device.

The accuracy of the displacement timings was checked using a stopwatch. Stimulus durations of 400, 200, 100 and 50 msec per cycle were timed over 50 oscillations to ensure a measurable value. The mean of three tests was calculated for each stimulus duration. For the computer used (Viglen Genie ATX Intel Pentium 200 MHzMMX processor, 32mb RAM) timings of < 200 msec per cycle were found to be increasingly inaccurate, the stimuli taking longer than the programmed time to complete their presentation (table 1-2).

Figure 1-8. Time diagrams illustrating change of MDT presentation by variation of stimulus duration and oscillation.

(i) variation of stimulus oscillation

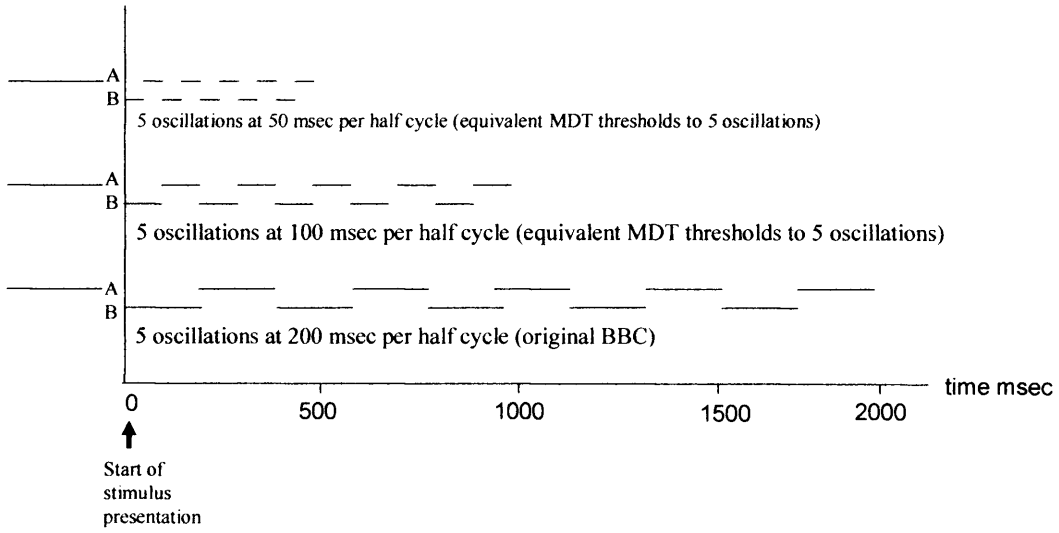

(ii) variation of stimulus duration

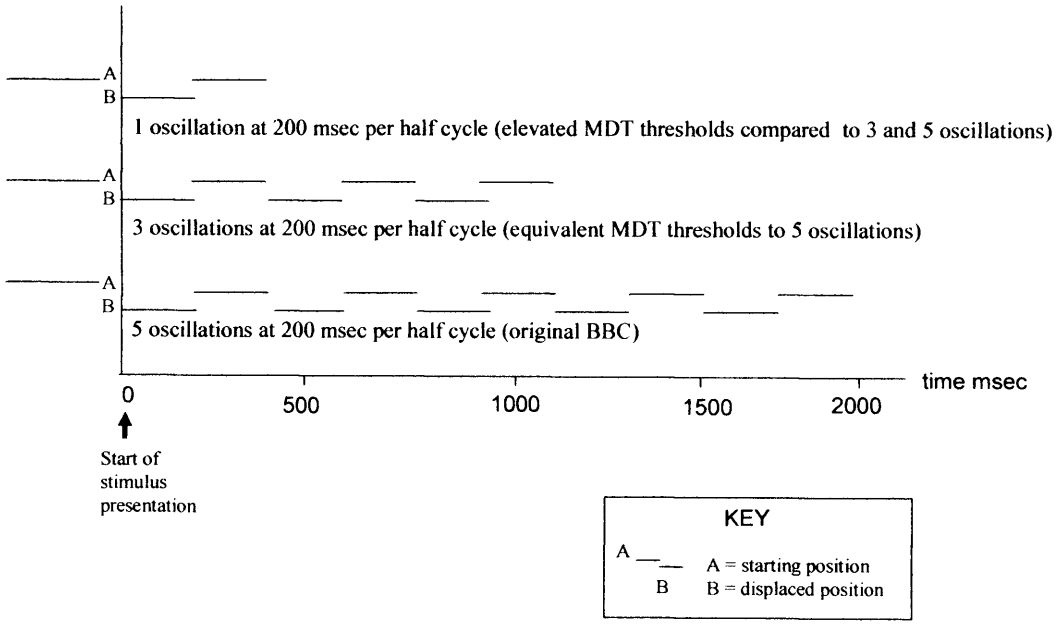

Table 1-2. Results of computer timings.

Time (t) per cycle (msec)	No Cycles	Calculated t (sec)	Mean Measured t (sec)	% error
400	50	20	22	10%
200	50	10	11.5	15%
100	50	5	6	20%
50	50	2.5	5	50%

It is possible that the findings may have been due to stopwatch error. An alternative methodology might have been to have kept time constant and varied the number of oscillations.

The MDT stimulus presentation was set to a new standard of 3 oscillations per cycle. The stimulus duration was set to 200 msec per cycle (figure 1-9). This allows for the possible limitation imposed by computer processing speeds and consideration of the findings of Post, who found elevation of motion threshold for short stimulus presentations of less than 80 msec per cycle (Post et al. 1984).

Figure 1-9. Time diagram illustrating the new standard MDT stimulus presentation.

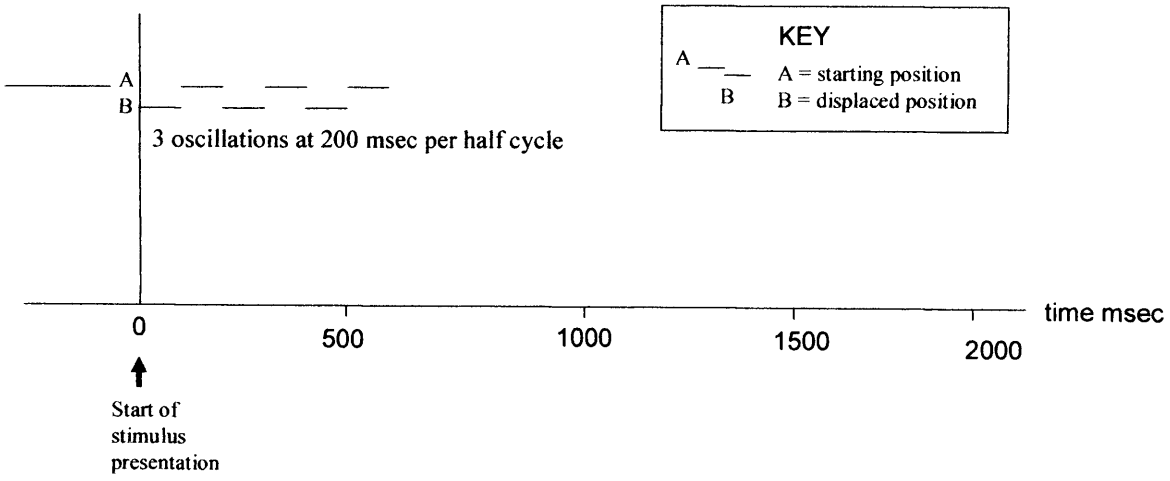

The minimum displacement MDT threshold that can be measured by the test monitor (0.255 dot pitch) at the test distance of 30cm is ~ 2-4 min arc, depending on stimulus orientation and eccentricity, enabling the detection of early focal defect.

Further advantages of MDT are that it shows high tolerance to media opacity and changes in pupil size, consequently offering good test specificity (Membrey 2000; Membrey and Fitzke 2000). It is possible that MDT resistance to media blur is achieved by the test being run at high contrast (original BBC 60%; new version 85%), which may it give it advantage over SAP and FDT. An alternative explanation may be the detection mechanism of vernier motion displacement.

1.8.1.2 RANDOM DOT KINETOGRAMS (RDK)

RDKs are comprised of computer-generated displays of dots. The illusion of movement is created by selective displacement of the dots from one frame to the next. The advantage of RDKs over MDT are that they are uncontaminated by form and positional cues (Nakayama and Tyler 1981). RDKs represent global processing (Baker and Braddick 1982), compared to the local processing of MDT. This would infer that RDKs are more suited to the detection of diffuse defects and MDT to focal lesions.

When the dots of RDK undergo a constant displacement in a uniform direction at short inter-stimulus intervals of < 100 msec a "short range of apparent motion" is perceived with motion detection occurring between two thresholds (Braddick 1974).

(i) D_{min} the lower limit of apparent motion describing the minimum dot displacement that can be detected [figure 1-10 (i)].

(ii) D_{max} the upper limit of apparent motion describing the maximum displacement for the perception of motion [figure 1-10 (ii)].

The limitation of spatial range between D_{min} and D_{max} enables the tracking of objects over time when viewing a screen (Morgan 1992). D_{max} is found to

vary with spatial frequency (Boulton and Baker 1991) and field size (Baker and Braddick 1982). It has been suggested that the variation in D_{max} with field size is explained by the recruitment of larger, more eccentric neural units (Baker and Braddick 1982; Baker and Braddick 1985). An alternative view is that D_{max} is determined by the spacing of the elements within a pattern and is dependant upon spatial filtering, which precedes motion detection (Morgan 1992; Morgan et al. 1997). When displacements are increased beyond D_{max} the illusion of two unrelated patterns is perceived (Bullimore et al. 1993).

In addition to D_{max} and D_{min}, coherence thresholds may be measured, where a selected percentage of the dots move in a uniform direction against a background of embedded noise (figure 1-10 (iii) where the coherence is 50%). The noise may be at a constant speed in a random direction (Bullimore et al. 1993) or entirely random.

RDK thresholds are generally measured by forced choice of one of the four cardinal positions (up; down; right; left). Bullimore investigated central motion and found D_{min} discriminated glaucomatous from control eyes, but that D_{max} and coherence thresholds failed to do so. This was a high contrast test where the stimulus dots where 100 cd/m^2 and the background 0.5 cd/m^2.

Figure 1-10. Three thresholds of measurement using Random Dot Kinetograms (from Bullimore et al., 1993).

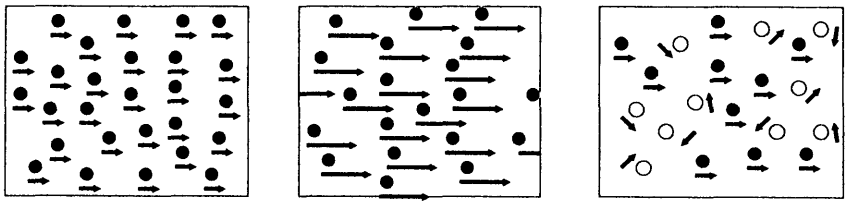

(i) d_{min} (ii) d_{max} (iii) coherence

Wall devised a "Random Dot Motion Perimetry" test for glaucoma where 44 locations were tested, corresponding to the Humphrey 24-2 test locations, but with the far nasal and top and bottom rows eliminated. Coherence was held constant at 50% and threshold gauged as the minimum size of circular RDK (0.25 - 21 degrees) where motion could be perceived, thereby giving a measure of RDK summation properties. Accuracy of response was measured by computer touch pen. Random Dot stimuli size threshold was increased in OHT and glaucoma compared with control, with an accompanying increase in spatial localization error in glaucoma. The disadvantage of this methodology is that the circular stimulus may introduce pattern discrimination (Wall and Ketoff 1995; Wall et al. 1997).

"Motion Automated Perimetry" (MAP) is a RDK based test designed by Bosworth, Sample and Weinreb (Bosworth et al. 1997a). It is a modified version of an earlier RDK test designed by Silverman, which showed deficits of motion detection in POAG and OHT (Silverman et al. 1990). Circular RDKs, each subtending 7.3 degrees of visual angle and consisting of 20 dots, are used to measure coherence ranging between 0% - 100% at 14 retinal locations (figure 1-11). The dot luminance is 59 cd/m^2 against a grey background of 26 cd/m^2, giving a moderately low contrast of 38%. The threshold is measured by staircase analysis, with a starting point of 80% coherence and a step size of 20% coherence. There is a halving of step size with each staircase reversal to a minimum of 5% coherence. Each pixel subtends 7.4 min arc at the test distance of 16.5 cm.

The stimulus parameters limit the smallest area of the field that can be sampled, giving it a lower spatial resolution to detect focal defects than the MDT. It is time consuming (~ 15 minutes) and shows high test variability (Sample et al. 2000b). Patients often find the forced-choice of methodology demoralizing in that they may be forced to respond for a long periods when in fact they have seen nothing. There is no RDK test commercially available for routine clinical testing.

Figure 1-11. Distribution of test locations used for Motion Automated Perimetry (from Sample et al., 2000a).

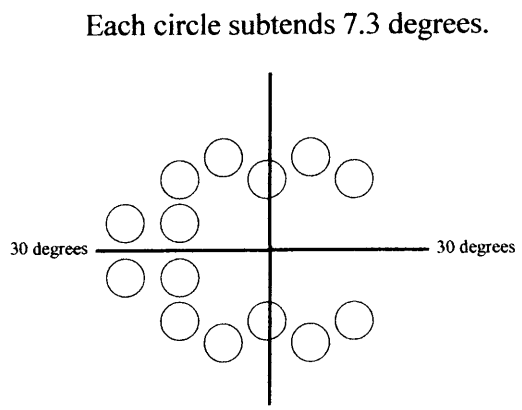

1.8.1.3 FREQUENCY DOUBLING TEST (FDT)

The Frequency Doubling illusion describes a phenomenon where a low spatial frequency sinusoidal grating (≤ one cycle per degree), undergoing high temporal frequency counterphase flicker (≥ 15Hz), appears to double in spatial frequency i.e. the stimulus appears to have twice as many light and dark bars as are actually present (Kelly 1966). It has been suggested that the frequency doubling illusion is specifically directed to the non-linear Mγ cells comprising 15-25% of a sub-population of the M pathway (Maddess and Henry 1992; Johnson and Samuels 1997). It is thought the Mγ in primates are vestigial from the non-linear Y cells found in cats (Enroth-Cugell and Robson 1966).

Electrophysiology experiments indicate that only 6% of cells are non-linear in primates at the LGN (Derrington and Lennie 1984). A recent study by White found no evidence of a non-linear subset of ganglion cells. He suggests that the frequency doubling illusion is a cortical phenomenon due to loss of temporal phase discrimination, with a doubling across time not space (White et al. 2002).

FDT [also referred to as FDP: Frequency Doubling Perimetry] is a contrast sensitivity test using a grey and white grating stimulus to create the frequency doubled illusion (Johnson and Samuels 1997). It is commercially available and widely used for glaucoma screening. FDT uses a low frequency grating stimulus presented at high counterphase flicker (25Hz). The grating consists of an alternate white and grey five-line stimulus presented on a white background (luminance 100 cd/m^2).

There is resemblance of FDT to MDT in the way the illusions of frequency doubling and movement are created (figure 1-12). Both are line stimuli that are displaced over time between computer frames. The MDT is a single line white stimulus presented on a grey background and programmed to present over a small range of displacement (0-30 min arc). The frequency doubling illusion is created by a 2-degree displacement of the vertical grey lines, alternating from a three-line to two-line grey stimulus on a white background. The inter-stimulus duration of FDT (25 Hz) is less than MDT (5 Hz).

The original FDT (FDT-1) stimulus has low spatial resolution compared to the MDT. The visual field is covered by 17 FDT grating stimuli (four per quadrant and one central), with the peripheral stimuli each subtending 10 x 10 degrees. The four central stimuli are cut out to accommodate a central circular stimulus of 5 degrees (figure 1-13). The peripheral gratings subtend 0.25 cycles per degree and the central grating 0.5 cycles per degree. By comparison, the original MDT stimulus dimension was 2 degrees x 2 min arc. The stimuli of the new multi-location test remain small and each stimulus size is scaled according to an estimate of non-specific GCD.

A choice of three strategies is offered: a) Suprathreshold C20 (~ 1 minute duration) b) Threshold C20 (~ 4 minute duration). c) Threshold N30, which is as C20 but includes two additional nasal locations which extend out to -30 degrees. The fast test times are achieved by using a modified binary search (MOBS) strategy.

Figure 1-12. Comparison of Frequency Doubling and MDT stimulus presentation.

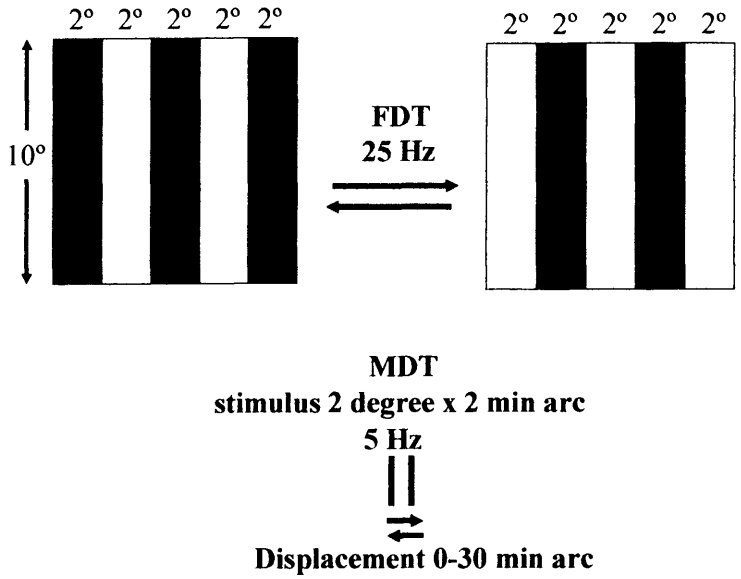

Figure 1-13. Distribution of FDT-1 test locations (from FDT manual).

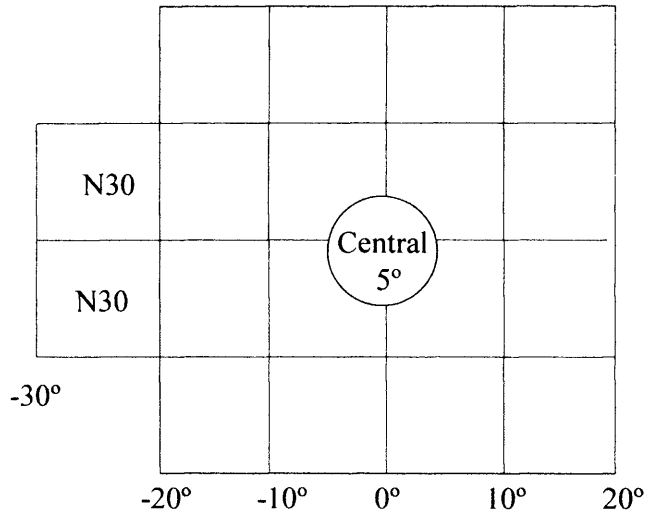

Strategy C20: out to 20 degrees

Strategy N30: two additional nasal locations extending to -30^0

FDT-1 has been shown to predict future scotoma development by SAP (Kogure S, et al., *IOVS* 2004; 45: ARVO E-Abstract 2129) and has been shown to offer increased sensitivity to detect glaucoma when compared to SAP (Sample et al. 2000a).

A major disadvantage of the FDT compared to MDT is its poor resistance to media blur, making it vulnerable to false positive referral from cataract (Membrey et al. 1998; Membrey and Fitzke 2000). This is likely because FDT is a test of contrast sensitivity. In the normal eye, the contrast at FDT threshold is < 10% (personal communication with Paul Artes). The new MDT has a high contrast of 85% and it is therefore anticipated that it will be less vulnerable to the effects of media opacity. Test resistance to cataract is of particular importance because of the age (> 40 years) of the population being screened for glaucoma. A modified version of FDP, "Quadravision," was developed using a 24-2 Humphrey format and offering higher spatial resolution (Johnson et al. 1999). However, this system required the simultaneous use of four 21-inch monitors and as such is not a practical clinical tool.

A new version, "The Matrix" (FDT-2) (Johnson et al. 1999) has recently been released (Johnson CA, et al. *IOVS* 2004; 45: ARVO E-Abstract 3470). It has 54 locations corresponding to those of the Humphrey 24-2 program. Each FDT stimulus measures 5 degrees x 5 degrees with higher spatial resolution of 0.5 cycles per degree. There are 4 presentations per location, each ~ 700 msec duration, giving a test time ~ 6 minutes. The presentations are selected using a test algorithm named "Zest" (zippy estimation of sequential testing) which was developed using Bayesian methods. It is based on the analysis of previous FDT data and models "maximum likely-hood estimation" (Turpin et al. 2002b; Turpin et al. 2002a). The subject response determines the step of the subsequent presentation: if "seen" the following presentation will be at a reduced contrast and if "unseen" at an increased contrast.

The Matrix has been found to show more uniform test re-test variability with eccentricity than SAP (Artes et al. 2005). This may be explained by the 5 x 5 degree stimulus covering a large number of receptive fields, resulting in greater cortical

pooling and reproducibility. Noise from uncorrected peripheral refractive error may be another contributing factor (Ferree et al. 1931; Millodot 1981).

FDT has been reported to be resistant to the effect of central defocus up between + 1.00 and + 6.00 DSph (Anderson and Johnson 2003). There are no publications to inform on the effect of peripheral refractive blur.

An advantage of FDT over the current MDT is that it has an in-built fixation monitor, which is used for assessing patient reliability in maintaining fixation. However, a disadvantage of this apparatus is its weight (18 kg), which means it is not a practical tool for mobile screening purposes.

Elevated FDT thresholds have also been demonstrated for foveal vision in glaucoma. The FDT was modified to test vernier acuity and used a display of two sinusoidal gratings of 1 cyc/deg, which were vertically separated by 10 min arc. The gratings were counterphased at 25 Hz and presented at high contrast (90%). The spatial phase of the upper grating was randomly selected. The lower grating was horizontally displaced from the upper grating, giving a maximum displacement of 0.5 cyc/deg. The task was to determine by forced choice whether the lower grating was displaced to the left or right, relative to the upper grating (McKendrick et al. 2002).

1.8.1.4 FLICKER PERIMETRY

Flicker perimetry gives a measure of high temporal frequency and as such provides a selective indication of M function. The threshold is traditionally measured by Critical Flicker Fusion (CFF), which represents the maximum rate at which flicker can be resolved, above which the stimulus appears steady (Cronly-Dillon 1991).

Early work by Delange (using a 2-degree patch) and Kelly (using a 65-degree patch) showed that flicker shows a specific temporal contrast sensitivity (TCS)

function. The peak of frequency response is shifted to higher frequency with an increase of flickering field size (Delange 1958; Kelly 1961; Cronly-Dillon 1991).

Various versions of automated flicker perimetry have been developed, measuring threshold either as a function of CFF or TCS, but none commercialized (Tyler 1981; Feghali et al. 1991; Lachenmayr et al. 1991; Austin et al. 1994; Horn et al. 1997; Yoshiyama and Johnson 1997; Gonzalez de la Rosa et al. 1998; Junemann et al. 2000; Langley-Hawthorne 2003). Comparison of CFF and temporal modulation perimetry (TMP), measuring TCS, suggests that TMP is more effective in separating normal subjects from glaucomatous and is therefore the method of choice (Yoshiyama and Johnson 1997).

A major advantage of flicker perimetry is that it is robust to the effects of optical and media blur (Lachenmayr and Gleissner 1992; Junemann et al. 2000). Disadvantages include flicker adaptation and subject confusion in response if the time-average luminance of the flickering stimulus differs from the background. If this is the case the patient may respond to the flicker, luminance step or both (Lachenmayr 1994).

The sensitivity to detect glaucoma is frequency dependant: Tyler found temporal modulation sensitivity at high frequency flicker (30 – 40 Hz) for a 5 degree flickering field to be a predictor of future field loss in suspect glaucoma in both central and peripheral (20 degree) fields. By contrast, low frequency sensitivity and CFF were often unaffected (Tyler 1981). Robson found a relationship between spatial and temporal properties whereby the higher the temporal frequency the lower the spatial acuity and vice versa (Robson 1966).

It is of interest that Feghali reported improved separation of glaucomatous from control eyes when using an increased size of stimulus for a perimetric flicker test operating at 25 Hz (Feghali et al. 1991).

Casson and Johnson developed a test of TMP that tested three temporal frequencies (2, 8, and 16 Hz) at 45 test locations in the 27-degree central field. Early loss in glaucoma was most reliably detected by the two higher frequencies of 8 and 16 Hz. The test consisted of 700-800 presentations with a duration in the region of 25 minutes (Casson and Johnson 1993). An age-related loss, most pronounced at 16 Hz, was found in the peripheral field (Casson et al. 1993a).

1.8.2 SHORT WAVE AUTOMATED PERIMETRY DIRECTED TO KONICELLULAR PATHWAY

Short wave automated perimetry (SWAP) is directed to the small population of "blue-on" bistratified cells of the konicellular pathway which comprise between 1% and 7% of the total population of retinal ganglion cells, depending on eccentricity (Dacey and Lee 1994). Traditionally, "blue-on" cells are thought to be inhibited by the red and green "off" bipolars, but recent psychophysical evidence supports the existence of a blue "off" pathway (Vassilev et al. 2003).

SWAP has been found to be sensitive for the early detection of glaucoma (Sample and Weinreb 1992; Johnson et al. 1993; Johnson et al. 2003). The advantage of SWAP is that it can be tested on an adapted standard perimeter. A bright yellow background is used in order to adapt out the long and medium wave-length pathways (Anderson 2005). Optimum test parameters, recommended by Sample and Johnson, are a 440-nm Goldmann size V (1.8 degrees) stimulus presented at 200 msec duration on a bright yellow background of 100 cd/mm^2 (Sample et al. 1996).

Disadvantages include poor specificity in the presence of cataract (Moss et al. 1995; Kim et al. 2001). SWAP has higher re-test variability than SAP (Kwon et al. 1998) and a longer test duration than FDT (Delgado et al. 2002). A limitation of SWAP is the relatively small dynamic range in which the blue wave length operates in isolation, which is estimated in the region of ~ 35-15 db (Felius et al. 1995; Sample et

al. 2000b). A bright stimulus (< 15dB) may stimulate the long and medium wave-length cones / P pathway.

Elevated blue-on-yellow thresholds also have been demonstrated for foveal vision in glaucoma. Two blue dots of 24 min arc were presented with a vertical separation of 15 min arc between the dots. The location of the upper dot was constant and the task was to determine by forced choice whether the lower dot was displaced to the right or left of the upper dot (McKendrick et al. 2002).

1.8.4 NON-SPECIFIC PSYCHOPHYSICAL TESTS

1.8.4.1 HIGH-PASS RESOLUTION PERIMETRY (HPRP)

High-pass resolution perimetry (HPRP) is a computer driven test that has been shown to offer improved sensitivity to detect glaucoma compared to SAP (Sample et al. 1992; Martinez et al. 1995; Chauhan et al. 1999). The stimulus is high spatial frequency filtered, ring-shaped test target (figure 1-14) which would suggest specific targeting of the P pathway. The mean luminance of the two rings of the stimulus and its inner core [(15 + 25)/2 cd/m^2] is calculated to give a space-averaged luminance at equi-luminance with the background (20 cd/m^2), (Wall et al. 2004).

The Michelson contrast [contrast = % (L max – L min)/ (L max + L min)] of the rings of the stimulus (luminance 15 cd/m^2) and the test background (luminance 20 cd/m^2) is low (14%), therefore favouring M contribution (figure 1-14).

50 locations are tested over a 30 degree field with short test duration ~ 6 minutes. Threshold is recorded at the "vanishing point of the optotype," which is determined by the smallest detectable size of test stimulus. An increase in ring size

at threshold is found in the periphery, which reflects the physiological reduction of retinal GCD. HPRP therefore reflects underlying ganglion cell summation properties, [in a similar way to the RDK of Wall (Wall and Ketoff 1995; Wall et al. 1997)], with larger rings required at threshold in the presence of glaucoma.

A large variation in HPRP results between test centers has recently been reported (Wall et al. 2004).

Figure 1-14 Diagrammatic Representation of the High Pass Resolution Stimulus.

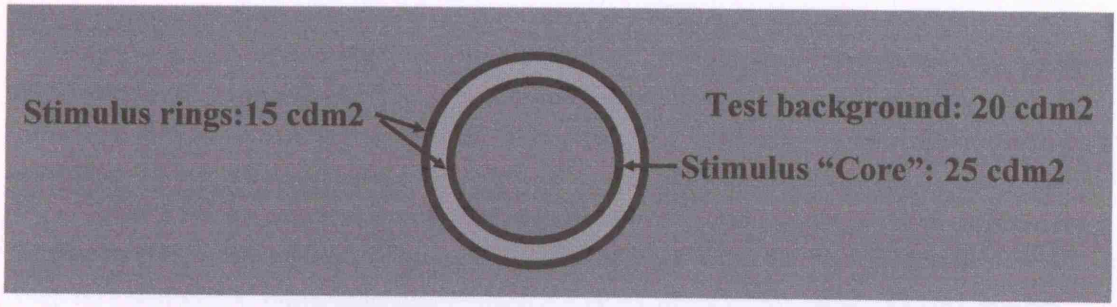

1.8.4.2 TUMBLING E'S

Anderson suggests that HPRP is inappropriately named a test of resolution, and would be more correctly termed a test of detection (Anderson and Ennis 1999). Detection may be defined as the highest spatial frequency for which luminance gratings can be discriminated from a uniform field, whereby resolution describes the correct identification of a spatial pattern.

Threshold for detection and resolution are very similar in foveal vision, where acuity is limited by the optics of the eye. In the retinal periphery acuity is limited by the GCD and resolution thresholds are consequently elevated relative to detection thresholds (Anderson and Ennis 1999). Peripheral resolution thresholds therefore reflect ganglion cell sampling. On this basis, Anderson suggests that a test of peripheral retinal resolution would give a more sensitive mechanism of determining ganglion cell loss in glaucoma than a test of peripheral retinal detection (Anderson and Ennis 1999).

The Bergmann-Helmholz rule of sampling states that for two points to be discriminated, at least one relatively unstimulated photoreceptor must lie between two relatively stimulated photoreceptors (figure 1-15), (Thibos 1997). Thibos hypothesizes that where under-sampling occurs, erroneous peripheral resolution thresholds may be achieved by "alias sampling" of ganglion cells (figure 1-16). This may be a cortical adaptation achieved by "in-filling" (Thibos et al. 1987a; Thibos et al. 1987b; Thibos 1998).

Tumbling E's offer a combined perimetric test of detection by contrast sensitivity and of resolution by discrimination of letter orientation (Anderson and Ennis 1999), (figure 1-17). A test has been designed with 16 locations (figure 1-18).

Figure 1-15. Diagrammatic illustration of neural sampling of the retinal image (from Thibos 1997).

Upper diagram shows location of three rows of neural receptive fields relative to the image of a sinusoidal grating. Top row, over sampled; middle row, critically sampled; bottom row, under sampled. Lower diagram shows strength of response of each neuron (bar graph). Interpolation of neural responses (dotted curves) faithfully reconstructs the original image in the top two rows, but misrepresents the grating's frequency in the bottom row

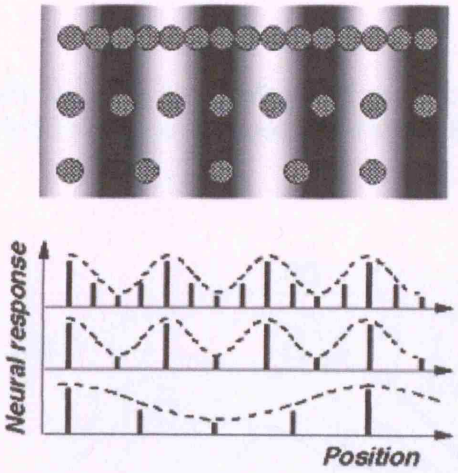

Figure 1-16. Diagrammatic illustration of aliasing through neural under-sampling (from Thibos 1997).

Under-sampling of a two-dimensional grating misrepresents orientation and spatial frequency. Strength of neural response is coded by the luminance of the circles at each sample point in the lower diagram. Dashed lines interpolate between neurons responding maximally, thus indicating the orientation and frequency of the aliased pattern.

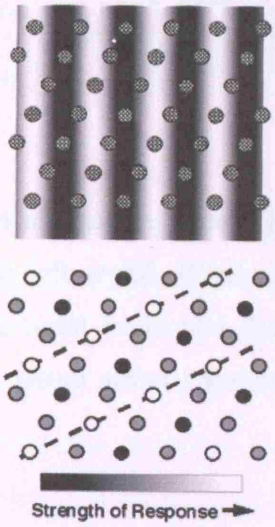

Figure 1-17. Estimation of peripheral resolution acuity using Tumbling E's 25 degrees eccentricity (from Ennis et al., 1999).

Numerals in black refer to c/deg. Numerals in red give the Snellens equivalent and those in brackets give the min arc subtended (refer to the conversion table, appendix table 14-1).

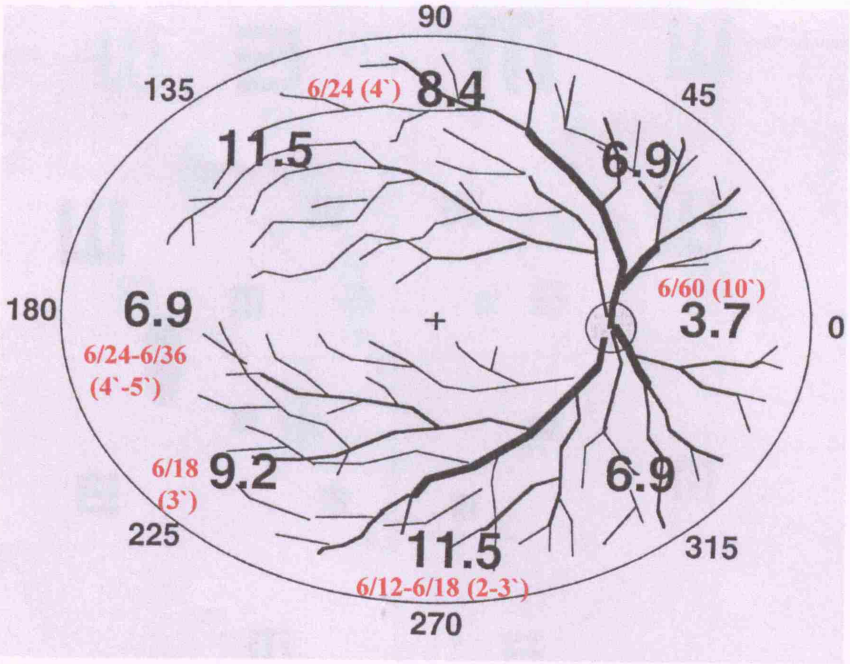

The Tumbling E task is 4-alternative forced choice discrimination of letter E orientation (horizontal; vertical; left; right), (Ennis et al. 1999). Greater powers of resolution are found along the nasal horizontal meridian in accordance with the relatively high GCD along the visual streak (Anderson et al. 1992). This is not a commercially available test.

Figure 1-18. Distribution of Retinal Locations for Tumbling E test (from Ennis et al., 1999).

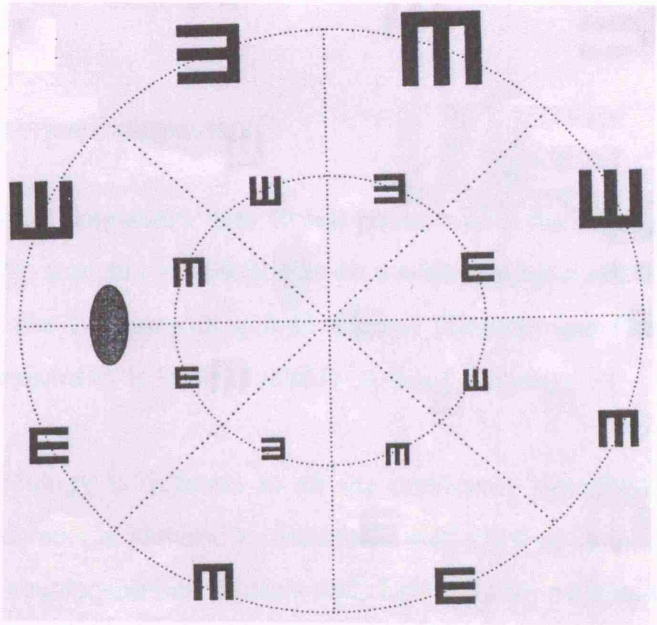

1.8.4.3 PATTERN DISCRIMINATION PERIMETRY

Pattern discrimination perimetry (PDP) consists of 28 locations positioned over the central 30-degree field. The subject is required to detect a static black and white checkerboard against a background of black and white dots that randomly reverse over time. The percentage of pixels used to form the stimulus is varied and threshold determined as the minimum percentage coherence required to perceive the pattern.

Drum hypotheses that groups of ganglion cells are required for the perception of pattern discrimination as opposed to single ganglion cells for SAP and that PDP will be therefore more sensitive to early glaucomatous loss (Drum et al. 1988; Drum and Bissett 1991). It is probable that both SAP and PDP each invoke mixed responses from both M and P pathways. The test time is long (14-18 minutes per eye). PDP is reported to show a poor correlation with SAP (Chauhan et al. 1993a) and to be less effective than SAP in monitoring progression (Ansari et al. 2000).

1.8.4.4 MULTIFIXATION CAMPIMETRY

Multifixation Campimetry uses 42 test points within the 24 degree central field (figure 1-19a). The stimulus is a black spot on a white background. It is the same size as a Goldmann size III, subtending 0.43 degrees (Damato and Groenewald 2003). Multifixation Campimetry is freely available on-line (Damato).

The methodology is different to all the previously described psychophysical tests in that the subject is required to constantly shift fixation onto each consecutive stimulus. This is counter-intuitive to most clinicians and also patients who are familiar with conventional perimetry.

The Multifixation Campimetry task is to place the computer cursor over the stimulus when it is seen and simultaneously to click on the computer mouse.

Weaknesses include the instructions, which are particularly confusing for the patient (figure 1-19b). There is no allowance for difference in monitor screen size and the test has been released prior to validation.

Figure 1-19. On-line Multifixation Campimetry (from Damato web site: http://wwwtestvisionorg/.).

(a) Distribution of stimuli

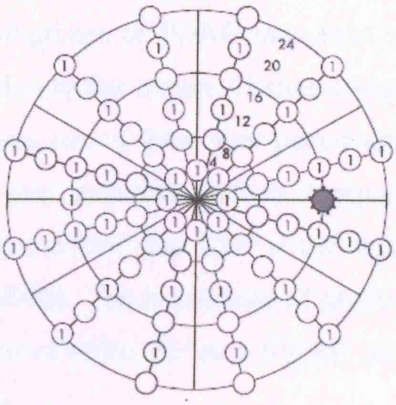

(b) Instructions

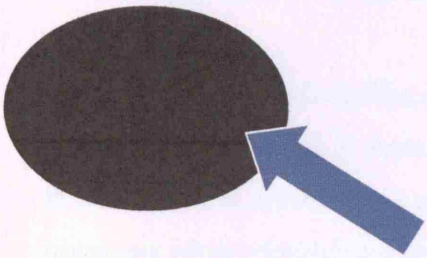

"IF YOU SEE A BLACK SPOT MOVE THE CURSOR OVER THAT POI
WHEN YOU PLACE THE CURSOR OVER THE AREA A SMILEY FAC
WILL APPEAR. IF THE SCREEN GOES BLANK LOOK AROUND UNT
YOU SEE A STATEMENT SAYING YOU HAVE MISSED A SPOT!
CLICK ON BLACK SPOT TO CONTINUE"

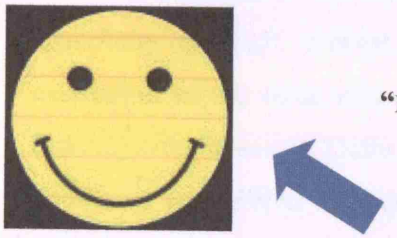

"MOVE YOUR CURSOR OVER THE SMILEY FACE AND CLICK ON IT"

1.8.3 COMPARISON BETWEEN TESTS DIRECTED TO DIFFERENT GANGLION CELL FUNCTION

Different tests directed to selective pathways may yield opposing results for different patients, and this has been interpreted that different mechanisms may contribute to POAG (Ruben et al. 1994; Sample et al. 1997; Sample et al. 2000b). This infers that different sub-groups of POAG may exist which are yet to be identified. However, in contradiction to this notion, Casson compared TMP, SAP and SWAP in OHT and early glaucoma over a three year period and found that TMP and SWAP produced similar or more extensive defects compared to SAP. Maximal bundle overlap occurred between SWAP and TMP at the higher frequencies tested of 8 and 16Hz (Casson et al. 1993b). The hypothesis of preferential pathway damage would predict different patterns of defect between SWAP, mediated by the K pathway, and TMP, by the M Pathway.

The theory of preferential pathway damage is also challenged by Martin who found similarity of HPRP and FDP results and concluded that either P and M cell populations are similarly affected by glaucomatous damage or that both methods measure activity in the same cell populations (Martin et al. 2003).

Many published studies comparing psychophysical tests are flawed because the diagnosis of glaucoma is made on the basis of one of the psychophysical tests under evaluation. It is preferable to use structural evidence as the benchmark for glaucoma diagnosis when comparing tests of visual function and vice versa.

For example, in the best study of its kind, Sample compared the sensitivity and specificity of SAP, SWAP, FDT and MAP, with glaucoma defined by photo evaluation of the optic disc and RNFL. 136 eyes (71 glaucoma; 37 OHT and 28 control) were assessed. Defects were detected by SAP in 46% of patients with GON, compared with SWAP (61%), FDT-1 (70%) and MAP (52%). In OHT figures were 5%, 22%, 46% and 30% respectively. It was concluded that improved sensitivity to diagnose early glaucoma might be gained by combining SAP with at least one specific

visual function tests. However, this was with the caveat of slight loss of specificity (Sample et al. 2000b).

1.9 RATIONAL FOR FURTHER DEVELOPMENT OF MDT

The early MDT work gave evidence that the single line BBC test offers a more sensitive method for the detection of early glaucoma than SAP. The BBC system is now out of date and equivalent MDT results have been shown using a modern computer Windows format (Viswanathan et al. 2000). This opens the opportunity to develop a new MDT test that would have wide global accessibility and be economically competitive to purchase.

The BBC MDT has been shown to offer greater resistance to media blur than FDT and SAP, showing improved test specificity to cataract (Membrey et al. 1998; Membrey and Fitzke 2000). This is important to avoid false positive diagnoses of glaucoma. With the increased rate of visual field testing in the primary care setting (optometry practices) large numbers of false positive "glaucoma" cases are referred to hospital eye clinics with a consequent rise in the economic burden to the health service.

The major limitation of MDT, in its original form, is that it tests only a single location. Baez followed the normal fellow eye of 51 patients with confirmed NTG over a three-year period. Elevation of the MDT threshold was found to be a predictor of future development of field loss in locations close to the MDT test site: an initially abnormal MDT threshold showed a sensitivity of 73% and a specificity of 90% in predicting field deterioration within the cluster of four Humphrey locations closest to the MDT test location at 15,9 above the blind spot. Sensitivity was lower (40%) in predicting progression at locations distant from the supero-temporal field, although specificity remained high (Baez et al. 1995).

It is therefore hypothesized that improved sensitivity will be achieved if the MDT is expanded to a multi-location format and targeted to specific areas of the visual field which are known to be subject to damage in early glaucoma. This will enable simultaneous determination of diffuse and focal loss.

A limitation of using a standard computer as a screening tool is that there is no means for monitoring fixation. Fixation error is monitored as an index of reliability in SAP, together with false positive and false negative responses. Both fixation error and false positive response have been shown to be poor predictors of variability by test-retest assessment. The best predictor of variability is false negative response (Bengtsson 2000; Bengtsson and Heijl 2000).

1.10 AIMS OF PHD

The principal objective set out at the start of this PhD was to create a novel multi-location MDT test for the early diagnosis of glaucoma. The aim was to achieve optimum test sensitivity and specificity through detailed exploration of the psychophysical properties of the MDT stimulus and incorporation of recommendations from earlier research.

It was planned for the test initially to use the location format of the Humphrey 24-2 test, to enable direct comparison with SAP. It was decided that all stimuli should be presented concurrently to avoid the confusion of target onset and target motion (Johnson et al. 1995). In addition, it was decided that line stimuli should be orientated with the RNFL (Westcott et al. 1996) and scaled in size according to estimate of GCD (Curcio and Allen 1990), in order to offer maximum sensitivity. The stimulus presentation was adjusted to adopt the time saving measures of shorter duration (200 msec per cycle) and reduced number of oscillations (3 oscillations per presentation) as previously described (Verdon-Roe et al. 2000; Westcott et al. 2000b).

The test was designed with the aim to convey the following attributes in order to comply with the modern requirements of health care economics and evidence based medicine and to satisfy the varying needs identified by epidemiology studies:

1. Improved sensitivity to detect glaucoma
2. Good specificity: distinction between subjects who do/do not have glaucoma
3. Be of short duration to ensure economic use of clinician time and prevent subject fatigue.
4. Be easily understood by both patient and examiner
5. Robust to the effect of learning
6. Robust to refractive error
7. Good reproducibility
8. Competitively priced
9. Portability to enable access to remote global areas (planned future lap-top version)

1.11 SUMMARY OF ACCOMPLISHMENTS OF PHD

1.11.1 DEVELOPMENT OF PROTOTYPE MDT

During the first six months of this PhD a multi-location MDT was created using the principles of the original single line test. The same retinal locations were used as for the 24-2 Humphrey visual field test to enable comparison of thresholds with SAP. The stimuli were orientated with the RNFL (Westcott et al. 1996) and scaled according to estimates of GCD. The first pilot study of the new multi-location MDT suggested that the test is able to identify established glaucoma. MDT defects were found to follow a similar topography to SAP and, in some cases, were found to cover more extensive areas of the visual field.

This pilot study was presented as a poster presentation ARVO, Florida, 2001
(Verdon-Roe GM, et al. *IOVS* 2001; 42: ARVO Abstract 4417).

1.11.2 EXPLORATION OF THE PSYCHOPHYSICAL PROPERTIES OF MDT

During the following two years the psychophysical properties of the MDT stimulus were explored and results applied to the development of the new test. GMVR was the first subject for all experiments undertaken. Results were then validated by assessment of a second subject experienced in psychophysical testing.

1.11.2.1 THE EFFECT OF PERIPHERAL REFRACTIVE BLUR ON MDT THRESHOLDS

MDT testing was shown to be robust to the effects of peripheral blur by cylinders, which produced only small elevation of MDT (< 2 min arc) up to +/- 6.0 DCyl. This is of interest with respect to the use of an orientated line stimulus, and is also of relevance in the context of peripheral astigmatism, which is reported to increase physiologically with eccentricity (Ferree et al. 1931; Millodot 1981).

The effect of peripheral spherical blur on MDT thresholds was quantified for lens strengths up to +/- 6.0/DSph. MDT thresholds were found to be more resistant to the effect of refractive blur than SAP (Anderson et al. 2001). Blurring by lens strengths up to +/- 6.0 DSph produced only small elevations in MDT of less than 5 min arc, with 2 outlying exceptions (< 9 min arc).

An earlier investigation using the BBC MDT format with a larger line length (2 degree x 2 min arc) at a more central location (15,3) suggested only small differences in MDT thresholds between glaucoma suspects [8.7 ± 3.4 (5.0 - 17.6) min arc], glaucoma patients [12.9 ± 5.8 (5.2 - 34.2) min arc] and normal subjects [5.9 ± 1.7 (2.6 - 8.9) min arc]. It is envisaged that separation between groups will be widened using the multi-location format. However, to ensure optimum test sensitivity and specificity, correction of spherical refractive error may be required and this will be kept under review.

The peripheral optical blur study was presented as a poster presentation ARVO 2003
(Verdon-Roe GM, et al. *IOVS* 2003; 44: ARVO E-Abstract 78).

1.11.2.2 THE EFFECT OF CENTRAL REFRACTIVE BLUR ON MDT THRESHOLDS

All central MDT responses were found to be suprathreshold for the emmetropic subject, including the smallest possible stimulus size of 1 pixel x 1 pixel, which subtends only 3 x 3 min arc at a test distance of 30 cm. It was therefore not possible to quantify the MDT response to central blur but only make points of observation. Results suggest that small lines subtending ≤ 14 min arc should be avoided if the test is to be run with refractive error uncorrected. However, use of larger lines may be less sensitive to detect glaucoma. The optimum balance between central line resistance to refractive error and sensitivity to detect glaucoma will be investigated as a post-doctorate study.

1.11.2.3 STUDY OF MDT SUMMATION PROPERTIES

Summation properties of single and multi-line stimuli were investigated to give insight into how MDT thresholds vary with line size, number and separation. Equivalent thresholds were found for equivalent line lengths, whether single or distributed amongst three shorter lines. This novel finding may be used to predict motion displacement thresholds when testing within the target dimensions investigated.

The results were presented at the International Perimetry Society (IPS) meeting June 2002 and accepted for publication in Perimetry Update 2002/3 (Verdon-Roe et al. 2002).

It has been suggested that MDT thresholds are determined by the length of the stimulus line-edge orthogonal to the direction of motion (Foley-Fisher 1973). The hypothesis that it is the stimulus area, rather than the edge-length, that determines the threshold response, was tested by comparing MDT thresholds for constant stimulus area but changing line-edge length. Results supported the hypothesis that the MDT threshold is determined by stimulus area.

The summation studies were extended to investigate the effect of changing line length and luminance. MDT thresholds were recorded at five values of Michelson contrast (25% - 84%) for each of five line lengths (11 - 128 min arc). FOS curves were generated and MDT thresholds and interquartile range (IQR, 75% - 25% seen) determined by probit analysis.

A novel approach was taken whereby the MDT threshold was calculated as a function of stimulus energy (stimulus area * luminance) in order to explore the application of Ricco's law to MDT stimuli. SAP measures DLS and, where the stimulus lies within Ricco's critical area, the product of the area and intensity of the stimulus at threshold is constant (Glezer 1965).

Elevations of MDT thresholds and IQR were demonstrated as line length and contrast were reduced. Log IQR was linearly related to log MDT displacement threshold (slope 1.3). Equivalent MDT thresholds were found for MDT stimuli of equivalent energy, in accordance with Ricco's law.

There was a linear relationship (slope –0.5) between log MDT displacement threshold and log stimulus energy ([stimulus area] * [stimulus luminance – background luminance]).

A new law, the 'threshold-energy-displacement' (TED) law, is proposed to apply to MDT summation properties, giving the relationship $T = K \sqrt{E}$ where T = MDT threshold; K= constant; E = stimulus energy.

The results were considered in the context of MDT as a hyperacuity stimulus. Ideal detector modelling was found a useful platform for considering the range of factors that may contribute to the TED law.

It is anticipated that the linear relationship found with MDT threshold and stimulus energy has the potential to be used as a basis for modelling the MDT

response to neural loss in glaucoma, using the principles described for SAP (Garway-Heath et al. 2000a; Harwerth et al. 2004; Swanson et al. 2004).

The findings were presented as a poster presentation at ARVO, Florida, 2004
(Verdon-Roe GM, et al. *IOVS* 2004; 45: ARVO E-Abstract 2122)
and have been submitted to IOVS (November 2005).

1.11.2.4 STUDY OF MDT RESPONSE TIME

Study of subject response showed a shortening of response time using the new MDT stimulus test parameters when compared with the original BBC. This was deduced to be due to shorter stimulus duration employed by the new test and explained by altered properties of temporal integration. The shortened response time enabled the stimulus timings to be adjusted with consequent reduction in test duration. Modification of the test programming was recommended to record false positive response of < 180 msec as an index of reliability (Woodworth and Schlosberg 1954). It was suggested that, where a false positive response has been made, the stimulus presentation should be repeated at the same displacement (as opposed to erroneously proceeding to a lower displacement down the staircase).

1.11.2.5 STUDY OF THE EFFECT OF ATTENTION ON MDT THRESHOLD

Attention is a cognitive process of selective concentration. Attention may be focused on a single task or divided into multi-tasks (Kastner and Pinsk 2004). The MDT methodology presents all the line stimuli concurrently, with only one line stimulus programmed to be displaced at any one time. It was hypothesized that the stationary lines would act as distracters to the detection of a single moving stimulus, and that the magnitude of the distraction would depend on the number of lines present and their positioning in the visual field. It was found that only small changes of MDT threshold occurred with up to 26 locations present and that clustering the locations

together minimized these differences. Only small changes in MDT thresholds were found using the 6-degree stimulus spacing of the Humphrey format.

1.11.2.6 SELECTION OF MDT LOCATIONS

A novel method of selection of test locations was made by application of the visual field-ONH correspondence map described by Garway-Heath (Garway-Heath et al. 2000b). The test locations were reduced in number and clustered together, with the aim of minimizing the effect of attention and reducing test duration.

1.11.2.7 AMALGAMATION OF STUDY RESULTS

The results gained within the PhD and earlier studies were combined to achieve an operational multi-location MDT.

In conclusion, as a result of this PhD, a novel multi-location MDT has been successfully produced that is ready to be embarked on its first clinical pilot studies.

1.12 POST-DOCTORATE MDT DEVELOPMENT PLAN

Pilot studies have been initiated to follow on from this PhD work. Ethical approval has been given by Moorfields Eye Hospital (reference VERG 1001) to proceed.

Chapter 2

DEVELOPMENT OF PROTOTYPE MULTI-LOCATION MDT

2.1 DEVELOPMENT OF MULTI-LOCATION MDT

2.1.2 SELECTION OF MDT LOCATIONS

A novel multi-location MDT was created using the same retinal locations as the 24-2 Humphrey visual field. Each location was allocated an individual reference number (figure 2-1).

Figure 2-1. Multi-location MDT test locations with allocated stimulus numbers (right eye).

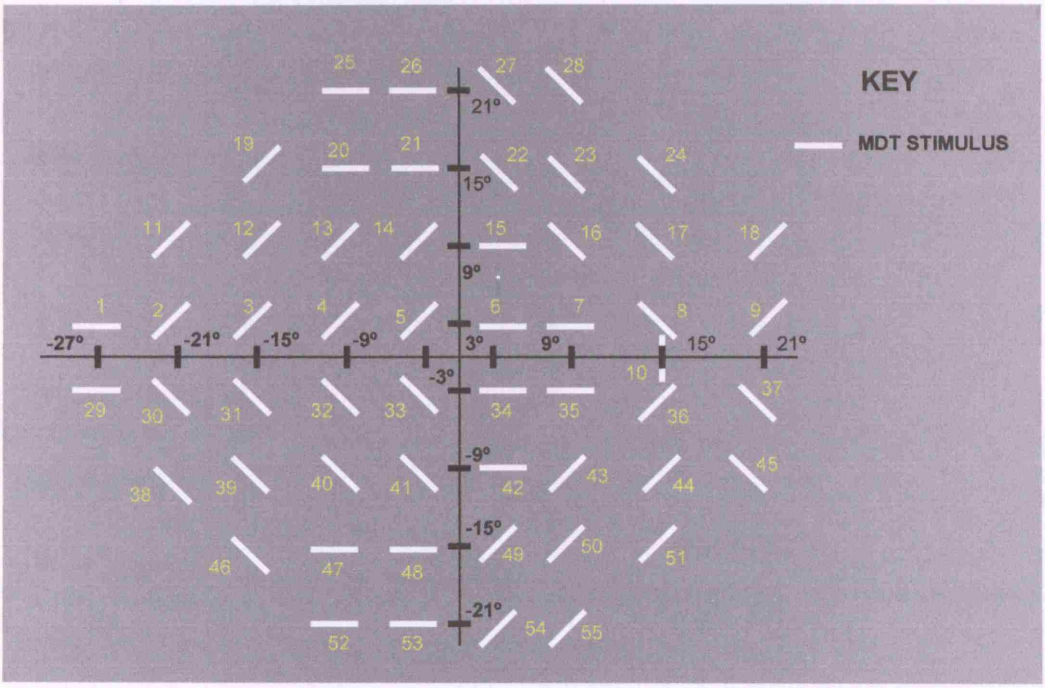

The test was designed to run on a modern PC using a 21-inch monitor. A short test distance of 30cm was adopted in order to achieve a visual field subtending 30 degrees. Stimulus locations were calculated according to the example for location 1 (figure 2-2).

Figure 2-2. Calculation of stimulus position.

Example: stimulus 1 (-27,3)

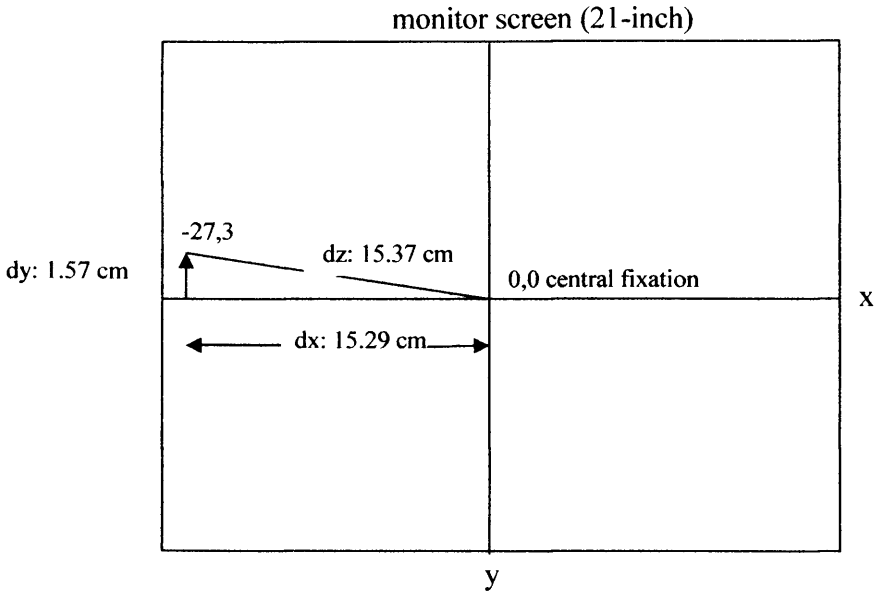

Test distance = 30cm

1 pixel = 0.03 cm

$dx = \frac{\tan 27 \text{ degrees}}{30} = 15.29$ cm (459 pixel) $\quad dy = \frac{\tan 3 \text{ degrees}}{30} = 1.57$ cm (47 pixel)

$dz = \sqrt{(dx^2 + dy^{2)}} = 15.37$ cm

The MDT software was developed by Ananth Viswanathan and designed to be flexible, enabling selective modification of the following test parameters:

1. Stimulus size, orientation and position in the visual field.
   Bitmaps for all stimuli were created individually by GMVR for each location using computer software Paintshop Pro 4.

2. Test contrast
   The luminance of stimulus and background was adjusted by modification of the red, green and blue (rgb) values. The luminance (cd/m^2) was measured using a Minolta Chroma Meter CS-100.

3. Stimulus presentation:
   (i) stimulus duration per cycle
   (ii) number of stimulus oscillations per presentation
   (iii) adaptation period on start of test
   (iv) fixed pre-displacement (period prior to each stimulus presentation)
   (v) random pre-displacement period (to prevent predictable rhythm)
   (vi) listening window (wait period for subject response)
   (vii) post response wait (wait period following stimulus response before subsequent stimulus presentation)

The stimuli were orientated to correspond with the RNFL in order to take advantage of the improved sensitivity described by Westcott (Westcott et al. 1996). The visual field was divided into six zones (figure 2-3), which were calculated according to estimates of total human GCD (Curcio and Allen 1990). The stimulus line lengths were scaled with eccentricity by applying the estimates of total human GCD along horizontal and vertical meridia (Curcio and Allen 1990; Garway-Heath et al. 2000a).

Figure 2-3. MDT zones selected according to estimate of ganglion cell density (right eye).

Numerals refer to allocated MDT stimulus Number

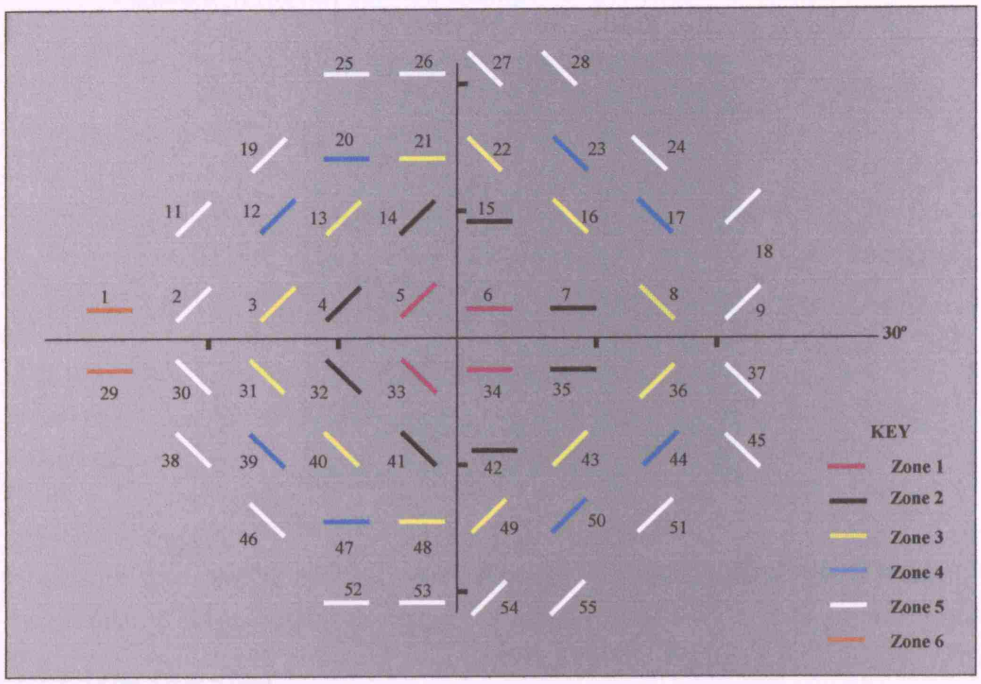

2.2.2 CREATION OF BITMAPS

2.2.2.1 LUMINANCE VALUES

The test background was set to a luminance of 10 cd/m^2 (65 rgb), corresponding to the standard Humphrey. The stimulus was set to the maximum white luminance of the monitor, which measured 112 cd/m^2 (255 rgb). This was calculated to give a test contrast of 85% using the Michelson equation:

Michelson's contrast = % (Lmax –Lmin/Lmax+Lmin) where L =Luminance

2.2.2.2 HORIZONTAL STIMULI

All stimuli were allocated a standard width of 2 pixels and the calculated pixel length was drawn for each individual location using paint shop pro software (figure 2-4).

Figure 2-4. Screen capture example of horizontal stimulus.

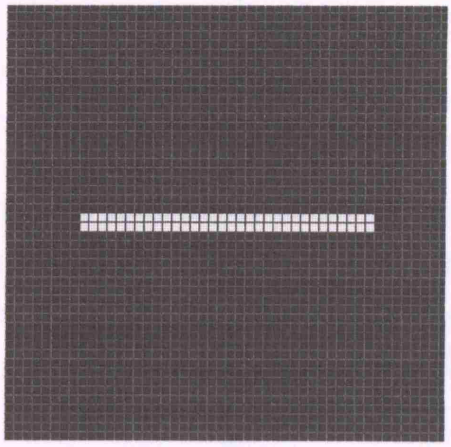

Horizontal line lengths selected varied from 1- 32 pixels (1 pixel = 0.03 mm).

2.2.2.3 OBLIQUE STIMULI

Oblique stimuli are orientated at 45 degrees and require fewer pixels along the length of the stimulus compared to horizontal to achieve equivalent line length. This is illustrated by figure 2-5 and calculations of equivalent lengths for each of the test stimuli are given in table 2-1.

Figure 2-5. Calculation of oblique Axis.

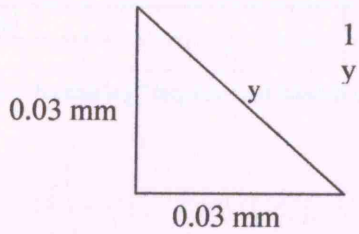

1 pixel = 0.03 mm

$y = \sqrt{(0.03^2 + 0.03^2)} = 0.04$

Table 2-1. Calculation of equivalent oblique length.

Equivalent oblique Length = horizontal length x 0.03 / 0.04

Horizontal Pixels	32	16	8	4	2	1
Oblique Pixels	24	12	6	3	2	1

As oblique stimuli require fewer pixels along the length of the stimulus, compared to horizontal for equivalent length, an adjustment needs to be made in order to achieve equivalent energy of stimuli of the same length. This was accomplished by "feathering" the sides of the oblique stimuli by the addition of light grey 128 rgb pixels to the long edge to give approximately equivalent total stimulus energy (table 2-2 and figure 2-6).

Table 2-2. Calculation of equivalent pixel elements for horizontal and oblique stimuli.

	Pixels@ 255 rgb	Pixels @ 128 rgb	Total Values Pixel x rgb
Horizontal	64	0	16320
Oblique	48	32	16336
Horizontal	32	0	8160
Oblique	24	16	8168
Horizontal	16	0	4080
Oblique	12	8	4084
Horizontal	8	0	2040
Oblique	6	4	2042
*Horizontal	2	0	510
* Oblique	2	0	510
*Horizontal	1	0	255
*Oblique	1	0	255

* No "feathering" required for stimuli of 2x1 and 1x1 pixels

Figure 2-6. Screen capture example of orientated stimulus.

6 x 2 pixel (255 rgb) oblique stimulus, with 4 x 2 pixel (128 rgb) "feathering."

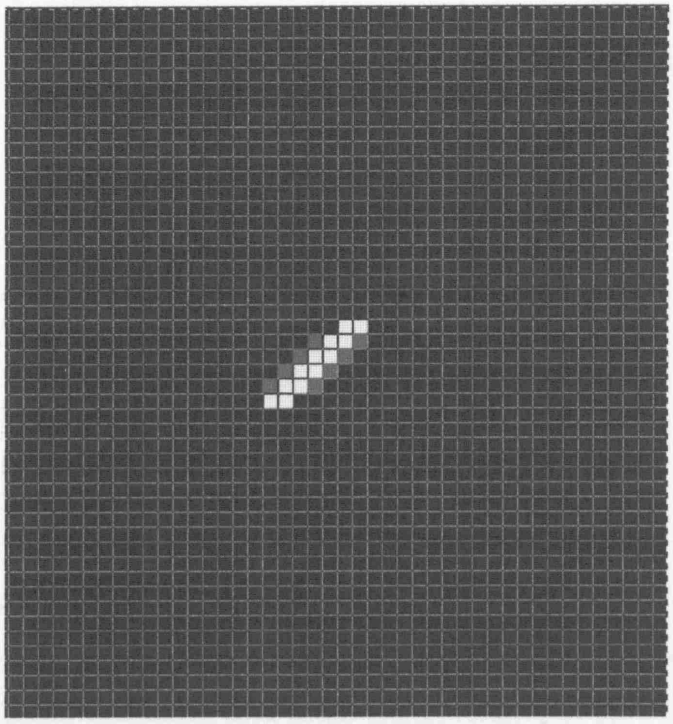

2.2.2.4 LIMITATIONS OF OBLIQUE STIMULI

In order for an oblique stimulus to move perpendicular to its axis the stimulus is required to move one pixel horizontally and one pixel vertically for each presentation (figure 2-7). The minimum displacement that can be achieved for oblique stimuli is therefore elevated when compared to horizontal, as shown by the examples in table 2-3), which were calculated according to figure 2-8.

Figure 2-7. Displacement of orientated stimuli.

The orientated stimulus moves one pixel horizontally (H) and one pixel vertically (V) to achieve apparent movement (M) perpendicular to the axis of the obliquely orientated stimulus.

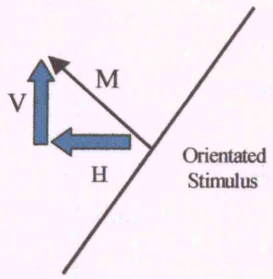

2.2.2.5 LIMITATIONS OF CENTRAL LOCATIONS

Limitations are imposed when testing the central locations due to constraints of the test: a test distance of 30 cm is required in order to gain a field of vision extending to 30 degrees. Central stimuli subtend larger angles relative to the periphery (table 2-3). At three degrees from fixation, a single pixel displacement for a horizontal stimulus subtends 3.42 min arc when using a test distance of 30 cm. This is significantly greater than the unidirectional thresholds (1.5 - 1.9 min arc) reported by Scobey and Johnson for line stimuli of 10 - 110 min arc length, at three degrees eccentricity (Scobey and Johnson 1981). One would predict lower thresholds for the MDT stimulus of this study, which uses 3 oscillations per presentation (Verdon-Roe et al. 2000). One would therefore predict that the central locations will prove suprathreshold in normal subjects, which may prove a barrier to the detection of early central glaucomatous loss.

Figure 2-8. Calculation of stimulus displacement angle.

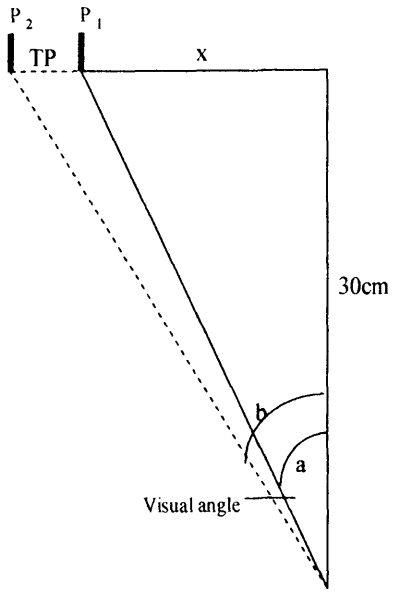

P 1 = starting position

P 2 = new position

TP = true pixel displacement

1 pixel displacement = 0.03 (horizontal stimulus)
0.04 (pixel oblique stimulus)

Starting angle a = tan $\frac{x}{30}$

Final angle b = tan $\frac{(x + TP)}{30}$

Displacement angle = a - b

Table 2-3. Displacement angles for equivalent oblique and horizontal stimuli.

Displacement (Pixels)	Displacement angle (min arc)			
	Central locations (zone 1)		Peripheral locations (zone 5)	
	Oblique	Horizontal	Oblique	Horizontal
	Location 5 (-3,3)	Location 6 (3,3)	Location 52 (9,21)	Location 52 (9,21)
1	4.84	3.42	2.93	4.15
2	9.67	6.84	5.86	8.29
3	14.50	10.26	8.79	12.42
4	19.34	13.67	11.71	16.56
5	24.17	17.09	14.64	20.69

2.2 INVESTIGATIONS

2.2.1 PILOT STUDY 1

AIM

To estimate normal MDT threshold by zone and determine the appropriate length of stimuli.

METHOD

Two pilot strategies were devised as summarized by table 2-4.

All the stimuli were presented concurrently as recommended by Johnson who found that presentation of a single target caused confusion of target onset and target motion resulting in false positive response (Johnson et al. 1995). The line length and range of displacement were estimated by zone by taking into account the estimate of GCD (Curcio and Allen 1990; Garway-Heath et al. 2000a) and the characteristics of a normal MDT FOS curves gained from previous studies (Westcott et al. 1999).The desired normal response was one of a threshold, with the smaller displacements unseen and all larger displacements seen. The blind spot is represented by location 10, zone 3 (refer figure 2-1), where 3 displacements at 1 pixel act as a catch trial.

Each strategy was tested in a random order on three individuals:
1. Psychophysically experienced observer aged 45 years
2. Psychophysically experienced observer aged 39 years
3. Naïve observer aged 23 years

The test was run without refractive correction as previously recommended for the BBC single line computer (Fitzke et al. 1989).

Table 2-4. Pilot study 1: multi-location strategies A and B.

	Zone 1	Zone 2	Zone 3	Zone 4	Zone 5	Zone 6
Strategy A Line length (min arc)	3	7	13	25	47	86
Strategy B Line length (min arc)	14	27	51	50	94	86
Displacement Range (min arc)	3.42-10.26	4.73-14.18	4.52-18.08	4.23-21.09	8.45-25.3	A 8.16- 29.83 B 27.1- 37.92
Number of Locations	4	8	12	8	20	2
Number of presentations	*3 H *2 O	*4 H *3 O	4	4	5	5
Total number of presentations	10	28	48	32	100	10

* H: number presentations for horizontal stimuli * O: number of presentations for oblique stimuli

N.B.$_1$ note limitation of the number of presentations achievable, within the min arc range of displacement set, for the oblique stimuli in zones 1 and 2 when compared with horizontal (refer table 2-3).

N.B.$_2$ the angle subtended by equivalent line length in pixels varies with eccentricity e.g. strategy B where a horizontal line length of 32 pixels subtends 94 min arc within zone 5 but only 86 min arc within zone 6.

RESULTS

Analysis of each location raised the following observations:

Zones 1- 4: inconsistent seen/unseen responses which were most marked for strategy A.

Zone 1: unexpectedly, not suprathreshold for either strategy.

Zone 5 and 6: Some locations were found to be suprathreshold.

Observer 3, in many instances, was found to have more seen responses than observers 1 and 2.

The number of presentations totalled 231 and the test duration was approximately 15 minutes.

The inconsistent, noisy responses found in zones 1-4 possibly indicate that longer line lengths should be used. Unexpectedly, Zone 1 was not suprathreshold. This may be explained by the simultaneous presentation of 55 locations introducing problems of selective visual attention.

It was difficult to interpret the results for the oblique stimuli of zone 1 due to the limitation of two displacements. This could be overcome by increasing the range of displacement beyond 10 min arc (table 2-4).

The suprathreshold results of zones 5 and 6 indicate the need to reduce the first displacement from two to one pixel or, alternatively, to reduce the size of the stimulus.

Naïve observer 3, in many instances, is better than psychophysically experienced observers 1 and 2. This possibly suggests little learning effect or increased MDT threshold with age.

The test duration was 15 minutes. Although longer than required for the final version, it is manageable for both patient and control. It is envisaged that in due course the duration can be shortened by adoption of an efficient test strategy, rationalization of the number of locations tested and adjustment of stimulus timings.

The results of the first pilot strategies gave useful information as to how the test parameters may be altered to reduce noise and improve specificity of the test to determine a normal response.

2.2.2 PILOT STUDY 1

AIM

To assess separation of known glaucoma from aged-matched control by the new multi-location MDT.

METHOD

A test strategy (table 2-5) was developed, based on the format of the 24-2 program of SAP, whilst incorporating the recommendations from the first pilot study, described previously. Figure 2-9 gives a screen capture of the computer image of the MDT multi-location program.

8 POAG patients (mean age 52 years, range 25 - 63 years), with reproducible glaucomatous focal Humphrey defects, were recruited from the Glaucoma Research Unit at Moorfields Eye Hospital and compared against 8 aged matched controls (mean age 47, range 23 - 69 years). The criteria for selection of patient and controls and the setting of the MDT adhered to the protocol described in the standard test procedures.

One eye of each patient and control was tested: the patient eye was selected according to the eye with the earlier focal defect, determined by the Advanced Glaucoma Intervention Study (AGIS) scoring procedure (1994). Control eyes were randomly selected.

DATA ANALYSIS

Motion displacement results were graded 1 - 3 for each location: 1 = suprathreshold (all presentations seen); 2 = threshold response (1 – 2 presentations unseen); 3 = poor response (3 or > presentations missed). Comparison between patient and control was made by zone to assess the efficacy of the line lengths and

Table 2-5. Pilot study 2: multi-location MDT strategy.

	Zone 1	Zone 2	Zone 3	Zone 4 & 5	Zone 6
line length (min arc)	14	27	51	96	86
Displacement (min arc)	3.42-14.50	4.73-14.1	4.52-18.08	4.43-21.09	5.44-24.42
No locations	*2 O *2 H	*4 O *4 H	12	28	2
No presentations	*3 O *4 H	*3 O *4 H	4	5	5
Total number Presentations	14	28	48	132	10

* H: number presentations for horizontal stimuli. O: number of presentations for oblique stimuli.

Figure 2-9. Screen capture: MDT pilot study 2 (right eye).

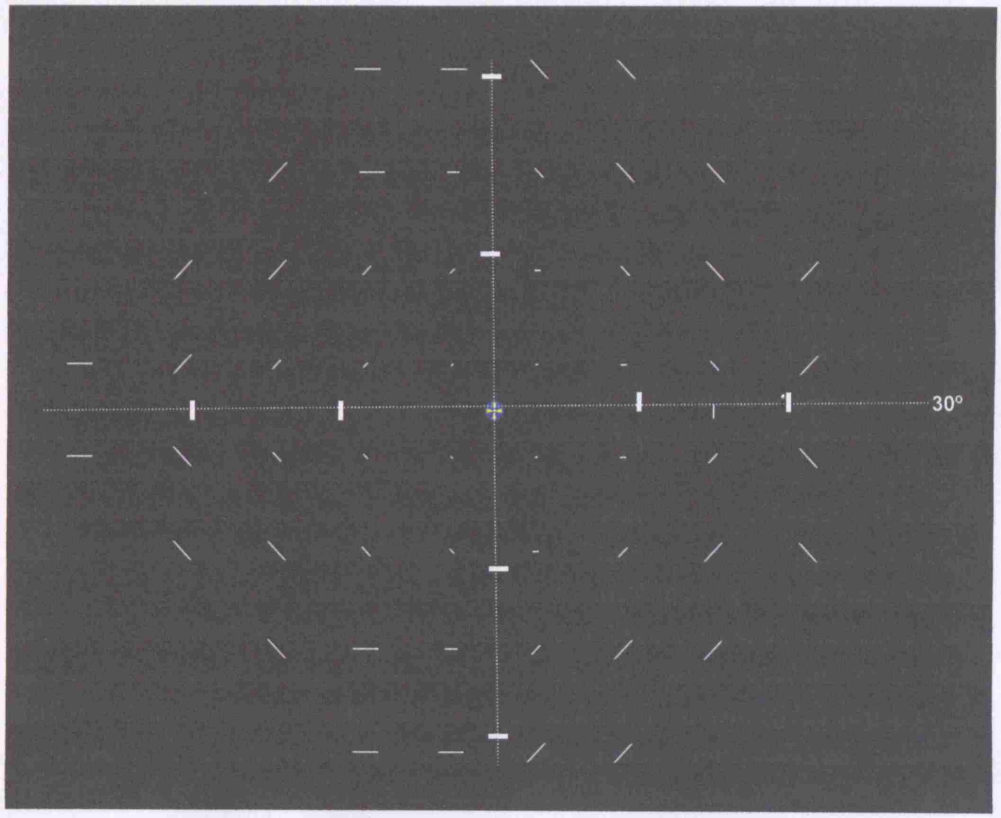

range of displacements between the two groups. Motion results were compared against the total deviation (TD: the difference in decibels between the test results and age-corrected normal) and pattern standard deviation (PSD: measure of standard deviation of points from the age-corrected average, after adjusting the hill of vision for deviation from the average age-adjusted hill) plots for each individual location of the Humphrey Visual Field.

RESULTS

A small percentage of control responses were poor in zones 1 - 5 (figure 2-10). All glaucoma patients were found to have motion loss (category 3) concordant with the Humphrey loss on the TD and PSD plots ($P < 5\%$), when compared by field quadrant. In all glaucoma cases, however, the deficit of motion was more widespread than the loss of Humphrey visual field as illustrated by the patient example (figure 2-11).

The screen capture of the test strategy (figure 2-9) was overlaid on a fundus photograph. Locations 8 and 36 were found to overlap with vessels near the optic disc and will be deleted from further studies. Location 22 was found to produce poor results in both patients and controls. It is possible that this may be also be due to an overlying retinal vessel and requires to be kept under review.

Figure 2-10. Bar Plots illustrating the percentage of subjects categorized within each MDT category and zone.

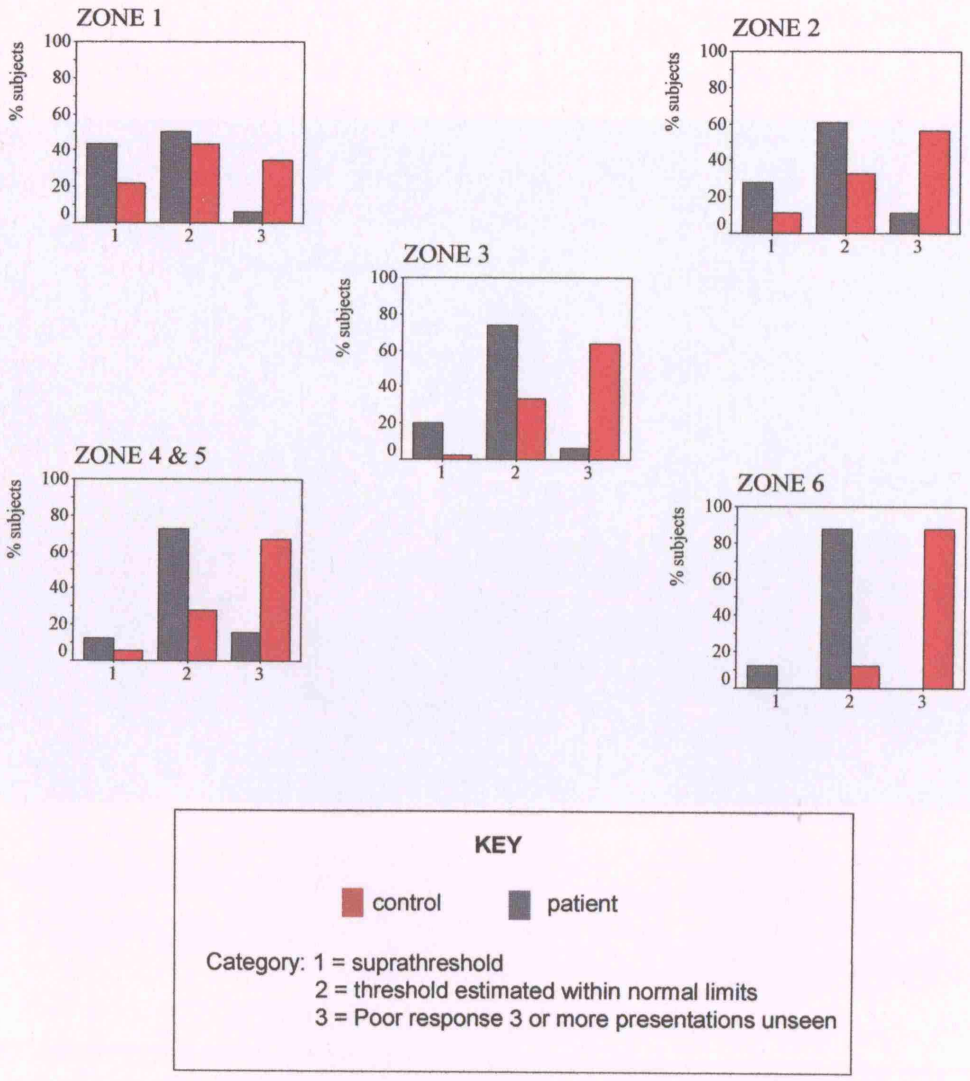

Figure 2-11. Comparison between Humphrey total deviation and pilot MDT.

Patient Example: Left Eye.

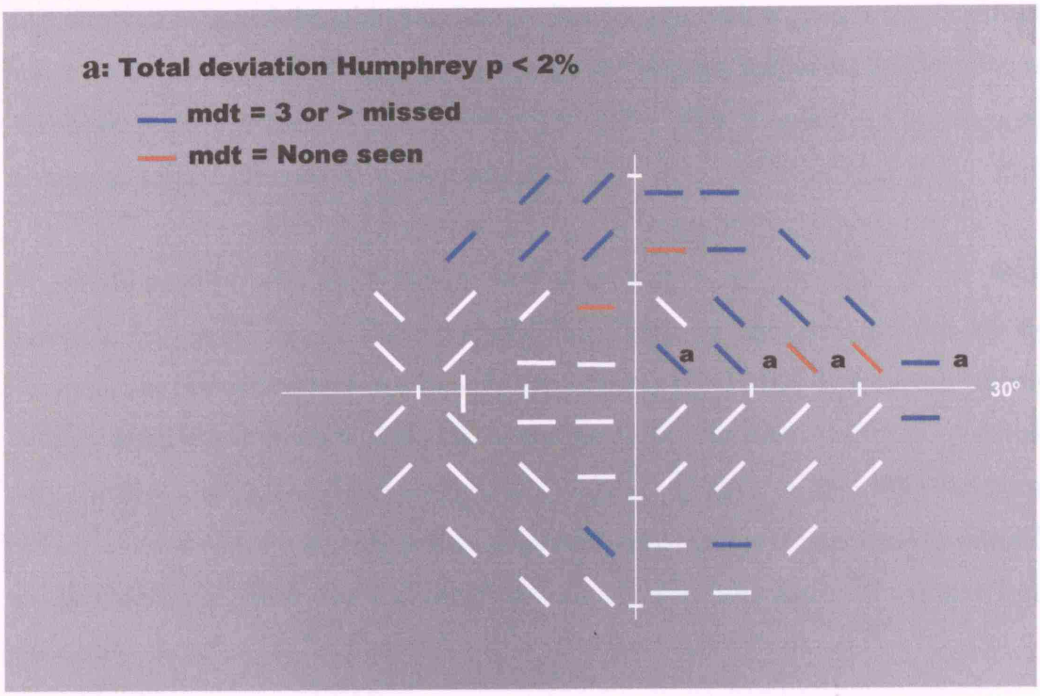

The first study of the new multi-location MDT suggests that the test is able to identify established glaucoma and may have the potential to identify more extensive damage than SAP.

Modification of the MDT is required to improve separation of glaucomatous from control eyes. This may be done by adjustment of either the line length and/or displacement range of the stimulus. Longer line lengths and/or greater displacements may be required in some zones where there are inconsistent responses in control eyes. An understanding of the summation properties of the MDT stimulus is a pre-requisite in order to select optimum stimulus parameters.

It is possible that other factors may contribute to an elevation of the MDT threshold in control eyes. These include the effects of attention induced by the simultaneous presentation of test stimuli. The original BBC MDT was run on patients without refractive correction, but previously the MDT threshold had been evaluated only for the effect of moderate myopia (-5.0 DSph), (Fitzke et al. 1989) Peripheral refractive error varies with eccentricity (Millodot 1981) and it is important to quantify the threshold elevation due to refractive blur if good separation of normal from glaucomatous eyes is to be achieved.

A thresholding strategy is required to estimate MDT thresholds for the multi-location test format. Previously, for the single line BBC test, MDT thresholds were estimated as the 50% seen response, determined by probit analysis, but this is not practical for the multi-location test due to unacceptable test duration. A staircase strategy is recommended as a starting point.

In due course, when a normal database has been established for the final selected strategy, a reduction in test duration may be achieved by analysis of response

time and predictive techniques (e.g. Bayesian methods), (Bengtsson et al. 1997; Bengtsson and Heijl 2003).

SUMMARY

The preliminary test results illustrate that a wider understanding of the psychophysical properties of the MDT stimulus is necessary if optimal test parameters are to be realized. This includes investigation of the following:

(i) Summation properties of the MDT stimulus to enable appropriate selection of stimulus size.

(ii) The effect of central and peripheral optical blur to identify the need for refractive correction and/or adjustment of line dimension.

(iii) The effect of visual attention to identify the effect on MDT thresholds of the simultaneous presentation of 55 locations at spacing of 6 degrees.

The MDT duration is currently unacceptably long (~15 minutes). It may be shortened by a variety of measures including the development of an efficient test strategy (e.g. staircase, Bayesian) adjustment of the stimulus timings and reduction in the number of locations tested (Bengtsson et al. 1997; Bengtsson and Heijl 2003).

The above issues will be addressed in the following chapters.

The results of the second pilot study were presented as a poster presentation at ARVO, Florida 2001 (Verdon-Roe GM, et al. *IOVS* 2001; 42: ARVO Abstract 4417).

Chapter 3

GEOMETRY OF THE STIMULUS

3.1 INTRODUCTION

The pilot studies described in chapter 2 identified variability in responses in normal subjects for the line dimensions selected. In order to achieve good test specificity, a clear separation is required between normal and glaucomatous subjects. It is therefore essential that robust, reproducible responses be gained from control. The following chapters address this requirement by undertaking a detailed exploration of the normal psychophysical properties of the MDT stimulus. This chapter specifically explores the MDT spatial summation response.

Temporal and spatial summation properties are determined by the anatomical configuration of retinal elements and their neural integration and should be considered in the context of a coordinated cortical spatio-temporal response (Anderson and Burr 1991).

Spatial summation describes the relationship of the threshold response with stimulus area and has been shown to vary with eccentricity and background luminance (Glezer 1965; Wilson 1970; Dannheim and Drance 1971; Scholtes and Bouman 1977; Johnson and Scobey 1980; Scobey and Johnson 1981) and to show specific properties for different ganglion cell types (Felius et al. 1996; Volbrecht et al. 2000; White et al. 2001).

SAP measures DLS and the threshold is defined by the relationship of the area (A) and intensity (I) of the stimulus giving the relationship IA^n = constant. The summation coefficient (n) varies for different conditions: where the stimulus lies

within Ricco's area n = 1. For larger stimuli summation is incomplete and the threshold is determined by probability of recruitment of adjacent receptive areas (Robson and Graham 1981). For these larger stimuli the relationship $A^n \times I$ = constant. Piper's law holds when n = 0.5 (Glezer 1965; Lachenmayr and Vivell 1993).

Glaucomatous visual field loss represents underlying ganglion cell loss and the choice of the test stimulus size is a critical determinant for the expression of a defect. Small stimuli may be required for the detection of focal defect. Large stimuli may be useful to assess remaining visual function by probability summation in advanced glaucoma (Fellman et al. 1988).

Felius investigated spatial summation for selected cell mosaics: white-on-white, red-on-white and blue-on-yellow detection thresholds for different sizes of stimuli were assessed. In controls, red-on white and white-on-white summation functions were similar, suggesting both are mediated by the P pathway, although white-on-white is generally considered to be non pathway specific (Sample et al. 1994). The critical stimulus area (A_c) was found to be greater for the blue-on-yellow stimulus and summation to occur to larger sizes in keeping with the concept of the parallel, independently driven, bistratified pathway. Glaucoma patients were found to have larger values of A_c for white-on-white perimetry in areas of visual field loss. This finding was absent for the red-on-white condition and was therefore concluded by the authors to be caused by a shift involving other ganglion types (Felius et al. 1996). No equivalent work has been conducted for motion displacement stimuli.

3.1.1 SPATIAL AND TEMPORAL SUMMATION PROPERTIES OF MOTION DISPLACEMENT STIMULI

Johnson and Scobey investigated the effect of varying line length (3 -120 min arc) for foveal and peripheral (18 degrees nasal field) line displacement thresholds using an "A-B" motion stimulus (Johnson and Scobey 1980). The stimulus was unidirectional, compared to the oscillatory stimulus of the MDT (figure 3-1).

Foveal thresholds were unchanged by variation in line length and remained constant at approximately 1.5 min arc. By contrast, increasing line lengths up to 90 min arc significantly reduced the peripheral displacement threshold, where the smallest displacement threshold achieved was 3.5 min arc (Johnson and Scobey 1980). Johnson and Scobey did further work at five nasal locations (3, 5, 10, 17 and 30 degrees nasal eccentricity) and found an increase in the mean and standard deviation of thresholds with eccentricity (Scobey and Johnson 1981).

MDT thresholds reduce as the number of oscillations per stimulus presentation increases from one to three, in line with different patterns of temporal summation (Verdon-Roe et al. 2000). One would therefore predict lower MDT thresholds when using the three-oscillation stimulus of the MDT compared to the unidirectional stimulus of Johnson and Scobey.

Post compared motion displacement thresholds for unidirectional stimuli (A-B) and oscillatory stimuli (A-B-A) for six durations of motion ranging 2.5 – 80 msec per half cycle (figure 3-1). Unidirectional stimuli threshold results were found to be independent of duration of motion. Oscillatory stimuli of > 40msec duration produced lower thresholds, and oscillatory stimuli of < 40msec duration higher thresholds, when compared with the unidirectional stimulus. This effect was attributed to a failure of temporal summation for short durations (Post et al. 1984).

The duration of the Johnson's unidirectional stimulus was 80 msec and the current MDT is 100 msec, per half cycle. On the basis of Post's findings one would again predict lower thresholds for the MDT stimulus.

Figure 3-1. Time diagram comparing unidirectional and oscillatory MDT stimuli.

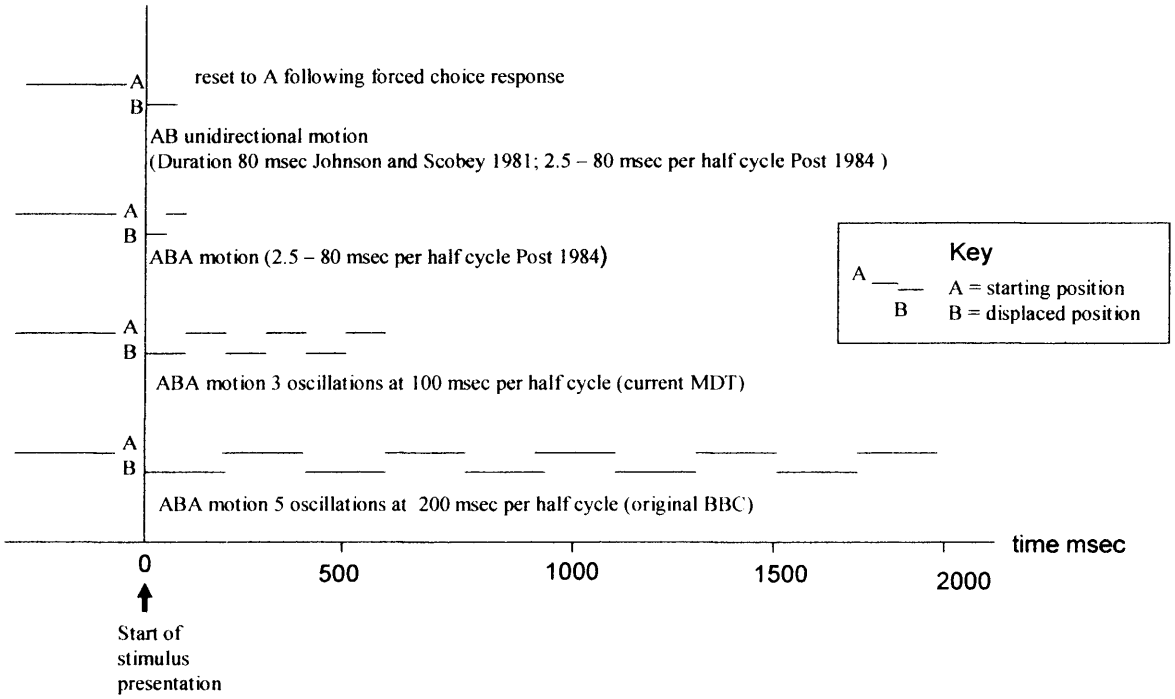

The aim of this chapter is to explore the spatial summation properties of the MDT stimulus to further our understanding of the normal psychophysical response and to apply this knowledge to the development of the MDT.

Different temporal summation properties for unidirectional and oscillatory MDT have been demonstrated as discussed, but comparisons in their spatial summation properties have not previously been investigated. It was therefore decided there would be merit in estimating the effects of different line length for the oscillatory MDT stimulus, using a similar methodology to Scobey and Johnson's unidirectional experiment (Johnson and Scobey 1980).

In addition, a 3-line stimulus was evaluated to provide insight into the spatial summation properties of the FDT stimulus, which, although generally perceived to be different to the MDT, has common features, as discussed in chapter 1 (figure 1-12).

All testing was performed at nasal location -27,3. The reason for this choice was because it represents the most eccentric location of the MDT and has the lowest GCD, thereby allowing a greater range of threshold measurements to be recorded for small line lengths. Another advantage is that, within the context of the MDT, -27,3 is a horizontal stimulus and therefore requires no "feathering" and is more easily manipulated in dimension. In addition, this nasal location is often associated with early glaucomatous defect and thus provides a particular interest of study.

3.2 INVESTIGATIONS

3.2.1 SINGLE LINE STIMULI

QUESTION

What is the effect of changing the MDT stimulus line length?

METHOD

5 Bitmaps were created of lines of the following line length: 128, 86, 43, 22 and 11 min arc (48, 32, 16, 8 and 4 pixels respectively). Each line width measured 5 min arc (2 pixels). Subject GMVR fixated the central fixation target through a centrally placed –5.0 DSph, in line with her central myopic correction. The stimulus was therefore seen through the periphery of the lens. The lines were selected in a random order and each programmed to pass through 5 presentations, of each of 6 randomized displacements, measuring 0, 5, 8, 14, 19 and 24 min arc (0, 2, 3, 5, 7 and 9 pixels respectively). FOS curves were generated and the threshold taken as the displacement corresponding to 50% of the probit-fitted curve.

RESULTS

A clear reduction in threshold was demonstrated as the length of line was increased, as shown in table 3-1 and figure 3-4).

Table 3-1. MDT thresholds with varying single line length

Stimulus line length (min arc)	MDT threshold min arc (50% seen)
128	4.5
86	8.2
43	12.8
22	19.8
11	19.7

3.2.2 THREE-LINE STIMULI

QUESTION

Do single line and equivalent length of three-line stimuli result in the same threshold?

METHOD

A bitmap was created of a three parallel line stimulus consisting of 3 white lines each measuring 11 x 5 min arc (4 x 2 pixels) and presented at location -27,3. Each line was separated by 2 pixels so that the entire stimulus subtended 11 x 27 min arc (figure 3-2). The background was as for the standard MDT, giving a contrast of 85%. Subject GMVR fixated the central fixation target through a centrally placed –5.0 DSph. The three-line stimulus was programmed to pass through 5 presentations of each of 6 randomized displacements measuring 0, 5, 8, 14, 19 and 24 min arc (0, 2, 3, 5, 7 and 9 pixels respectively).

Figure 3-2. Three-line stimulus.

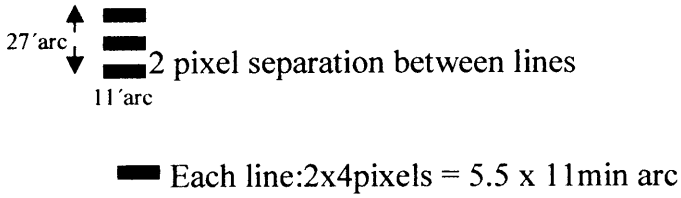

RESULT

MDT threshold: 18.7 min arc.

3.2.3 THE EFFECT OF LINE SEPARTION USING A 3-LINE STIMULUS

QUESTION

What is the effect of line separation of a three-line stimulus?

METHOD

This was identical to the previous experiment (3.2.2), except the separation of lines was increased to 21 pixels. The entire stimulus subtended 11 x 128 min arc (figure 3-3).

RESULT

MDT threshold: 7.9 min arc.

DISCUSSION

By referring to figure 3-4 it can be seen that the three-line stimulus with 2-pixel spacing between lines achieved near equivalent threshold to a single line of 11 min arc length, with no evidence for additional summation. It is possible that the threshold was elevated due to variable overlap of the retinal area that is stimulated as the line stimulus is displaced. By referring to figure 3-2 one can visualize that for the first

Figure 3-3. Three-line stimulus: increased separation of lines.

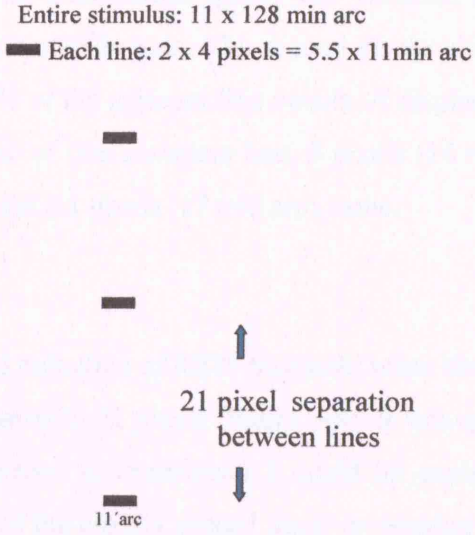

Figure 3-4. Threshold results for single and three-line stimuli (central lens correction: –5.0 DSph).

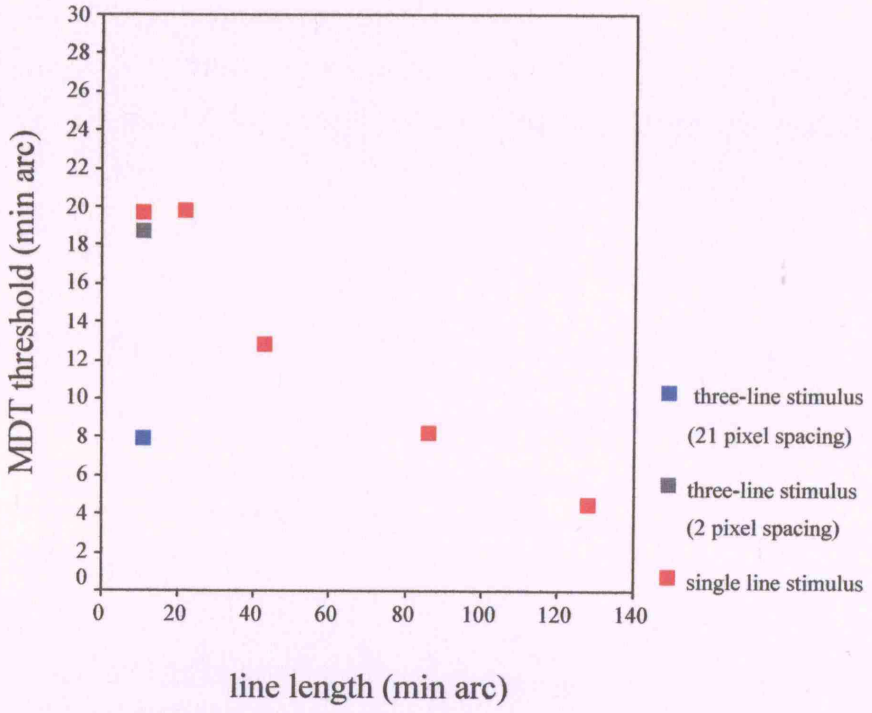

displacement of 2 pixels (6 min arc) there is no overlap as the two-pixel width line moves to the adjacent two-pixel width space. The stimulus therefore moves from stimulated retina to un-stimulated retina. The second displacement is 3 pixels (8 min arc). Here, overlap of 50% of the adjacent line occurs. A displacement of 4 pixels (11 min arc) results in overlap of one complete line, 5 pixels (14 min arc) an overlap of 50% of the adjacent line and six pixels (17 min arc), none.

There was a marked reduction of MDT threshold when the line separation of the 3-line stimulus was increased to 21 pixels (figure 3-4). It was questioned whether the absence of spatial summation in experiment 2 could be explained by the stimulus overlap on displacement of the closely spaced lines, or whether it might be attributed to error of peripheral refraction causing the lines to blur into one.

Investigation into the effects of peripheral refraction was undertaken as a next step on the basis of these test results.

Chapter 4

OPTICS

4.1 BACKGROUND

The previous chapter raised the question of whether MDT thresholds may be subject to the effect of refractive blur. This chapter addresses the effects of central and peripheral optical blur. Clinical Optics (Elkington and Frank 1991) and Clinical Visual Optics (Bennett and Rabbetts 1984) were used as general text of reference.

Central acuity is achieved through high cone density and a 1:1 ratio with retinal ganglion cells. Central detection and resolution sensitivity are equivalent, but limited by the physiological optics of the eye. By contrast, peripheral acuity is limited by reducing receptor and retinal ganglion cell density with eccentricity, with increasing ratio of convergence of cone to ganglion cell (Curcio and Allen 1990). The laterally spreading horizontal and amacrine cells enhance detection. In consequence, peripheral resolution thresholds are elevated by comparison with peripheral detection thresholds (Thibos et al. 1987a; Thibos et al. 1987b; Anderson 1996; Thibos 1998).

Thus, central vision is limited by the optics of the eye, whereas peripheral sensitivity is limited by the underlying retino-neural configuration.

4.2. THE EFFECT OF PERIPHERAL REFRACTIVE BLUR ON MDT THRESHOLDS

4.2.1 INVESTIGATION INTO THE EFFECT OF PERIPHERAL REFRACTIVE BLUR ON MDT THRESHOLDS

QUESTION

What are the effects of spherical refractive blur on peripheral MDT thresholds for single line and three line stimuli of different lengths?

METHOD

Subject GMVR fixed the central MDT fixation target as previously, but without her central refractive correction (- 5 DSph). Lens strengths of: +/- 6 DSph, +/- 4DSph, +/- 2DSph and plano were selected in random order and supported on a clamp positioned so that the test lens was centered on location -27,3. The first experiment of chapter 3 was repeated for single lines of 128, 86 and 11 min arc length. The second experiment of chapter 3 was repeated for an 11 min arc length three-line stimulus. This time the lines were separated by 3 pixels, as opposed to 2 pixels, because of a subjective improvement on the screen (using 2 pixels the separation between lines appeared less than the width of the lines. Using 3 pixels, lines and their separation appeared equivalent in width). The three-line stimulus subtended 11 x 33 min arc.

The experimental set up, using a peripheral lens centered on the stimulus, excluded the influence of prismatic displacement on the threshold results. Concave lenses simulate hypermetropia and convex lenses, myopia (Henson and Morris 1993).

RESULTS

a) single line stimuli

The 11 min arc line length stimulus showed lower displacement thresholds for lens strengths ranging from - 4 DSph to + 6.0 DSph (figure 4-1) when compared to the central –5.0 Dsph correction of the previous chapter (figure 3-4).

The lowest MDT threshold was seen when using a lens strength of - 2.0 DSph. There was smaller elevation in MDT threshold with increasing strength of convex lenses compared to concave. Three threshold values were suprathreshold for line lengths of 128 and 86 min.

b) three-line stimuli

The three-line stimulus showed greater response to lens defocus than the 11 min arc single-line stimulus (figure 4-1b). The lowest threshold was achieved with a plano lens and was considerably reduced when compared with the results obtained with a centrally placed lens of the previous chapter (figure 3-4). The MDT threshold rose markedly with increasing strengths of both convex and concave lens.

DISCUSSION

The reduction in MDT threshold seen for the single-line and three-line stimuli, when using a low power concave lens, suggests there is a difference in subject GMVR's central and peripheral refractive error. In the presence of axial myopia, one would expect a reduction of myopic error in the periphery of approximately - 2.0 DSph. The test distance of 30 cm corresponds to + 3.0 DSph. It is therefore credible for there to be no need for refractive correction at -27,3 in the nasal periphery at 30 cm viewing distance. It was therefore planned to investigate this theory by assessing peripheral refraction as the next procedure.

Figure 4-1. The effect of refraction on MDT thresholds for single-line and three-line stimuli (lens centered –27,3).

a) single-line lengths.

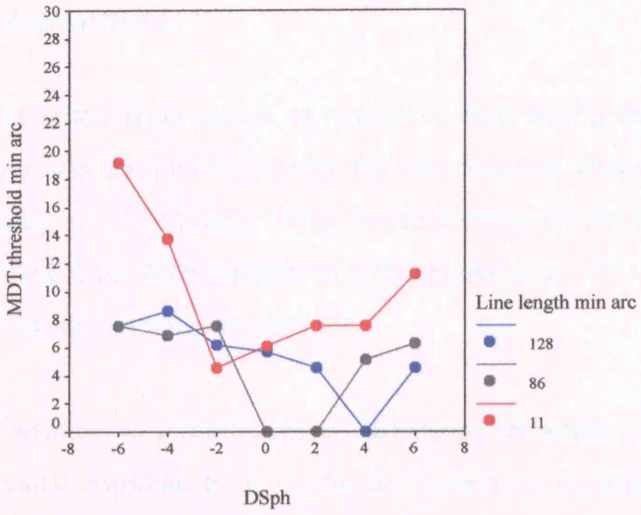

b) single-line and three-line stimuli (each 11 min arc line length).

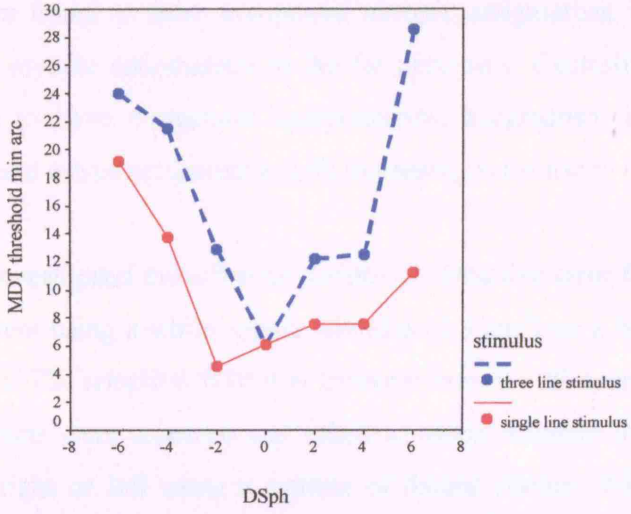

The test results showed a notable asymmetry in the 11 min arc single-line thresholds, with a greater increase in threshold with concave versus convex lenses. Subjectively, GMVR thought that this might be due to magnification of the MDT image when viewed through a convex lens and minification when viewed through a concave lens.

4.2.2 PERIPHERAL REFRACTION

Peripheral refraction is an aspect of psychophysical testing that is frequently over-looked. Young was the first to identify the physiological change in astigmatic error with eccentricity in 1801 (Young 1801). Ferree investigated peripheral refractive error using a modified Zeiss Refractometer in 1931 (Ferree et al. 1931). His work was later supported by Millodot (Millodot 1981).

Millodot conducted a comprehensive peripheral refraction of 62 eyes and assessed the horizontal meridian from 60 degrees nasally to 60 degrees temporally using a Topcon refractometer. Astigmatism was found to increase toward the periphery in 91% of the eyes and to vary according to the central correction. Centrally emmetropic eyes were found to have mixed astigmatism in the periphery. Centrally myopic eyes were found to have compound myopic astigmatism in the periphery becoming simple myopic astigmatism in the far periphery. Centrally hypermetropic eyes were found to have compound hypermetropic astigmatism in the periphery becoming compound mixed astigmatism with increasing eccentricity (Millodot 1981).

Leibowitz investigated the effect of peripheral refractive error for unidirectional motion displacement using a white square stimulus (1.3 cm^2) on a black background viewed at 78.7 cm. The temporal field was assessed from 0 - 80 degrees in 10 degree steps. Three subjects were assessed and asked to select whether the unidirectional stimulus moved right or left using a system of forced choice. When uncorrected, thresholds were found to increase by a factor of 10 from 0 - 80 degrees eccentricity.

This reduced to a factor of 6 when peripheral refractive error was corrected (Leibowitz et al. 1972).

4.2.1.1 ESTIMATION OF GMVR'S PERIPHERAL REFRACTION

On the evidence of the above, subject GMVR's central myopia and the effects of spherical blur on MDT thresholds described at the beginning of this chapter, it was decided the next logical step would be to estimate subject GMVR's peripheral refraction.

METHOD

Mr Andrew Milliken, Senior Optometrist, Moorfields Eye Hospital, performed retinoscopy using a standard manual retinoscope. Subject GMVR's right eye was dilated using tropicamide. Refraction test distance was 67cm. String, measuring 31cm in length, was used to approximate 25 degrees from fixation.

RESULTS (refer appendix figure 14-1, table 14-2)

Central refraction was confirmed to be - 5.0DSph for distance viewing. Peripheral refraction was estimated as - 2.75 / - 1.75 axis 105 degrees, at 25 degrees temporal retina (nasal field) at 6 meters. An approximate correction of α / - 1.75 axis 105 degrees, would be required for a test distance of 30 cm.

DISCUSSION

The results of GMVR's refraction are consistent with the findings of Ferree and Millodot. Physiological changes in peripheral, compared to central, refraction are common and frequently considerable. It is therefore imperative that any psychophysical test involving the periphery is robust to the effect of refractive error. Peripheral astigmatism is of particular relevance and concern in the context of the orientated line stimuli of the MDT.

4.2.3 REPEAT OF INVESTIGATION INTO THE EFFECT OF PERIPHERAL REFRACTIVE BLUR ON MDT THRESHOLDS WITH PERIPHERAL REFRACTION IS CORRECTED

QUESTION

What is the effect of spherical and cylindrical peripheral blur, calculated in addition to corrected peripheral refraction, on MDT thresholds?

METHOD

A horizontal line stimulus was presented in the nasal field at -27,3 degrees. The right eye of subject GMVR and a second normal subject, experienced in psychophysical testing, was tested. A central target was fixated and randomly selected lens strengths [(i) +/- 0, 2, 4, and 6 DSph and (ii) +/- 0, 2, 4, and 6 Dioptre cylinder (DCyl) at 90-degree/180-degree axis], additional to peripheral refractive correction determined by retinoscopy under mydriasis (appendix: table 14-2; figure 14-1)], were centered at -27,3 degrees.

The line stimulus (lengths 43, 86 or 128 min arc for DSph; 86 min arc only for DCyl) was programmed to pass through 5 presentations of 7 randomized displacements (0, 3, 5, 8, 13, 19, 24 min arc; 0, 1, 2, 3, 5, 7, 9 pixels). Note inclusion of smaller first displacement to address the suprathreshold response of the previous experiment. Each parameter was tested 3 times, FOS curves obtained and 50% seen threshold calculated by probit analysis.

RESULTS

1. DSph

Blurring by lenses of varying strength from - 6.00 to + 6.0 DSph showed only small elevations of mean MDT thresholds of < 5 min arc (table 4-1), when compared with the un-blurred baseline measurements, which were corrected for peripheral

refraction. There were two exceptions in the case of subject 1, where blurring by concave lenses resulted in elevation of MDT threshold > 5 min arc: [(i) 128 min arc line length blurred with – 4.0 DSph (< 7 min arc); (ii) 43 min arc line length blurred with – 6.0 DSph (< 9 min arc)].

In all cases, the effect of spherical blur resulted in a percentage change in log MDT threshold of <100 % (figure 4-2). No consistent effect of line length was observed for subject 1. Subject 2 showed the largest percentage change in threshold for the longest line length of 128 min arc, which showed the lowest base-line threshold measurement (table 4-1; figure 4-2).

Subject 1 showed greatest resistance to blur by convex lenses, with an increase of threshold and standard deviation when blurred with concave lenses. Subject 2 showed a more symmetrical response to the effect of blur by convex and concave lenses, with a tendency to increase of standard deviation for the highest strength of convex lens (table 4-1; figure 4-2).

2. DCyl

With the exception of one outlier, all cylinders produced only small variation in MDT (< 2 min arc) for both subjects (table 4-2). This represents a change of < 35% when the blurred log MDT thresholds are compared to the base-line un-blurred log MDT thresholds (figure 4-3). No consistent effect of cylinder axis is observed.

Table 4-1. MDT thresholds for varying amounts of peripheral spherical lens blur.

Mean MDT threshold results (range) and ± SD (min arc) for three line lengths (43, 86 and 128 min arc).

(a) Subject 1

Line length (min arc)	43	86	128
Un-blurred (Peripheral refraction corrected)	6.1 (5.6 – 6.3) ± 0.40	5.9 (5.3 – 6.2) ± 0.52	4.4 (4.2 - 4.8) ± 0.35
-2.0	9.4 (8.2 – 10.3) ± 1.10	8.8 (7.5 - 11.3) ± 2.19	8.8 (8.0 - 10.3) ± 1.33
-4.0	10.6 (6.6 - 12.0) ± 3.52	9.6 (8.4 - 11.3) ± 1.53	10.9 (9.8 – 11.9) ± 1.01
-6.0	14.8 (13.4 - 16.8) ± 1.78	10.0 (8.4 – 12.7) ± 2.33	8.5 (8.2 - 8.9) ± 0.36
+2.0	6.4 (5.6 - 7.1) ± 0.75	4.8 (3.4 – 5.6) ± 1.19	4.8 (4.2 - 5.3) ± 0.55
+4.0	7.4 (6.8 - 8.0) ± 0.60	6.0 (5.3 – 6.5) ± 0.64	4.3 (4.1 - 4.6) ± 0.29
+6.0	7.3 (6.3 - 8.0) ± 0.87	5.6 (4.8 – 6.3) ± 0.76	4.8 (3.4 - 5.6) ± 1.19

(b) Subject 2

Line length (min arc)	43	86	128
Un-blurred (Peripheral refraction corrected)	4.9 (4.2 - 5.3) ± 0.64	3.8 (2.9 - 4.2) ± 0.75	2.6 ± 0.69 (2.2 – 3.4)
-2.0	7.3 (6.3 - 8.2) ± 0.96	4.7 (4.6 - 4.8) ± 0.12	4.9 ± 1.78 (3.6 – 6.9)
-4.0	8.3 (7.1 - 9.4) ± 1.15	4.6 (3.4 - 5.6) ± 1.11	5.8 ± 0.84 (4.8 - 6.3)
-6.0	7.2 (6.2 - 8.0) ± 0.93	5.2 (4.2 - 6.2) ± 1.00	5.3 ± 0.81 (4.8 – 6.2)
+2.0	5.1 (4.2 - 6.8) ± 1.50	3.1 (2.5 - 4.1) ± 0.90	3.1± 0.9 (2.5 - 4.1)
+4.0	6.8 (6.5 - 7.0) ± 0.29	4.7 (4.2 - 5.2) ± 0.50	4.4 ± 0.35 (4.2 - 4.8)
+6.0	9.8 (8.4 – 12.6) ± 2.42	7.0 (5.1 - 9.4) ± 2.19	6.9 ± 0.98 (5.8 - 7.5)

Figure 4-2. Percentage change in mean log MDT threshold in response to spherical lens blur.

(i) Subject 1

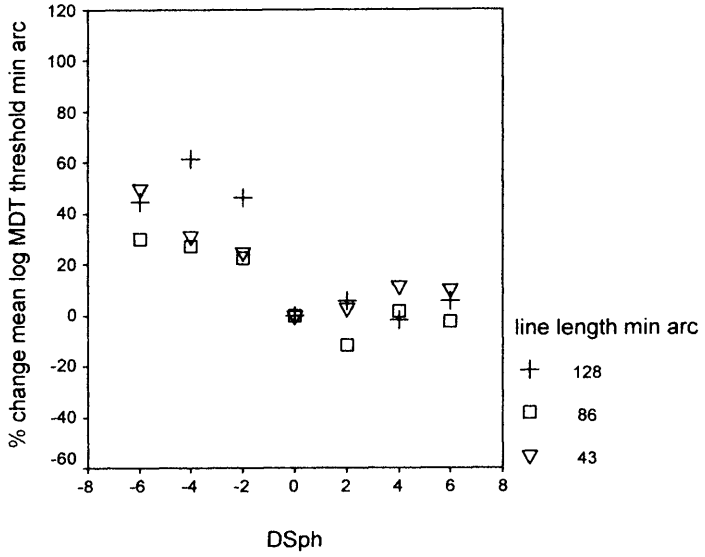

(ii) Subject 2

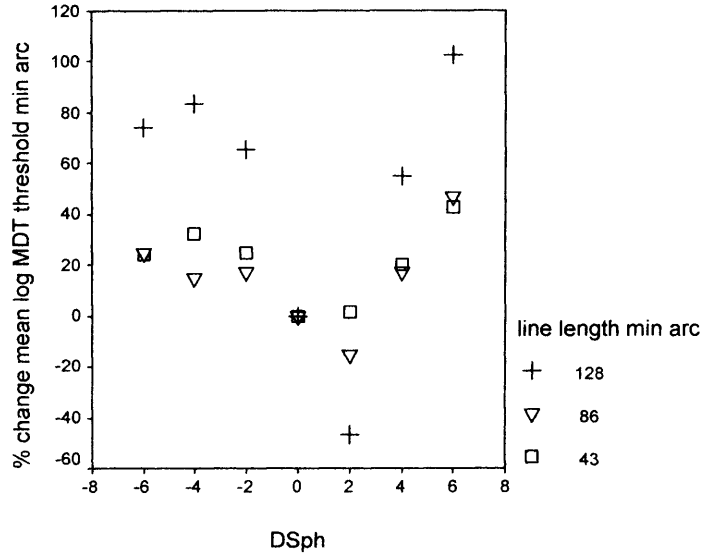

Table 4-2. MDT thresholds for varying amounts of peripheral cylindrical lens blur.

* Mean MDT threshold results (range) and ± SD (min arc) for a single line length of 86 min arc.

AXIS	DCyl	Subject 1*	Subject 2*
	Un-blurred (peripheral refraction corrected)	6.7 ± 1.04 (5.5 - 7.5)	4.1 ± 0.70 (3.4 – 4.8)
90 degrees	-2.0	8.5 ± 0.90 (7.6 - 9.4)	4.1 ± 0.70 (3.4 - 4.8)
	-4.0	7.2 ± 0.35 (6.8 - 7.5)	3.2 ± 0.29 (2.9 - 3.4)
	-6.0	8.7 ± 1.43 (7.1 - 9.9)	3.5 ± 0.66 (2.9 - 4.2)
	+2.0	7.0 ± 0.87 (6.3 - 8.0)	3.7 ± 0.42 (3.4 - 4.2)
	+4.0	7.9 ± 0.71 (7.1 - 8.5)	4.1 ± 0.70 (3.4 - 4.8)
	+6.0	5.6 ± 0.75 (4.8 - 6.3)	4.2 ± 0.00 (4.2 - 4.2)
180 degrees	-2.0	7.8 ± 0.25 (7.5 - 8.0)	5.0 ± 0.74 (4.2 - 5.6)
	-4.0	12.6 ±2.93 (9.4 - 15.1)	3.8 ±1.07 (2.9 - 5.0)
	-6.0	8.3 ±1.30 (7.0 - 9.6)	4.6 ±0.40 (4.1 - 4.8)
	+2.0	6.4 ± 2.17 (5.6 - 8.9)	4.3 ± 1.27 (2.9 - 5.3)
	+4.0	6.6 ± 0.96 (5.6 - 7.5)	5.8 ± 2.27 (4.2 - 8.4)
	+6.0	8.5 ± 0.81 (8.0 - 9.4)	5.2 ± 0.40 (4.8 - 5.6)

Figure 4-3. Percentage change in mean log MDT threshold in response to cylindrical lens blur.

(i) 90 degree axis

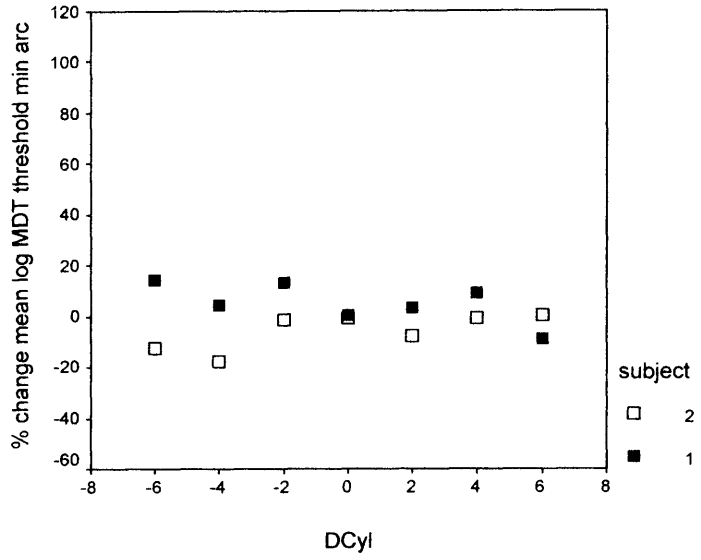

(ii) 180 degree axis

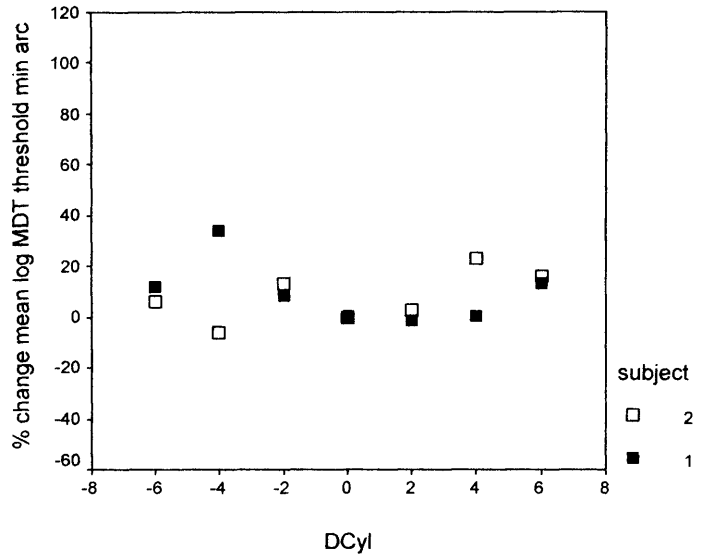

DISCUSSION

MDT testing has been shown to be robust to the effects of blurring by DCyl, producing only small elevations of MDT thresholds (< 2 min arc). This is of particular interest in the development of the new test, with respect to the use of an orientated line stimulus and in consideration of peripheral astigmatism, which is reported to physiologically increase with eccentricity (Ferree et al. 1931; Millodot 1981).

Blurring by spherical lenses also produced elevations of MDT of < 5 min arc. An earlier investigation, using the BBC MDT format with a larger line length (2 degree x 2 min arc) at a more central location (15°, 3°), suggested only small differences in MDT thresholds between glaucoma suspects 8.7 ± 3.4 (5.0 - 17.6), glaucoma patients 12.9 ± 5.8 (5.2 - 34.2) and normal subjects: 5.9 ± 1.7 (2.6 - 8.9) [mean ± SD (range) min arc], (Westcott et al. 1998b). Separation of glaucomatous from normal eyes may be increased using the multi-location test format, but, for optimal test sensitivity, correction of spherical refractive error may be required and will be kept under review as post-doctorate work.

Subject 1 (GMVR) showed an asymmetrical elevation of MDT threshold to the effect of spherical concave and convex blur, when compared to subject 2. Subjectively, GMVR suspected this was due to the magnification effect of the convex lens. Spectacle Magnification (SM) describes the factor by which the initial size of the image is magnified/minified (Elkington and Frank 1991).

$$\text{Relative Spectacle Magnification (RSM)} = \frac{\text{corrected ametropic image size}}{\text{emmetropic image size}}$$

Image size is magnified in corrected refractive hypermetropia and minified in refractive myopia. Magnification of the image may result in the stimulation of more ganglion cells.

Anderson assessed the effect of localized defocus on DLS in the fovea and periphery (at 30 degrees). He used circular white stimuli ranging from 0.2 - 6.4 degrees in diameter (the four smallest stimuli approximately corresponding to Goldmann sizes II -V, with two additional larger sizes) and a system of forced choice (Anderson et al. 2001). Peripheral lenses were positioned in line with the stimulus, as with the above MDT methodology, using spherical lenses up to ± 4.0 dioptre. Anderson found foveal thresholds increased immediately with increasing refractive error especially for small target size (figure 4-4).

Figure 4-4. The effect of defocus on foveal contrast sensitivity (Anderson et al. 2001).

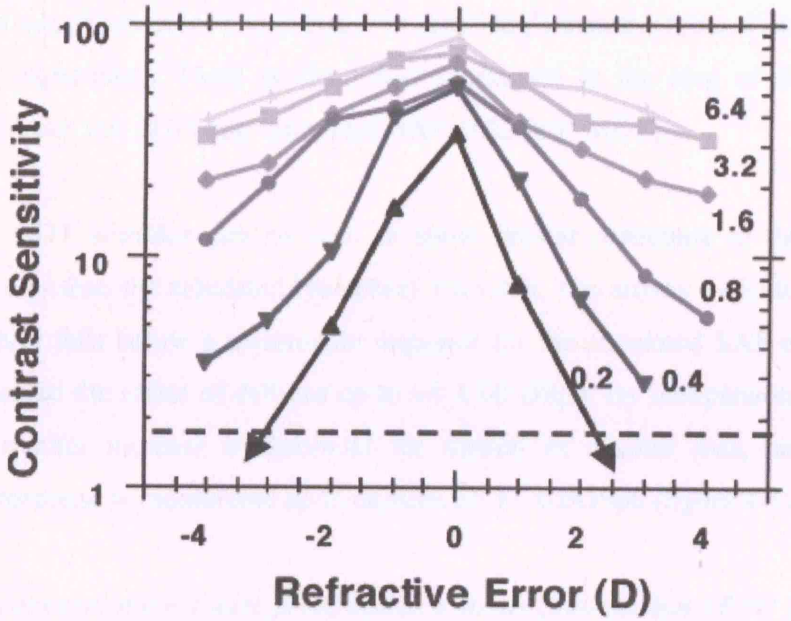

The thresholds for a peripheral stimulus (positioned at 30 degrees) were less affected by defocus initially and then increased more sharply (figure 4-5 a). Anderson suggested these properties may be explained by the different receptive field properties of central and peripheral retina. When a stimulus is defocused its image decreases in luminance, but increases in size, so that the energy of the blurred image is only slightly less than that of the focused image.

Anderson postulated that thresholds are maintained when an image is defocused, so long as the image is retained within its receptive field. Anderson hypothesized that a small stimulus would almost immediately fill the capacity of a stimulated central receptive field. An increase in image size would cause adjacent receptive fields to be stimulated, with a spread of the total energy and a consequent rise in threshold response. Peripheral receptive fields are larger. Thus, a blurred image would remain within the confines of a receptive field for longer, with no change in threshold (Anderson et al. 2001).

It is interesting to compare the effect of defocus on the simulated peripheral Humphrey stimuli of Anderson [figure 4-5 (a)], with that of MDT stimuli [figure 4-5 (b)]. The second smallest stimulus of the Anderson experiment corresponds to the Goldmann size III stimulus and is larger in area (deg^2) than the three stimuli used for the MDT experiment. There is close correspondence in the area of the smallest stimulus of each test (0.03 deg^2 simulated SAP; 0.02 deg^2 MDT).

The MDT stimulus can be seen to show greater resistance to the effect of refractive blur than the simulated Humphrey stimulus. The arrows indicate where the effect of blur falls below a measurable response for the simulated SAP experiment, which assessed the effect of defocus up to +/- 4.00 DSph. By comparison, the MDT shows a smaller increase in threshold for stimuli of smaller area, and a MDT threshold response is measurable up to defocus of +/- 6.0DSph (figure 4-5).

The results of experiment 2 were presented as a poster presentation ARVO 2003 (Verdon-Roe GM, et al. *IOVS* 2003; 44: ARVO E-Abstract 78).

Figure 4-5. The effect of spherical defocus on peripheral contrast sensitivity (from Anderson et al., 2001) and MDT thresholds.

(a) Peripheral contrast sensitivity thresholds (30 degrees eccentricity). The effect of refractive blur on peripheral contrast sensitivity thresholds (30 degrees eccentricity), (Anderson et al. 2001). The dashed lines indicate the lowest measurable contrast sensitivity under the experimental conditions. The arrows indicate where performance fell below this level. The area of each stimulus is as follows: 0.03, 0.13, 0.50, 2.10, 8.04 and 32.17 deg^2 (corresponding to the stimulus diameters of 0.2, 0.4, 0.8, 1.6, 3.2 and 6.4, as notated in the diagram). The smallest stimulus (0.3 deg^2) therefore closely corresponds in area to the smallest MDT stimulus (0.2 deg^2) in diagram (b).

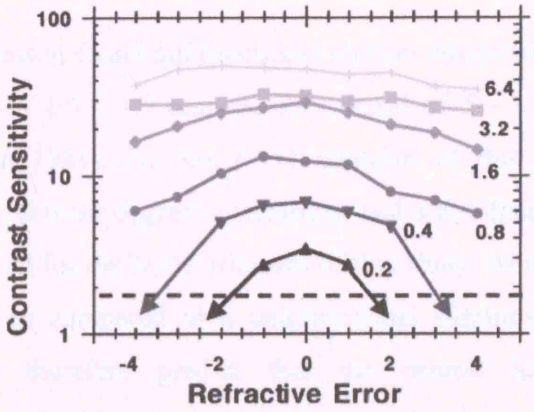

(b) Log MDT thresholds (-27,3 degrees eccentricity). The log MDT threshold is multiplied * -1 to draw comparison with peripheral contrast sensitivity thresholds in (a). The test points within the vertical dotted lines correspond to the range of defocus (+/- 4.0 DSph) tested by Anderson with +/- 6.0 DSph being additional defocus.

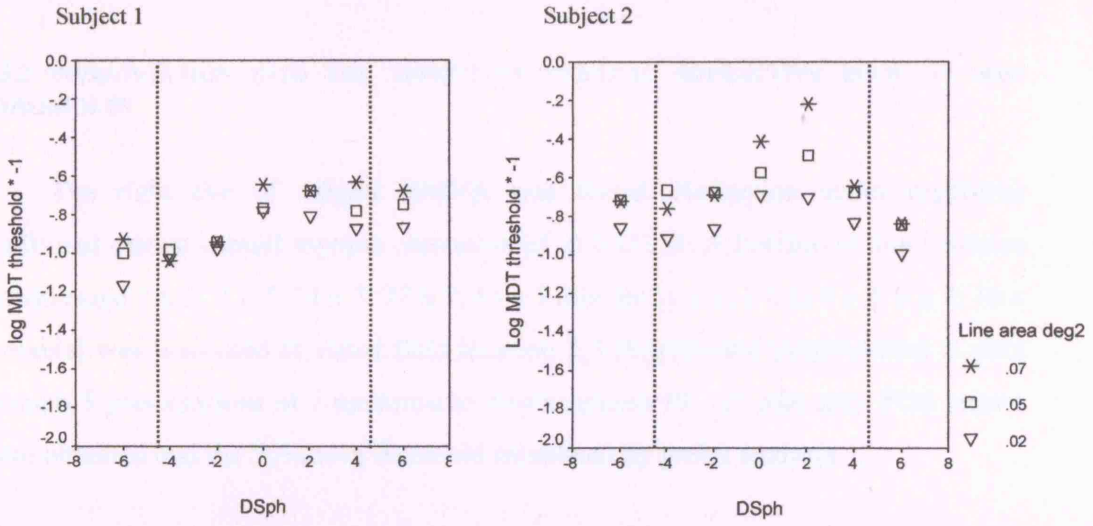

4.3. THE EFFECT OF CENTRAL REFRACTIVE BLUR ON MDT THRESHOLDS

4.3.1 BACKGROUND

The effect of optical blur has been described by the previous experiment for a peripherally placed stimulus at -27,3. This study sought to investigate the effect of central blur.

Scobey and Johnson found unidirectional motion thresholds, at 3 degrees in the nasal field, to measure 1.5 - 1.9 min arc for stimuli of 5 - 110 min arc in length (Scobey and Johnson 1981). For the MDT stimulus of this study a single pixel subtends 3.42 min arc at three degrees eccentricity and a test distance of 30 cm. Lower thresholds are predicted for the MDT stimulus of this study, which uses 3 oscillations per presentation, when compared to a unidirectional stimulus (Verdon-Roe et al. 2000). One would therefore predict that the central locations may prove suprathreshold in normal subjects, which may prove a barrier to the detection of early central glaucomatous loss. Thus, short stimulus lengths for central locations would be preferred, providing they are robust to the effect of refractive blur.

4.3.2 INVESTIGATION INTO THE EFFECT OF CENTRAL REFRACTIVE BLUR ON MDT THRESHOLDS

The right eye of subject GMVR was tested. Refraction under mydriasis confirmed distant central myopic correction of -5.0 DSph. A horizontal line stimulus (randomized 3 x 3; 7 x 7; 14 x 7; 27 x 7; 55 x 7 min arc [1 x 1; 2 x 2; 4 x 2; 8 x 2; 16 x 2 pixels] was presented at visual field location 3,3 degrees and programmed to pass through 5 presentations of 7 randomized displacements (0 - 21 min arc). FOS curves were obtained and the 50% seen threshold calculated by probit analysis.

The right eye was dilated (using 1% Tropicamide, 2 applications, 10min apart) in order to overcome the problem of accommodation induced by using a near, centrally placed target. The dilated pupil measured 8.5 mm.

Optical blur was achieved by the wear of contact lenses, thereby avoiding the effects of prismatic displacement. Lens strengths ranged + 4.0 to - 8 DSph to give defocus of + 6 to - 6 DSph in subject GMVR (calculated to adjust for her central distance correction of - 5.0 DSph and the test distance of 30 cm, therefore requiring a near correction of - 2.0 DSph).

RESULTS

Table 4-3 summarizes the results.

Table 4-3. MDT thresholds for varying stimulus line length and central optical blur.

	Line length x width				
Min arc	3 x 3	7 x 7	14 x 7	27 x 7	55 x 7
Pixels	1 x 1	2 x 2	5 x 2	10 x 2	20 x 2
+ 6 DSph	US	5.8	ST	ST	ST
+ 4 DSph	3.4	ST	ST	ST	ST
+ 2 DSph	ST	ST	ST	ST	ST
0 DSph	ST	ST	ST	ST	ST
- 2 DSph	3.5	ST	ST	ST	ST
- 4 DSph	US	5.1	ST	ST	ST
- 6 DSph	US	US	23.5	2.8	ST

ST: suprathreshold US: unseen

In the un-blurred state, suprathreshold responses were achieved even for the smallest possible stimulus size of 1 pixel x 1 pixel, which subtends 3 x 3 min arc at a test distance of 30 cm. It is therefore not possible to calculate the effects of central blur but only make points of observation.

It is notable that the stimulus displacement was unseen for the 3 x 3 min arc stimulus, when blurred by a + 6.0, - 4.0 and - 6.0 DSph lens, as was the case for the 7 x 7 min arc stimulus when blurred by a - 6.0 DSph. The MDT threshold was markedly elevated from suprathreshold to 24 min arc when using a 14 x 7 min arc stimulus blurred by a - 6.0 DSph lens. This would suggest that if the test were to be run with refractive error uncorrected small lines subtending $\leq$ 14 min arc should be avoided.

When selecting stimulus line length, there may therefore be a trade-off between the convenience of the test being run with refraction uncorrected and the sensitivity of the test to detect central glaucomatous defects.

It is recommended that the issue of central refractive error should be kept under review and investigated as part of a future pilot study.

Chapter 5

MDT SUMMATION PROPERTIES (PERIPHERAL REFRACTION CORRECTED)

5.1 INTRODUCTION

The findings of the previous chapter indicated that spherical peripheral refractive error may have a significant effect on the MDT threshold. The objective of this chapter was to further the MDT summation studies of chapter 3 with peripheral refraction corrected.

5.2 INVESTIGATIONS

5.2.1 INVESTIGATION OF MDT THRESHOLDS FOR SINGLE LINE STIMULI OF DIFFERENT LENGTH

METHOD

Experiment 1 of chapter 3 summation experiments was repeated for subject 1, (GMVR), with peripheral refraction corrected. Five horizontal line lengths (128, 86, 43, 22 and 11 min arc; 48, 32, 16, 8 and 4 pixels), each of uniform width (5 min arc; 2 pixels) were randomly selected, presented at –27,3 and programmed to pass through 5 presentations of each of 7 randomized displacements (0, 3, 5, 8, 14, 19 and 24 min arc; 0, 1, 2, 3, 5, 7 and 9 pixels).

Each parameter was tested three times to achieve a mean value. Note inclusion of smaller first displacement to allow for an expected reduction in threshold when compared with experiment 1, which used the central correction of – 5.0 DSph. Comparison was made between the results of this experiment, those of the first experiment chapter 3 and the unidirectional line stimulus of Scobey and Johnson, which was tested in the nasal field at 30 degrees eccentricity (Scobey and Johnson

1981). The relationship between log MDT threshold and log stimulus line length was explored by linear regression analysis.

RESULTS

A reduction in MDT threshold was found with peripheral refraction corrected. The difference in thresholds with and without refractive correction reduced as the line length became longer, with no difference seen for the longest line length of 128 min arc (figure 5-1).

Comparison between the unidirectional stimulus and the oscillatory MDT showed a reduction in MDT threshold for the longer lines tested, but little difference for the shorter line lengths (figure 5-1).

A plot of log MDT threshold as a function of log line length demonstrated a linear relationship [slope - 0.42; 95% confidence intervals (95% CI) - 0.41, - 0.43], (figure 5-2).

DISCUSSION

The apparent increasing effect of refractive error with decreasing length of line (figure 5-1) may be misleading. The previous chapter showed no increase in threshold to refractive blur with reduction of line length, when calculated as a percentage threshold change (figure 4-2).

Comparison of MDT and unidirectional thresholds (Scobey and Johnson 1981), (figure 5-1), indicates similar results for the smaller lines, but lower MDT thresholds for the longer lines tested. This may indicate different patterns of spatial and temporal summation for unidirectional and oscillatory motion displacement presentation.

Figure 5-1. Effect of single line length on unidirectional and oscillatory MDT.

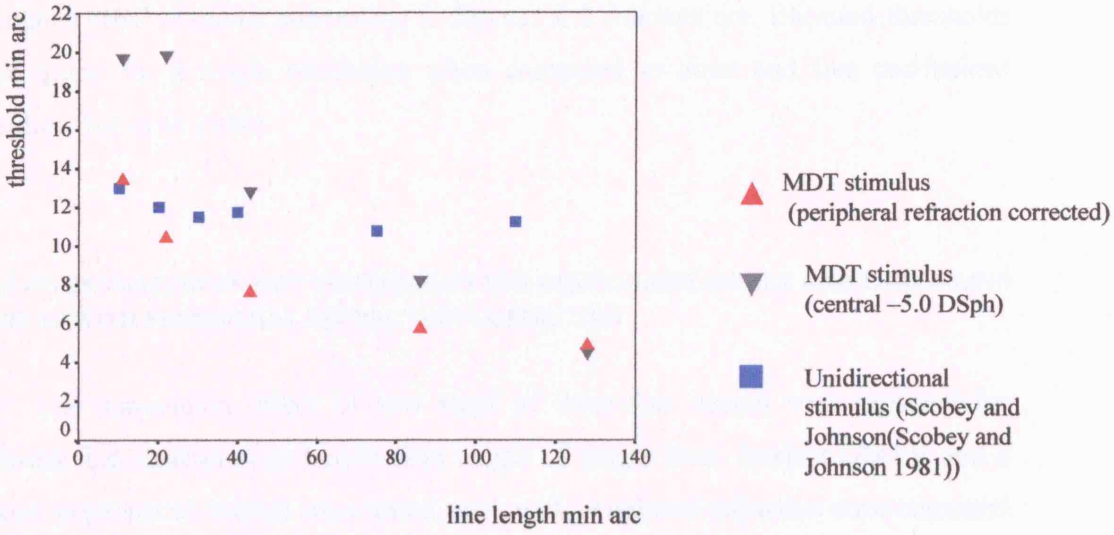

Figure 5-2. Log MDT threshold as a function of log single line length.

Regression slope - 0.42 (95% CI -0.41, - 0.43; $R^2 = 1.00$; $P < 0.001$).

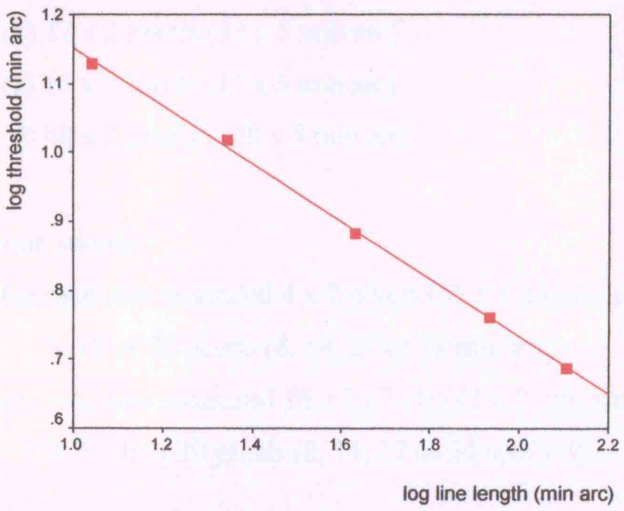

The reduction of threshold found for the oscillatory MDT compared to the unidirectional stimulus for the longer line lengths (figure 5-1) is consistent with earlier work, which investigated the effect of different number of stimulus oscillation for a simulated BBC stimulus subtending 2 degrees x 2 minutes arc. Elevated thresholds were found for a single oscillation when compared to three and five oscillations (Verdon-Roe et al. 2000).

5.2.2 INVESTIGATION OF MDT THRESHOLDS FOR EQUIVALENT SINGLE AND THREE-LINE STIMULI WITH PERIPHERAL REFRACTION CORRECTED

The summation effect of two sizes of three-line stimuli was explored for different line separation and equivalent length of single lines. Subject GMVR and a second experienced subject were tested, each with peripheral refractive error corrected (appendix: table 14-2; figure 14-1).

METHOD

Bitmaps were created of the following dimensions (figure 5-3)

(i) single line stimuli:

(a) 4 x 2 pixels (11 x 5 min arc)

* (b) 12 x 2 pixels (33 x 5 min arc)

(c) 16 x 2 pixels (43 x 5 min arc)

† (d) 48 x 2 pixels (128 x 5 min arc)

(ii) 3-line stimuli:

* (a) each line measured 4 x 2 pixels (11 x 5 min arc) and was separated by 3, 5, 10 or 20 pixels (8, 14, 27 or 54 min arc).

† (b) each line measured 16 x 2 pixels (43 x 5 min arc) and was separated by 3, 5, 10 or 20 pixels (8, 14, 27 or 54 min arc).

* / † denotes stimuli of equal area

Figure 5-3. Illustration of single line and 3-line stimuli of equal area.

A
(i) Single line stimulus measuring 12 x 2 pixels (33 x 5 min arc) in length.

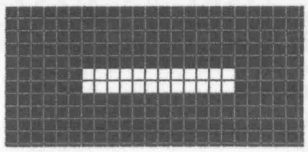

(ii) 3-line stimulus: each line measures 4 x 2 pixels (11 x 5 min arc) and, in this case, is separated by 5 pixels (14 min arc). The entire stimulus subtends 43 x 11 min arc. The total number of pixels comprising the 3-line stimulus is 24 and equivalent to the 12 x 2 pixel single line stimulus above.

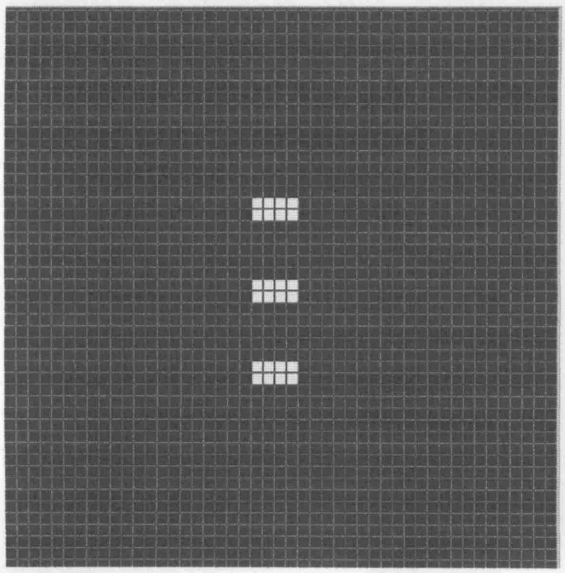

(B)

(i) Single line stimulus measuring 48 x 2 pixels (128 x 5 min arc) in length.

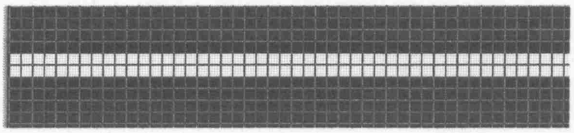

(ii) 3-line stimulus: each line measures 16 x 2 pixels (43 x 5 min arc) and, in this case, is separated by 10 pixels (26 min arc). The entire stimulus subtends 70 x 43 min arc. The total number of pixels comprising the 3-line stimulus is 96 and equivalent to the 48 x 2 pixel single line stimulus above.

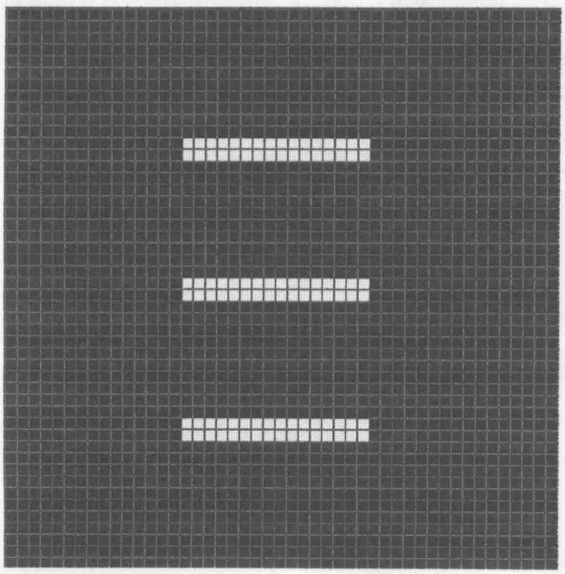

5 presentations of each of the following displacements were made in a randomized order: 0, 3, 5, 8, 14, 19 and 24 min arc (0, 1, 2, 3, 5, 7 and 9 pixels) for each three-line and single line stimulus. Each test was repeated three times in order to achieve a mean value.

Results

The motion displacement threshold decreased as single line length increased (figure 5-4).

Similar thresholds were seen for equivalent three and single line stimuli (table 5-1).

Table 5-1. Mean MDT thresholds for equivalent single and 3-line stimuli.

	33 min arc single-line	11 min arc three-line*	128 min arc single-line	43 min arc three-line*
Subject 1	8.4 ± 0.9	7.5 ± 0.6	4.9 ± 0.7	5.2 ± 0.1
Subject 2	7.4 ± 0.9	7.9 ± 1.0	5.0 ± 0.7	5.4 ± 0.4

* mean threshold results of the four line separations

No effect of changing line separation was seen for the 43 min arc 3-line stimulus. A small increase in threshold was seen for subject 2 for the 11 min arc 3-line stimulus as line separation is decreased (figure 5-5).

Figure 5-4. Log MDT thresholds as a function of log single line length.

(i) Subject 1

Regression slope: – 0.40 (95% CI - 0.39, - 0.41; $R^2 = 1.00$; $P < 0.001$).

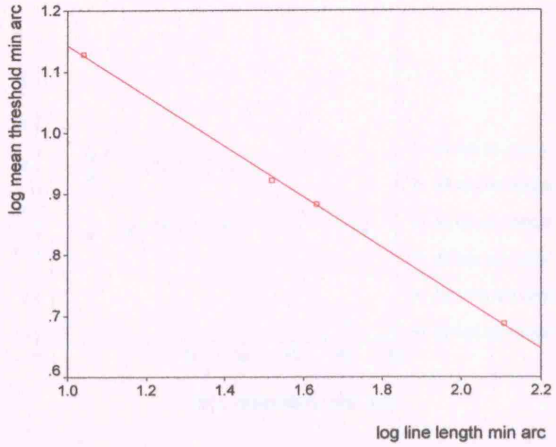

(ii) Subject 2

Regression slope: – 0.33 (95% CI -0.22, - 0.44; $R^2 = 0.91$; P 0.047).

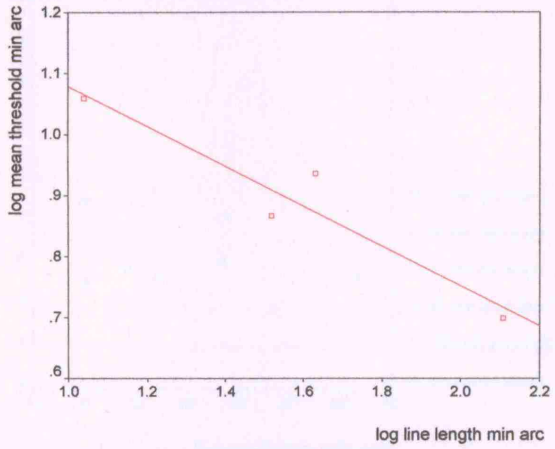

Figure 5-5. MDT thresholds for equivalent single and three-line stimuli.

(i) Subject 1

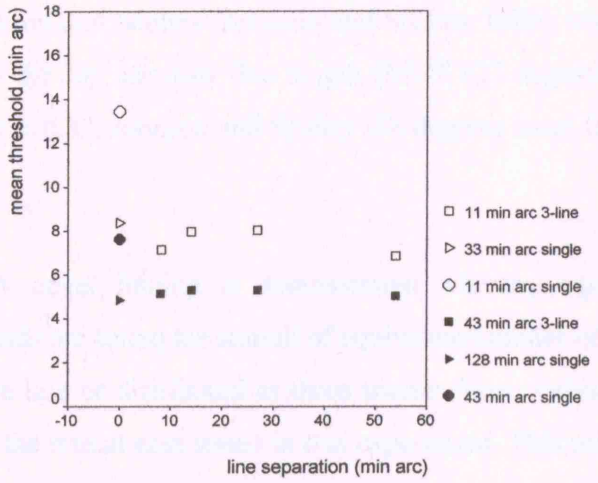

(ii) Subject 2

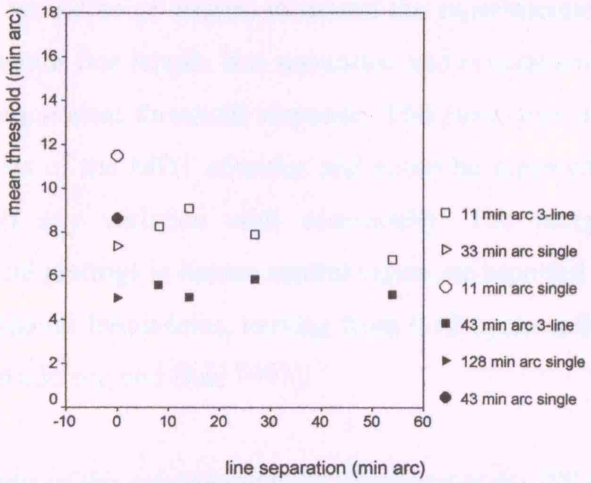

DISCUSSION

This study demonstrates that decreased motion displacement thresholds are achieved with increasing line length indicating spatial summation, in keeping with the findings of the unidirectional stimuli of Johnson and Scobey (Johnson and Scobey 1980; Scobey and Johnson 1981). Similar line slopes are found for this study and that of Johnson and Scobey (Johnson and Scobey 1980) when the log threshold is plotted against the log stimulus line length [MDT (27 degrees nasal field) subject 1: 0.40; subject 2: 0.33. Johnson and Scobey (18 degrees nasal field) subject 1: 0.34; subject 2: 0.22].

A novel finding is demonstrated whereby equivalent motion displacement thresholds are found for stimuli of equivalent number of pixels, whether configured as a single line or distributed as three shorter lines, indicating linear summation occurs within the retinal area tested in this experiment. This principal may be used to predict motion displacement thresholds when testing within the described dimensions. The three line stimulus could be used in a clinical setting to sample a wide retinal area, if required. For example, to uncover seeing areas of the field in end-stage glaucoma, or for rapid assessment of neurological defects e.g. hemianopia or quadranopia.

It would be of interest to extend the experimental design to vary further the 3-line stimulus line length, line separation and orientation to ascertain the critical limits of the equivalent threshold response. This may give insight into the receptive field properties of the MDT stimulus and could be repeated for different retinal areas to establish any variation with eccentricity. The receptive field size for drifting sinusoidal gratings in human central vision are reported to be as long as they are wide for all spatial frequencies, varying from 0.12 cycle at 0.1 c/deg to 0.52 cycle at 10.0 c/deg (Anderson and Burr 1991).

The results of this experiment were presented at the IPS meeting June 2002 and accepted for publication in Perimetry Update 2002/ (Verdon-Roe et al. 2002).

5.2.3 INVESTIGATION OF MDT THRESHOLDS FOR STIMULI OF EQUAL AREA BUT DIFFERING EDGE LENGTH

It has been suggested that vernier thresholds are determined by the stimulus edge (Foley-Fisher 1973; Watt and Morgan 1983; Mather 1987; Lee et al. 1993; Fendick and Swindale 1994; Lee et al. 1995; Ruttiger and Lee 2000). In this study we test the hypothesis that it is the MDT stimulus area, rather than the edge length, that determines the threshold response, by comparing MDT thresholds for constant stimulus area but changing line edge length.

METHOD:

MDT thresholds were estimated for three stimuli of equivalent area but different line edge length at two levels of Michelson contrast (table 5-2). The stimuli at 85% contrast are illustrated by screen capture images (figure 5-6).

Table 5-2. Specification for stimuli of equivalent area but differing line edge length.

Michelson contrast	85 %			40%		
Luminance (cd/m^2)	112			24		
Stimulus area pixels	96	96	96	40	36	36
Stimulus dimensions pixels (min arc) Horizontal (X) x Vertical (Y)	12 X 8 (128 x 5)	24 X 4 (64 x10)	48 X 2 (128 x 5)	5 X 8 (14 x 22)	9 X 4 (24 x 11)	18 X 2 (49 x 5)
Aspect Ratio Stimulus width / height	1.5:1	6:1	24:1	0.625:1	2.25:1	9:1
Stimulus edge length (pixels)	24	48	96	10	18	36

Figure 5-6. Screen capture of stimuli of equivalent line area but different edge length.

The arrows indicate the vector of motion.

(a) 12 x 8 pixels (32 x 20 min arc)

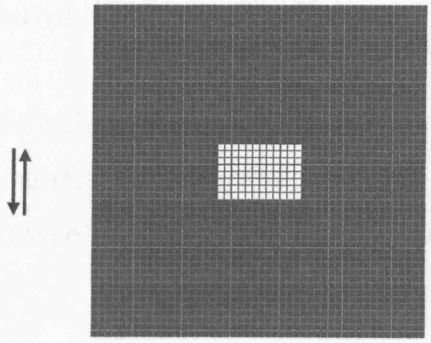

(b) 24 x 4 pixels (64 x 10 min arc)

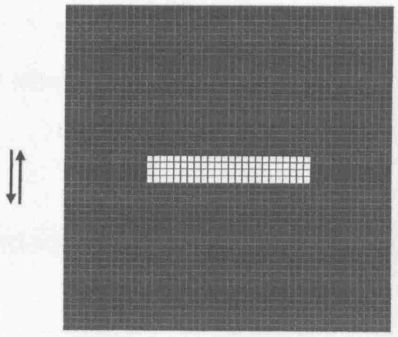

(c) 48 x 2 pixels (128 x 5 min arc)

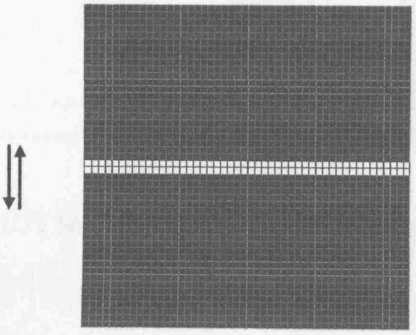

The methodology of the previous experiment was repeated: each stimulus configuration was positioned at –27,3 and programmed to pass through 5 presentations of each of following displacements: 0, 3, 5, 8, 14, 19 and 24 min arc (0, 1, 2, 3, 5, 7 and 9 pixels). Subjects 1 and 2 from the previous experiment were tested, with peripheral refraction corrected. Three tests were performed for each stimulus variation in a randomized order.

The three test results for each parameter tested were merged for each individual. FOS curves were generated and the threshold was taken as the displacement corresponding to 50% seen of the merged probit fitted curve.

RESULTS

This experiment used two variations of constant stimulus area, 96 pixels and 36 - 40 pixels, and found that a four-fold change in edge-length had minimal impact on MDT thresholds (table 5-3). There was an elevation of MDT threshold, with widening of 95% CI, for smaller, lower contrast stimuli (figure 5-7).

Table 5-3. MDT threshold for stimuli of equivalent area, but varying edge length.

% contrast	Stimulus dimension length x width (min arc)	MDT threshold (range) and standard deviation (min arc)
85%	12x8	5.6 (4.4 - 6.8) ± 0.85
	24x4	6.0 (4.9 - 7.3) ± 0.91
	48x2	5.2 (3.6 - 7.2) ± 1.28
40%	5x8	19.1 (14.1 - 26.0) ± 4.15
	9x4	20.8 (16.4 - 27.8) ± 3.98
	18x2	18.7 (14.2 - 22.2) ± 2.89

(comparison between MDT thresholds of merged and unmerged FOS curves is given in the appendix, table 14-4).

Figure 5-7. MDT thresholds for stimuli of equal area, but differing line length-edge.

(a) Subject 1

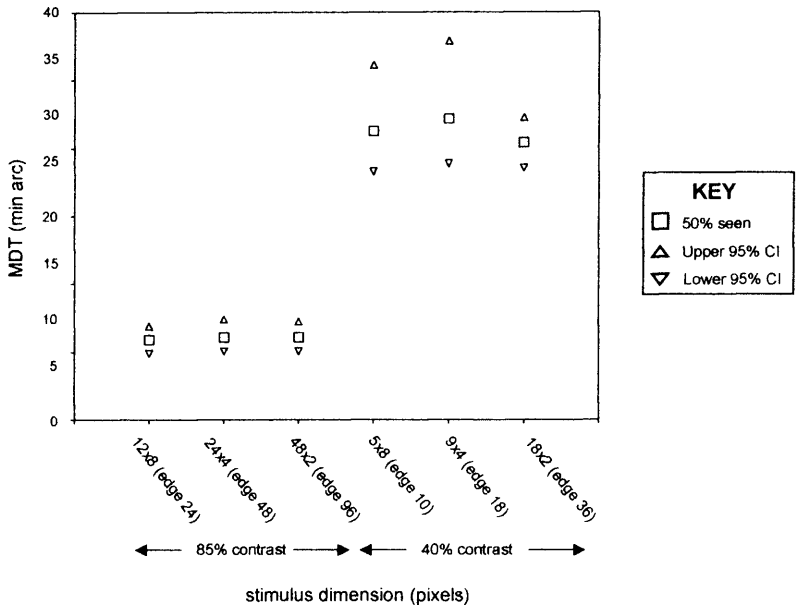

(b) Subject 2

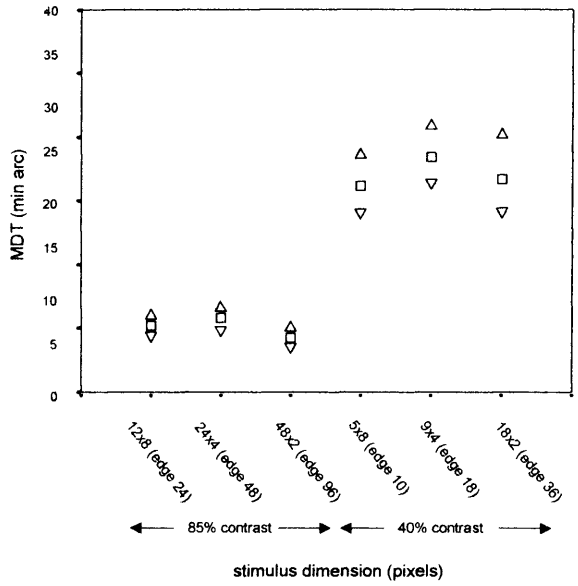

Displacement acuity is traditionally considered as a function of edge jump, with summation calculations made in relation to line edge length (Foley-Fisher 1973; Lee et al. 1995). The results of this experiment suggest that it is the total area of the stimulus, as opposed to its edge length, that is the contributing factor. However, a limitation of the experiment is that all stimuli, with the exception of one (5 x 8 vertical rectangle, aspect ratio 0.625), were horizontal rectangles, with aspect ratios from 1.5 to 24 (table 5-2). In order to conclude that it is always the area of the stimulus that is the determining variable, one should demonstrate equivalent thresholds should be demonstrated for a wider variety of aspect ratios e.g. horizontal rectangle 48 x 2 (aspect ratio 24:1) and vertical rectangle 2 x 48 (aspect ratio 0.042:1). Figure 5-8 illustrates an example in the difference in overlap between the resting and displaced positions of two such stimuli.

Future work could explore at what aspect ratio stimulus area ceases to be the relevant variable for horizontal rectangles.

An increased threshold, with widening of 95% confidence intervals, is found as the line area and the contrast is reduced (figure 5-7; table 5-3). The next chapter will further explore this relationship.

The results of this experiment, together with those of the following chapter, have been submitted to IOVS for publication (November 2005).

Figure 5-8. Diagrammatic illustration of overlap of stimulated retina by MDT displacement.

(i) Horizontal rectangle (48 x 2 pixels (128 x 5 min arc); aspect ratio 24:1).

There is no overlap of the retinal retina stimulated between position 1 and position 2 for displacements greater than the stimulus width [2 pixels (5 min arc)].

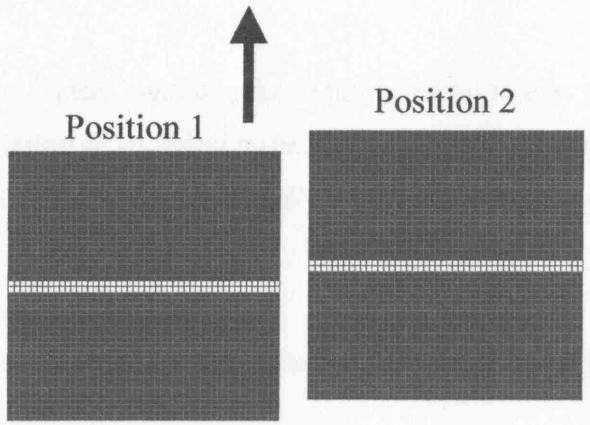

(ii) Vertical rectangle (2 x 48 pixels (2 x 128 min arc); aspect ratio).

Overlap of stimulated retina occurs for displacements up to 128 min arc.
"A" indicates the overlap that occurs for a displacement between positions 1 and 2.

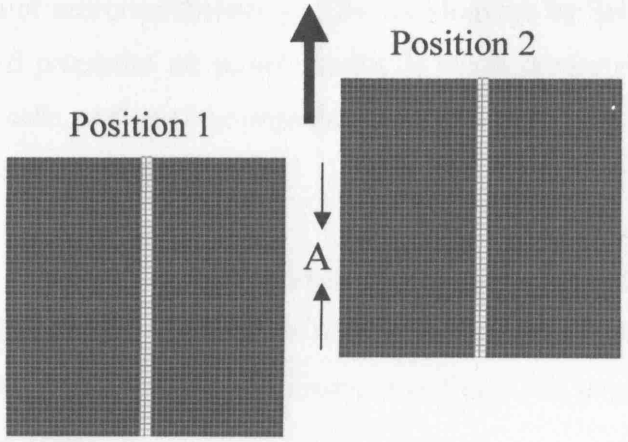

Chapter 6

STIMULUS CONTRAST, LINE LENGTH AND TOTAL STIMULUS ENERGY

6.1 CONTRAST SENSITIVITY

6.1.1 BACKGROUND

The ability to discern contrast plays a fundamental role in visual processing and determines the visibility of an object against its background. In psychophysical testing contrast is generally defined by Michleson's law, which states:

Contrast = % (L_{max} –L_{min}/L_{max}+L_{min})
L_{min} and L_{max} refer to the minimum and maximum luminance, respectively

Contrast sensitivity is achieved by a differential response to light increment and decrement by the on-off centre-surround properties of the retinal ganglion cells, which are mutually antagonistic (figure 6-1).

On-off cell properties were first identified in 1953 by electrophysiological studies in response to spots of light in the cat (Kuffler 1953) and rabbit (Barlow 1953). Selective blocking of neurotransmission on Rhesus Monkeys by Schiller in the 1980s revealed that on-off properties are present earlier in visual processing, at the level of the retinal bipolar cells, and continue segregated through to the visual cortex (Schiller 1984; Schiller et al. 1986; Schiller 1992).

On-off cells are characterized by circular ganglion receptive fields. A classical receptive field (CRF), figure 6-2) may be defined as the area of visual space where stimulation of photoreceptors causes an increase or decrease of a visual neuron's firing rate (Solomon et al. 2002).

Figure 6-1. Illustration of on-off properties of retinal ganglion cells, from Principles of Neuroscience (Kandel ER 1991).

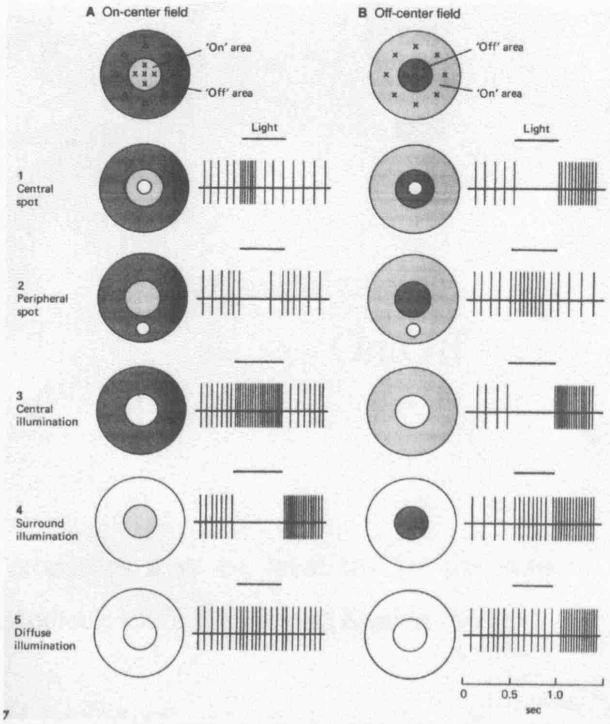

Central illumination (3): gives maximum response to on centre cells. Off centre cells are inhibited but response increases as stimulus is removed. Surround illumination (4): inhibits on centre and excites off center. Diffuse illumination (5): gives weak response (both centre and surround inhibited)

The extraclassical receptive field (ECRF), (figure 6-2) is a region of space where an appropriate stimulus can modify the response from a CRF (Solomon et al. 2002). Modification is achieved by differential neurotransmission. It may be inhibitory or excitatory and occurs at all stages of the visual pathway. For example, the responses of receptive fields at the level of the LGN are regulated by neuronal feed-back from V1 (Webb et al. 2002). Kapadia found the central receptive field (2-7 degrees from fovea) response in the occipital cortex of the macaque monkey to be adaptive in response to changes in contrast and texture. The excitatory receptive field is reported to be four times greater for a low-contrast stimulus than for a stimulus at high contrast (Kapadia et al. 1999). It is therefore appropriate to view a receptive field not as a static dimension, but one that is dynamic, constantly fluctuating in size in response to both local and global influences (figure 6-2).

Figure 6-2. Diagrammatic representation of the modulation exerted by the extraclassical receptive field on the on-off classical receptive field.

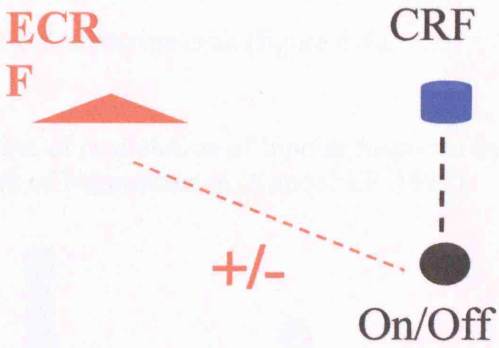

Receptive field properties may be idealized by the sum of two Gaussian functions (figure 6-3), (Rodieck 1965; Croner and Kaplan 1995).

Figure 6-3. Idealized receptive field properties by the sum of two Gaussian functions (from Rodieck 1965).

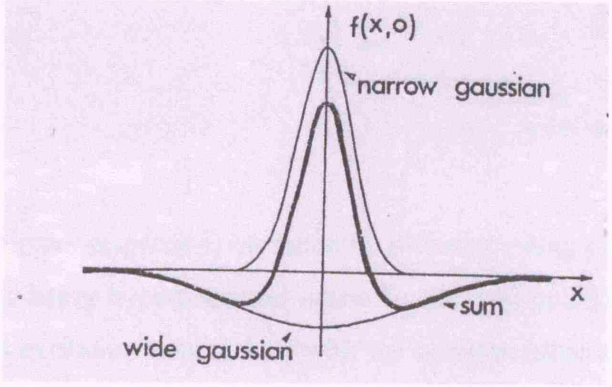

The central area of the receptive field increases with retinal eccentricity in direct relationship to estimates of the anatomical dendritic field size (Glezer 1965; Scobey and Horowitz 1976; Derrington and Lennie 1984; Croner and Kaplan 1995; Volbrecht et al. 2000).

Local retinal summation and receptive field properties are determined by dendritic arborization. This is quantified by the convergence ratio of the number of receptors to a single ganglion nerve fiber and the modulatory effects of the laterally spreading horizontal and amacrine cells (figure 6-4).

Figure 6-4. Illustration of modulation of bipolar response by horizontal and amacrine cells, from Principles of Neuroscience (Kandel ER 1991).

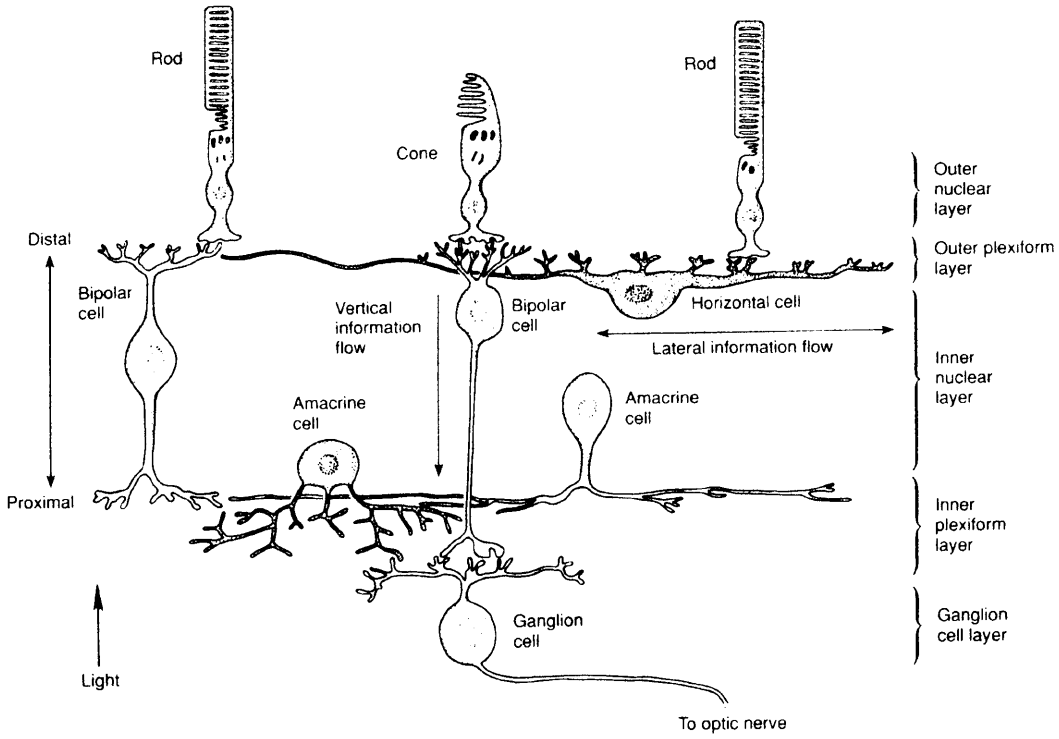

The on-off bipolar response is mediated by different gating properties of ions to glutamate: on-cells being hyperpolarized and off-cells hypopolarized. Each class of bipolar cell makes excitatory connections with the corresponding ganglion cell type, but the response is neuro-chemically adjusted by amacrine cells, whose dendritic endings are found in the inner plexiform layer (Schiller et al. 1986; Kandel ER 2000), (figure 6.4). Gaudiano suggests a model of "push-pull" bipolar cells which enables retinal ganglion cells to remain sensitive to deviations about the mean of non-linear photoreceptors (Gaudiano 1994).

Selective blocking of the "on" channel by a glutamate analogue is reported by Schiller to cause only slight impairment of colour, flicker and movement but longer times are required for their discrimination. No effect was noted on the centre-surround antagonism of off-cells or cortical orientation and direction selectivity (Schiller et al. 1986).

Contrast sensitivity function (CSF) varies with spatial frequency and is characterized by an asymmetric U-shaped curve (figure 6-5).

Figure 6-5. Contrast sensitivity as a function of spatial frequency under photopic conditions (from De Valois et al., 1974).

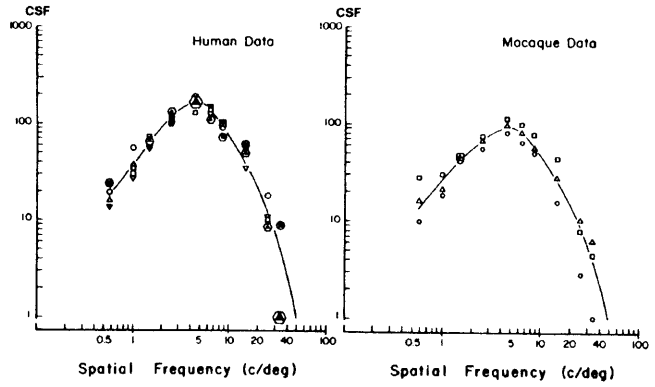

CSF is the reciprocal of the contrast necessary to detect a pattern at threshold. The peak of CSF varies with luminance and retinal eccentricity. CSF is determined by the density and spacing of retinal photoreceptors, the on-off properties of ganglion cells and probability summation.

6.1.2 MAGNOCELLULAR AND PARVOCELLULAR CONTRIBUTIONS TO CONTRAST SENSITIVITY AND MOTION PERCEPTION

There remains a widespread assumption that tests of motion are directed to the M pathway, which may be an over simplification. Clear segregation of the retino-geniculate pathways exists up to the LGN, but within the cortex multiple inter-connections occur, making the pathways less independently driven than once thought (figure 6-6), (DeYoe and Van Essen 1988; Maunsell et al. 1990; Merigan and Maunsell 1993; DeYoe et al. 1994).

Figure 6-6. Schematic diagram of magnocellular, parvocellular and konicellular pathways (from Merigan and Maunsell, 1993, Shabana et al., 2003).

Note segregation of pathways up to Lateral Geniculate Nucleus, with multiple crossovers thereafter.

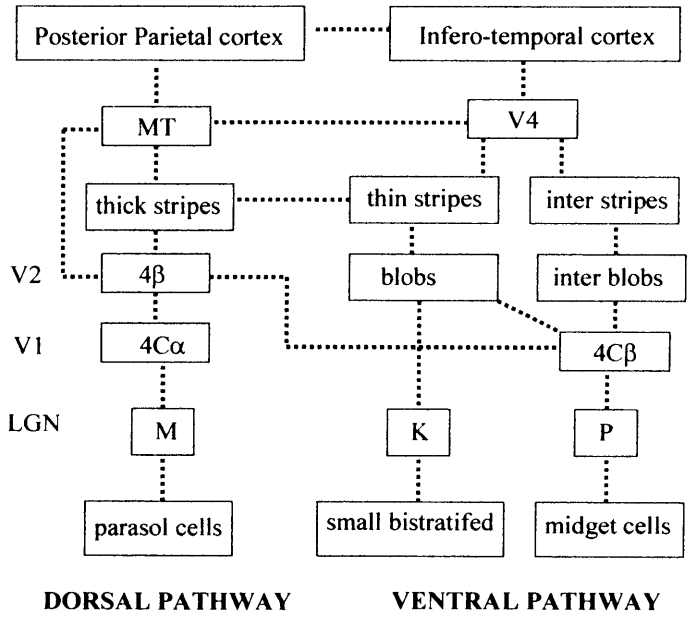

Electrophysiology studies on the LGN of primates show that both M and P cells show on-off properties. Both M and P cells begin to respond at 1 - 2% contrast, but M

cells saturate at 15% contrast and P cell responses increase more slowly, saturating at higher contrasts (Shapley et al. 1981).

Merigan assessed the effect of discrete lateral geniculate lesions in the macaque by testing sensitivity to grating stimuli of varying contrast and spatial frequency. The P pathway was shown to be principally responsible for contrast detection at low temporal and high spatial frequencies (Merigan et al. 1991b) and the M pathway for the visibility of motion at low spatial and high temporal frequencies (Merigan et al. 1991a).

Derrington investigated the electrophysiological response of M and P pathways to change of temporal frequency at the LGN of the Macaque using grating stimuli of varying contrast and spatial frequency. P cell responses were found to peak in the region of 10 Hz and M at 20Hz (Derrington and Lennie 1984).

The work of Merigan, Maunsell and Derrington suggest that it is appropriate to think of both M and P pathways as contributing to contrast and motion perception in primates. The M pathway acts as a motion detection system, showing greater sensitivity relative to the P pathway, to stimuli of high temporal frequency, low spatial frequency and low contrast.

In the central retina midget ganglion cells connect to a single cone via a bipolar connection. A central parasol ganglion cell, by comparison, may be supplied by ~ 40-140 cones with convergence ratios increasing with eccentricity. Dacey estimates the difference in dendritic field size between parasol to midget as 3:1 in the periphery and 10:1 at 3 degrees eccentricity (Dacey and Petersen 1992). Parasol cells are therefore characterized by large convergence ratios and spreading dendritic fields, which increase in size with eccentricity. Midget cells show low convergence with relatively small dendritic fields with maximal density at the fovea. This may represent an environmental adaptation, favoring motion detection in the periphery and fine spatial perception centrally.

Dendritic fields of parasol cells are larger in humans than macaques. Neural convergence would predict lower resolving ability, but higher luminance contrast sensitivity, for a motion stimulus (Dacey and Petersen 1992).

Raymond reported evidence of a parvocellular functional response for an induced motion stimulus (illusory motion, perceived from a variable contrast central grating, viewed against a variable contrast moving surround grating), (Raymond and Darcangelo 1990). The author suggested that the pattern of the observed responses was compatible with the initial processing of motion being performed by the transient response of the magnocellular pathway and the more detailed interpretation of contour being performed by the sustained response of the parvocellular pathway, a concept first described by Livingstone and Hubel (Livingstone and Hubel 1987; Livingstone and Hubel 1988).

Stephen Anderson provided psychophysical evidence that the sampling density of P cells, calculated from histological data, limits the motion acuity of drifting sinusoidal gratings, even for high velocity targets (Anderson et al. 1995).

Derrington found that change in temporal frequency altered the shape of both P and M spatial contrast sensitivity curves. He suggested that these patterns may be explained by the on-off centre and surrounds of retinal ganglion cells having different temporal properties, with the surround less sensitive to higher temporal frequencies (Derrington and Lennie 1984).

The receptive field size of both M and P cells increase with eccentricity, with the central radii of the M cells being twice that of neighboring P cells, giving an estimated contrast gain of x 6 (Croner and Kaplan 1995).

Bernadete and Kaplan reported both linear and non-linear dynamics of the primate P system. The first order response of centre and surround depends linearly on contrast. A time delay of approximately 8 msec was found in the first order surround

response which extended to a further 1-5 msec at the LGN (Benardete and Kaplan 1997a). A non-linear response was found in the second order response at the LGN, steady illumination of the surround increasing the contrast gain (the cellular response to change in contrast (Croner and Kaplan 1995) of off-cells and decreasing the contrast gain of on-cells (Benardete and Kaplan 1997b).

Bernadete and Kaplan found that the temporal frequency response of M cells is altered by the level of stimulus contrast: as contrast increases, the peak of frequency of response is shifted to higher temporal frequency whilst P cells respond uniformly (Benardete et al. 1992). The contrast gain of magnocellular cells is approximately ten tines greater than the parvocellular, with the difference in sensitivity being evident at a retinal level (Kaplan and Shapley 1986). Multi-electrode recording in primates by Chichilnisky demonstrated functional asymmetry between the on and off responses of parasol cells. On-cells were found to be 20% larger in diameter than off-cells and to show faster response times (Chichilnisky and Kalmar 2002).

Modulation of centre and surround response is indicated by the Neuropeptide Y class of amacrine cells, where selective ablation results in both on and off cells showing a decrease in the size of the surround, with loss of tuning to low spatial frequencies (Sinclair et al. 2004).

The hypothesis of asymmetry of on-off pathways and amacrine modulation is supported by anatomical evidence. Dacey found the dendritic field of human on-centre cells to be 30-50% larger than off-centre for both parasol and midget cells (on-centre and off-centre were identified by stratification in the inner-third and outer-third of the inner plexiform layer respectively), (Dacey and Petersen 1992). Anatomical tracers reveal coupling of at least two different sub-groups of amacrine cells to parasol cells which is not evident to midget cells (Dacey and Brace 1992).

Psychophysical correlates of magnocellular and parvocellular contrast gain in human subjects have been demonstrated for temporal and spatial sensitivity (Pokorny

and Smith 1997; Leonova et al. 2003). Burr compared response times for detecting the onset of motion of sinusoidal gratings modulated in luminance or colour contrast. Responses to luminance gratings indicated very low saturating contrast and high gain and colour gratings high semi-saturating contrast and low gain. This suggests each is controlled by different mechanisms, possibly M and P systems (Burr and Corsale 2001).

6.1.3 ON-OFF CELLS IN GLAUCOMA

When modelling altered patterns of response in glaucoma it is of interest to consider that off-centre cells are reported to be more resistant to induced IOP elevation than on-centre and the centre more resistant than the surround (Zhou et al. 1994).

One would predict from Shiller's work that the unequal resistance of on-centre and off-centre cells would not impair motion sensitivity but longer times would be required for their discrimination (Schiller et al. 1986). Chichilnisky's research would suggest greater delay for the M pathway (Chichilnisky and Kalmar 2002). Clinically, this would be expressed by longer response times.

The lower resistance of the on-off surround compared to the centre would alter the temporal modulation function with reduction in contrast gain. From the work of Derrington, and the Neuropeptide experiment cited above, one would predict loss of tuning to high temporal and low spatial frequencies respectively (Derrington and Lennie 1984; Sinclair et al. 2004), functions normally associated with the M pathway.

6.2 THE PSYCHOPHYSICS OF MOTION DISPLACEMENT

The MDT uses small stimuli (< 2 degree) of high luminance value (112 cd/m^2) set against a lower luminance background (10cd/m^2), giving a high contrast of 84%. The stimulus oscillates at 200 msec per cycle, which is equivalent to 5Hz. These features would suggest both parvocellular and magnocellular contributions if Derrington, Merigan and Maunsell's findings, using a grating stimulus, are applicable to the single line stimulus of MDT (Derrington and Lennie 1984; Merigan et al. 1991a; Merigan et al. 1991b).

The MDT methodology creates the illusion of apparent motion by spatial displacement of the line stimulus between computer frames. It is regarded as "local motion," which assumes the sampling of the image at two points in space at slightly different times by "bilocal" detectors (Snowden and Braddick 1989).

Motion displacement has long been recognised as a hyperacuity stimulus, offering a sensitivity that is beyond that which would be predicted from anatomical ganglion cell spacing (Exner 1875; Westheimer 1975; Scobey and Horowitz 1976). The MDT task is to discriminate the positional change between two lines and may thus be categorized as a temporal form of vernier acuity.

Scobey and Horowitz explored receptive field properties of displacement sensitivity by electrophysiological testing in cats (Scobey and Horowitz 1972) and primates (Scobey and Horowitz 1976; Scobey 1981).

The centre diameter of a receptive field was measured by the "constant response" method, where the distance between two test sites that gave an auditory response to the brightest spot of light available was measured (Scobey and Horowitz 1976).

Different responses to unidirectional spot displacement were found within the receptive field. Maximum sensitivity to unidirectional spot stimuli was recorded in the border zone of the centre-surround area of a retinal receptive field. By contrast, there was no recordable response to displacement at the geometric centre of the receptive field. Displacement to a site of increased sensitivity was only effective for on-centre cells and decreased sensitivity only for off-cells (Scobey and Horowitz 1976). They concluded that motion displacement threshold (D_l) may be predicted by the sensitivity gradient of the retinal ganglion cell receptive field (RF) and the incremental threshold (ΔI) at that site (figure 6-7). They suggested that as stimulus luminance is increased more eccentric areas of the RF will be stimulated where the sensitivity gradient is steeper with consequent reduction in D_l (Scobey and Horowitz 1976; Johnson and Scobey 1980).

Scobey and Johnson investigated the effect of changing line length and luminance using a unidirectional stimulus in humans. Elevation of displacement threshold was found as line length and luminance were decreased, with an increase in mean threshold and standard deviation with eccentricity (Johnson and Scobey 1980; Scobey and Johnson 1981). MacVeigh found similar results using as oscillatory displacement stimulus, presented at low temporal frequency (2Hz), in the presence of stationary references (MacVeigh et al. 1991).

Johnson drew attention to the similarity of the psychophysical peripheral displacement results in humans with those of the rhesus monkey (Scobey and Horowitz 1976). Johnson concluded that variation in threshold with changes in stimulus size and luminance can be predicted from receptive field properties (figure 6-7, (Johnson and Scobey 1980; Scobey and Johnson 1981).

Figure 6-7. Prediction of motion displacement threshold based on receptive field characteristics (from Johnson and Scobey, 1980).

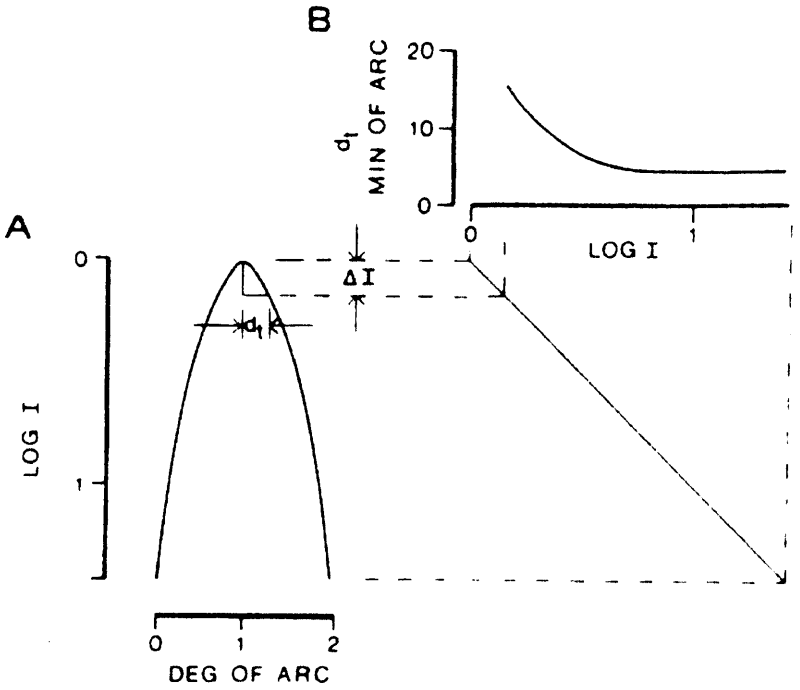

Δ1 incremental threshold; d_t: displacement threshold min arc

A: Sensitivity profile of an on-centre retinal ganglion RF

B: Displacement threshold sensitivity (D_t min arc) is plotted as a function of log I.

ΔI: average incremental threshold for the central region of receptive field

D_t: predicted displacement threshold based on the assumption that movement through the sensitivity gradient equal to ΔI will generate a threshold response.

The previous chapter demonstrated constant MDT threshold for equivalent stimulus line length, whether the stimulus was a single line or distributed amongst three shorter lines, independent of their line separation. These findings give insight into MDT receptive field properties and suggest that the testing was conducted within an area of linear summation for the dimensions investigated.

It is interesting to consider how MDT summation properties compare to those of SAP. SAP measures DLS and the threshold is defined by the relationship of the area (A) and intensity (I) of the stimulus giving the relationship IA^n = constant. The summation coefficient (n) varies for different conditions: where the stimulus lies within Ricco's critical area n = 1. (AI = constant). For larger stimuli summation is incomplete and the threshold is determined by probability summation, which is achieved by recruitment of adjacent receptive areas (Robson and Graham 1981). Piper's law holds when n = 0.5 (Glezer 1965).

Wilson estimated Ricco's area under photopic conditions (Wilson 1970). Anderson applied Wilson's estimates to SAP and calculated that the standard stimulus (Goldmann III) is the same size as Ricco's area at 40 degrees, 2.5 times Ricco's area at 25 degrees and approximately 13 times at 5 degrees eccentricity. This means the SAP threshold is determined by probability summation and covers many receptive fields (Anderson 2005).

Ricco's area is psychophysically defined and it has been hypothesized that it may correlate with the central area of retinal on-off ganglion cells found in electrophysiological animal studies (Barlow 1953; Kuffler 1953; Glezer 1965; Wilson 1970). However, in man and the macaque Ricco's area measures larger than the measured dendritic field size (Watanabe and Rodieck 1989), suggesting summation across retinal ganglion cells and possible higher neural input. The magnification effect serves to compensate for the decreasing GCD with eccentricity, with corresponding diminution of the representative area of visual cortex (Swanson et al. 2004).

Estimates of Ricco's critical area vary according to the type and size of the stimulus, indicating different patterns of spatial filtering (Swanson et al. 2004). Ricco's area changes with eccentricity and this is thought to reflect differences in ganglion cell type, density and neural convergence (Felius et al. 1996; Volbrecht et al. 2000).

Average receptive field diameters of macaque M and P cells are given in figure 6-8 and show a clear increase in size with eccentricity. In human vision, central motion receptive fields, estimated using drifting sinusoidal gratings, are reported to be as long as they are wide for all spatial frequencies, varying from 0.12 cycle at 0.1 c/deg to 0.52 cycle at 10.0 c/deg (Anderson and Burr 1991).

A larger critical area has been found for blue-on-yellow stimuli, directed to the konicellular pathway, compared to red-on-white stimuli, directed to the parvocellular (Felius et al. 1996). Volbrecht measured the maximum area of complete summation in humans for short and long wavelength cone mechanisms. Ricco's area was found to increase monotonically for long wavelength from 0-20 degrees eccentricity but was more erratic for short wavelength. The pattern of results was interpreted as representative of the anatomical differences in ganglion cell density of different cell types and their neural convergence (Curcio and Allen 1990; Dacey and Petersen 1992; Volbrecht et al. 2000).

S-cone stimuli show differences in incremental and decremental response, supporting the existence of both an "on" and "off" short-wave pathway (Vassilev et al. 2003). Currently unpublished work by Vassilev found Ricco's area to be constantly in the region of 1.6 -1.8 times larger than the small bistratified dendritic tree, independent of eccentricity (Anderson 2005).

There are no publications to inform whether Ricco's Law is applicable to a MDT stimulus, which is historically assumed to be specifically directed towards the magnocellular pathway (Livingstone and Hubel 1987).

Figure 6-8. Average receptive field centre diameters of Macaque magnocellular and parvocellular cells (Swanson et al., 2004a).

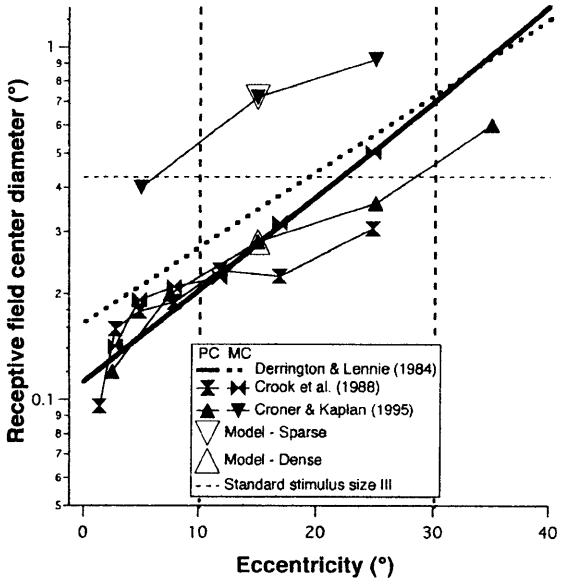

6.3 INVESTIGATION OF THE RELATIONSHIP OF STIMULUS AREA AND CONTRAST WITH MDT THRESHOLD, WITH RESPECT TO RICCO'S LAW

A study was designed to explore the relationship between stimulus area and contrast with MDT stimulus threshold. The MDT stimulus, which is composed of three oscillations at 200 msec per cycle, may show different patterns of summation when compared to the unidirectional displacement stimulus of Johnson (Verdon-Roe et al. 2000) and the oscillatory displacement stimulus of MacVeigh, which was performed in the presence of stationary references at a temporal frequency of 2Hz (MacVeigh et al. 1991).

A further aim of this study was to assess the characteristics of MDT frequency of seeing curves in response to change of contrast and line length. In addition, an entirely novel approach was taken, whereby the MDT threshold was calculated as a combined relative energy function of the stimulus (stimulus area * [stimulus luminance – background luminance]), in order to investigate the application of Ricco's Law to MDT.

METHOD

The MDT stimulus was presented in the nasal field (-27,3°) and the right eye of two experienced subjects (aged 47 and 31 years) was tested with peripheral refractive error corrected, as previously described (chapter 4). The test background was maintained at 10 cd/m^2 throughout. Five values of stimulus luminance (112, 56, 34, 24, 17 cd/m^2) were used to achieve 5 values of Michelson contrast (84%, 70%, 55%, 40%, 25%). Each contrast value was assessed for five horizontal line lengths of 48, 32, 16, 8 and 4 pixels (128, 86, 43, 22, 11 min arc). The stimuli of this experiment were of constant width (2 pixels, 5 min arc) and the change in area therefore equals the change in line length.

For each test, the line stimulus was programmed to pass through 5 presentations each of 7 randomized displacements (0, 1, 2, 3, 5, 7, 9 pixels; 0, 3, 5, 8, 14, 19, 24 min arc). The 25 test paradigms were applied once in a randomized order. This was repeated twice, so that each subject underwent 75 tests in total. The number of tests was limited to eight per session, with rest intervals of five minutes between tests to avoid subject fatigue. Additional tests were undertaken where no responses were generated (all presentations unseen) for small lines of low contrast. Where this occurred the upper limit of displacement was increased to 40 min arc (5 presentations of 7 displacements: 0, 5, 7, 9, 11, 13, 15 pixels; 0, 14, 19, 24, 30, 35, 40 min arc).

DATA ANALYSIS

The three test results for each parameter were merged for each individual. FOS curves were generated and the threshold was taken as the displacement corresponding to 50% seen of the probit fitted curve.

The results of subjects 1 and 2 were averaged. The mean MDT threshold was plotted as a function of contrast (for each line length) and stimulus area (for each value of contrast) on both linear and log coordinates. The interquartile range (IQR; difference between 75% and 25% of the probit fitted curve) was calculated to give an indication of the psychometric function slope (Chauhan et al. 1993b; Westcott et al. 1999). The relation between mean log MDT threshold and log IQR was explored by linear regression analysis.

Stimulus energy was calculated relative to background luminance as follows: relative stimulus energy = stimulus area * (stimulus luminance – background luminance). The background luminance was deducted from the stimulus luminance to account for the fact that when the MDT stimulus is displaced it moves to an area that is not black, but of constant background luminance (10 cd/m^2). The relation between mean log MDT threshold and log relative stimulus energy was explored by linear regression analysis.

The FOS curves of each subject illustrate a similar pattern of shallowing of the slope and widening of the 95% CI and IQR, as contrast and line length is reduced, as shown by the selected examples in figure 6-9. Differences in function slopes remained when MDT thresholds were plotted on a logarithmic scale. Note the steep curve of the longest line length (128 min arc) at the highest contrast (85%), with low IQR and narrow CI (figure 6-9A). A complete record of this study's FOS curves is given in the appendix (figure 14-2).

No threshold was recorded for the smallest range of displacements (0 - 24 min arc) when testing the smaller line lengths at low contrast (subjects 1 and 2: 11, 22 and 43 min arc line lengths at 25% contrast and the 11 min arc line length at 40% contrast; subject 1: 22 min arc line length at 40% contrast). The increase in the upper limit of displacement to 40 min arc enabled only one further FOS curves to be measured for each subject (subject 1: 22 min arc line length at 40% contrast; subject 2: 43 min arc line length at 25% contrast).

Analysis of MDT threshold as a function of percentage contrast showed a curvilinear relationship for each line length, with an increase of 50% seen threshold and widening of 95% CI as contrast was reduced (figure 6-10). Relationships became linear when plotted in log-log coordinates. (figure 6-11; table 6-1). [Comparative 50% seen threshold results are given in the appendix (table 14-5) for merged FOS curves data (FOS curves merged for each individual parameter prior to probit analysis) and unmerged FOS data (probit analysis performed for each individual FOS curve)].

A linear relationship (slope 1.3) was found between log MDT threshold and log IQR (figure 6-12). A linear relationship was also found between log MDT threshold and log relative stimulus energy. The slope measured -0.5, indicating that the MDT threshold is related to the square root of the stimulus energy (figure 6-13).

Figure 6-9. Examples of MDT frequency of seeing curves for individual subjects.

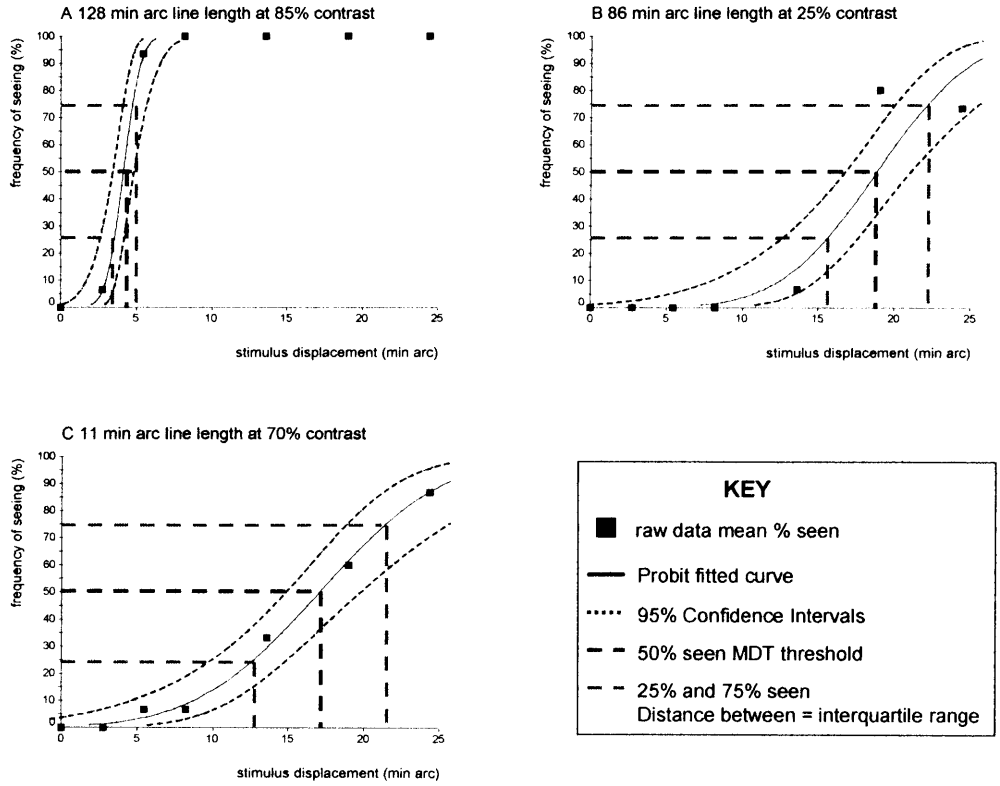

Figure 6-10. Mean MDT thresholds, with 95% confidence intervals, as a function of percentage contrast for each line length.

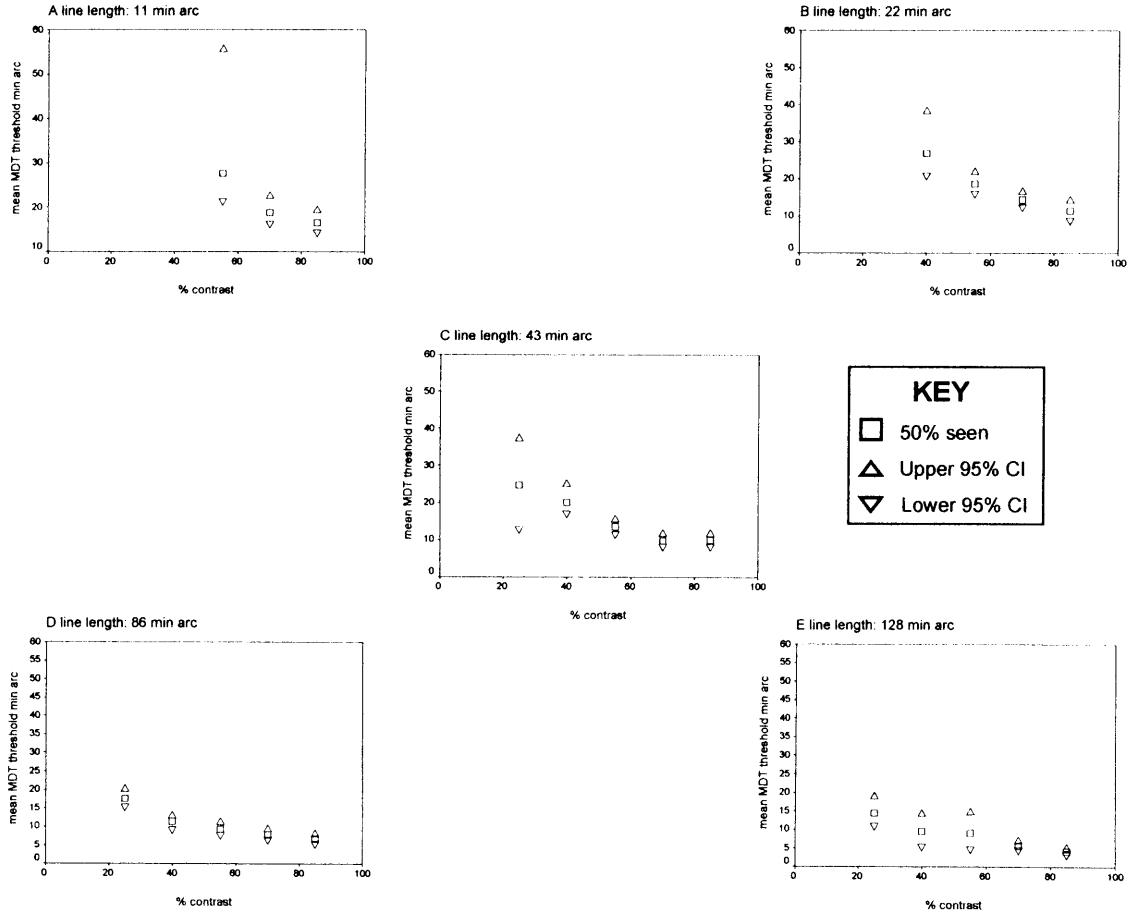

Figure 6-11. Plot showing linear relationship of log mean MDT threshold and log percentage contrast for each line length.

Plots of each individual subject are given in the appendix, figure 14-3.

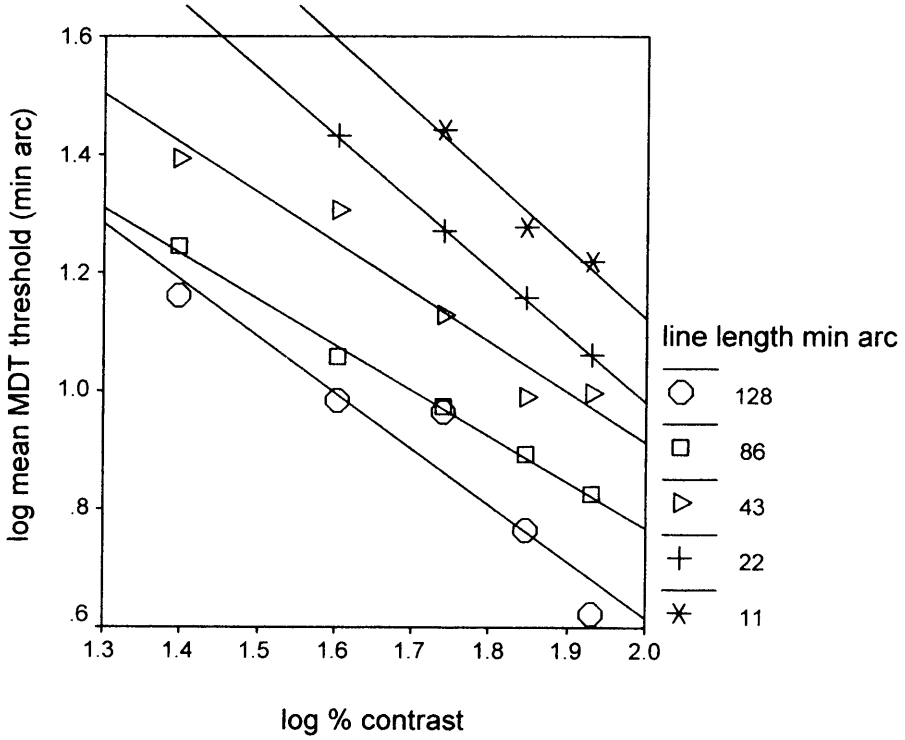

Table 6-1. Slope values of log MDT threshold as a function of log percentage contrast.

Data from figure 6-11.

Line Length (min arc)	Slope (95% CI)	R2	P
128	- 0.95 (- 1.28, - 0.62)	0.92	0.011
86	- 0.78 (- 0.84, - 0.71)	1.00	< 0.001
43	- 0.84 (-1.07, - 0.61)	0.95	0.005
22	-1.12 (- 1.16, - 1.10)	1.00	< 0.001
11	-1.18 (- 1.69, - 0.68)	0.96	0.136

Figure 6-12. Plot of log interquartile range as a function of log MDT threshold.

Slope: 1.26 (95% CI 0.98, – 1.54; $R^2 = 0.79$; P: < 0.001).

Plots of each individual subject are given in the appendix, figure 14-4.

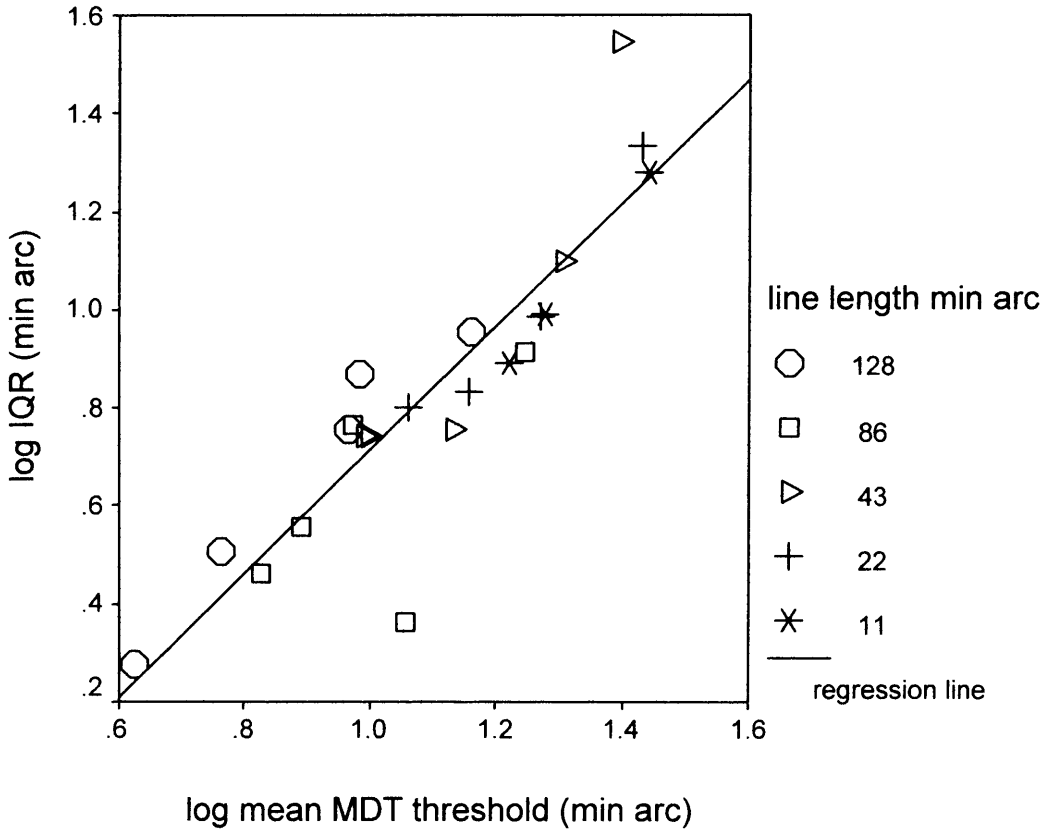

Figure 6-13. Plot of log MDT threshold as a function of log stimulus energy.

Stimulus energy = stimulus area * [stimulus luminance – background luminance].

Slope: – 0.45 (95% CI - 0.49, - 0.41; $R^2 = 0.96$; P: < 0.001).

Plots of each individual subject are given in the appendix, figure 14-5.

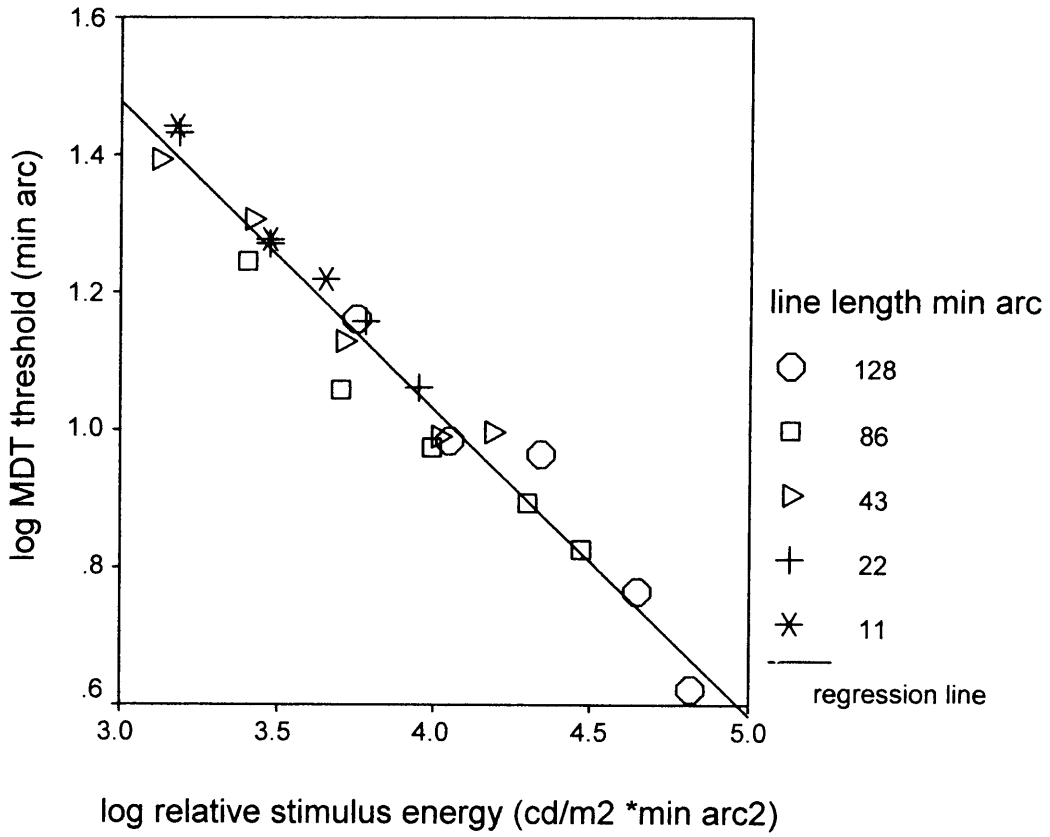

Displacement acuity is traditionally considered as a function of edge jump, with summation calculations being made in relation to line edge-length (Foley-Fisher 1973; Lee et al. 1995). The results of the second experiment of the previous chapter suggest that it is the total area of the stimulus, as opposed to its edge-length, that is the determining factor (figure 5-7; table 5-3). The results of this experiment indicate that it is the total energy of the stimulus with respect to its background that is the important (figure 6-13).

A clear trend of decreasing oscillatory MDT threshold with increasing line length and luminance is found (figure 6-10), which is consistent with previously reported findings of summation experiments for line displacement stimuli (Johnson and Scobey 1980; MacVeigh et al. 1991).

A re-analysis of 14 studies, which examined the relationship between contrast and vernier threshold as a power function, found log-log slopes ranging between - 0.4 and - 1.0 (McIlhagga and Paakkonen 2003). In this study we report slopes ranging between - 0.8 and -1.2 (table 6-1).

The IQR is directly scaled with the MDT threshold (figure 6-12). As line length and contrast are reduced there is shallowing of the FOS slope with elevation of IQR (figure 6-9), which is of similar appearance to that seen in glaucoma, (Westcott et al. 1999) where retinal ganglion cell function is impaired (Quigley et al. 1989; Harwerth et al. 1999). The increased variability seen with reduction in sensitivity is similar to that found by Henson, when assessing SAP in normal and diseased eyes, and which he attributed to a difference functional ganglion cell density (Henson et al. 2000).

The conventional view is that the M pathway acts as a motion detection system which shows greater sensitivity relative to the P pathway, to stimuli of low contrast,

high temporal frequency and low spatial frequency (Derrington and Lennie 1984; Merigan et al. 1991a; Merigan et al. 1991b). The MDT test conditions of this study operate at a moderate temporal frequency (5 Hz), for stimuli of high spatial frequency, over a wide range of contrast (25%-85%). It is therefore possible that responses from both M and P contributions are invoked. However, this view is contradicted by a recent study, which suggests that the M pathway is primarily responsible for vernier acuity thresholds, with higher neural mechanisms being responsible for spatiotemporal integration (Sun et al. 2004). Oscillatory displacement thresholds, measured in the presence of stationary references, have been previously shown to saturate at contrasts below 15%, consistent with the M pathway contrast response function (Watkins and Buckingham 1992).

The energy plot (figure 6-13) shows a constant stimulus/response relationship over the range of contrasts assessed, which could apply to either a single or multiple pathway contribution. There is no evidence for a transitional shift in threshold or slope, which would be a possible finding if different pathways were to predominate under different stimulus conditions within the experimental design. All stimuli were presented at contrasts equal to, or greater than, 25%, which is above the level at which the M pathway responses are generally considered to saturate.

However, the results of this study suggest that it is not the contrast *per se* that modulates the response, but the stimulus energy (figure 6-13), so that saturation for higher contrast stimuli occurs only if the stimulus is also large. Saturation is generally measured with grating stimuli and so the "total energy" within a "receptive field" may be much larger than with the single line displacement stimuli used for this experiment. It is not possible, therefore, to hypothesize mediation of the response by a particular cell type for these experimental conditions.

Table 6-2 shows the estimated number of RGCs stimulated by lines of varying length. Values were approximated using estimates of human, non-specific GCD (Curcio and Allen 1990) and coverage values. The methods of the calculations follow the table.

The table may under-estimate the actual number of receptive fields stimulated, in that no allowance is given for the optical effect of line spread (Westheimer 1987; Wachtler et al. 1996).

Table 6-2. Estimated number of retinal ganglion cells stimulated by MDT stimulus, in the nasal field at 30 degrees eccentricity (Curcio and Allen 1990; Dacey and Brace 1992; Dacey and Petersen 1992; Dacey 1993; Dacey 1994).

RGC: retinal ganglion cell

Each length was of uniform width of 2 pixels (5 min arc).

		Number of RGCs stimulated by target			
Line Length Min arc	Total RGCs	M "on" and "off"	P "on" and "off"	P "on"	P "off"
128	18	12	8	3	5
86	12	9	5	2	3
43	6	6	3	1	2
22	3	3	2	<1	1
11	2	1	1	<1	<1

Calculation of number of ganglion cells stimulated by line stimulus at -27,3

Line length mm: degree subtended x magnification factor.

Eccentricity = $\sqrt{(x^2) + (y^2)}$
Therefore eccentricity at x = 27 and y = 3 is: $\sqrt{[(27 * 27) + (3 * 3)]} = 27.16$

Magnification = $0.286 - [(0.000014 * (ecc^2)]$, (Rudnicka et al. 1998).
Therefore, magnification at 27.16 is $0.286 - ((0.000014 * (27.16 * 27.16)) = 0.276$

Number of ganglion cells stimulated = line length mm x linear estimate of ganglion cell numbers.
Estimated ganglion cell density at 27.16 degrees = 877 ganglion cells per mm^2 (Curcio and Allen 1990; Garway-Heath et al. 2000a)
Linear estimate = $\sqrt{GCD}$ = 30 ganglion cells per mm.

Example of calculation of the number of retinal ganglion cells stimulated at 27,3 by a 128 min arc line length:

Line length is 128 min = 2.13 degrees = (0.276 * 2.13) mm = 0.588 mm
Line width is 5 min = 0.08 deg = 0.02208 mm

Estimated ganglion cell density at 27 degrees = 877 ganglion cells per mm^2 (Curcio and Allen 1990; Garway-Heath et al. 2000a).
Linear estimate = 30 ganglion cells per mm
Therefore stimulus length stimulates 0.588 x 30 = 17.6 ~18 ganglion cells (all types)
width stimulates 0.02208 x 30 = 0.66 ganglion cells (all types)

Calculation of the number of P and M cells and coverage values for each "on" and "off" mosaic

The number of P (midget) and M (parasol) cells was estimated from percentage estimates of each cell type from primate histological data. At 30° eccentricity this approximated to 20% parasol and 45% midget (Dacey 1994).
Coverage is defined as the average number of cells whose receptive-field centre includes the same point in visual space. It is identical to overlap (the average number of cells whose receptive field cover that of a given cell (Schein and de Monasterio 1987). The anatomical estimate of coverage is given by cell density mm^2 * dendritic field area mm^2 (Dacey 1994). The calculations are adjusted for coverage of each "on" and "off" mosaic (Dacey and Petersen 1992; Dacey 1993). The estimated coverage is 3:1 for the parasol cells and 1:1 for the midget cells (Dacey 1994). Calculations are further adjusted for the higher cell density of "off" P cells, located in the outer inner plexiform layer (IPL), compared to "on" P cells which are located in the inner IPL (outer: inner density ratio of 1.7:1), (Dacey 1993). M cells are assumed to be divided equally between "off" and "on" mosaics.

All presentations at all displacements for the two shortest line lengths (11 and 22 min arc) were unseen, when testing at low contrast (25% – 40%), even when the displacement range was increased to 40 min arc. The two smallest lines stimulate only small numbers of ganglion cells (table 6-2). It is possible that the energy these stimuli exert at low contrast is insufficient to generate a response. Alternatively, the displacement required at these energy levels may be greater than the detector receptive field.

The anatomic extent of the dendritic tree corresponds to the electrophysiological central receptive field, but may be smaller than the psychophysical receptive field estimate (Wassle et al. 1983; Croner and Kaplan 1995). In humans, dendritic tree measurements approximate to 60 min arc diameter for M cells and 20 min arc diameter for P cells, at 30 degrees eccentricity, in the nasal field (Dacey and Petersen

1992). Human dendritic trees are larger than their counterparts in the macaque, predicting larger receptive fields (Dacey and Petersen 1992). The estimated psychophysical receptive field size in the Macaque, at 30 degrees eccentricity, for drifting sinuoisoidal gratings approximates 42 min arc (Derrington and Lennie 1984; Crook et al. 1988; Swanson et al. 2004). The estimated coverage is 3:1 for the parasol cells and 1:1 for the midget cells (figure 6-14), (Dacey 1994).

Figure 6-14. Estimated dendritic central receptive field size and overlap for parasol and midget cells at 30 Degrees eccentricity for each "on" and "off" mosaic (from Dacey and Petersen, 1992; Dacey 1994).

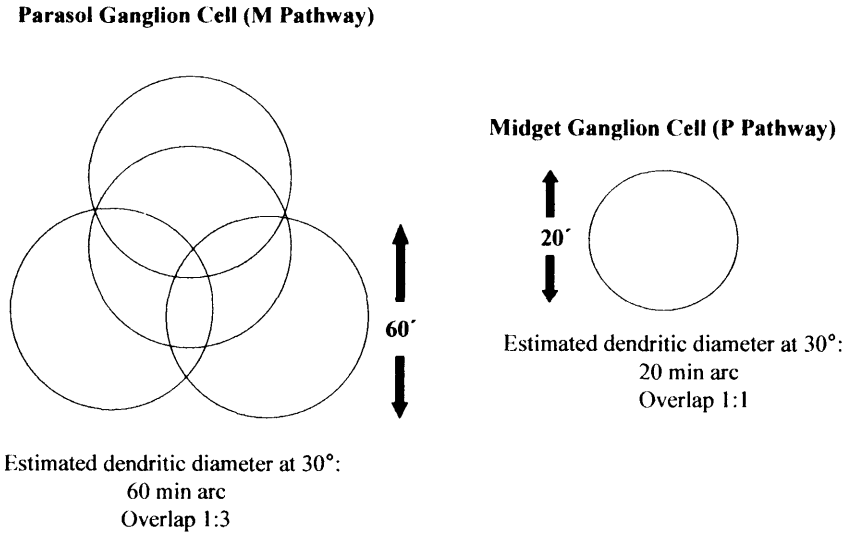

As the longer line lengths extend over many ganglion cells, yet result in the same threshold as shorter, brighter lines of equivalent energy (area x luminance, figure 6-13), it may be deduced that linear summation of retinal ganglion cell responses occurs for the line lengths used in these experiments.

Ricco's law is therefore applicable to the MDT stimulus, within the experimental conditions described. That Ricco's law holds may be deduced from figure 6-13, where the same MDT threshold is found for different combinations of constant product of line length and luminance.

The slope of approximately 0.5 of log MDT threshold against stimulus energy (figure 6-13) is of special interest. In order to interpret this finding the different processing mechanisms associated with SAP and MDT need to be considered.

SAP measures DLS and the threshold is defined by the relationship of the area (A) and intensity (I) of the stimulus giving the relationship IA^n = constant. By contrast with DLS, electrophysiological studies of spot light displacement in primates indicate that all retinal ganglion cells respond to movement of < 10% the diameter of their receptive field. It is thought that intra-receptive field directional sensitivity is achieved by pooling of the excitatory and inhibitory responses of overlapping on-off receptive fields (Scobey and Horowitz 1976; Scobey 1981). The displacement threshold is thus determined by the sensitivity gradient between the two stimulus positions (Johnson and Scobey 1980; Zhang and Reid 2005). It is possible that as the line stimulus moves from one position to another off-cells and on-cells are stimulated as an alternating decremental-incremental response.

A route to understanding the relationship between stimulus energy and MDT threshold lies in ideal detector modelling, whereby a hypothetical model of optimal performance is created for known variables.

Geisler predicted a slope of 0.5 between log threshold and log stimulus intensity for a hyperacuity stimulus, calculated on the basis of a number of pre-neural factors and an ideal detector. Performance was predicted to increase with longer line length. The calculation estimated the average total number of effectively absorbed quanta per light source for receptor size of 0.28 min arc^2 at 0.2 sec duration. A hexagonal retinal

receptor lattice (figure 6-15) was used to generate predictions for foveal spot stimuli, with the diameter of the receptors assumed to be 0.6 min arc.

Figure 6-15. Hexagonal Lattice Configuration: assumes centre-centre distances of any neighbouring elements form an equilateral triangle (from Geisler, 1984).

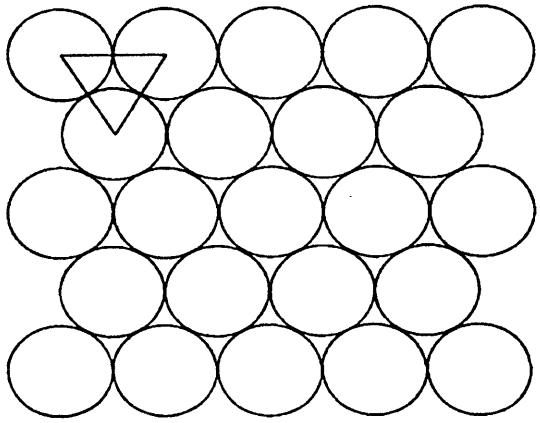

Line spread function was used to estimate the retinal distribution of light for a 2 mm pupil (figure 6-16). The optimal receptive field was built by simple linear summation and inhibition (Geisler 1984).

Figure 6-16. Calculation of retinal line spread for a 2 mm pupil (represents the sum of two gaussian functions), (from Campbell and Gubisch, 1966, Geisler, 1984).

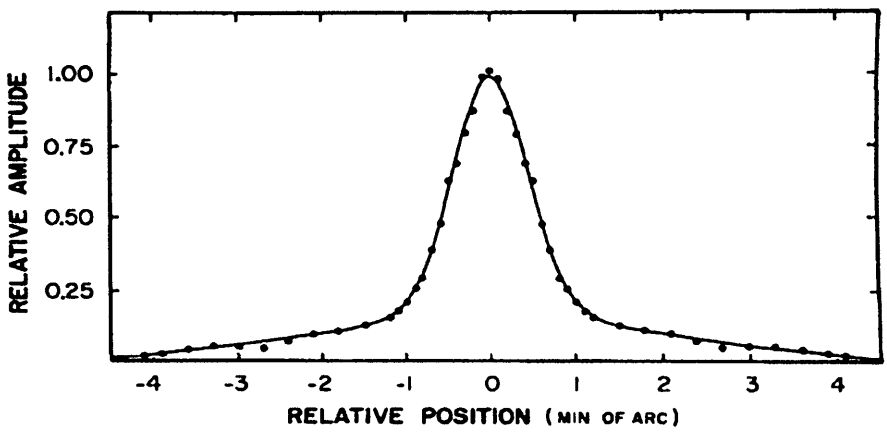

The quantal absorption of photons by the retinal detectors is a source of noise,

In a later paper, Geisler advises consideration of both pre-neural and neural factors, with receptive fields regarded as free parameters (Geisler and Diehl 2002). Receptive fields are dynamic and neuro-chemical contributions contribute to their state of flux at any stage of the visual pathway which is described by the Poisson distribution. Noise is a constant feature in all sensory pathways and signal detection is dependant on the average number of quantal absorptions to elicit one extra impulse. This determines gain control and the signal-to-noise ratio grows in proportion to the square root of the stimulus area (Rose 1948a; Rose 1948b; Barlow and Levick 1969). M cells have more inherent noise and therefore greater gain. This manifests at low to moderate contrasts of < 20 - 40% and therefore may only apply to the lowest contrast condition of this study, although the MDT stimulus differs from a grating in the total energy delivered (Lee et al. 1993; Wachtler et al. 1996).

Previous studies have suggested that vernier acuity is predicted from changes in the relative luminance of the retinal image (Westheimer and McKee 1977; Morgan and Aiba 1985; Levi et al. 2000). The results of the present study suggest that MDT sensitivity is achieved by detection of the total energy difference as the stimulus is displaced with respect to its environment. The MDT stimulus is displaced in position over time and is therefore probably best modelled using a three-dimensional space-space-time filter input (Anderson and Burr 1991).

Adelson and Bergen suggested a two-stage hierarchal model of local motion signals, in which the first stage represents pairs of linear filters that are orientated in space and time and tuned in spatial frequency. The response of each pair is squared and summed. The second stage computes "motion energy" on the assumption of neural opponence (Adelson and Bergen 1985; Georgeson and Scott-Samuel 1999; Rainville et al. 2005). The MDT stimulus is presented as an oscillating square "A-B-A" stimulus of apparent motion. The displacement threshold may therefore represent the summed difference of the on-off response and also opposing directional filters, as

the stimulus is displaced from position "A" to second position "B" and back to starting position "A."

The novel finding of this study is that the MDT threshold is related to the square root of the stimulus energy for the stimulus conditions described. Thus, a new principle, TED (threshold energy displacement), is proposed to apply to MDT summation properties, giving the relationship: $T = K \sqrt{E}$ (where T = MDT threshold; K= constant; E = stimulus energy [stimulus area)* [stimulus luminance – background luminance]). TED offers a numerical basis for modelling the structural-functional relationship of MDT thresholds and will be applied to the new multi-location MDT test under development. It is anticipated that there is the potential to quantify neural losses from glaucoma with MDT using the principles described for SAP (Garway-Heath et al. 2000a; Harwerth et al. 2004; Swanson et al. 2004).

Future work includes exploration of the limits of linearity for the relationship of MDT threshold with stimulus energy, and the variation of the relationship between threshold and stimulus parameters with eccentricity. Ricco's area of complete summation decreases as the square root of the background illumination increases (Glezer 1965). It would therefore also be of interest to investigate the relationship of MDT threshold with stimulus energy for different background illumination. Fellman found increasing sensitivity with decreasing background luminance for both normal and glaucomatous subjects, with the improvement being greater in the control group (Fellman et al. 1988). Anderson therefore suggests that use of a lower background illumination may improve detection of glaucoma (Anderson 2005).

The Findings were presented as a poster presentation at ARVO, Florida, 2004

Verdon-Roe GM, et al. *IOVS* 2004; 45:ARVO E-Abstract 2122)

and have been submitted to IOVS (November 2005).

Chapter 7

REFINEMENT OF MULTI-LOCATION MDT

7.1 DEVELOPMENT OF STAIRCASE STRATEGY

All experiments described within the thesis to this point have been performed using software designed for calculation of MDT threshold by probit analysis. This is ideal for accurate measurement of threshold for single locations, but would prove too time consuming for a multi-location test. To overcome this hurdle, new computer software was produced by Ananth Viswanathan to measure MDT threshold by staircase analysis (Cornsweet 1962), as used in standard automated perimetry (Heijl 1985). More recently introduced Humphrey field programs, such as SITA, use mathematical models of known threshold estimates to shorten test duration (Bengtsson et al. 1997) and give improved estimates of reliability (Olsson et al. 1997). These methodologies could be a future consideration for motion testing, once normative and glaucomatous MDT data has been collated.

METHOD

The staircase computer software was designed to allow selection of the range and starting displacement for each stimulus location with an optional number of "reversals." The program operates so that if a stimulus is registered as "seen" on the starting presentation subsequent stimuli are presented in a descending stair until "unseen." This marks the point of "reversal" and the stimulus is then presented in an ascending stair until registered as "seen" again. The reverse occurs for a stimulus "unseen" on the initial presentation. Threshold is recorded as "the last seen" response.

A multi-location MDT grid was created using the same locations as the "gold standard" Humphrey visual field test (figure 2-1, chapter 2). The stimuli were orientated with the RNFL and scaled according to estimates of GCD (Curcio and Allen 1990; Westcott et al. 1996; Garway-Heath et al. 2000a). Two versions were produced using central line lengths of 6 pixels (21 min arc) and 8 pixels (27 min arc) respectively as the determining scale (table 7-1), in accordance with the results of the central blur experiment, which suggest that small lines subtending ≤14 min arc should be avoided (Optics chapter 4 section 4.3). Peripheral line widths were adjusted to allow for the reduced angle subtended with eccentricity.

Table 7-1. Stimulus dimensions for strategies (i) and (ii).

	Strategy (i) pixels (min arc)	Strategy (ii) pixels (min arc)
Zone 1	8 x 2 (27 x 7min arc)	6 x 2 (21 x 7min arc)
Zone 2	16 x 2 (53 x 7min arc)	12 x 2 (40 x 7 min arc)
Zone 3	32 x 2 (103 x 7 min arc)	24 x 2 (76 x 7 min arc)
Zone 4	32 x 3 (99 x 9 min arc)	24 x 3 (74 x 9 min arc)
Zone 5	32 x 3 (94 x 9 min arc)	24 x 3 (71 x 9 min arc)
Zone 6	32 x 3 (86 x 8 min arc)	48 x 3 (128 x 9 min arc)

Equivalent energy exposure with horizontal and oblique stimuli was obtained using the principle described in chapter 2. An even spread of "feathering" was attained by calculating the difference between the energy of each horizontal and oblique stimulus pair and dividing this value by the number of pixels along the two sides of the oblique axis of the stimulus (table 7-2).

Table 7-2. Calculation equivalent pixel elements: horizontal and oblique stimuli.

Strategy (i)

	Stimulus Length	Pixels @ 255 RGB	Pixels @ 172 RGB	Pixels @ 153 RGB	Pixels @ 128 RGB	Pixels @ 116 RGB	Total Values Pixel x RGB
Horizontal	32	96	0	0	0	0	24480
Oblique	22	66	44	0	0	0	24398
Horizontal	32	64	0	0	0	0	16320
Oblique	22	44	0	0	0	44	16324
Horizontal	16	32	0	0	0	0	8160
Oblique	11	22	0	0	0	22	8162
Horizontal	8	16	0	0	0	0	4080
Oblique	5	10	0	10	0	0	4080

Strategy (ii)

	Stimulus Length	Pixels@ 255 RGB	Pixels @ 128 RGB	Pixels @ 191 RGB	Total Values Pixel x RGB
Horizontal	48	144	0	0	36720
Oblique	32	96	0	64	36704
Horizontal	24	72	0	0	18360
Oblique	16	48	0	32	18352
Horizontal	24	48	0	0	12240
Oblique	16	32	32	0	12256
Horizontal	12	24	0	0	6120
Oblique	8	16	16	0	6128
Horizontal	6	12	0	0	3060
Oblique	4	8	8	0	3064

Locations were matched in pairs for upper and lower hemi-fields. Staircase parameters were estimated by zone. Minimum, maximum and start displacements were selected by application of knowledge of MDT threshold and FOS characteristics gained both prior to, and within, this study doctorate (table 7-3; appendix, table 14-7).

Strategy (i) and (ii) were attempted by subject GMVR after 3 practice sessions to avoid the effect of learning (figure 7-1).

Table 7-3. Selection of staircase parameters by location.

Upper and lower hemi-field locations are matched in pairs.

Start position is indicated in bold.

DMA: Displacement min arc.

Location	zone	DMA1	DMA2	DMA3	DMA4	DMA5
1;29	6	5	8	**14**	19	22
2;30	5	4	8	**13**	17	21
3;31	3	5	9	**14**	18	
4;32	2	5	9	**14**	19	
5;33	1	5	**10**	15	19	
6;34	1	3	7	**10**	14	17
7;35	2	3	7	10	**13**	17
9;37	5	4	8	**13**	17	21
11;38	5	4	8	**12**	17	21
12;39	4	4	9	**13**	18	
13,40	3	5	9	**14**	19	
14,41	2	5	9	**13**	19	
15,42	2	3	7	**10**	13	17
16,43	3	5	9	**14**	18	
17,44	4	4	9	**13**	18	
18,45	5	4	8	**12**	17	21
19,46	5	4	8	**13**	17	21
20,47	4	6	9	**13**	16	22
21,48	3	6	10	**13**	16	19
22,49	3	5	9	**14**	18	23
23,50	4	4	9	**13**	18	22
24,51	5	4	9	**13**	17	21
25,52	5	6	9	**12**	18	20
26,53	5	6	9	**12**	18	21
27,54	5	4	8	**13**	17	21
28,55	5	4	8	**12**	17	21

Figure 7-1. Preliminary Staircase Strategies.

(A) strategy (i)
(a) stimulus dimension and range of staircase displacement by zone.

Numerals refer to allocated MDT stimulus number (right eye).

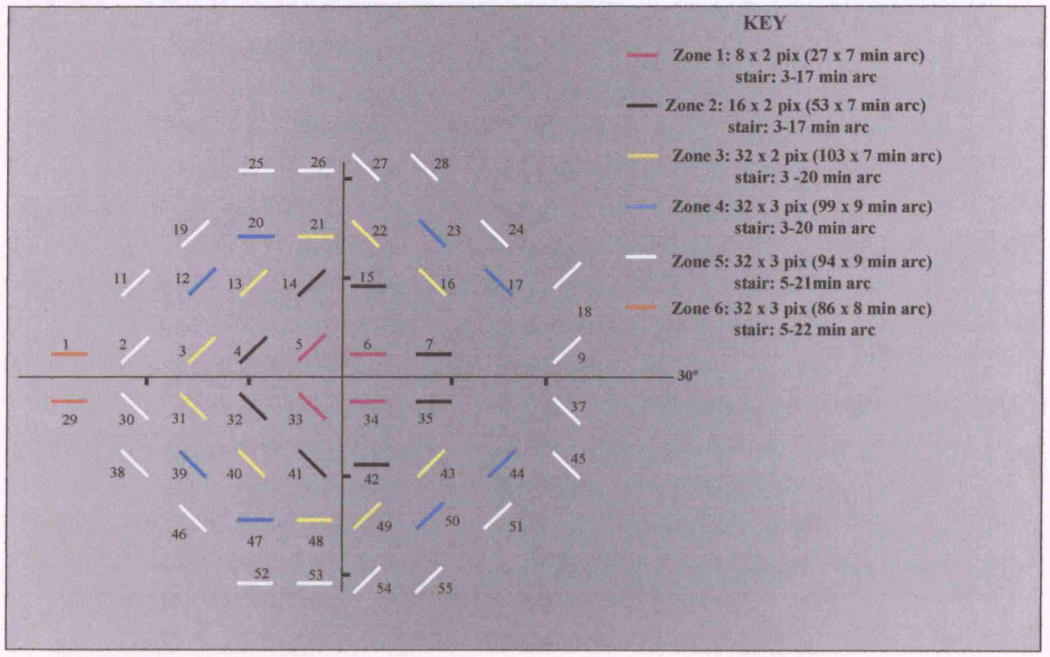

(b) threshold results (min arc). Right eye.

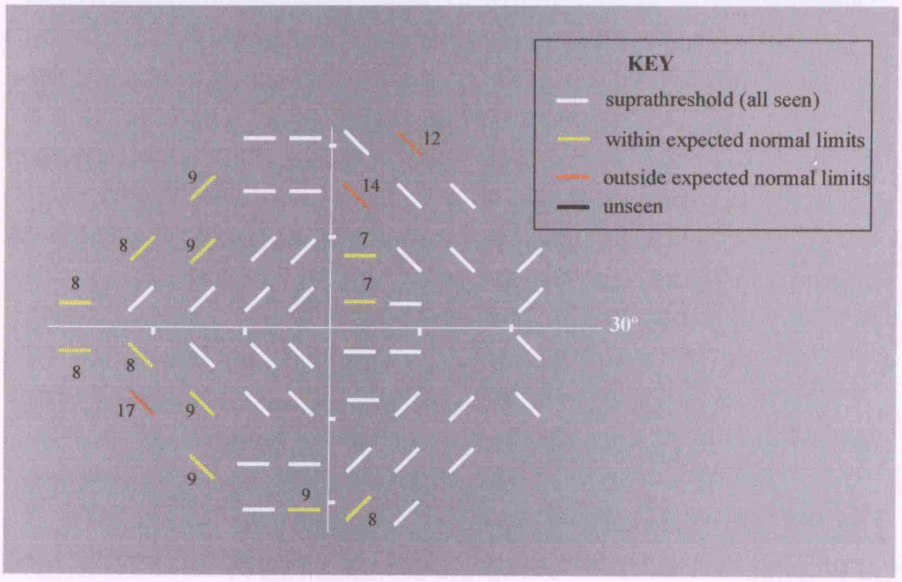

(B) strategy (ii) (a) stimulus dimension and range of staircase displacement by zone. Numerals refer to allocated MDT stimulus number (right eye).

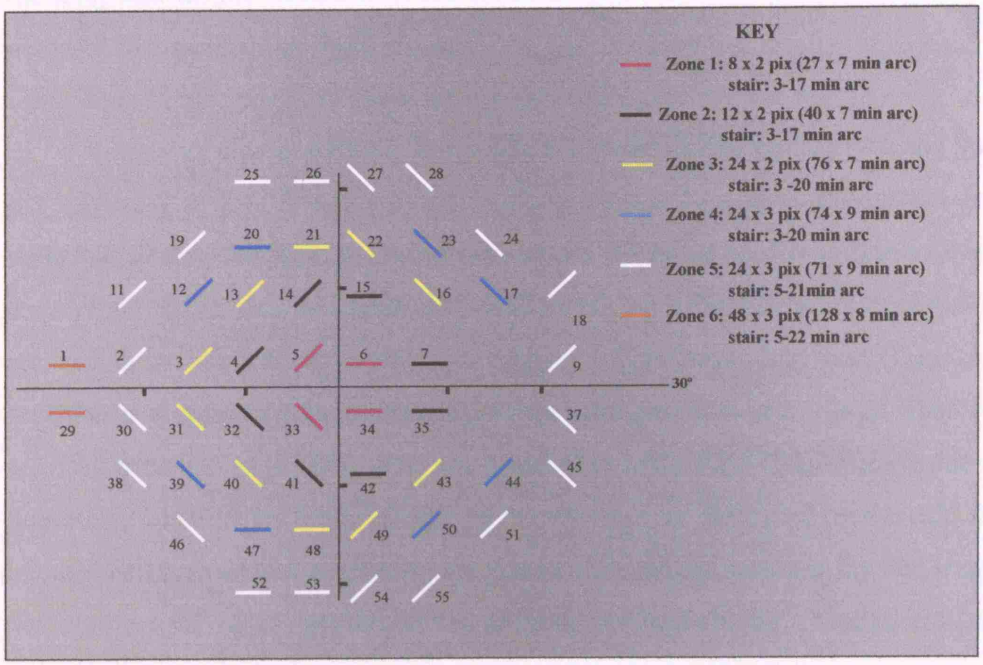

(b) threshold results (min arc). Right eye.

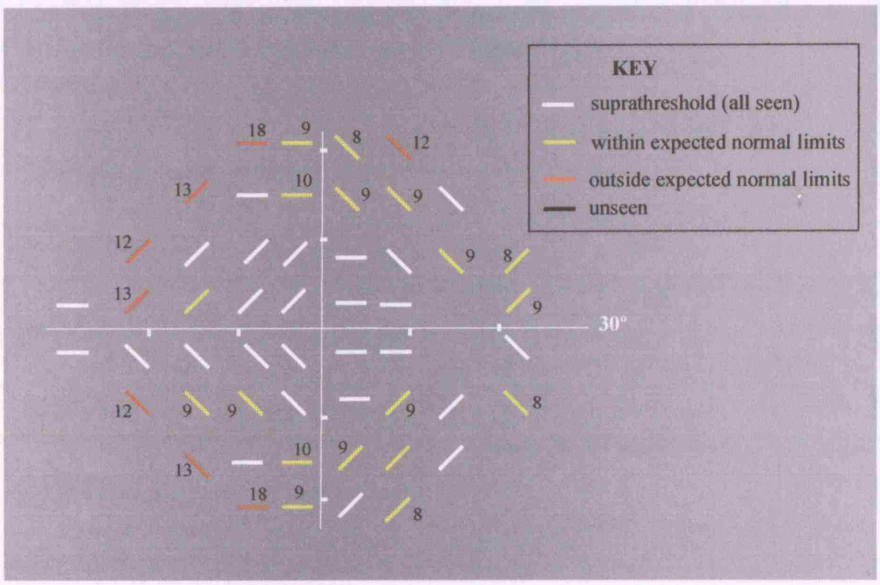

Analysis of the pilot multi-location test threshold responses showed predominantly suprathreshold results for strategy (i), (figure 7-1 Ab). Small threshold responses were found for locations 6 and 15 and those in the nasal periphery, despite the long line lengths selected. Three locations (one in zone 3; two in zone 5) show higher than expected threshold results.

Numerous elevated MDT thresholds are found in the periphery using strategy (ii), (figure 7-1 iib). The line lengths of the stimuli for the multi-location test are scaled according to GCD. In theory one would therefore predict uniform thresholds across the field. A uniform threshold is unlikely to be a fixed measure in terms of min arc, but more likely to be uniform in relation to receptive field size. Therefore we would expect small thresholds centrally when measured in min arc, even when stimuli are scaled according to GCD. It is not possible to scale the MDT staircase due to the limitations imposed by the pixel size of the monitor, as illustrated by the calculations of table 7-4. It would be possible to compensate for this by reducing the line lengths of the more central zones, but the effects of refractive blur will be a limitation to size of the stimuli in zone one, as previously discussed in chapter 4.

Table 7-4. Estimated number of ganglion cells stimulated along the nasal horizontal mid-line by the proposed MDT stair of table 7-3.

Zone	Location	Stair (min arc)	Ganglion cells
1	-3,3	1-19	2 – 13
2	-9,3	1-19	1 – 8
3	-15,3	1-18	<1 – 5
5	-21,3	1-21	<1 – 4
6	-27,3	1-22	<1 – 3

Some of the peripheral MDT thresholds are higher than would have been predicted from earlier work in this study, when a stimulus was tested in isolation at – 27,3 degree eccentricity. This raises the question whether the constant presence of a large number of locations may cause elevation of threshold due to difficulty in attention. This would be consistent with Hock's description of a neural model of large, foveally centered receptive fields driving attention (Hock et al. 1998). An alternative explanation is that the staircase strategy underestimates the MDT threshold, as found for SAP and FDT (Spry et al. 2003).

The duration of the test was excessive (strategy (i) 11.5 minutes; strategy (ii) 12.4 minutes). Presentation of the stimuli was in a predictable regular rhythm, inferring that the random pre-displacement should be increased from 500 msec. The waiting time from the end of one stimulus presentation to the beginning of the next appeared unnecessarily long, suggesting that a reduction in test time could be achieved by modification of stimulus timings.

7.2 ANALYSIS OF MDT STIMULUS TIMINGS

MDT stimulus timings include the following components, each one of which needs to be carefully considered in order to produce a test which runs optimally to the minimum time, thus avoiding subject fatigue and increasing hospital efficiency, whilst maintaining test sensitivity.

(i) Adaptation: the period of acclimatization prior to first stimulus presentation. (Current selection: 5000msec).

(ii) Fixed Pre-displacement: the interval prior to each stimulus presentation (Current selection: 1500msec).

(iii) Random Pre-displacement: randomized time added to the fixed pre-displacement listening window to remove predictability of subject response (Current selection: randomized time of anything between 0-500 msec).

(iv) Cycles: the number of cycles selected for each stimulus presentation. One cycle is composed of the displacement of a stimulus to a new position and its return to the starting position (figure 7-2). Earlier research determined 3 cycles to be optimal with a time saving over the original BBC of 5 oscillations (Verdon-Roe et al. 2000).

(v) Duration: the time taken to complete each cycle. The original BBC was set to duration of 400 msec per cycle (figure 7-2).. Subsequent research showed equivalent MDT for durations of 200 and 100 msec per cycle. A new standard of 200 msec per cycle (Westcott et al. 2000b) was set in accordance with the findings of Post (Post et al. 1984), as discussed in chapter 3.

(vi) Listening Window: the period allocated for subject response following presentation of the stimulus (current selection: 1500 msec).

(vii) Post Response Wait: the recovery time allowed between the end of one stimulus presentation and the start of the next (current selection: 1500 msec).

The time course of each MDT presentation sums to a maximum of 5.6 seconds if the motion displacement is unseen (figure 7-3). If the stimulus is registered as "seen" (recorded by the computer mouse click) the program automatically proceeds to the post-response wait. The setting of the listening window requires consideration of the subject response time. This is measured as the time taken from the commencement of the stimulus oscillation to the computer registration of a "seen" response.

Figure 7-2. Illustration of MDT stimulus presentation.

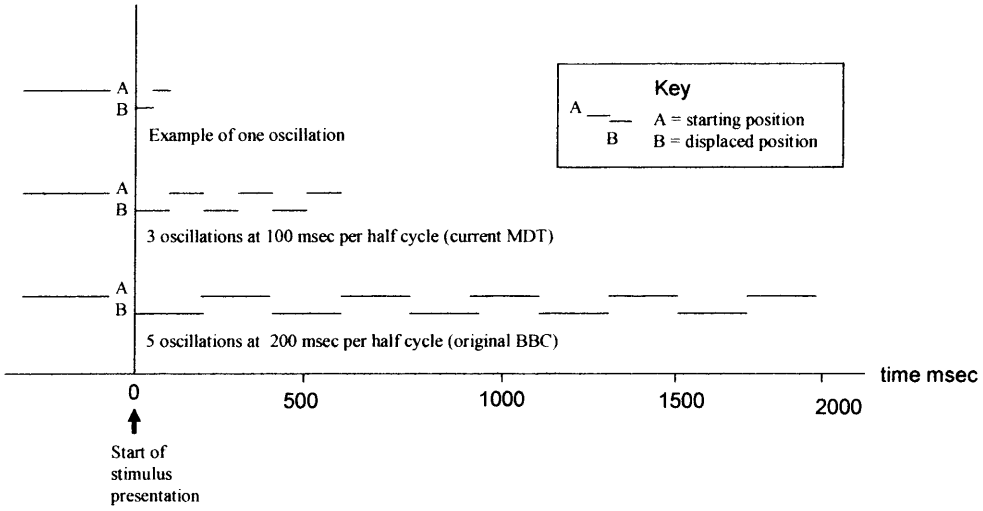

Figure 7-3. Time course of components of the MDT stimulus presentation.

If the stimulus is unseen the duration of the presentation totals 5.1 sec, with an additional random pre-displacement of anything between 0- 500 msec.

Key:
A: Adaptation
FP: Fixed Pre-displacement
RP: Random Pre-displacement
SP: Stimulus Presentation
LW: Listening Window
PRW: Post Response Wait

A:	FP:	RP:	SP:	LW:	PRW:	
5000	1500	0-500	600	up to 1500	1500	msec

7.2.1 MDT RESPONSE TIME

No subject was urged to respond as rapidly as possible for any of the MDT studies and therefore the term "response time " is used in preference to "reaction time" (Artes et al. 2002).

Response times are determined by the time taken for the following sequence:

(i) The eye to perceive the line stimulus movement.

(ii) The inter-cortical transfer of sensory information to the motor centre of the brain.

(iii) The passage of the impulse of response from the central nervous system to the peripheral nervous system controlling the hand.

The minimum physiological response time is 180 msec (Woodworth and Schlosberg 1954). Responses made within this period should be regarded as false positive and may be used as an indicator of reliability (Artes et al. 2002).

Variability in response time may arise due to the effects of learning, attention, age and fatigue. Coronel reported mean physiological reaction times of 304.33 ± 4.1 and 312.35 ± 4.5 msec for left and right hemispheres respectively. The faster time of the left hemisphere was attributed to the proximity of the motor centre, which is located in the left hemisphere in the majority of right-handed individuals. Longer response times were found in the left visual field compared to the right and for females compared with males (Coronel et al. 1999).

Different response times are reported for sensing motion as a function of luminance and chromatic contrast using sinuoisoidal gratings. This may indicate mediation by different mechanisms, consistent with the different conduction velocities of the M and P systems (Burr and Corsale 2001).

Increased response times may be an indication of pathology. This may be in relation to the eye [e.g. glaucoma (Wall and Ketoff 1995; Westcott et al. 2000a)], central nervous system [e.g. multiple sclerosis (Rao et al. 1989), HIV (Dunlop et al. 2002), Alzheimer's disease (Rizzo et al. 2000a), or benign intracranial hypertension (Wall and Montgomery 1995)] or local malfunction of the hand (e.g. arthritis).

The duration of the original BBC stimulus presentation and response window was 4000 msec, the stimulus undergoing 5 oscillations at duration of 400 msec per cycle with a listening window of 2000 msec [figure 7-4 (a)].

The stimulus presentation and response window was reduced to 2100 msec for the new multi-location MDT. This was achieved by applying time saving revisions to the number of stimulus oscillations and duration per cycle (Verdon-Roe et al. 2000; Westcott et al. 2000b). In addition, the listening window was reduced to 1500 msec [figure 7-4 (b)] in consideration of response times at threshold found using the original BBC (Westcott et al. 2000a).

The mean response times, standard deviation and range for the original BBC MDT were reported to be 1160 ± 140 (940-1430) msec for control subjects and 1370 ± 220 (980-1680) msec for aged- matched glaucoma (Westcott et al. 2000a). When the data were re-plotted to show the relationship between response times at 50% seen threshold, there was no significant difference between the two groups, in agreement with research done by Wall testing differential light sensitivity using Humphrey Visual Fields (Wall et al. 1996). MDT response times were found to decrease with increasing stimulus displacement, with a linear negative fit as the stimulus moved from threshold to suprathreshold levels (Westcott et al. 2000a).

The mean and range of the BBC MDT at threshold were 1470 (1000 - 2050) msec and 1360 (980 - 1800) msec for control and glaucoma groups respectively (Westcott et al. 2000a). It is of interest that the MDT response times at threshold are more than twice those reported by Wall using Humphrey field perimetry (Goldmann

Figure 7-4. MDT presentation windows.

(a) Original BBC MDT stimulus presentation window.

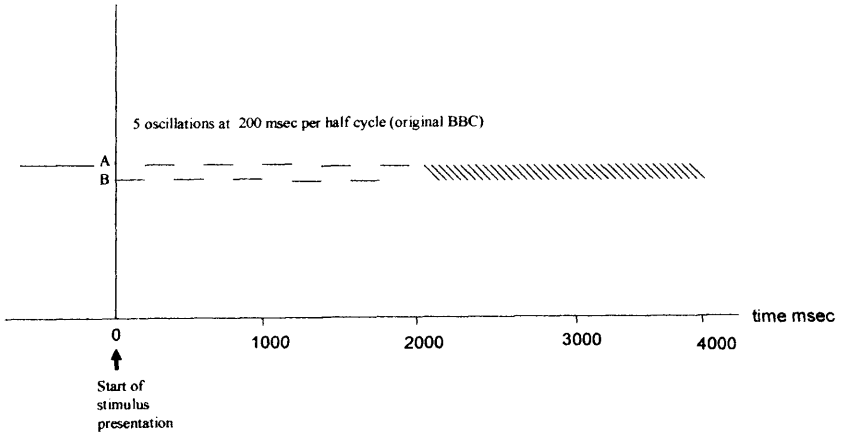

(b) Multi-location MDT presentation window.

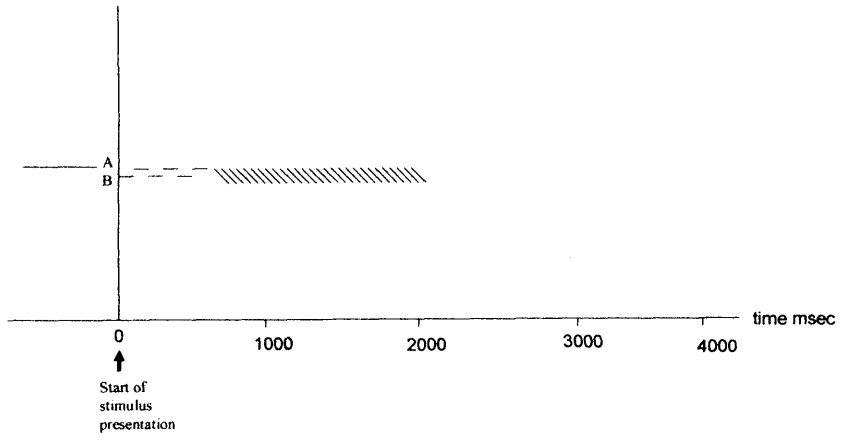

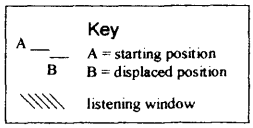

stimulus size III of 200 msec duration), where response time was also measured at the 50% frequency of seeing threshold from the stimulus onset (Wall et al. 1996).

Response times were examined for the preliminary pilot studies of new multi-location test (figure 7-1) to determine whether there might be further scope to shorten the listening window in order to reduce the long test duration. The response time for each location was recorded at threshold.

When mean response times are plotted against stimulus area, lines of greater area within the same zone show shorter response times, with a clear trend of increased duration of response with eccentricity (figure 7-5; appendix, table 14-8).

Figure 7-5. Mean response time at threshold by zone for multi-location MDT (strategies i and ii).

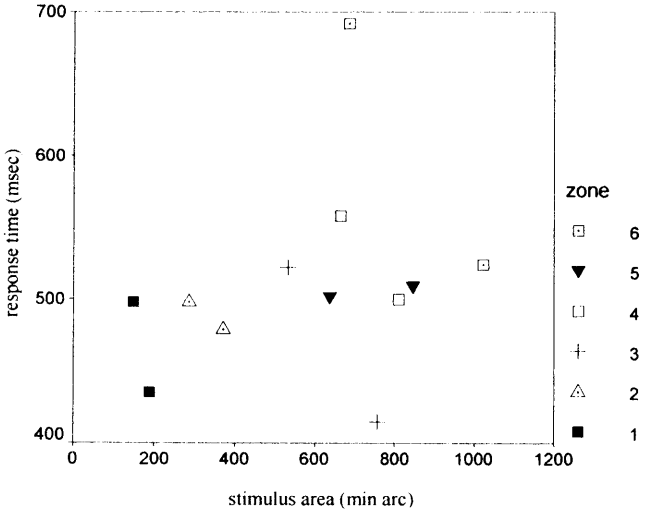

A reduced mean response time at threshold was found for the multi-location test [500 ± 157 (265-925) msec (mean, sd (range)] when compared with the BBC controls

(Westcott et al. 2000a). It was questioned why this should be the case. Could it be explained by the fast response speeds of the well-practiced author or is it due to the change in the temporal summation properties of the stimulus presentation adopted for the new test? If the latter is the case, would this allow for further time saving modifications to be made to the stimulus timings?

Records of data relating to change of stimulus duration collated by GMVR prior to the start of this study were re-examined to address the question of differences in MDT response time. Tests were conducted on a Viglen Genie ATX Pentium 200 PC. A single line stimulus (2 degrees x 2 min arc) was presented at location 15,3 and programmed to pass through 10 randomized displacements, ranging between 1 and 18 min arc, at a test distance of 1.24 m. MDT thresholds were estimated by probit analysis. The stimulus presentation timings included a simulated BBC duration of 400 msec per cycle and two reduced stimulus durations of 200 and 100 msec per cycle. Each stimulus presentation underwent 5 oscillations.

The threshold response was similar for the simulated BBC [1248 ± 386 (841-1782) msec (mean, sd (range))] as the reported values for the original BBC (Westcott et al. 2000a). However, there is a trend towards shortening of response times as stimulus duration is decreased (table 7-5), suggesting altered patterns of temporal integration as the duration of the stimulus presentation is changed.

Table 7-5. Response times for varying stimulus duration (Westcott et al. 2000b).

Four controls (mean age 46 years (range: 33-68 years).

Stimulus Presentation Osc x duration (msec)	Total Stimulus Presentation (msec)	MDT threshold Min arc	Response time at Threshold (msec)
5 x 400	2000	3.3 ± 1.1	1248 ± 387 (841-1782)
5 x 200	1000	2.5 ± .4	862 ± 163 (657-1107)
5 x 100	500	3.5 ± .3	617 ± 235 (392-1011)

Bloch's law is applicable for stimulus duration of $\leq$ 100 msec where stimulus duration * luminance = constant. Beyond $\geq$ 100 msec sensitivity is independent of time and directly proportional to the luminance intensity (Lachenmayr and Vivell 1993). However, we know from the discussion in the previous chapter that the MDT stimulus may be regarded as a noise-limited vernier process and may therefore exhibit different temporal summation properties, through different patterns of neural integration.

SUMMARY OF MDT RESPONSE TIMES

The revised multi-location MDT has been shown to produce lower response times than the BBC, which may be explained by alteration of the stimulus presentation time. MDT response time is found to depend on stimulus size, varying with eccentricity, suggestive of a spatial summation effect. Alternatively, this may reflect sub-optimal scaling of the stimuli.

The response time of the multi-location test is found to be at least 700 msec less than that found with the single line BBC. Response for the new test was made within 1000 msec under all stimulus conditions (appendix, figure 14-8), suggesting that there is opportunity to reduce the response window (stimulus presentation time plus listening window), which is currently set at 2100 msec [figure 7-4 (b)].

A preliminary study is recommended using a reduction of 500 msec to the listening window of the new test, giving a response window of 1600 msec (figure 7-6). This will allow for possible variation in response with age, practice and attention. Final selection of response window will depend on selection of stimulus size with eccentricity.

When the MDT normative database has been collated the principles of maximum likelihood of response time could be applied to MDT to provide a measure of reliability and reduce variability (Olsson et al. 1997; Artes et al. 2002).

Figure 7-6. Proposed revised response window for multi-location MDT.

Listening window is reduced to 1000 msec giving a response window of 1600 msec and time saving of up to 500 msec per unseen presentation.

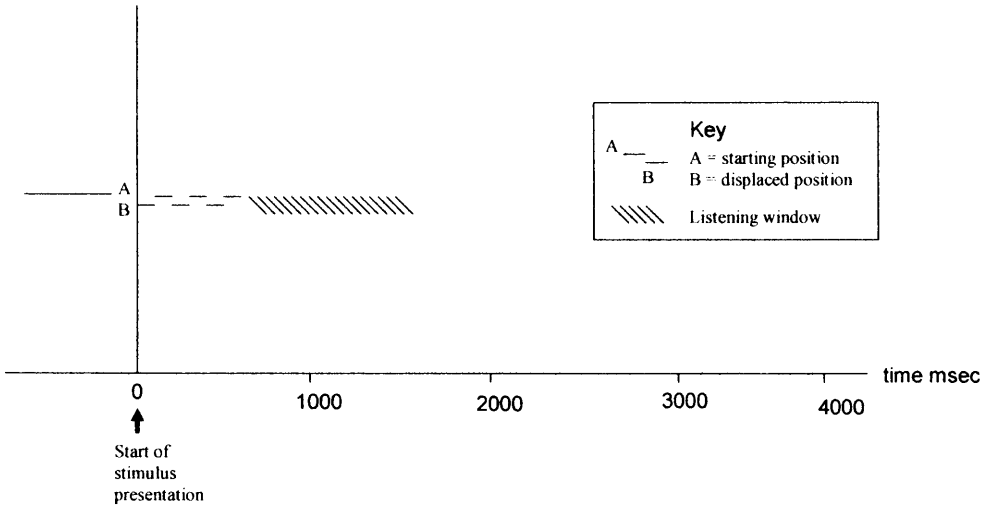

7.2.2 RANDOM PRE-DISPLACEMENT

The preliminary pilot studies of the multi-location test found the presentation of the stimuli to be too predictable suggesting an increase of the random pre-displacement period would be appropriate. The random pre-displacement was therefore increased to 750 msec. Re-assessment of the test by subject GMVR and two other volunteers found the modification ensured the test was unpredictable. A new standard random pre-displacement of 750 msec was therefore set.

7.2.3 FIXED PRE-DISPLACEMENT AND POST RESPONSE WAIT

The fixed pre-displacement describes the period prior to stimulus displacement and the post-response wait the recovery period following subject response. In practice the fixed pre-displacement and post response wait run consecutively from the end of one stimulus to the start of the next (figure 7-3). Each has an allocated duration of 1500 msec giving a total resting period of 3000 msec stimuli. Subjectively, subject GMVR and other observers found this break between stimuli unnecessarily long.

A pilot test was undertaken by subject GMVR, with both the fixed pre-displacement and post response wait reduced from 1500 msec to 750 msec. A large time saving of 37% (4 minutes 4 seconds) was found over the original test timings. However, the speed of successive stimulus presentations was found to be too fast and to result in raised motion displacement thresholds (figure 7-7, pilot timings 1).

The fixed pre-displacement and post response wait were in consequence each increased to 1000 msec. The revised test was subjectively found to run at a satisfactory pace by subject 1 (GMVR) giving a 35% time saving (3 min 53 sec) over the original settings. A second subject verified it as acceptable (figure 7-8, pilot timings 2).

A general tendency for peripheral MDT thresholds to be elevated was observed. This was less evident for subject 2, but still present. For example, it was surprising to see a threshold of 14 min arc in the far nasal periphery [-27,-3], (figure 7-8 b). Much testing has now been done at its fellow location above [-27,3]. A threshold of < 5 min arc would have been predicted for a single line length of 86 x 8 min arc presented in isolation. It was questioned whether the raised threshold is caused by difficulty in attention due to the large number of stimuli present. This will be investigated in the next chapter.

Figure 7-7. Multi-location MDT threshold results for pilot timings 1 (fixed pre-displacement 750 msec; post response wait 750 msec).

Test Duration 7 mins 1 sec. Right eye.

Note increase in thresholds compared with original timings (figure 7-1).

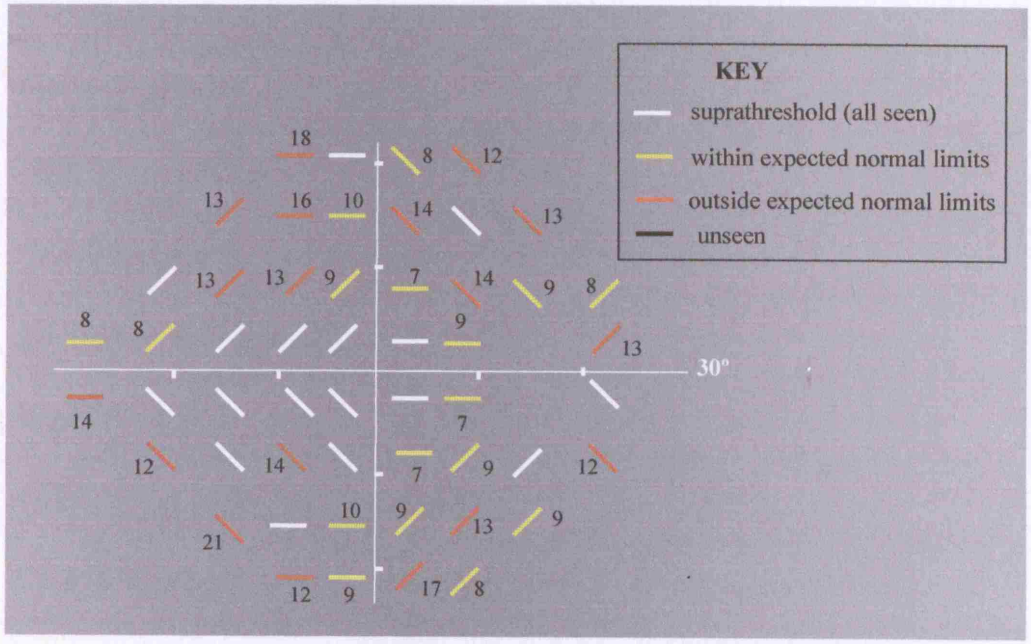

Figure 7-8. Multi-location MDT results for pilot timings 2 (fixed pre-displacement 1000 msec; post response wait 1000 msec).

a) Subject 1, Right Eye. Test Duration: 8 min 12 sec.

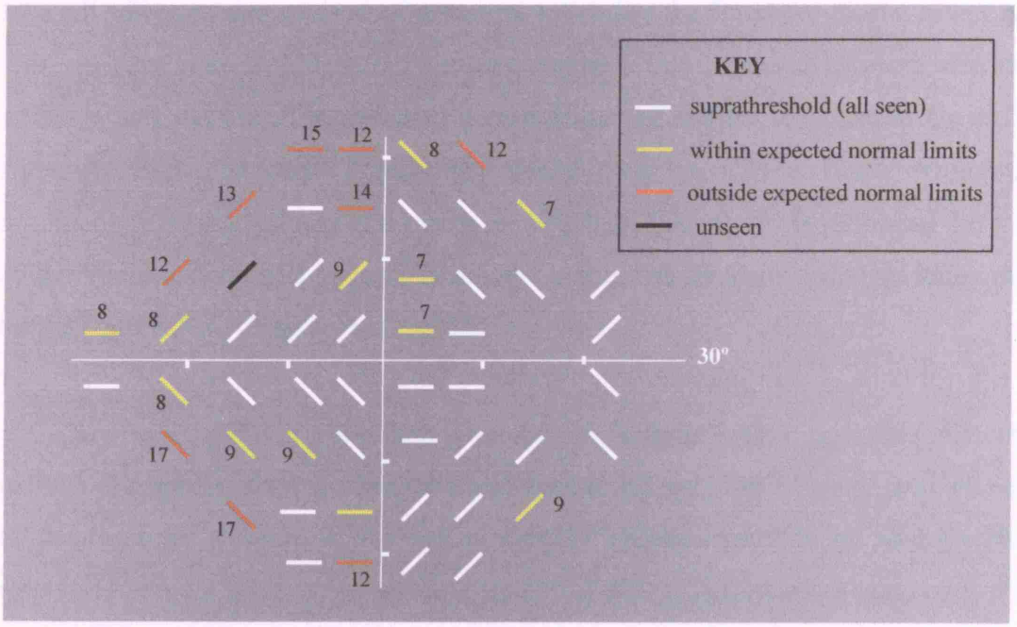

b) Subject 2, Right Eye. Test Duration 7 min 48 sec.

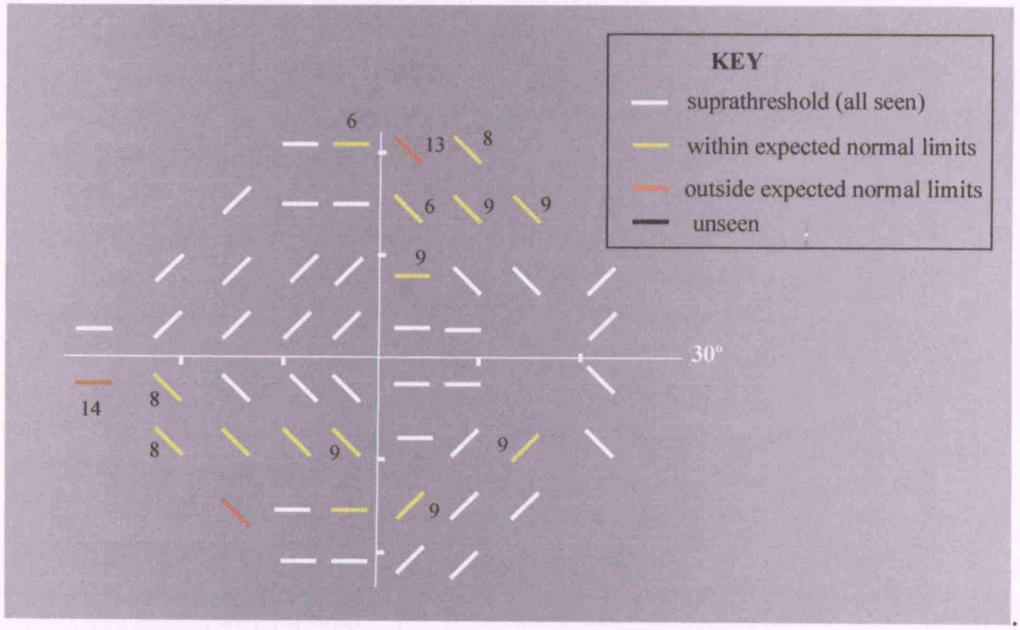

7.2.4 FALSE POSITIVE INDICES

Both fixed pre-displacement and post response periods should be "silent" and may be used as an indicator of false positive response (Olsson et al. 1997). In order to take advantage of this method of assessing reliability the fixed pre-displacement and post response wait should be incorporated together into a second listening window, which would run after the allocated period given for subject response to the MDT stimulus. Two indicators of reliability would then be offered, firstly within the minimum physiological response period of 180 msec (Greve 1973) following the start of the stimulus presentation and, secondly, within the allocated post response wait period (figure 7-9), (Olsson et al. 1997).

The current SITA Humphrey test uses a flexible timing algorithm whereby individual response time is monitored throughout the test with frequent readjustment of the response window as the test proceeds. Optimal detection of false positive responses may be achieved by monitoring the latency of responses of each patient in comparison to their average. It is recommended that in due course this principal be adopted for the MDT (Henson and Artes 2002).

Figure 7-9. Proposed MDT modifications to give two indices of false positive response.

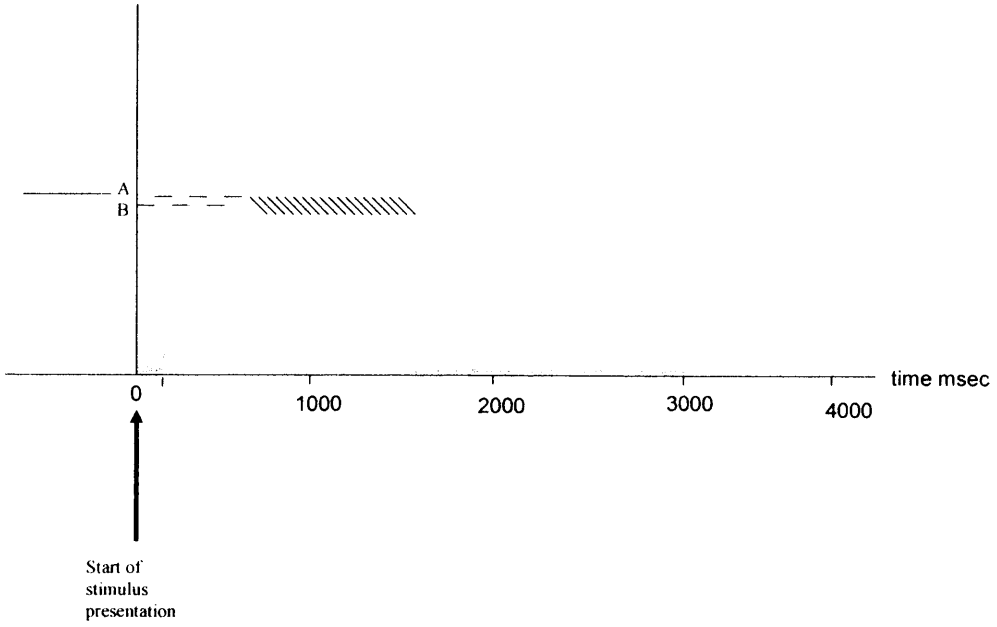

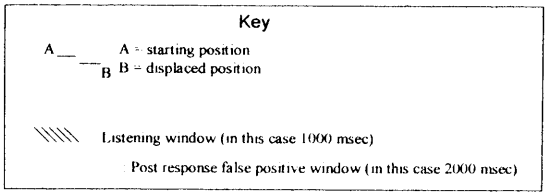

7.2.5 SUMMARY OF MODIFIED STIMULUS PRESENTATION

On the basis of this chapter's investigations the multi-location test was set to a new standard of timings of a fixed pre-displacement of 1000 msec (previously 1500 msec), a listening window of 1000 msec (previously 1500 msec), a post response wait of 1000 msec (previously 1500 msec) and a random pre-displacement of 750 msec (previously 500 msec).

This gives a maximum duration of a stimulus presentation, if no response, of 3.6 sec [+ random pre-displacement up to 750 msec], (figure 7-10), over the previous settings of 5.1sec [+ random pre-displacement up to 500 msec], (figure 7-4).

The tailoring of the computer software to individual response time and the monitoring of false positive response requires change of the MDT computer programming and will be incorporated into post-doctorate work.

Figure 7-10. New standard MDT timings.

Key:
A: Adaptation
FP: Fixed Pre-displacement
RP: Random Pre-displacement
SP: Stimulus Presentation
LW: Listening Window
PRW: Post Response Wait

A:	FP:	RP:	SP:	LW:	PRW:	
5000	1000	750	600	1000	1000	msec

Chapter 8

THE EFFECT OF ATTENTION ON MDT THRESHOLD

8.1 BACKGROUND

In cognitive neuroscience attention describes the selective filtering of information, with the purpose of sorting relevant from non-relevant information. Modern imaging techniques indicate that neuro-filtering for selective visual attention is a multi-level process, occurring from the LGN through to higher orders of visual processing in the frontal and parietal cortex. The pulvinar of the thalamus is thought to be an integrator of attentional function (Kastner and Pinsk 2004).

Attention varies according to the state of alertness, diminishing with fatigue. Visual attention is diminished in dementia, such as Alzheimer's disease, where visual acuity, stereo-acuity and motion direction performance are unaffected (Rizzo et al. 2000a; Rizzo et al. 2000b).

Visual attention is thought to be primarily driven by luminance and contrast, with cues that preferentially excite the M system predominantly capturing visual attention (Steinman et al. 1997). Neuro-imaging demonstrates that selective attention, for a specific change of visual feature (e.g. shape, colour, motion) within the visual field, results in enhanced activity of specific areas within the extra-striate cortex. This supports the hypothesis that attention is driven by specific neuronal populations (Corbetta et al. 1991; Chawla et al. 1999).

Visual attention may be affected by the presence of neighbouring stimuli in the visual field which may act as "distracters" (Montaser-Kouhsari and Rajimehr 2005). This phenomenon of interference amongst adjacent features is known as "crowding" (Bex et al. 2003; Bex and Dakin 2005) and is found to vary according to the character

size, the spacing between the characters and the attentional focus (Strasburger et al. 1991).

Crowding is reported to increase with eccentricity in the presence of moving stimuli (Bex et al. 2003). Parkes suggests that crowding is related to texture perception and that under crowded conditions orientation signals are pooled in the primary visual cortex before reaching consciousness (Parkes et al. 2001).

Chapter 6 considers MDT in the context of a vernier stimulus. Spatial interference is found to occur over large areas, with respect to hyperacuity thresholds, and is thought to represent central inhibition (Westheimer and Hauske 1975). Levi found vernier acuity to degrade with the presence of abutting linear flanks. This was applicable to both foveal and peripheral stimuli, with complete isolation only occurring when flanks are placed at 60-times the un-flanked threshold (Levi et al. 1985).

The single stimulus MDT allows a subject to focus attention on a particular location. The multi-location MDT test, by contrast, has 53 stimuli, which are presented concurrently, thereby forcing attention to be broadly spread. Hock suggests that "broadly spread attention enhances the sensitivity of relatively large spatial filters, which increases the perceiver's spatial scale but reduces spatial resolution." Attentional spread of spatial resolution is accounted for by a "neural model of large foveally centered receptive fields, with cooperatively interacting sub-units at the level of MST or higher" (Hock et al. 1998).

Poor attention is accompanied by increase response time. Occipital electrophysiological measurements indicate that periods of inattention increase variability and reduce reproducibility of psychophysical tests (Henson D, et al. *IOVS* 2003; 44: ARVO E-Abstract 4343).

During preliminary work, higher MDT thresholds were observed at nasal peripheral location, -27,3, using a multi-location format, than when testing in isolation. An experiment was designed to assess whether this could be attributed to the effects of attention by analysis of MDT thresholds and response times at threshold, at both a peripheral location (-27,3) and a central location (-9,9).

A further experiment was specifically designed to assess the attentional effects of crowding. A mid-central location (-9,9) was selected to ensure the test location was surrounded on all sides by other locations, thereby giving maximum distracter interference within the format of the multi-location test.

8.2 INVESTIGATION OF THE EFFECT OF ATTENTION ON MDT THRESHOLDS

8.2.1 PERIPHERAL LOCATION 1 (-27,3)

METHOD

MDT threshold of location 1 (-27,3) was assessed for subject GMVR using a staircase strategy. Six tests were designed with a varying number of randomly selected locations, equally divided between upper and lower hemi-fields (figure 8-1).

The tests were conducted in random order using the same stimulus length and displacements per location as described for the first staircase strategy (figure 7-1(A)). Each test was repeated three times. Location 1 was repeated at the end in isolation to assess the effect of fatigue.

Modified timings were used as indicated by the results of the previous chapter (the fixed pre-displacement, listening window and post response wait were each 1000 msec and the random pre-displacement 750 msec). MDT threshold was recorded as the last seen response.

The following tests were each conducted three times (figure 8-1):

Test 1

52 locations present

Test 2

26 locations present:

Upper hemi-field stimulus numbers:* 1, 2, 6, 7, 9, 13, 14, 17, 18, 19, 22, 23, 26

Lower hemi-field stimulus numbers*: 29, 32, 33, 34, 35, 38, 39, 41, 42, 49, 50, 51, 53

Test 3

12 locations present:

Upper hemi-field stimulus numbers*: 1, 3, 11, 24, 15, 18

Lower hemi-field stimulus numbers*: 31, 37, 40, 42, 46, 55

Test 4

6 locations present:

Upper hemi-field stimulus numbers*: 1, 16, 21

Lower hemi-field stimulus numbers*: 33, 43, 54

Test 5

2 locations present:

Upper hemi-field stimulus numbers*: location 1

Lower hemi-field stimulus numbers*: location 29

Test 6.

1 location present:

Upper hemi-field stimulus number*: location 1

* stimulus number: refer figure 2-1.

Figure 8-1. Distribution of locations to assess attention at -27,3 (right eye).

(location 1, -27,3*).

Test1: 52 locations present

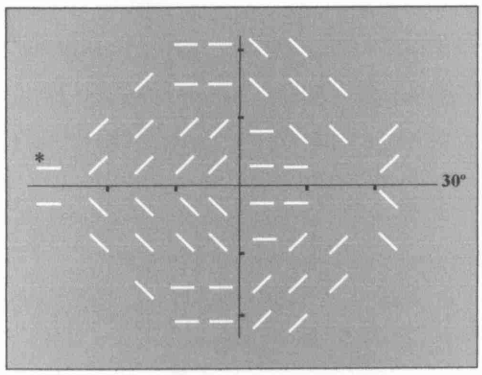

Test 2: 26 locations present

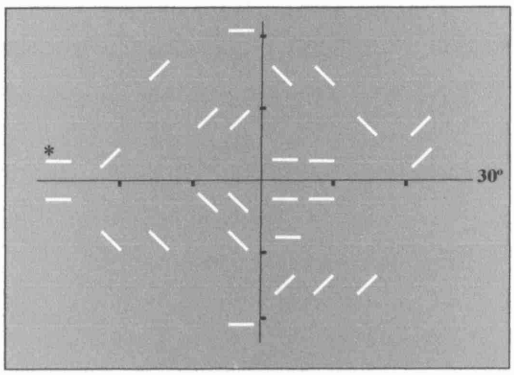

Test 3: 12 locations present

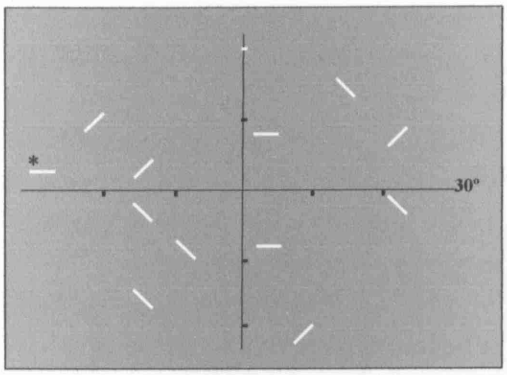

Test 4: six locations present

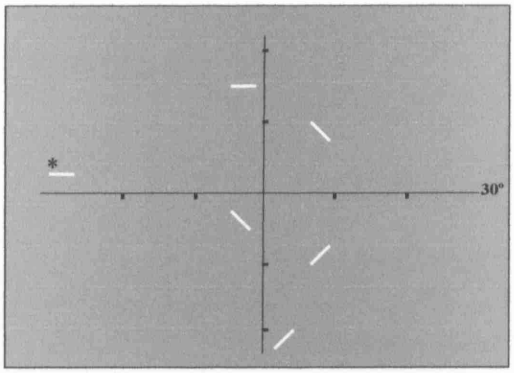

Test 5: two locations present

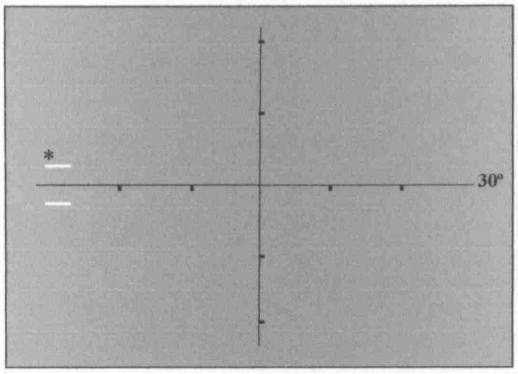

Test 6: location 1 in isolation

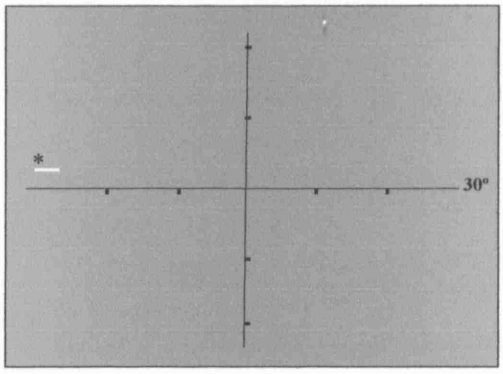

A trend towards elevation of MDT threshold was observed at location 1 (-27,3) as the number of locations present was increased (table 8-1). Mean values were not calculated due to several results being suprathreshold. Location 1 remained suprathreshold when tested in isolation at the end.

Table 8-1. MDT threshold at location -27,3 for varying number of locations present.

< 5 = suprathreshold response.

TEST	locations	MDT 1	MDT 2	MDT 3
1	52	14	14	8
2	26	8	14	8
3	12	< 5	8	8
4	6	8	< 5	< 5
5	2	< 5	< 5	< 5
6	1	< 5	< 5	< 5
REPEAT 6	1	< 5		

8.2.2 CENTRAL LOCATION 13 (-9,9)

METHOD

The attention test was repeated for the more central location 13 (-9,9). Location 13 was observed to be suprathreshold for both multi-location test strategies in the previous chapter (figure 7-1). A reduced line length was therefore used and all zones scaled accordingly (figure 8-2).

Figure 8-2. Reduced line lengths used for assessment of attention (-9,9).

Numerals refer to allocated MDT stimulus number (right eye).

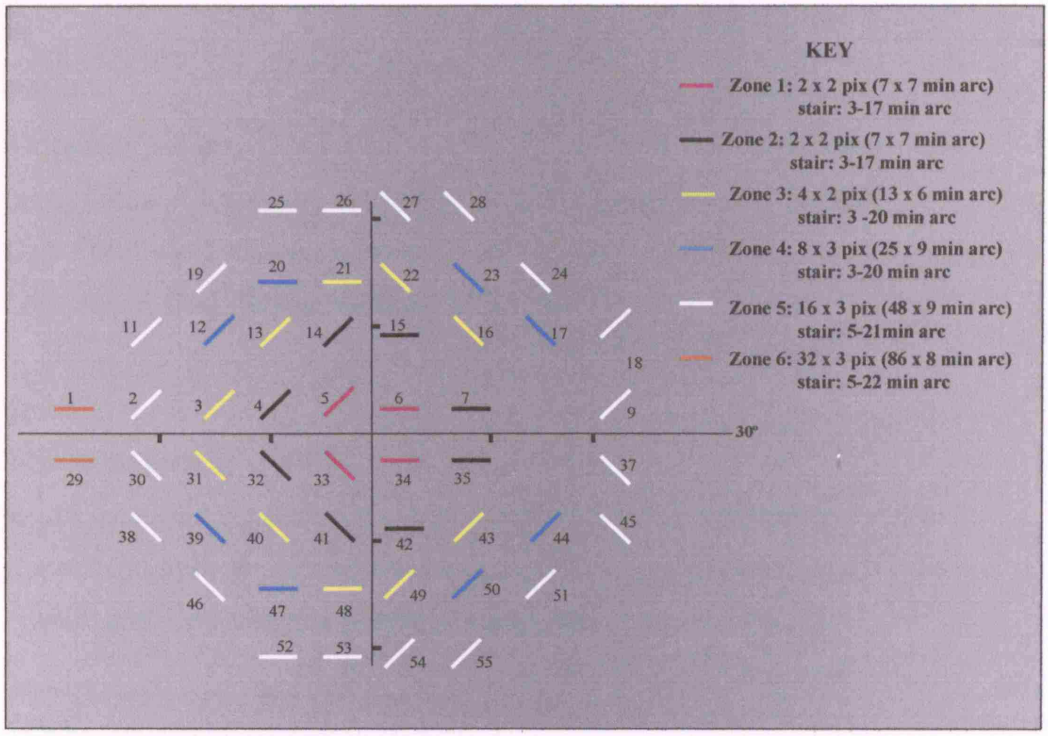

The following tests were each conducted three times:

Test 1

52 locations present (as for location 1 attention test)

Test 2

26 locations present (as for location 1 attention test):

Upper hemi-field stimulus number: 1, 2, 6, 7, 9, 13, 14, 17, 18, 19, 22, 23, 26

Lower hemi-field stimulus number: 29, 32, 33, 34, 35, 38, 39, 41, 42, 49, 50, 51, 53

Test 3

12 locations present

(as for location 1 attention test except location 13 added and 40 deleted):

Upper hemi-field stimulus number: 1, 3, 11, 13, 24, 15, 18

Lower hemi-field stimulus number: 31, 37, 42, 46, 55

Test 4

6 locations present

(as for location 1 attention test except location 13 added and 21 deleted):

Upper hemi-field stimulus number: 1, 16, 13

Lower hemi-field stimulus number: 33, 43, 54

Test 5

2 locations present

(as for location 1 attention test except location 13 added and location 1 deleted):

Upper hemi-field stimulus number: location 13

Lower hemi-field stimulus number: location 29

Test 6.

1 location present:

Upper hemi-field stimulus number: location 13

A small increase in mean MDT threshold was observed when six locations were present, compared to when only one or two. The MDT threshold remained constant between six and fifty-two locations present (figure 8-3).

Figure 8-3. MDT threshold for varying number of locations present (-9,9).

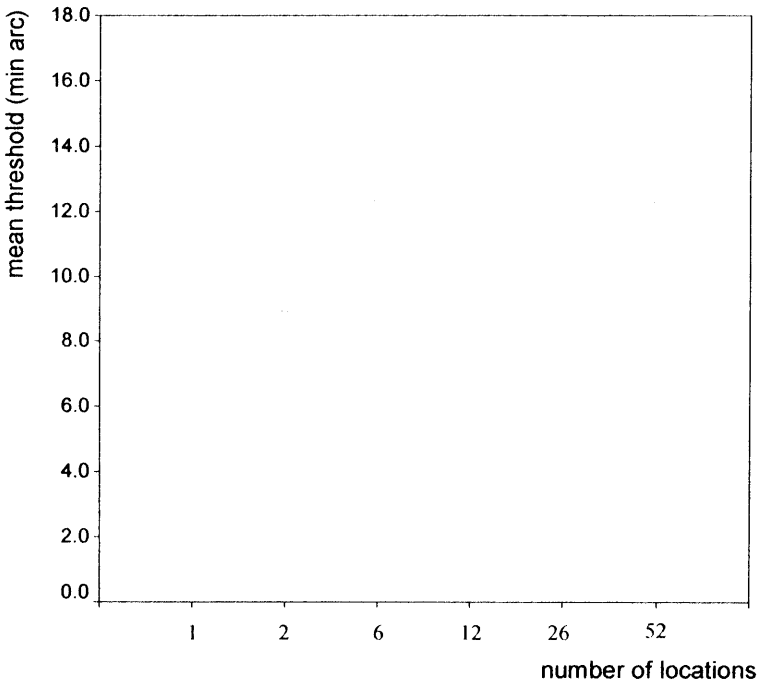

The results of the two attention experiments indicate an increase in MDT thresholds as the number of stimuli present is increased, in keeping with an effect of attention. The threshold effect appears more marked for peripheral location 1 (-27,3) compared with the more central location 13 (-9,9), consistent with Hock's attentional model of large foveally centered receptive fields (Hock et al. 1998). However, due to the numerous suprathreshold measurements at location 1 this cannot be quantified (table 8-1).

Threshold measurements could be obtained by adjustment of the staircase parameters and/or reduction of stimulus length.

The current methodology for location 1 uses the staircase parameters as described for the first multi-location study (2, 3, 5, 7, 8 pixels; 5, 8, 14, 19, 22 min arc) with the "start" displacement at 5 pixels (14 min arc). These were set to allow for inexperienced observers and glaucoma suspects and to provide economical use of time for a fifty-three location test. This experiment, by contrast, requires detailed evaluation of location 1 (-27,3) and uses experienced normal observers as subjects.

The MDT threshold at -27,3 ranges from < 5 min arc to a maximum of 14 min arc for subject 1, depending on the number of locations present (table 8-1). Sensitivity could be improved by inclusion of 1, 4 and 6 pixel (3, 11 and 16 min arc respectively) displacements to the stair. The "start" could be changed to 3 pixels (8 min arc).

The random selection of locations resulted in their being widely scattered, raising the question whether MDT thresholds were elevated due to attentional difficulties through the stimuli being broadly and irregularly spread. To test this theory an experiment was designed whereby MDT threshold values for location 1 (-27,3) were measured with surrounding locations clustered closely together.

8.2.3 CLUSTERED LOCATIONS

METHOD

The same methodology was used as described for the previous location 1 (-27,3) attention experiment for three tests of closely clustered locations (figure 8-4):

Test 1
26 locations present
Upper hemi-field stimulus number*: 1,2,3,4,5,6,7,13,14,15,16,21,22
Lower hemi-field stimulus number*: 29,30,31,32,33,34,35,40,41,42,43,48,49

Test 2
12 locations present
Upper hemi-field stimulus number*: 1,2,3,4,12,13
Lower hemi-field stimulus number*: 29,30,31,32,39,40

Test 3
6 locations present
Upper hemi-field stimulus number*: 1,2,3
Lower hemi-field stimulus number*: 29,30,31

* stimulus number: refer figure 2-1.

RESULTS

Clustering of stimuli results in a reduction of MDT thresholds compared with scattered stimuli. This is indicated by the suprathreshold response achieved when 26 locations are present (table 8-2 compared with table 8-1).

Figure 8-4. Distribution of clustered locations (right eye).
* location 1, -27,3.

Test 1: 26 locations

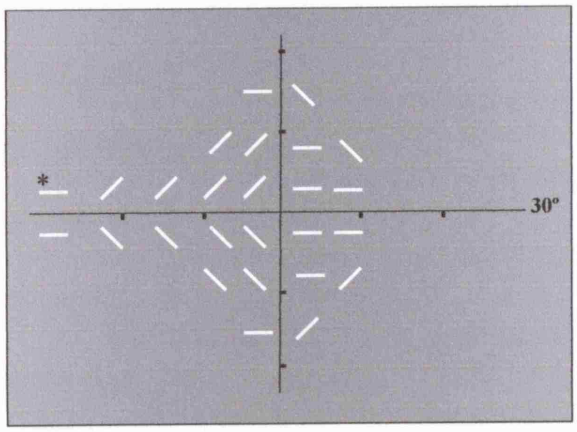

Test 2:12 locations

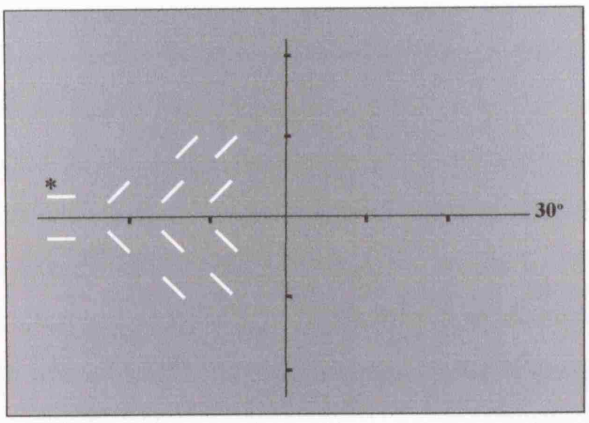

Test 3: 6 locations

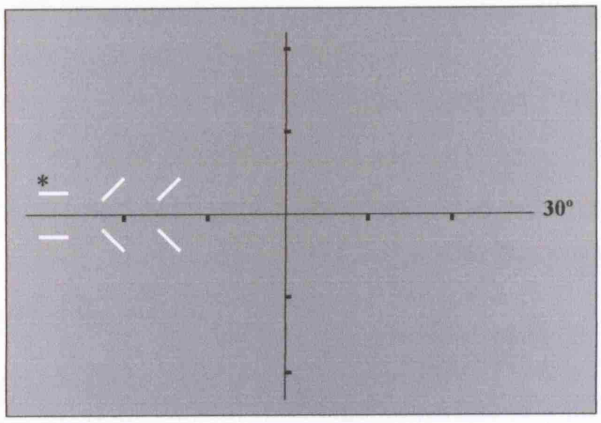

Table 8-2. MDT threshold for varying number of clustered locations present (-27,3).

< 5 = suprathreshold response

TEST	Number of locations	MDT 1	MDT 2	MDT 3
1	26	8	<5	<5
2	12	<5	<5	<5
3	6	<5	<5	<5

DISCUSSION

The preliminary results of this experiment suggest that MDT thresholds are lower when stimuli are clustered, compared with the same number of stimuli broadly spread. However, the lower MDT thresholds achieved with the clustered stimuli, which followed the experiment for the scattered stimuli, may be due to a learning effect. It was therefore decided that this experiment should be repeated, randomizing the scattered and clustered conditions. A smaller first displacement and reduced stimulus line length was selected to avoid a suprathreshold response.

8.2.4 REPEAT OF EXPERIMENTS FOR SCATTERED AND CLUSTERED LOCATIONS

The methodology of the preliminary attention experiments for Location 1 (-27,3) was repeated for both scattered and clustered locations. A smaller stimulus length and first displacement were used to avoid suprathreshold response (figure 8-5). Two experienced subjects were assessed. The tests were conducted in a randomized order and each repeated three times.

Figure 8-5. Test parameters for revised attention experiments (-27,3).

Numerals refer to allocated MDT stimulus number (right eye).

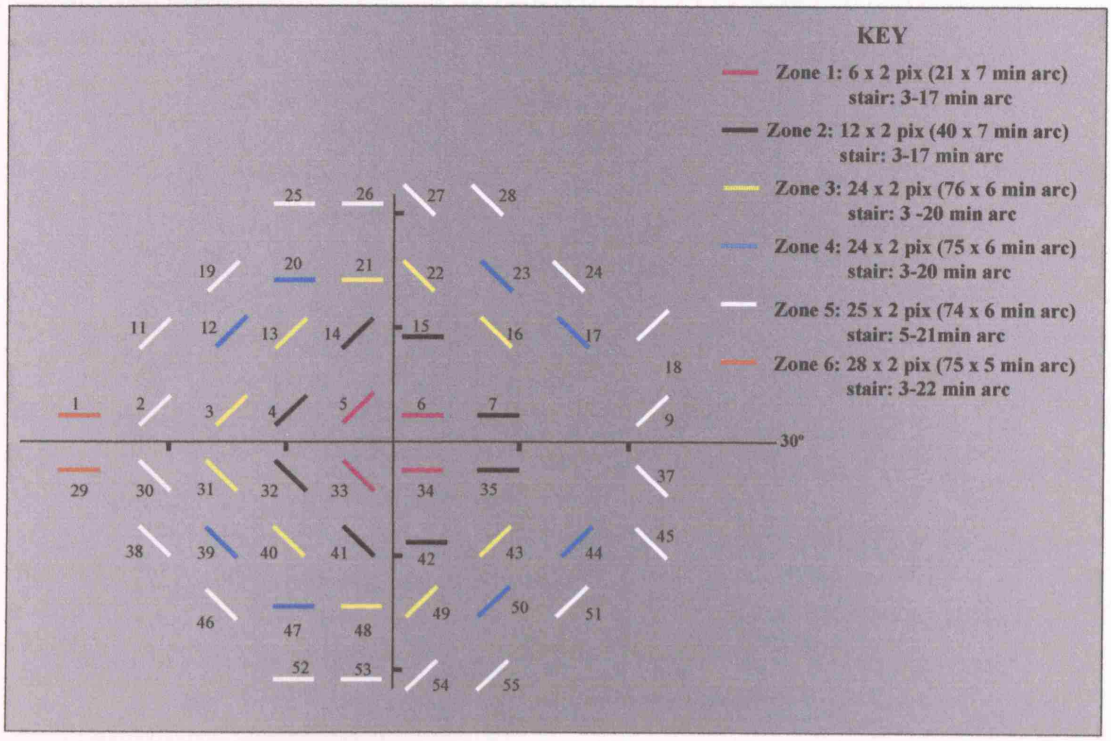

RESULTS

Both subjects showed elevation of mean MDT threshold as the number of scattered locations was increased from 6 locations to 26. Little difference in mean threshold was observed between when 26 irregularly scattered locations and 52 regularly spaced locations (at six degrees, corresponding to the Humphrey 24-2) were present. The effect of clustered stimuli was smaller and inconsistent between the two observers, but in each case lower mean MDT thresholds were observed when 26 clustered locations were present, compared to the 52 locations of the 24-2 program (figure 8-6; appendix table 14-9). An increase in the number of presentations made after reversal was observed when testing with 52 locations present (subject 2 > subject 1). A greater effect of fatigue was found for subject 1 on re-test of location 1 in isolation at the end of a test session.

Figure 8-6. Mean MDT threshold for different number of scattered and clustered locations.

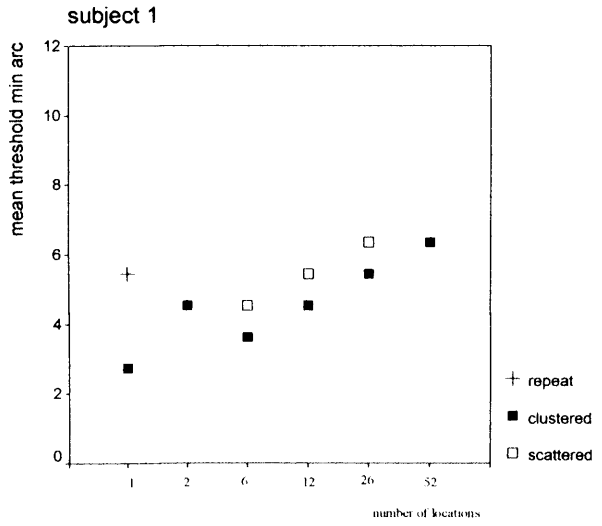

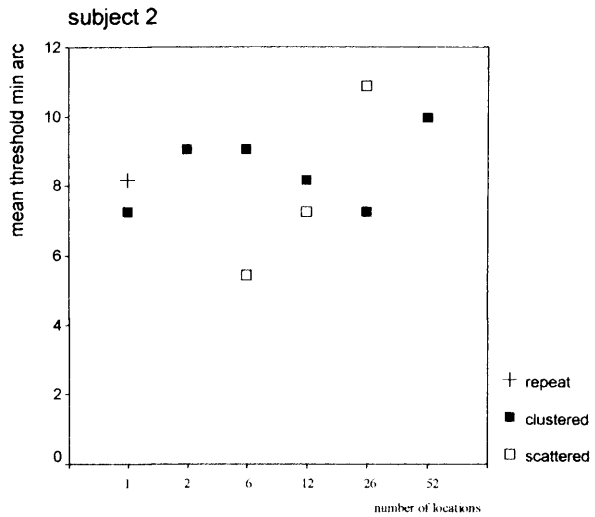

Subjects 1 and 2 showed different patterns of change in MDT threshold as the number of locations present was increased. However, an elevation of MDT threshold was found for both subjects when the number of locations present was increased from 12 to 26. This only occurred when the locations were scattered, indicating an effect of broadly spread attention.

The increase in the number of presentations made after reversal, when testing with 52 locations present, indicates increasing response fluctuation and may be attributed to uncertainty due to fatigue and/or difficulty in maintaining attention.

The elevation in MDT threshold on re-test of location 1 in isolation is indicative of fatigue, and is more evident in subject 1.

A summary perspective indicates that only small changes of MDT threshold will occur with up to 26 locations present and that clustering the locations together will minimize these differences.

The risk of glaucoma increases with age and the MDT test will therefore principally be directed towards the elderly. This experiment was conducted by two psychophysically experienced and relatively young individuals, who may differ from the glaucoma population. It is of paramount importance that the MDT is as robust as possible to the effects of attention in order to avoid false positive diagnosis and reduce test variability. A reduction in the number of test locations is therefore recommended.

The lower MDT thresholds of well practiced subject 1 (GMVR), who is older than subject 2, may indicate that a learning effect is associated with the multi-location format, and should be further explored.

8.2.5 EFFECT OF CROWDING (ADJACENT DISTRACTORS) ON MDT THRESHOLDS

METHOD

The effect of crowding (adjacent distractors) was assessed for location 13 (-9,9) using same line length configurations as described for the prototype multi-location test [figure 7-1 (A)]. MDT threshold of Location 13 was calculated by probit analysis of 5 presentations of 5 displacements between 0 - 18 min arc. Location 13 was suprathreshold using this format, its length was therefore reduced from 103 to 26 min arc. The remaining locations remained at the length selected for strategy (i) in order to maximize the adjacent distractor effect.

The following tests (figure 8-7) were conducted three times each for two experienced subjects:

Test 1

52 locations present.

Test 2 (crowded condition)

The seven stimuli immediately adjacent to location 13 are present (3,4,5,12,14,20,21), with remaining upper nasal quadrant locations stimuli removed (1,2,11,19,25,26).

Test 3 (uncrowded condition)

The seven stimuli immediately adjacent to location 13 were removed (3,4,5,12,14,20,21), with the stimuli of the upper nasal quadrant locations remaining present (2,11,19,25,26,1).

RESULTS

A slight increase in MDT threshold is seen for the crowded condition, when all stimuli are present, compared with the uncrowded condition. The effect is greater for subject 2 than subject 1 but is small in each case (< 1.5 min arc), [figure 8-8 and appendix table14-10].

Figure 8-7. Distribution of test locations for the assessment of crowding (right eye).

Test 1: all locations present (-9,9).*

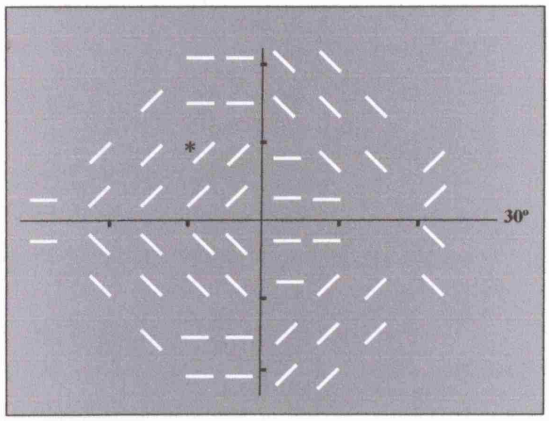

Test 2: upper nasal locations removed (-9,9).*

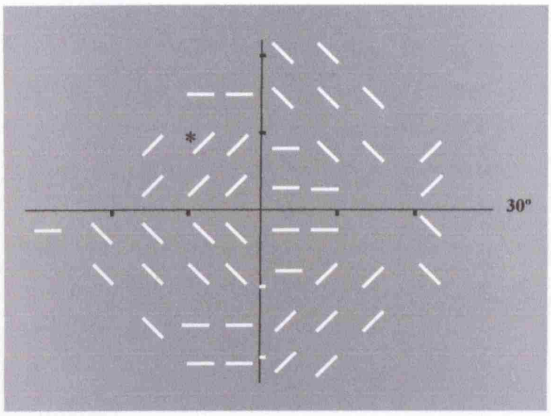

Test 3: adjacent locations removed (-9,9).*

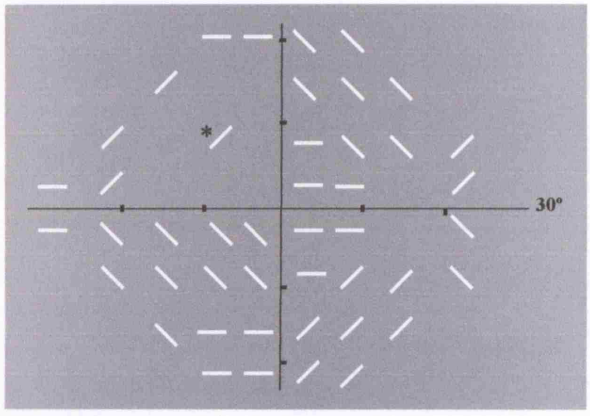

Figure 8-8. Mean MDT threshold for different crowding conditions (-9,9).

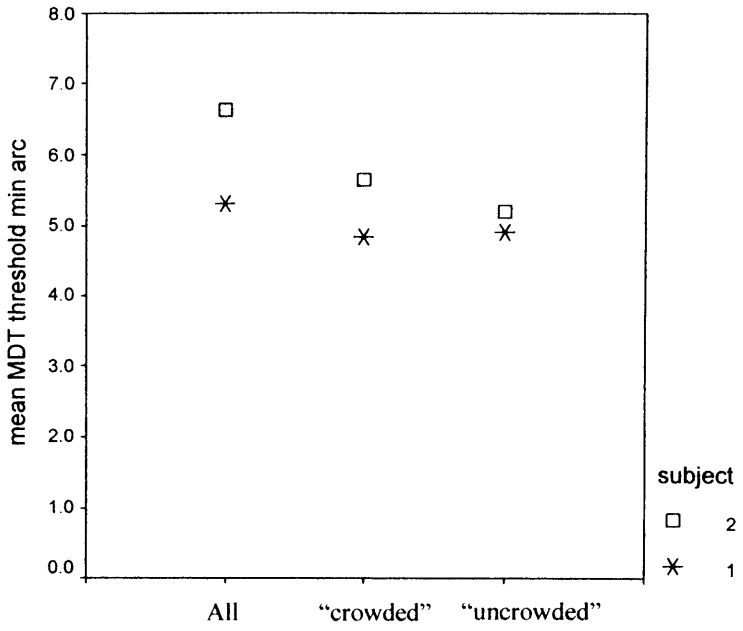

MDT threshold showed only a small effect of adjacent distractors under the experimental conditions set by this study. The un-flanked threshold at –9,9, is in the region of 5 minutes of arc for both subjects [figure 8-8 "uncrowded"]. Based on the observations in Levi's paper, MDT should be free of spatial interference within 5 degrees (Levi et al. 1985).

The spacing of the MDT stimuli is 6 degrees from the centre of one line to the centre of the next, with the line length scaled with GCD. This means that crowding may be greater in the periphery, where the stimuli are longer. Adjacent horizontal lines are more closely aligned than equivalent oblique and may therefore suffer greater interference.

The MDT format uses stimuli of different orientation and this may result in greater central inhibition than if the stimuli were all orientated in a similar direction. It would be interesting to compare MDT threshold using stimuli orientated with RNFL, with strategies where all stimuli are aligned vertically or horizontally.

It may be that future strategies will require smaller spacing between test locations in order to elicit focal glaucomatous defects. This should be done with caution if the distracter effects of crowding are to be avoided. A method of overcoming this would be by using the principal of fine matrix mapping (FMM). FMM has been previously used to give a detailed assessment of small areas of the Humphrey visual field. Westcott created a FMM of 9 x 9 degrees by using four grids of 25 locations, with a 2-degree separation between adjacent points. Each grid was offset with respect to each other by one degree. The grids were then merged to give a FMM of 100 locations, each separated by one degree (Westcott et al. 1997).

Chapter 9

REDUCED MDT STRATEGY BY OPTIC NERVE HEAD REPRESENTATION

9.1 BACKGROUND

The prototype design of the multi-location MDT uses the same location format as the "gold standard" Humphrey 24-2 visual field program and has been shown in the previous chapter to be vulnerable to the effects of attention and distraction. It may therefore be preferable to reduce the number of test locations, providing this is not at the expense of test sensitivity and specificity. It has been found that high sensitivity can be achieved with only a small number of optimally positioned stimuli and that, for screening purposes, it may be preferable to test a small number of locations with a suprathreshold strategy (Henson et al. 1988).

Calculation of the informational content of the visual field suggests that the superior arcuate and inferior nasal quadrant of the visual field give the most useful information in glaucoma, with the inferior temporal quadrant, the superior field beyond 20 degrees and the area around the blind spot the least (Henson and Chauhan 1985).

Study of RNFL bundles by photography shows that the 24-2 distribution of test points gives a disproportionate representation of some disc sectors, weighted in favour of the poles. The poles of the optic disc correspond to the arcuate areas of the visual field and are densely sampled. The superior and inferior parts of the lamina cribrosa have larger pores and thinner connective tissue at the level of the sclera. These regional differences are thought to make the poles more vulnerable to early glaucomatous damage (Quigley and Addicks 1981). However, bias in this interpretation may be introduced by the under-sampling of the central and temporal areas in SAP [figure 9-1 (Garway-Heath et al. 2000b)) and figure 9-2 (Sanchez et al. 1986)].

Figure 9-1. Topographic relationship of MDT test points to the optic nerve head of the right eye (adapted from Garway Heath et al., 2000).

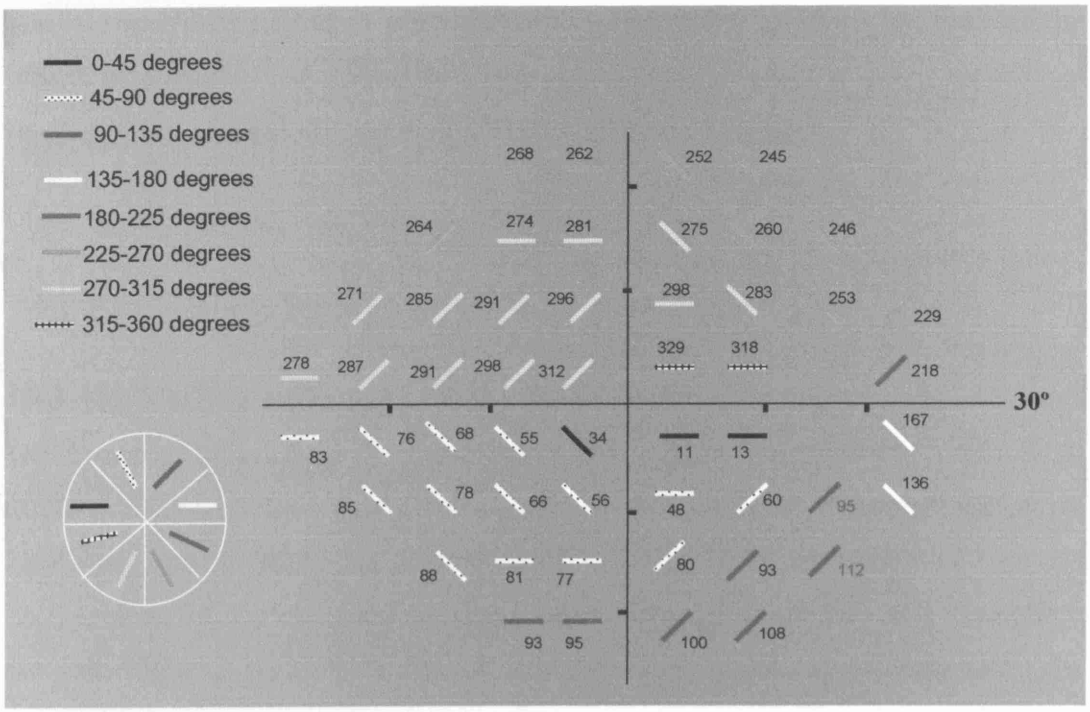

Figure 9-2. Diagrammatic representation of regional density of optic nerve fibers in the optic nerve head of the monkey (from Sanchez et al., 1986).

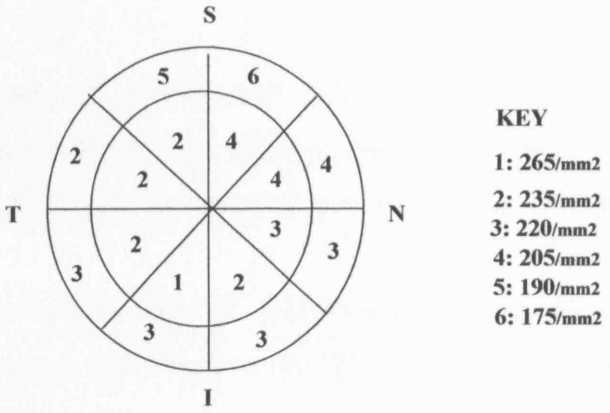

9.2 DEVELOPMENT OF REDUCED MULTI-LOCATION MDT STRATEGY

A reduced multi-location MDT strategy was designed using a novel format: the aim was to produce a test of a small number of clustered locations to minimize the effects of attention and distraction. Test points were selected to give proportional representation of the ONH spanning different optic nerve bundles.

METHOD

Five pilot MDT strategies (figure 9-3) were designed with reference to the Garway-Heath map of visual field-ONH correspondence (figure 9-1), (Garway-Heath et al. 2000b). Approximately three locations were selected per 45-degree sector. A limitation was imposed on central and temporal field representation by the confinements of the computer program, which was based on the 24-2 Humphrey template (figure 2-1). MDT thresholds were estimated by staircase analysis using the same stimulus parameters (line length, width and displacement) as described for the second multi-location study (figure 7-1B). Two experienced and two naïve control subjects were tested to give an indication of test performance and acceptability.

RESULTS (figure 9-4)

Subjectively, all subjects showed preference for version E where stimuli are clustered closely together. Subjects were disconcerted by strategies A - C where there are islands without test points. These areas were perceived as apparent "holes."

All subjects showed a reduced test time (< 4 min 45 sec) for all variations of the reduced MDT by comparison with the prototype 52-location test, where the test

Figure 9-3. Pilot versions of the MDT with selection of locations by optic nerve head sector (right eye).

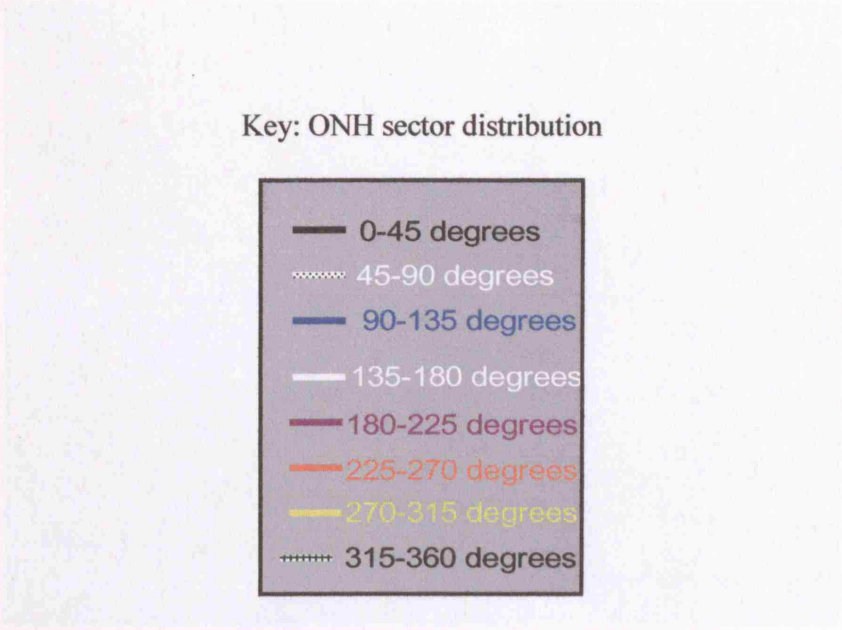

Version A

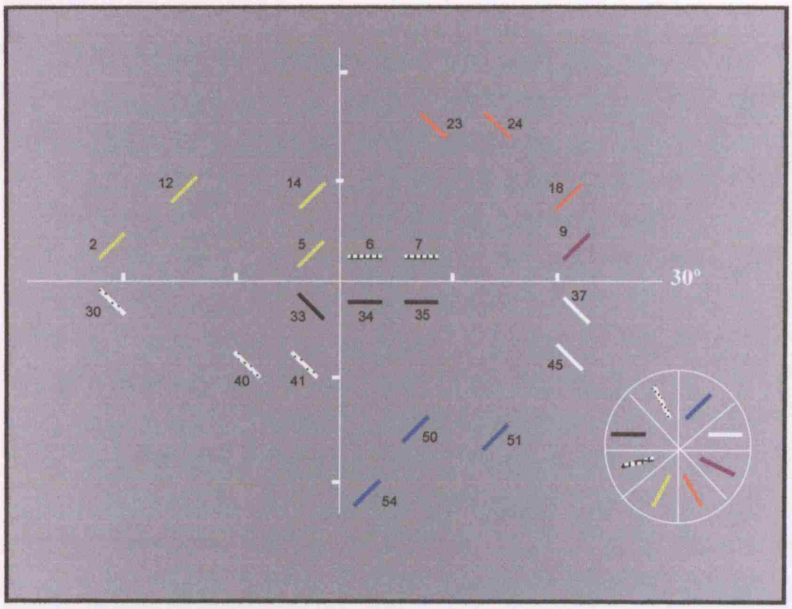

Version B

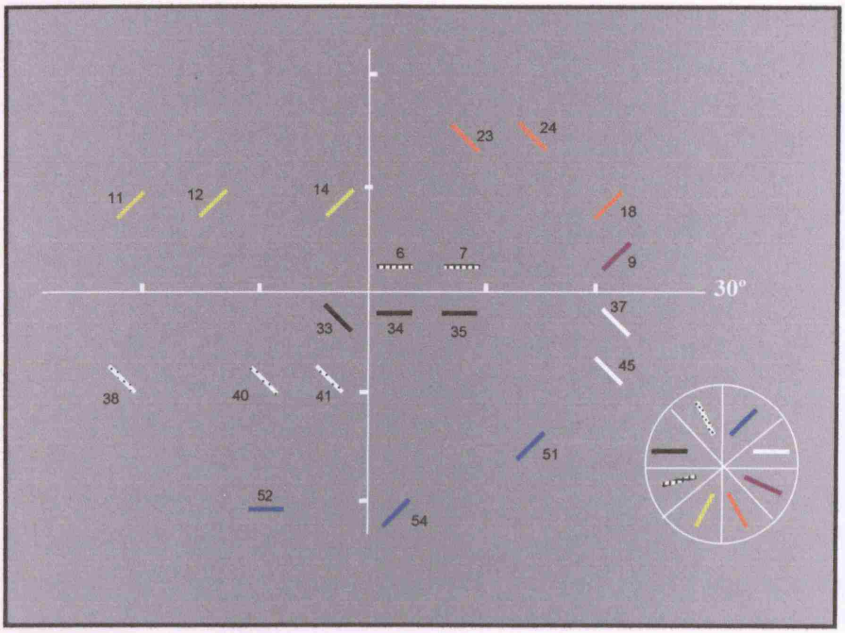

Version C

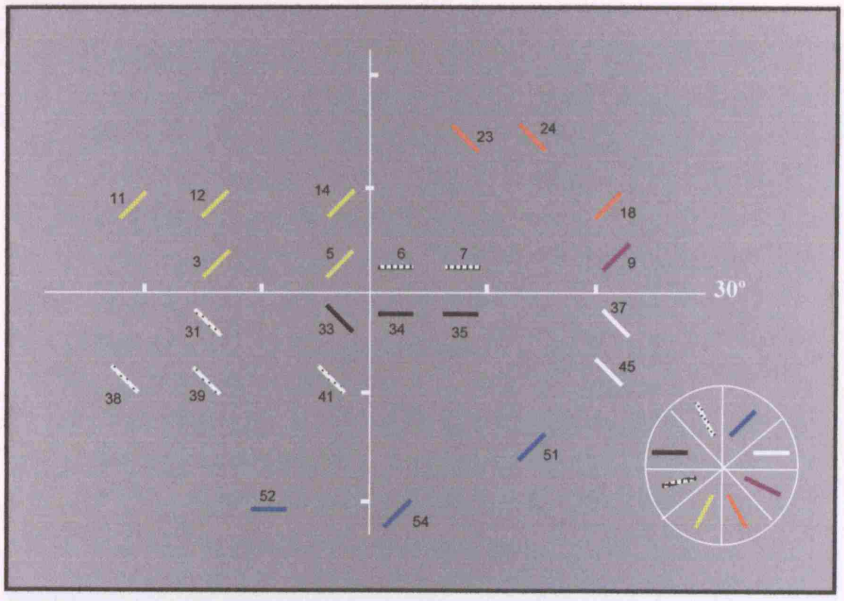

Version D

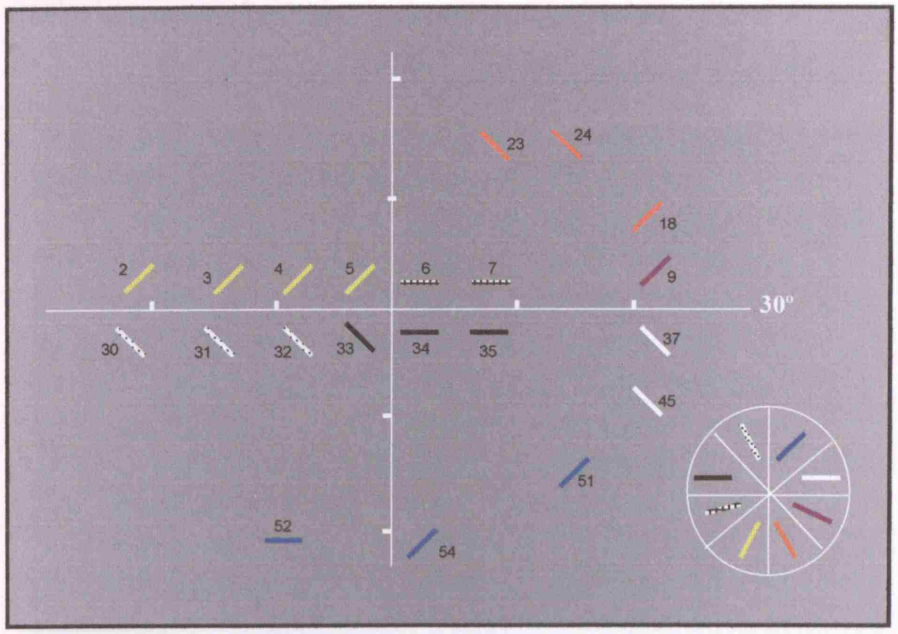

Version E

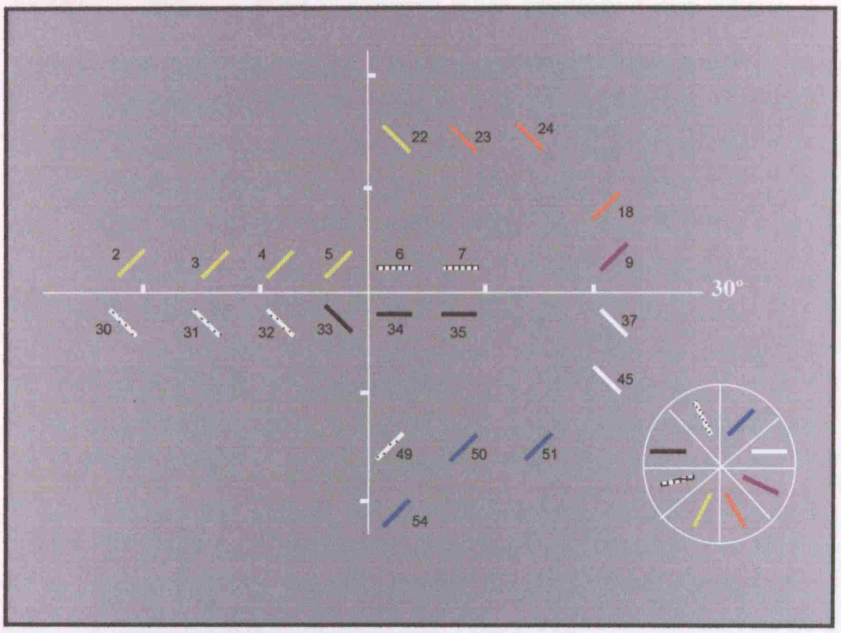

Figure 9-4. Examples of pilot reduced MDT (Strategy A).

Numerals adjacent to stimuli refer to the MDT threshold determined by the staircase strategy. Where there are no numerals for subject (i) the location is suprathreshold.

(i) Experienced subject (47 years). Test duration: 3 min 24 sec.

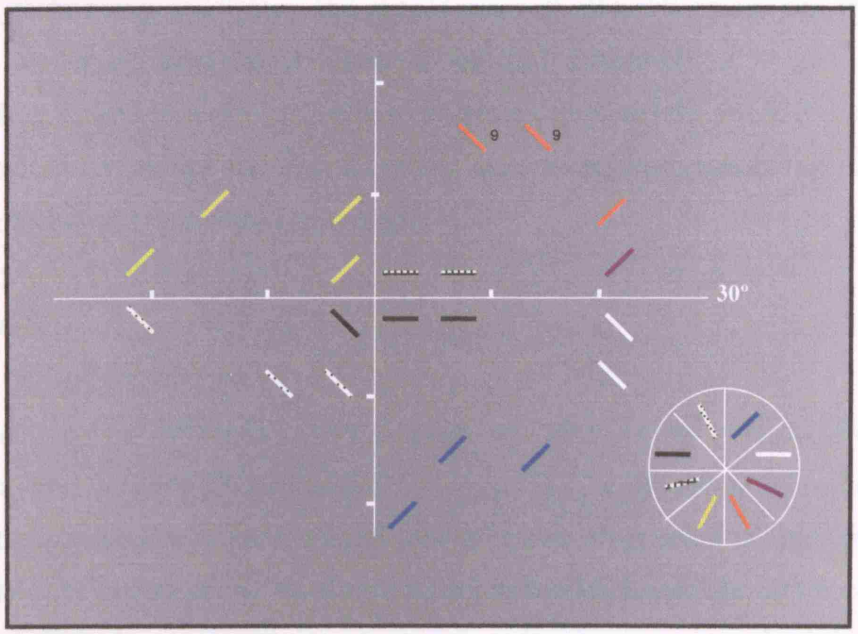

(ii) Naïve subject (34 years). Test duration: 4 min 33 sec.

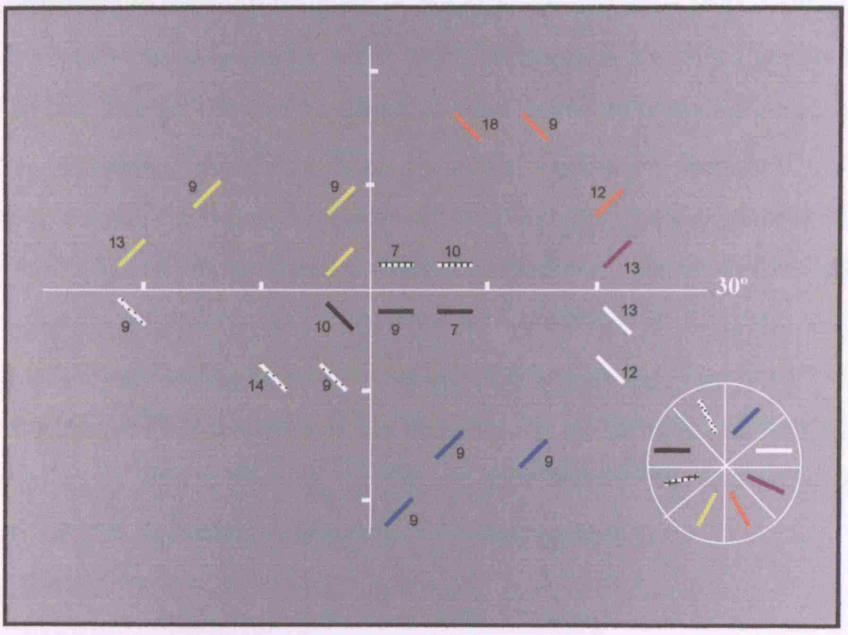

duration was in the region of 12 minutes. There was a tendency to an increased MDT threshold with eccentricity, which was more marked for the naïve subjects.

For example, experimental strategy A (figure 9-3): experienced subject GMVR, aged 47 years, completed the test in 3 min 24 sec, with all test locations suprathreshold except two upper temporal locations which had thresholds of 9 min arc. By comparison, a naïve younger subject aged 34 years completed the test in 4 min 33 sec. Only one central location was suprathreshold and increasing thresholds up to 13 min arc were found with increased eccentricity.

DISCUSSION

A substantial reduction in test duration was seen for the reduced pilot MDT strategies over the pilot 52-location MDT (chapter 7). The elevation of thresholds and the longer test duration of naïve subjects are indicative of an effect of learning, which should be kept under review. An allowance for increased thresholds with eccentricity may be made by increasing the stimulus length and/or displacement. Caution needs to be applied to ensure that this is not done at the expense of detecting early glaucoma.

Consideration needs to be given to the required response from normal subjects. A threshold response is desirable if the test is to be used for long-term follow-up of patients so that damage may be measured. A suprathreshold response is acceptable for screening purposes, providing there is good separation between control and glaucomatous eyes. Suprathreshold tests are normally designed to present stimuli at a fixed intensity above the estimated threshold, sometimes referred to threshold related suprathreshold tests. Here the suprathreshold increment is variable. A threshold response may be gained by adjustment of the stimulus energy. The linear relationship found with log MDT threshold and log stimulus energy (chapter 6) provides a basis for manipulating the stimulus to the desired parameters. The central locations are limited by current technology and sensitivity to optical blur.

It is recommended that in due course the computer software for the MDT should be re-designed to be independent of the 24-2 Humphrey format, in order to allow increased representation of the temporal and central field.

9.3 TROXLER FADING

Naïve subjects sometimes complain of Troxler fading when presented with the multi-location MDT test in its original (52 location) or reduced (21 or 23 location) form. Troxler fading describes the physiological habituation of a peripheral stimulus in the presence of a competing central stimulus (Jansiewicz et al. 2004) and is manifested by the subjective disappearance of the continuously presented line stimuli in the context of the multi-location MDT.

Lou investigated the effect of Troxler fading and voluntary attention by presenting six discs, three green and three red in alternate positions. 16 subjects were tested and each observer was asked to attend to three discs of the same colour. Some discs began to fade within a mean period of 11 msec. Of those beginning to fade, 81% were selected for attention, with the effect increasing with eccentricity (Lou 1999).

Experienced subjects become habituated to MDT Troxler fading over time. Study of focal brain lesions suggest the parietal cortex may be important in sustaining attention toward visual stimuli in peripheral space, whereas the frontal cortex may mediate selective attention through habituation to peripheral stimuli (Mennemeier et al. 1994).

Johnson developed a staircase (3 min – 5 degree) MDT test on a Macintosh computer using 60 continuously displayed square white stimuli subtending approximately 0.6 degrees. The test distance was 30 cm. Stimuli underwent unilateral displacement at a duration of 50 msec. Johnson found subjects with good fixation would experience Troxler fading after 30 - 40 seconds of continuous presentation.

Subjects with poor fixation tended to experience "negative after image shadow" which moved with the fixational instability.

Johnson overcame the problem of Troxler fading by fading the entire test grid out over a period of one second after every 8 - 10 stimulus presentations. The grid remained extinguished for 2 seconds and was then faded back over a further one second period. Testing was resumed 1.5 seconds after the grid had completely faded back in (Johnson et al. 1995).

Johnson's methodology would add significantly to the MDT test duration and could prove disruptive to the flow of the test. It is recommended that Troxler fading should be mentioned as a normal, physiological, occurrence within the instructions of the MDT. The subjective effect of Troxler fading on MDT acceptability should be kept under review.

Chapter 10

PILOT INVESTIGATION OF REDUCED MDT TEST STRATEGY IN GLAUCOMA

A pilot study was initiated to assess the optimal stimulus line length and displacement of the MDT by systematic investigation of a small number of glaucoma patients with reproducible focal defects in different areas of the visual field.

METHOD

The distribution of test locations in pilot test version E, described in the previous chapter (figure 9-3), was used to investigate the MDT in glaucoma. Five patients who were known to produce reliable, reproducible Humphrey fields were carefully selected. Subjects 1 and 2 were first evaluated. Test parameters were modified, according to their results, before testing subjects 3, 4 and 5.

Subject 1 (focal central field defect; left eye): two variations of central stimulus length were investigated for the left eye [figure 10-1 (i) and (ii)]. Stimulus length for zones 4 and 5 was increased by comparison with the pilot strategies of chapter 7 (figure 7-1) to investigate whether this would reduce peripheral noise. Equivalent pixel elements were calculated for horizontal and oblique stimuli using the methodology described in chapter 7 (appendix table 14-11).

Subject 2 (focal lower temporal field defect; right eye): the right eye was tested using strategy 2 [figure 10-1 (ii)].

Subject 3 (no field defect; ocular hypertension both eyes): the right eye was tested for strategy 1 [figure 10-1 (i)]. Both eyes were tested using strategy 3a [figure 10-1 (iii)], which uses shorter line lengths for peripheral zones, in view of the

Figure 10-1. Variations of MDT pilot strategy (right eye).

Numerals adjacent to stimuli refer to the reference number allocated to each stimulus.

(i) Strategy 1.

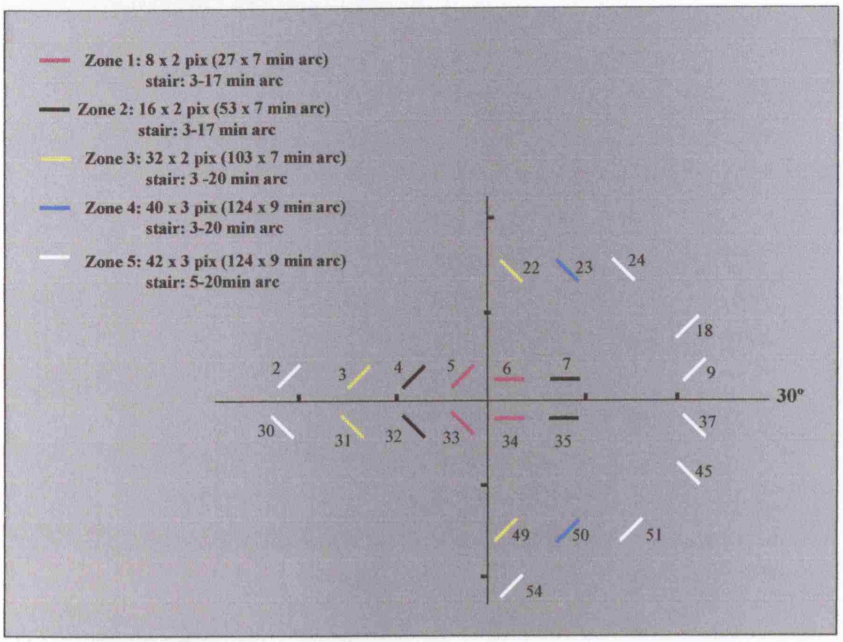

(ii) Strategy 2 (Note zones 4 and 5 remain the same).

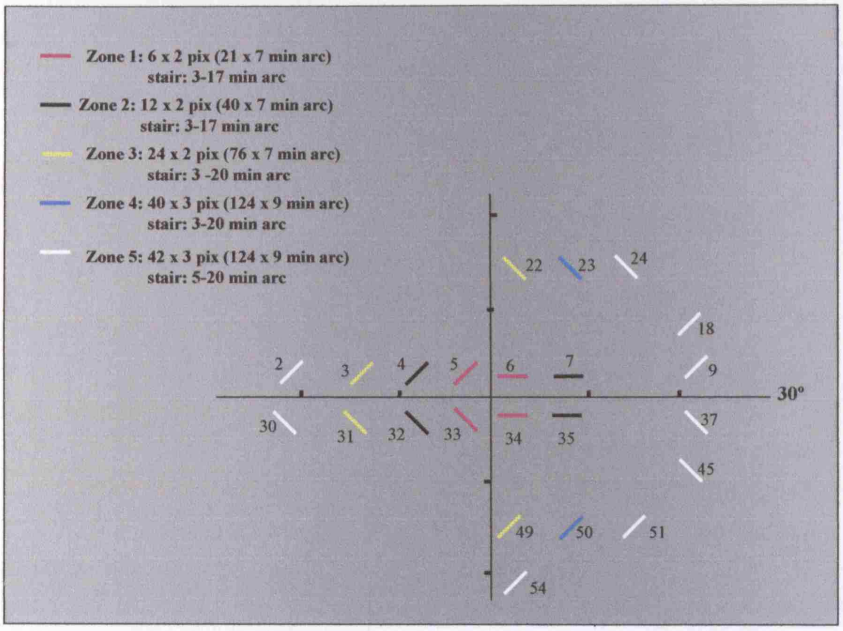

(iii) Strategy 3a.

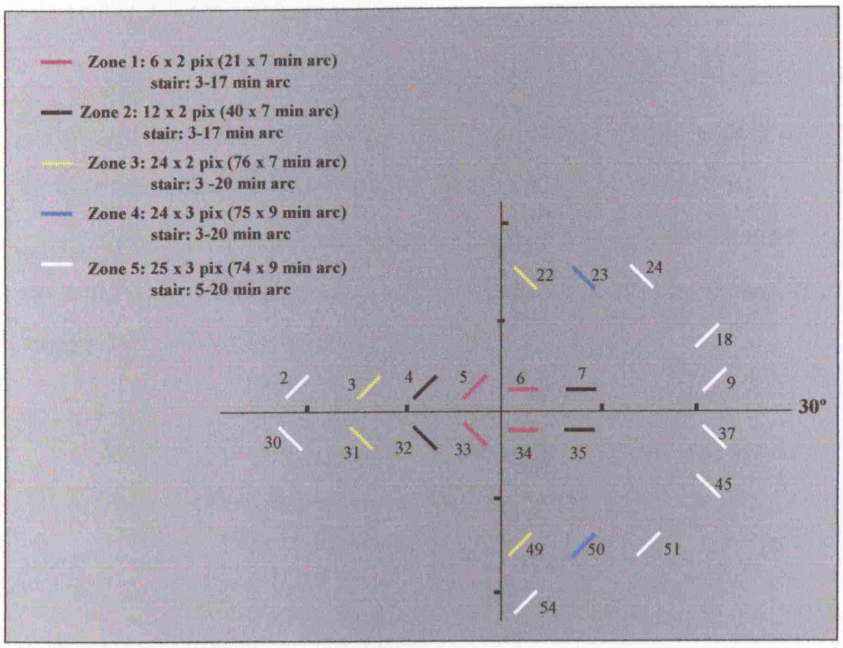

(iv) Strategy 3b.

Stimulus lengths are as described for strategy 3a above. Stair parameters are increased.

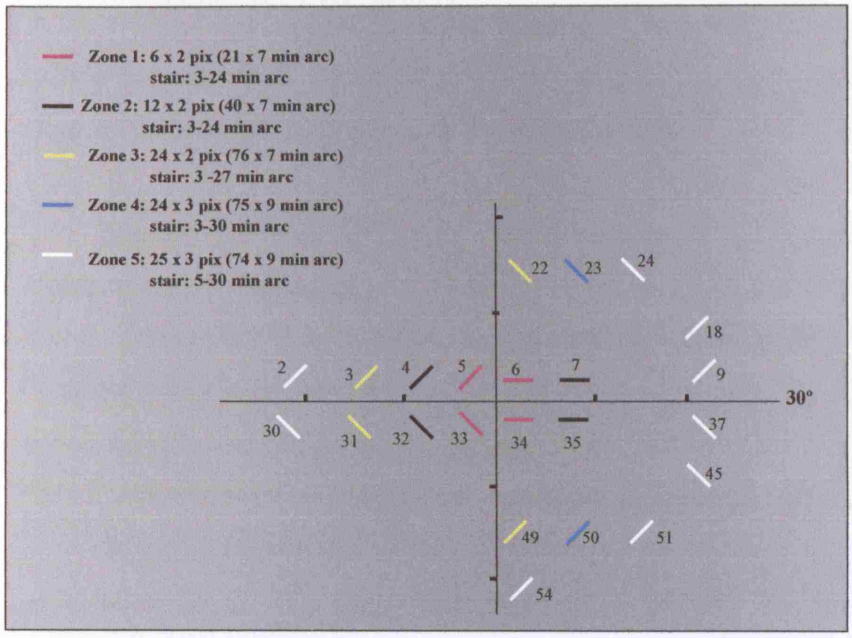

suprathreshold MDT response obtained for subject 2 at the site of a known Humphrey defect (figure 10-2)].

Subject 4 (nasal field defect): the right eye was assessed using strategy 1 [(figure 10-1 (i)] and strategy 3b [(figure 10-1 (iv)], which uses the same stimulus length as strategy 3a but the displacement stair is increased. This is to give a greater prospect of measuring thresholds where there is glaucomatous damage, as in this patient, who presents with a more widespread, denser defect than previous patients tested.

Subject 5 (lower field defect): the left eye was assessed using strategy 3b [figure 10-1 (iv)]. This strategy was selected for the same reasons as given for subject 4 (above).

RESULTS

A summary of patient details, test duration and number of presentations is given in table 10-1. Detailed analysis of the results from each strategy was made in relation to the point-by-point topography of the Humphrey pattern deviation (PD) index (figure 10-2). Results for each subject were as follows:

Subject 1 [figure 10-2 (i)]: central locations 6 (3,3) and 7 (9,3) showed Humphrey PD P values of $< 0.5\%$ and $< 1\%$ respectively. MDT strategy 1 failed to clearly differentiate these locations as abnormal. Locations 6 and 7 were recorded as "unseen" when using the smaller line lengths of MDT strategy 2. By contrast, low threshold values of MDT (10 and 7 min arc) were found for the matched-paired hemi-field locations (34 (3,-3) and 35 (9,-3) respectively) in the lower field.

Subject 2 [figure 10-2 (ii)]: MDT strategy 2 elicited the lower Humphrey defect at location 54 (3,-21), which was recorded as unseen, but poorly differentiated location 49 (3,-15; 14 min arc) and location 50 (9,-15; suprathreshold).

Subject 3 [figure 10-2 (iii)]: The order of tests was as follows: test 1, left Eye (strategy 3a); test 2, right eye (strategy 3a); test 3, right eye (strategy 1). An effect of fatigue, but not learning, was found. The left eye produced lower MDT thresholds using strategy 3a than the right eye, which was tested second. The right eye performed better for strategy 3a than for strategy 1, which used longer peripheral line length. Fatigue was also indicated by an increased number of presentations and test duration for the right eye, strategy 1, which was tested last in the sequence of tests (table 10-1).

Subject 4 [figure 10-2 (iv)]: an improved sensitivity to detect glaucoma was seen with the shorter lengths and longer displacement parameters of strategy 3b over strategy 1.

Subject 5 [figure 10-2 (v)]: strategy 3b showed a good correlation between the MDT thresholds and the Humphrey lower field defect. Differences occurred in the upper field at location 2 (-21,3), where the Humphrey estimation was normal and the MDT threshold was recorded as "unseen." Location 4 (-9,3) was suprathreshold by MDT estimation but had a Humphrey pattern deviation probability value of less than 1%.

Table 10-1. Summary of results for variations of MDT strategy in glaucoma.
Key:
POAG: primary open angle glaucoma; OHT: ocular hypertension; PxF: pseudoexfoliation glaucoma

	Subject 1		Subject 2	Subject 3			Subject 4		Subject 5
Sex	Male		Male	Female			Female		Male
Age (years)	68		72	68			61		65
Diagnosis	POAG		POAG	OHT			PxF		POAG
Strategy	1	2	2	1	3a	3a	1	3b	3b
Eye	LE	LE	RE	RE	RE	LE	RE	RE	RE
Duration (mins)	4:31	4:26	4:29	5:03	4:38	4:29	4:24	4:52	5:29
Number of Presentations	88	86	78	96	90	88	85	94	104

Figure 10-2. Topographical comparison of MDT thresholds with Humphrey 24-2 probability value for pattern standard deviation.

(i) Subject 1 (left eye).
Strategy 1 and Strategy 2 (min arc). Results for strategy 2 are given in brackets.

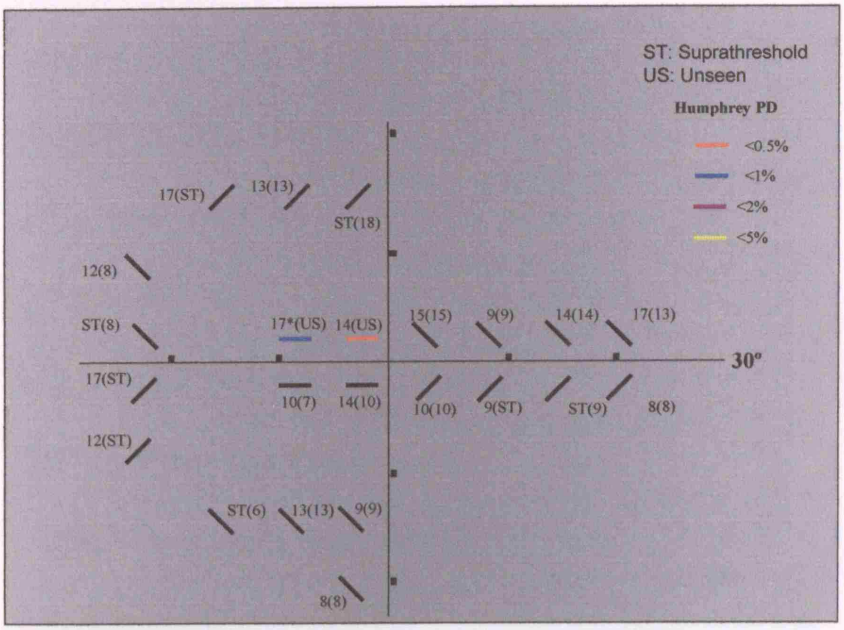

(ii) Subject 2 Strategy 2 (right eye).

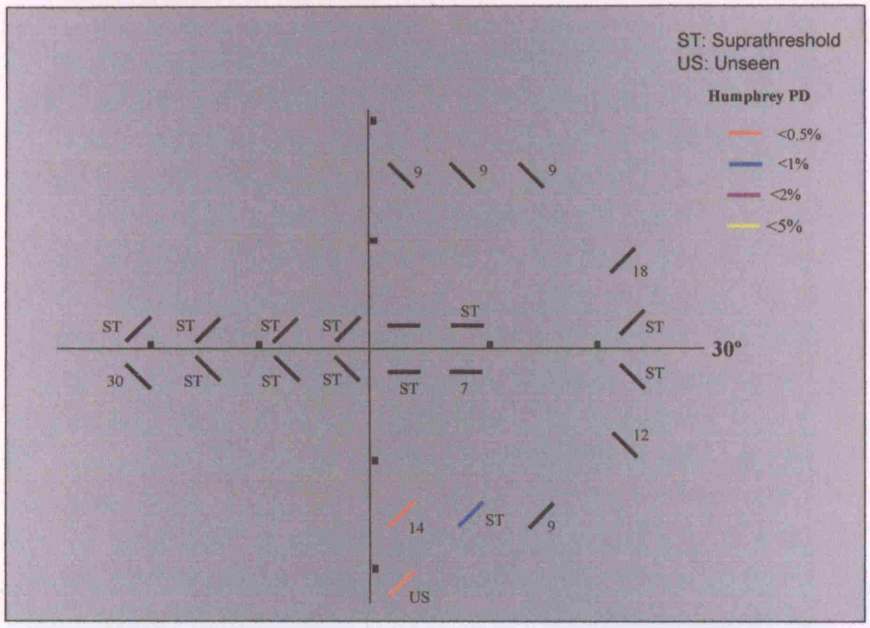

(iii) A) Subject 3 Strategies 1 and 3a (right eye).

Results for 3a are given in brackets.

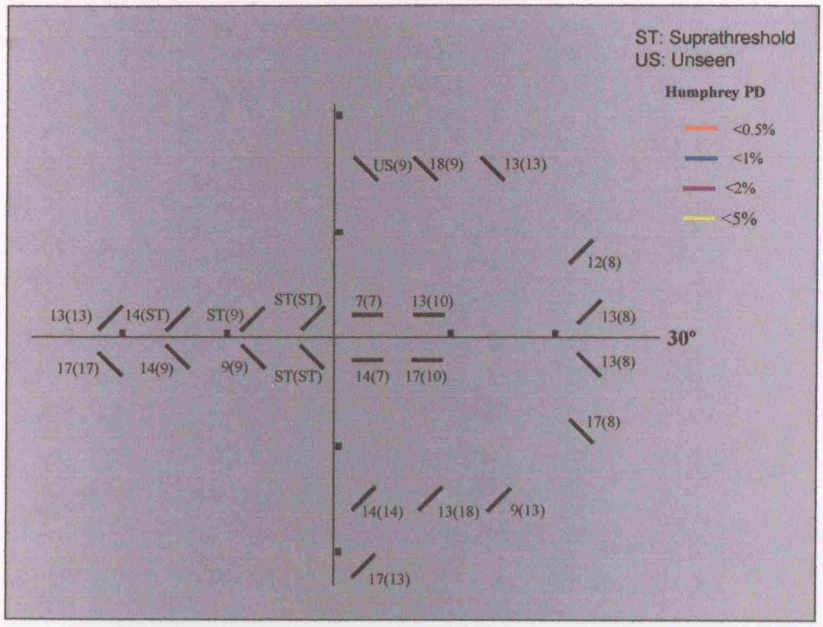

B) Subject 3 Strategy 3a (left eye).

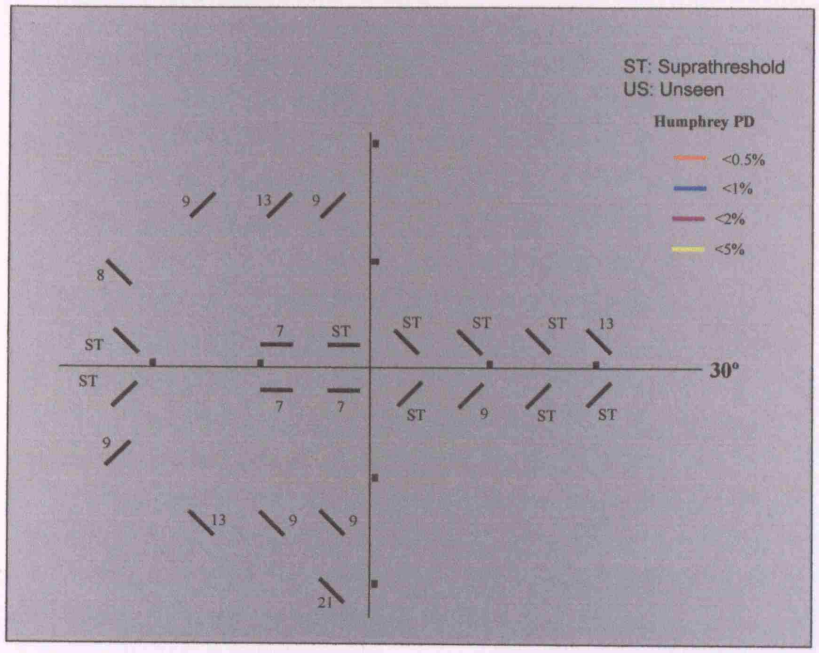

(iv) Subject 4 Strategies 1 and 3b (right eye)

Results for 3b are given in brackets.

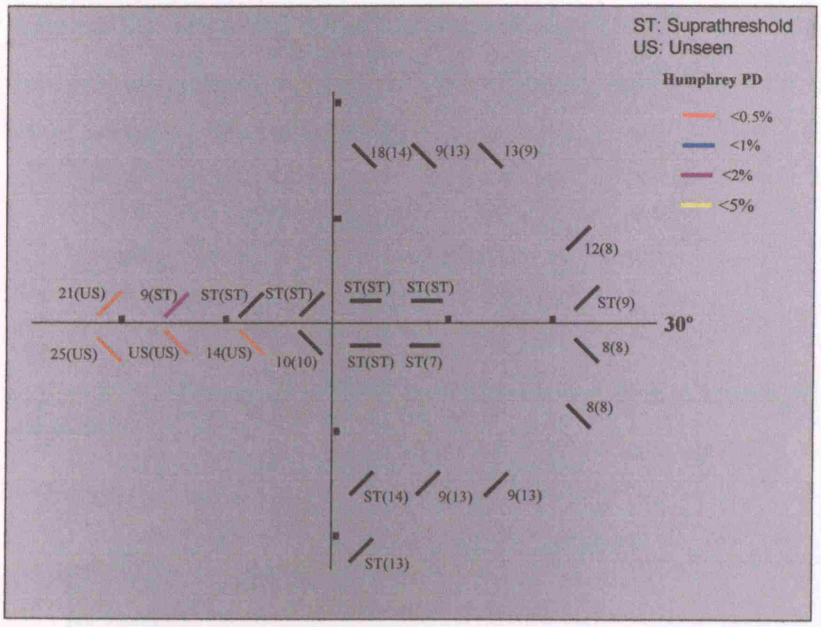

(v) Subject 5 Strategy 3b.

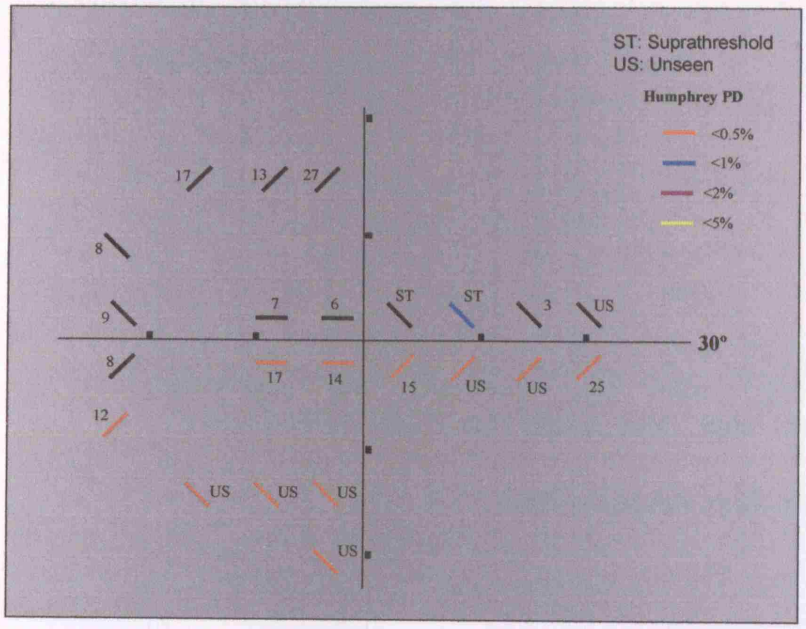

The age of the patients was 67 (61-72) ± 3.4 years (mean (range) ± standard deviation). The patient response times were 676 ± 177 (379 – 1279) msec (mean (range) ± standard deviation). Individual response times are given in the appendix table 14-12). The frequency of response time at threshold was plotted. This was done both with the glaucoma subject response times merged (figure 10-3) and for individual subjects (figure 10-4; table 10-2).

Figure 10-3. Histogram of frequency of response time at threshold (five glaucoma subjects).

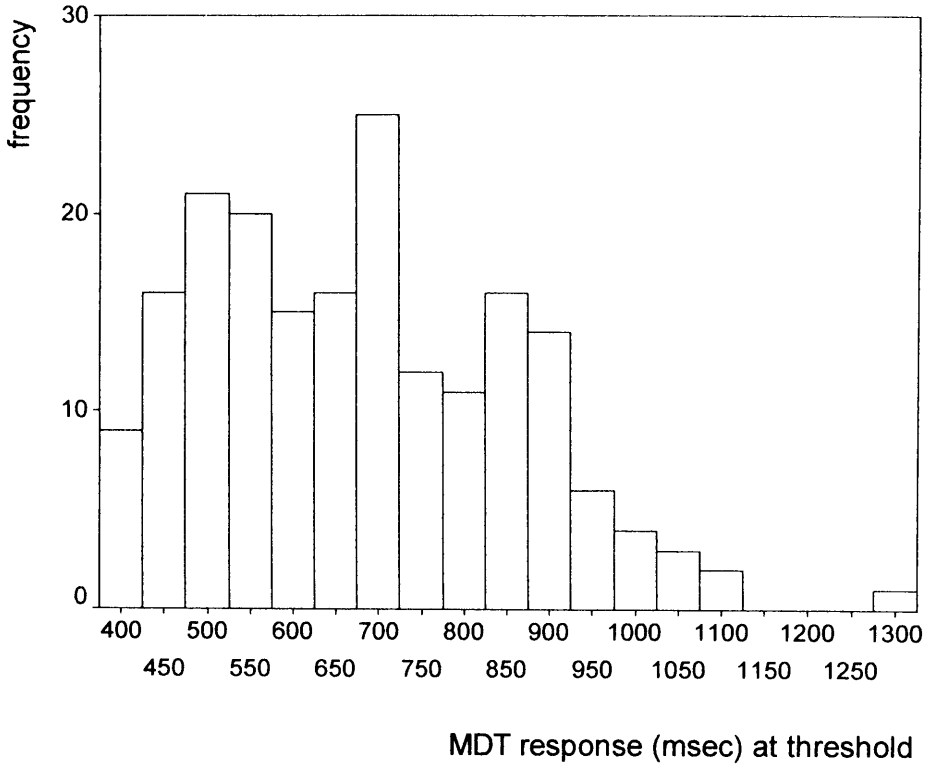

Figure 10-4. Frequency of response times at threshold for individual glaucoma subjects.

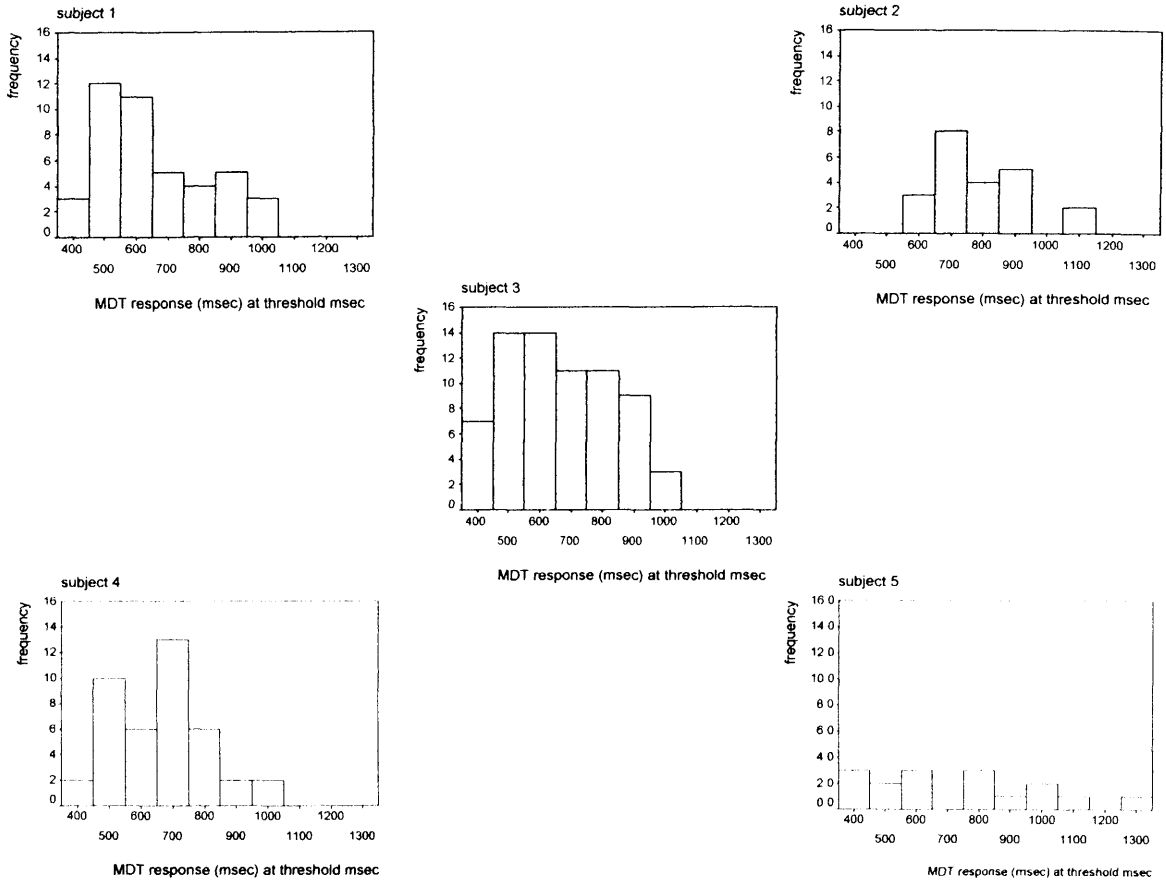

Table 10-2. Summary of percentiles and range of frequency of response time at threshold.

		Percentiles of frequency of response (msec)			
Subject	range (msec)	25	50	75	95
1	395 – 1045	504	585	774	998
2	575 – 1085	680	754	890	1080
3	394 – 984	515	640	825	938
4	379 – 690	513	675	750	952
5	420 – 1279	504	694	988	1279
All	379 – 1279	530	674	820	979

The preliminary results of the reduced multi-location test indicate that MDT loss in glaucoma follows a similar pattern to that seen for DLS in conventional perimetry. This is in agreement with the spatial relationship of RDK perimetry with optic disc topography in glaucoma and also Johnson's early unidirectional motion displacement test (Johnson et al. 1995; Bosworth et al. 1999).

Choice of MDT line length is shown to be critical in detecting motion displacement sensitivity loss in areas of known Humphrey field loss (Patients 1 and 4).

Fatigue may manifest as an elevation of MDT threshold, a greater number of stimulus presentations and longer response times, which will consequently lead to an increase in test duration.

It is interesting to compare the response time at threshold [mean (range) msec] of the elderly glaucoma patients of this study [676 (379 – 1279) with GMVR's response time for the 52 multi-location test [500 (265-925), (chapter 7)] and the original single line BBC [(1470 (1000 – 2050) and 1360 (980 - 1800 msec) for controls and glaucoma respectively), (Westcott et al. 2000a).

Chapter 7 suggested reducing the listening window from 1500 to 1000 msec. This gives a response time of 1600 msec, allowing for the stimulus presentation time of 600 msec (3 oscillations at duration of 200 msec per cycle). Analysis of the frequency of patient response times at threshold indicates a further reduction in the stimulus listening window may be achieved (figure 10-3). If the 95th percentile were used as the cut-off for the response window, a listening window of ~ 980 msec would be required (table 10-2). The stimulus presentation time is 600 msec. A listening window of 400 msec would give a total response window of 1000 msec from the stimulus onset (figure 10-5).

Figure 10-5. Illustration of proposed modified stimulus timings.

The listening window is reduced to 400 msec, which, together with the stimulus presentation of 600 msec, gives a response window of 1000 msec. The total time for each stimulus presentation is 3 sec (1000 fixed pre-displacement; 1000 msec stimulus presentation + response window; 1000 msec post response wait) plus a randomized pre-displacement of anything between 0 and 750 msec. This modification would give a potential time saving of 600 msec per unseen presentation.

Key:
A: Adaptation
FP: Fixed Pre-displacement
RP: Random Pre-displacement
SP: Stimulus Presentation
LW: Listening Window
PRW: Post Response Wait

A:	FP:	RP:	SP:	LW:	PRW:	
5000	1000	750	600	400	1000	msec

Lowering the listening window to 400 msec would give a potential time saving of up to 600 msec per presentation over the currently used response window of 1600 msec. All subjects have unseen presentations at the turning point of the stair, where displacement values are below threshold. The setting of the response window therefore has a significant effect on the test duration for both normal and glaucomatous patients.

The effect of lowering the response window to 1000 msec on MDT threshold can be estimated by analysis of the raw data and making a consequent prediction of the outcome on the MDT staircase. For example, table 10-3 (a) shows the step staircase response of subject 5 at location 3 (-15,3). The first presentation was "seen" with a response time of 860 msec. The MDT program consequently reduced the following

presentation to 2 pixels, where the response was 1094 msec. The stair therefore descended a further step to 1 pixel, which is "unseen." The stair then reversed and increased the next displacement to 2 pixels, which was also "unseen." A further increase in step displacement to 3 pixels yielded a "seen" response of 495 msec. One can predict that if a listening window of 1000 msec were imposed then the second displacement of 2 pixels would be registered as "unseen." The staircase would therefore reverse up to 3 pixels and one can estimate from the table that this would be recorded as "seen." From this one can deduce that there would be a time saving of two "unseen" presentations, which would total six seconds (three seconds per presentation) with two additional random pre-displacements of anything from 0 to 750 msec (figure 10-5).

Reduction in the listening window may improve separation of normal and glaucomatous eyes by removing uncertainty where there is pathology. For example, subject 5, location 35 (9,-3); strategy 3b [figure 10-2 (v)]. The Humphrey PD probability value for this location was $P < 0.5\%$. The MDT threshold was estimated as 17 min arc (6 pixels). If the response window were set at 1000 msec none of the presentations in the table would be seen and the threshold estimate would therefore be greater than 17 min arc [table 10-3 (b)].

There is a similar finding for patient 1, at location 7 (9,3), for strategy 1 [figure 10-2 (i)]. The PD probability value for this location was $< 0.5\%$. The MDT threshold was estimated as 17 min arc. If the response window were set at 1000 msec, the third presentation at 5 pixels would be recorded as "unseen" and the stair continue upwards. The threshold would therefore measure > 17 min arc.

When interpreting the stair response it should be noted that subject 5 was the slowest responder. When the individual response times are taken into account, two of the five glaucoma subject show 5% of responses above 1000 msec (table 10-2). If one tested a control, who was a similar slow responder, the response window of 1000 msec would result in a loss of specificity. Therefore a response window of 1000 msec may be a little on the short side.

Table 10-3. Examples of MDT staircase with response times.

(a) subject 5; location 3 (-15,3).

Displacement (pixels)	Response time (msec)
3	860
2	1094
1	0
2	0
3	495

(b) subject 5; location 35 (9,-3).

Displacement (pixels)	Response time (msec)
3	1615
2	1120
3	0
4	0
5	0
6	1004

c) subject 1; location 7 (9,3).

Displacement (pixels)	Response time (msec)
3	0
4	0
5	1005
4	0

The results of this study show a clear variation between subjects in response time (figure 10-4; table 10-2). In due course it is planned that the MDT will be tailored to the response times of the individual (Artes et al. 2002). This will be done as post-doctorate work. It is recommended that the response times of perimetrically naïve, elderly controls should be evaluated before the listening window is reduced.

Detection of glaucoma may be improved by the development of novel MDT strategies not confined to the Humphrey format (figure 2-1). These could be designed to assess specific areas of suspect ONH damage in detail. Areas of the visual field that are currently poorly represented by SAP could be investigated (figure 9-1). Small numbers of clustered locations would reduce the effect of distraction and fatigue. Reduction of the spacing between locations may improve sensitivity to detect early glaucoma (Westcott et al. 1998a) but the effect of crowding would need to be kept under review.

An overview of the results suggests that strategy 3b offers the optimum parameters of stimulus line length and displacement to detect glaucoma within this small group of patients with various focal defects. It is of interest to note the number of locations that are recorded as unseen, even when the range of the staircase is increased to 30 min arc, which exceeds the largest displacement tested within the original BBC computer test strategy. This raises the question whether it would be informative to increase the range of displacements of the staircase strategy further, in order to obtain threshold results. This will be considered in the next chapter.

Chapter 11

PILOT INVESTIGATION OF MDT SUMMATION PROPERTIES IN GLAUCOMA

The first pilot study of the reduced MDT in glaucoma found many locations were unseen, including where the range of displacement was increased beyond that of the BBC MDT (24 min arc). Longer lines were found to yield lower MDT thresholds in areas of known glaucomatous damage. This finding is consistent with Humphrey perimetry, where an increase in stimulus size enables the measurement of DLS in "blind" areas of SAP using the standard Goldmann stimulus size III (Fellman et al. 1988).

The increase in sensitivity with increase in stimulus size in glaucoma may in part be explained by probability summation of neighboring normal areas of the visual field. However, some glaucoma patients show levels of summation which are beyond what would be predicted physiologically ("pathological summation"), (Anderson 2005). Ricco's area increases in size in glaucoma (Fellman et al. 1988), which indicates altered patterns of spatial summation.

The enlargement of the critical summation area in glaucoma may be due to higher neural processes, which occur in compensation to ganglion cell loss. This may be achieved by the pooling of second-stage spatial filters (Swanson et al. 2004; Anderson 2005). Alternatively, or additionally, we know that Ricco's area enlarges as the background illumination declines (Glezer 1965), and in glaucoma, the ganglion cell loss may equate to reduced background illumination, resulting in an increased Ricco's area.

One questions exactly what the MDT is actually testing in glaucoma: where we find an elevated threshold, does it represent dysfunctional overlapping receptive fields

and consequent altered patterns of integration? Are we in effect mapping the MDT scotoma, where we convert an unseen response to a seen response by increasing the range of displacements?

An experiment was designed to investigate MDT summation properties in areas of reproducible Humphrey focal loss in glaucoma.

Subject 1, from the previous chapter, was invited to take part in the investigation. This patient was selected as he was known to have reliable, reproducible Humphrey fields with a dense, focal, central upper defect, associated with POAG in the left eye. The Humphrey defect corresponded to MDT locations 6 (3,3) and 7 (9,3) and the total deviation measured - 31db and - 4db respectively. It was unknown how these varying degrees of DLS loss would translate into MDT perception.

Earlier investigation of this patient found unseen MDT responses for locations 6 and 7 using a line length of 6 pixels (21 min arc). A longer line length of 8 pixels (27 min arc) produced MDT thresholds which were noted to be elevated when compared to the counterpart hemi-field locations [34 (3,-3) and 35 (9,-3)] in the lower field [figure 10-2 (i)].

The staircase parameters for central locations were restricted to a maximum of 17 minutes of arc for the pilot strategies 1 and 2 of chapter 7 (figure 7-1). This was expected to allow sufficient range for the detection of MDT thresholds in normal subjects on the basis of Johnson's work (Johnson and Scobey 1980) and investigation done during the course of this study (chapter 4).

The parameters clearly need to be increased to allow threshold measurement of MDT in glaucoma. Johnson tested a range extending to 5 degrees (un-scaled for eccentricity) for a 60-location unidirectional MDT performed on a Macintosh computer (Johnson et al. 1995).

It was decided that the summation effect in glaucoma could be most accurately measured by probit analysis of different lengths of a single line. A pilot study was undertaken taking displacements to a maximum of 4:30 degrees, having first checked the limit of computer accuracy for displacement. This was done by measurement of pixel displacement at location 1, one pixel equating to 0.03cm (table 11-1). Accuracy was maintained to 175 pixels (7:23 degrees at location –27,3).

Table 11-1. Estimation of accuracy of computer monitor pixel displacement

1 pixel = 0.03cm * 3% error

Pixel	Mm	min arc
200	58*	500
175	52	443
150	45	383
100	30	261
50	15	133
25	75	67

METHOD

MDT threshold was assessed for subject 1 by probit analysis of paired hemi-field locations 6 (3,3) and 34 (3,-3) for randomized horizontal line stimuli of 6, 12, 24 and 48 pixel (20, 41, 82, 163 min arc) lengths, each of 2 pixel (7 min arc) width, programmed to pass through 10 presentations of 10 displacements [0 – 80 pixels (0 - 271 min arc)].

Stimulus timings were adjusted as recommended in chapter 7: fixed pre-displacement, listening window and post response wait were each set at 1000 msec (previously 1500 msec). The upper limit of the random pre-displacement was increased to 750 msec (previously 500 msec). The subject wore reading correction (+3.5 DSph) supported in a trial frame to avoid any effect of refractive error. Only one MDT threshold was recorded for location 6 (3, 3). The test was therefore extended to

include location 7 (3, 9). Its lower field pair (location 33) was not included in this session because of limitation of test time and risk of introducing fatigue.

RESULTS

Increasing elevation of MDT threshold is found with decreasing line length. Only one measurement of MDT threshold was recordable for location 3,3. This was for the longest line length, the smaller lines being unseen (table 11-2).

Table 11-2. MDT thresholds for different line lengths in focal glaucoma.

Stimulus length min arc	LOCATION		
	3,3	9,3	3,-3
163	90	17	4
82	UNSEEN	50	2
41	UNSEEN	56	4
20	UNSEEN	60	8

Plot of log MDT (min arc) as a function of log stimulus area (min arc) shows a slight increase of slope at the damaged Humphrey location (9,3; slope - 0.56) compared with the normal Humphrey location (-3, 3; slope - 0.44). However, confidence intervals are wide and overlap (location 9,3: 95% CI -1.64, 0.52; location 3,-3: 95% CI -2.37, 1.50), (figure 11-1).

DISCUSSION

The central location (3, 3) of the glaucomatous subject is found to have a high MDT threshold of 90 min arc for the longest line length tested (163 min arc), with no MDT threshold recordable for the shorter lines tested. This corresponds topographically to a dense Humphrey total deviation defect of 31 db ($P < 0.5\%$),

indicating that a further increase in the stair parameter may be necessary if the MDT threshold is required to be measured in advanced glaucoma.

Figure 11-1. Log MDT threshold as a function of log stimulus area in glaucoma.

Location 9, 3: slope: - 0.56 (95% CI -1.64, 0.52; R^2: 0.77; P: 0.157).
3,-3: slope: - 0.44 (95% CI -2.37, 1.50; R^2: 0.32; P: 0.435).

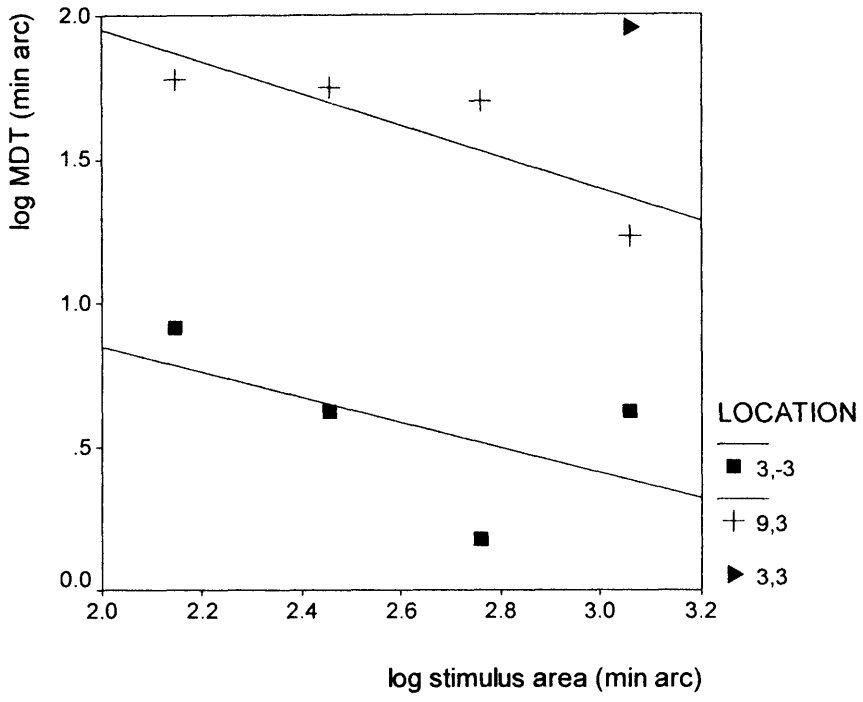

It is of interest that line lengths of up to 82 minutes of arc reveal grossly elevated MDT threshold for location 7 (9,3), where the Humphrey defect measures only 4db (P < 1%). It would be of interest to repeat the experiment for the counterpart hemi-field location (9, -3) to determine separation by hemi-field analysis.

The gradient of the summation slope (- 0.56) of location 9,3 is slightly greater than at undamaged location 3,-3 (-0.44) but the confidence intervals are wide and overlap, so it is not possible to conclude whether they differ.

One cannot draw accurate comparison of glaucoma with normal subjects for the central locations due to limitation of the computer pixel size. Normal subject GMVR was suprathreshold for line lengths between 1 and 55 min arc when testing MDT at central location 3,3 (chapter 4).

The slope found for the undamaged DLS central location (3,-3) of the glaucomatous patient (68 years) is similar to that found for subject 1 (46 years) and greater than that for subject 2 (30 years) for MDT thresholds at nasal peripheral location (-27,3), reported in chapter 5. It is greater than the slopes recorded for both subjects tested at 18 degrees by unidirectional MDT (Johnson and Scobey 1980).

The effect of age on MDT summation properties is unknown and would be of interest to explore at different eccentricity. The human optic nerve axon count declines at approximately 0.4% (Jonas et al. 1992) – 0.6% (Johnson et al. 1987) per annum. These estimates are supported by in vivo imaging of the RNLF by scanning laser polarimetry (Schlottmann et al. 2004). However, Dannheim found no effect of age for spatial summation properties of DLS under mesopic and photopic conditions (Dannheim and Drance 1971).

SUMMARY

This preliminary investigation of focal field loss in glaucoma suggests that there is a spatial correspondence of a dense Humphrey defect with elevation of MDT thresholds, as also reported for random dot and unidirectional motion perimetry (Johnson et al. 1995; Bosworth et al. 1999).

The findings indicate that the choice of line length for the new test will be critical to optimize separation of normal from glaucomatous eyes. Target size has been reported to be of significance in the detection of Humphrey field defect, size I being more sensitive than the generally used size 3, although variability is higher (Uyama et al. 1993). There is a delicate balance to be struck between reducing line length to increase sensitivity to detect glaucoma and increasing line length to reduce the effects of attention and central refractive error.

The upper limit of staircase parameters may need to be increased if measurement of threshold is required in advanced glaucoma. Restriction is placed both by the limit of computer accuracy (175 pixels) and the spacing distance between locations (currently six degrees).

The size of stimulus displacement at threshold may offer an indication of the magnitude of the motion receptive field scotoma in glaucoma, as the patient moves from an "unseen" to a "seen" response.

It would be of interest to relate future MDT summation results to the critical dimension of the equivalent summation (chapter 5).

Chapter 12

POST-DOCTORATE MDT DEVELOPMENT PLAN

12.1 OVERVIEW OF PHD

During the course of this PhD a novel MDT test has been developed and fundamental psychophysical properties of the MDT stimulus explored.

The preceding chapters give insight into the physiological summation properties of the MDT stimulus in relationship to retinal GCD. Ricco's law has been shown to apply to the MDT stimulus. A linear relationship of log MDT threshold has been found with log stimulus energy (stimulus area * luminance). This knowledge may be used to select appropriate stimulus dimensions and predict the outcome MDT threshold with precision.

The effect of peripheral optical blur on MDT threshold has been quantified and the effect of attention considered. A staircase MDT threshold strategy has been developed and response times investigated. The MDT stimulus timings have been adjusted, with the benefit of shortening the test duration. The minimum physiological response time is recommended to be used as an index of reliability.

The information acquired has been pooled to produce a reduced multi-location MDT, of short duration, with locations scaled with retinal GCD and selected to give a proportional representation by ONH sector.

However, several questions remain outstanding and pilot studies are planned to address these issues as post-doctorate work.

12.2 POST-DOCTORATE PLAN

12.2.1 NEW MONITOR

A new flat screen 1600 x 1200 monitor was purchased for the start of the post-doctorate pilot studies with a dot pixel resolution of 0.255. This provided a 15% gain in resolution compared to the previous Hitachi monitor of 0.28 dot pixel.

The new screen measurement of 40.8 x 30.6 cm gives the potential for testing within a 32-degree horizontal x 25-degree vertical field, with a perimeter allowance of 1 cm, calculated for a test distance of 30 cm.

The original MDT program was limited to the same test positions as the Humphrey 24-2. The software was re-designed to provide coordinates plotted at 1-degree intervals across the new screen, giving ultimate flexibility, with a choice of 3200 test locations for future work.

The set-up for the new monitor gives the opportunity to address the sampling imbalance of the visual field with respect to the ONH (chapter 9). This could be achieved by increasing the number of test locations in the temporal and central field. In addition, the separation of the nasal field between 3 and 21 degrees could be reduced from 6 degrees to ~ 4 degrees, subject to the effect of increased crowding. These potential modifications will be held in reserve for future consideration. It was decided pro tem to continue to use Humphrey locations as a standard, to enable pilot study comparison between FDT matrix and SAP. The proximity of locations 11 (3,-3) with 13 (9,-3) suggests that in due course one location could be excluded with the benefit of shortening the test duration (figure 12-1).

Figure 12-1. Topographic relationship of MDT test points to optic nerve head (right eye).

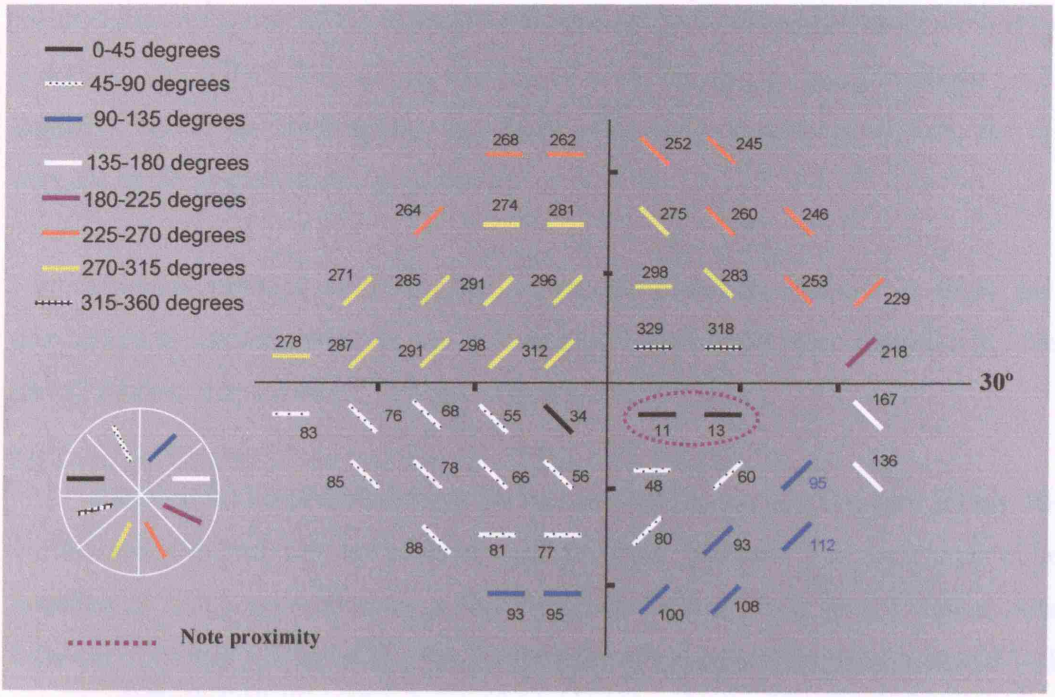

Luminance values of the new monitor were measured and the background and stimulus set to a contrast of 85% as follows:

Background: 10 cd/m^2 (rgb 68), [previously 10 cd/m^2 (rgb 65)].
Stimulus: 124 cd/m^2 (rgb 210), [previously 114 cd/m^2 (rgb 255)].

Note higher luminance value of white with new monitor.

12.2.2 SELECTION OF POST-DOCTORATE TEST STRATEGY

Version "E" (figure 9-3) was selected as the optimum test strategy based on the results of investigation of the reduced MDT strategy by ONH representation (chapters 9 and 10. On deliberation, it was decided to re-instate the far nasal locations (– 27 degrees), which are traditionally associated with early glaucomatous loss, for the purpose of the post-doctorate pilot studies.

Stimulus timings were adjusted as recommended in chapter 7: fixed pre-displacement, listening window and post response wait: 1000 msec (previously 1500 msec); random displacement: 750 msec (previously 500 msec).

The stimulus lengths of strategy 3b were adopted as the new standard [figure 10-1 (iv)] and adjusted for the pixel size of the new monitor. The additional nasal locations at –27,3 were allocated a line length of 48 x 3 pixels in accordance with estimate of scaled retinal GCD. The line lengths are standardized to stimulate 13-18 ganglion cells (table 12-1). The line width remains narrow measuring only 2-3 pixels and stimulating 1-4 ganglion cells. It would be possible to further standardize the stimulus size by increasing the width of peripheral locations, but this might be at the expense of detecting fine RNFL defects (Westcott et al. 1996). Alternatively, the central line width could be reduced to 1 pixel but there is concern this would introduce artifacts related to refraction.

The monitor area required by strategy 3b is reduced in height when compared with the Humphrey 24-2 equivalent. It would be possible to operate the test from a 14-inch lap top screen if the nasal locations were added as an optional extra at the end of the test program with the fixation placed off-center. Alternatively, the MDT test format would entirely fit on the new generation of wide lap-top screens. This is of fundamental importance in the test being eventually able to function as a portable screening tool.

Table 12-1. Summary of stimuli dimensions for the new monitor and the estimated number of ganglion cells stimulated by zone.

* zones are defined in Chapter 2, figure 2-3.

Zones *	Pixel dimensions Length x width	Min arc dimensions Length x width	Ganglion cells Length x width
1	7 x 2	20 x 6	13 x 4
2	14 x 2	40 x 6	15 x 2
3	21 x 2	57 x 5	16 x 1.5
4 & 5	28 x3	(69 - 74) x (7 - 8)	(13 – 18) x (1 - 2)
6	48 x 3	109 x 7	15 x 1

12.2.3 PILOT STUDY 1: DETERMINATION OF OPTIMUM CENTRAL LINE LENGTH

The optimum central line length remains undetermined.

The test strategy proposed favors the central zone in terms of the total number of ganglion cells stimulated (table 12-1). This means that the central zone may be less sensitive than peripheral zones in detecting focal defect. Currently, the central lines measure 7 x 2 pixels (20 x 6 min arc). We are reluctant to reduce the width to one pixel for fear of introducing refractive artifact. We know that we can change the stimulus configuration to achieve equivalent threshold. Therefore, an alternative option would be to try a 4 x 2 pixel stimulus (12 x 6 min arc), which may prove more robust to refractive blur than a 7 x 1 pixel stimulus (20 x 3 min arc).

The central blur experiments conducted within this PhD (Optics chapter 4; section 4.3) would suggest that line lengths of 14 x 7 min arc remain suprathreshold for myopia ≤ -6 DSph and hypermetropia $\leq +4.0$ DSph. This would suggest that, if the 4 x 2 pixel central line length is adopted as the final test strategy, near refractive correction may be necessary for subjects who require convex correction of $> +4.0$ DSph. This gives little latitude for patients who are both hypermetropic and presbyopic.

Requirement for refractive correction is not ideal in many respects. Firstly, time and skill is required to assess near correction. Secondly, increased cost is entailed to cover the purchase of wide aperture lenses. Wear of glasses is not recommended for the test in case the frame obscures the outer field locations. In addition, many patients have a reading correction incorporated in their glasses in the form of bifocals, which would result in a "prismatic jump" effect. Thirdly, use of lenses and a trial frame holder makes the test less portable, restricting access to remote areas.

Investigation of central focal glaucoma (chapter 11) indicated that an early Humphrey defect may be associated with a marked elevation of MDT threshold. This indicates that some tolerance of elevation of MDT threshold due to refractive error may be allowable whilst maintaining separation between glaucomatous and normal eyes.

On consideration of all of the above, it is proposed that the merits of different central line lengths (7 x 2; 7 x 1 and 4 x 2 pixel) be investigated by comparing glaucoma patients with a focal central defect against aged-matched normal subjects, testing both groups with and without correction of refractive error up to +/- 6.0 DSph.

ORIENTATION OF CENTRAL STIMULI

Westcott showed improved sensitivity to detect glaucoma if the MDT line stimulus was aligned with the RNFL. However, the threshold differences with changing line orientation were small and assessed in only a small number of individuals at 2 retinal locations (15,9 and 15,-9), (Westcott et al. 1996). The advantage of stimulus orientation with the RNFL may be outweighed by the limitation in the minimum size of displacement that can be achieved compared with a vertical or horizontally aligned stimulus (chapter 2).

It is therefore recommended that the first pilot study be performed with all stimuli aligned vertically. This may prove beneficial for the central zones where the MDT is expected to be close to suprathreshold. In zone 1 the smallest central displacement that can be achieved with an obliquely orientated stimulus is 4 minutes of arc. This reduces to 3 minutes of arc for a horizontally or vertically aligned stimulus.

12.2.4 PILOT STUDY 2: DETERMINATION OF THE OPTIMUM ORIENTATION OF THE STIMULUS, THE EFFECT OF LEARNING AND THE REQUIREMENT FOR PERIPHERAL REFRACTION

The benefit of stimulus orientation with the RNFL is unconfirmed within the context of the multi-location MDT format. In order to address this, it is proposed that a second pilot study is conducted comparing stimuli aligned as follows:

(i) all vertical
(ii) all orientated with RNFL
(iii) all orientated perpendicular to the RNFL

The study is planned additionally to assess the effect of learning and the requirement for central refractive error. This will be done by running a base-line test with the stimuli vertically aligned (with near refractive correction) followed by randomized testing of four strategies:

(i) all stimuli vertical (with near refractive correction)
(ii) all stimuli vertical (unaided)
(iii) all stimuli orientated with RNFL (with near refractive correction)
(iv) all orientated perpendicular RNFL (with near refractive correction)

Adequate rest periods will be given between tests to avoid fatigue. Learning will be assessed by comparison of the base line test with the repeat vertical strategy (with correction). The need for refractive error will be investigated by comparison of the

corrected and uncorrected vertical strategies following the base-line test. The effect of orientation will be assessed by comparison of the strategies with the stimuli orientated with the RNFL and perpendicular to the RNFL.

The staircase for the post-doctorate study was calculated by zone for the new monitor pixel size (table 12-2). The start positions and range of stair were allocated on the basis of knowledge of threshold responses measured through this PhD and earlier studies using the single line MDT.

MDT is expected to be near suprathreshold for the central zones. A start of 6 min arc is given to allow for the effects of learning.

The original BBC stimulus was at sited at 15,9 (zone 4) and subtended 2 degrees x 2 min arc when presented at a test distance of 124 cm. The BBC stimulus stimulates 28 x 0.43 RGC (calculated using the methodology described in chapter 6). The BBC MDT threshold was considered within normal limits if < 9 min arc (Baez et al. 1995; Westcott et al. 1998a). Using the proposed new multi-location dimensions the number of ganglion cells stimulated by stimulus length at zone 4 is approximately equivalent to the BBC MDT but the width is greater (1.7 RGC).

The single line summation studies indicate that at location -27,3, a 48 x 2 pixel stimulus (stimulating 15 x 0.6 RGC) yields a MDT threshold in the region of 4 min arc in a practiced individual. The selected stimulus size at -27,3 for the multi-location pilot study is slightly wider (48 x 3 pixels [15 x 0.9 RGC]).

A lower MDT threshold may therefore be predicted for zones 4 and 6 using the new multi-location test on the basis of the increased stimulus width, but the effects of attention may counteract this advantage. Preliminary start positions of 11 -12 min arc were accordingly allocated for zones 4-6.

The staircases for the vertical [table 12-2 (i)] and orientated [table 12-2 (ii)] strategies were approximated to be equivalent in range. However, it is important to

note that this means fewer presentations are made for the orientated strategy compared to the vertical strategy.

The displacements for the horizontally/vertically (h/v) aligned stimuli were approximated to be equivalent to that of the oblique (O) stimuli for the strategies aligned with and perpendicular to the RNFL [table 12-2 (ii)].

Table 12-2. Range of staircase displacement for post-doctorate work.

Stair: start (indicated in bold) and range by zone (min arc)
P = pixel.
Z = zone

(i) vertical strategy

	P 1	P2	P3	P4	P5	P6	P7	P8	P9	P10	P11	P12	P13
Z1	3	**6**	9	12	15	17	20						
Z2	3	**6**	9	11	14	17	20	23					
Z3	3	5	8	**11**	14	16	19	22	24	27			
Z4	3	5	8	**11**	13	16	19	21	24	27	29		
Z5	3	5	7	10	**12**	15	17	20	22	25	27	30	
Z6	2	5	7	9	**12**	14	16	18	21	23	25	28	30

(ii) orientated strategy

0 = oblique stimuli; h/v = horizontal/vertically aligned stimuli.

	P 1	P2	P3	P4	P5	P6	P7	P8	P9	P10	P11	P12	P13
Z1_0	4	**8**	12	16	21								
Z1_h/v	3		**9**	12	15		20						
Z2_0	4	**8**	12	16	20	24							
Z2_h/v	3		**9**	11		17	20	23					
Z3_0	4	8	**11**	15	19	23	26						
Z3_h/v	3		8	**11**		16	19	22		27			
Z4_0	4	8	**11**	**15**	19	23	27	30					
Z4_h/v	3		8	**11**		16	19		24	27	29		
Z5_0	4	7	**11**	14	18	22	25	29					
Z5_h/v	3		7	**10**		15	17		22	25		30	
Z6_h/v	2	5	7	9	**12**	14	16	18	21		25		30

12.2.5 PILOT STUDY 3: NORMATIVE DATA BASE

On completion of the pilot studies above a normative database will be established for the selected test strategy. The purpose will be to investigate the effect of age on MDT threshold and to give a basis for comparison of glaucomatous subjects against aged-matched control.

The human optic nerve axon count declines at approximately 0.4%– 0.6% per annum (Jonas et al. 1992). Random dot perimetry shows an age-related decline in sensitivity, which is reported to be most marked in the central field and to occur at a different rate and magnitude when compared to DLS (Wojciechowski et al. 1995). Bullimore investigated the effect of age for random dot D_{min} in normal subjects and found, by linear regression, an increase of ~ 3 min arc per decade of life (Bullimore et al. 1993). Frequency Doubling sensitivity decreases by approximately 0.7 dB per decade across all eccentricities (Anderson et al. 2005). A decline of sensitivity is also reported for flicker perimetry (for temporal frequencies of 2, 8 and16 Hz), (Casson et al. 1993a) and increasing duration of vernier oscillatory displacement (2 and 6 Hz), (Kline et al. 2001).

12.3 FURTHER MDT STUDIES

The format of the MDT computer programming for the new monitor is highly adaptable and gives it wide potential for further development. Possible ideas for further studies and test development include the following:

- Determination of the limit of equivalent summation effect (chapter 5).
- Determination at what aspect ratio stimulus area ceases to be the relevant variable for horizontal rectangles (chapter 5).

- Determination of the limits of linearity of MDT threshold with stimulus energy (chapter 6), and any variation with age, background illumination and eccentricity,
- Further investigation of MDT spatial summation characteristics in glaucoma.
- Development of mathematical models of known MDT threshold estimates on completion of the normative data base, with the aim to identify false positive response, reduce test duration and improve inter-test variability (Spenceley and Henson 1996; Bengtsson et al. 1997; Olsson et al. 1997; Artes et al. 2002; Henson and Artes 2002; Turpin et al. 2002b; Turpin et al. 2002a; Tucker et al. 2005). The number of fluctuations after reversal may be used as indicator of pathology/reliability.
- Techniques of spatial filtering could be considered to reduce noise and improve repeatability (Gardiner et al. 2004). Gaussian filtering gives a weighted average between neighboring points and thereby gives a predictive value of indirect relationships between adjacent test locations.
- Development of a motion displacement glaucoma hemifield test.
- Adjustment of stimulus spacing to give a balanced representation of the visual field with respect to the ONH (chapter 9).
- Development of specialized MDT strategies with the aim to detect early defects that may be beyond the resolution of SAP and the standard multi-location test. The principle of fine matrix mapping could be applied to motion displacement to give a detailed map of localized areas of the visual field under suspicion (Westcott et al. 1997; Westcott et al. 1998a).
- Development of a suprathreshold test on completion of the normative database. This will enable appropriate setting of "pass/fail" criteria (Henson and Artes 2002). Suprathreshold tests are useful for screening purposes, having the advantages of being quick and showing less test-retest variability than full threshold tests (Spry et al. 2000).
- It is envisaged that in order to achieve wide accessibility the test should be available for purchase on-line as a software product. This means that the

software will require to be upgraded for automatic monitor recognition to ensure standardized display of test coordinates and stimulus presentation.

- A laptop version of the MDT is planned to give good accessibility for glaucoma screening purposes. The nasal field could be assessed as an optional second part to the test where the screen is too small to accommodate a 30-degree field (a test distance of less than 30 cm is not recommended).
- The development of a dedicated MDT apparatus will be considered to address the issue of central refractive error and provide a standardized testing medium.
- Development of MDT for the assessment of driving standards. An integrated field of motion sensitivity could be created using the principle of the integrated visual field of SAP (Crabb et al. 1998; Crabb and Viswanathan 2005). The principal could also be applied to provide a motion test for use by the armed forces.
- A pilot study with the RNIB is planned to assess the role of a laptop MDT for patients where a domiciliary visit is required. An integrated field of motion displacement sensitivity could be used to give information on the binocular field in patients with severe visual impairment (Crabb et al. 1998; Crabb and Viswanathan 2005).

In conclusion, I hope that the content of this PhD will provide a useful foundation for further work and I wish the MDT every success for the future.

Ethical approval has been granted by the ethics committee at Moorfields for the post-doctorate pilot studies to proceed (reference VERG1001).

Chapter 13

ABSTRACTS OF PUBLICATIONS

Proceedings of the XIVth International Perimetric Society Meeting
Halifax (NS) Canada 2000

VALIDATION OF A NEW MOTION TEST

AC Viswanathan, MC Westcott, GM Verdon-Roe, FW Fitzke, RA Hitchings

The Institute of Ophthalmology and Moorfields Eye Hospital, London

Purpose: To compare a new PC-based system of motion detection testing against the previous 'gold standard' (Fitzke, 1987).

Methods: Frequency of seeing (FOS) curves were obtained for 9 normal volunteers using both the 'gold standard' test and the new PC-based system for a line stimulus in the temporal field undergoing displacements of between 2 and 18 minutes of arc.

Results: The 50% seen threshold for the 'gold standard' test was 6.13 ± 2.34 min arc (mean ± SD) and for the new test 5.19 ± 2.86 min arc. These are not significantly different ($p=0.1222$, paired t-test). The power of the study was 0.8.

Conclusion: Previous results obtained with the 'gold standard' test may be taken to apply to the new test during its further development.

This project was supported by IGA, LORS and MRC.

Proceedings of the XIVth International Perimetric Society Meeting
Halifax (NS) Canada 2000

(ii) OPTIMUM STIMULUS DURATION FOR MOTION DISPLACEMENT IN GLAUCOMA

MC Westcott, GM Verdon-Roe, AC Viswanathan, FW Fitzke, RA Hitchings

The Institute of Ophthalmology and Moorfields Eye Hospital, London

We are developing a new PC operated test for the detection of Glaucoma using the principal of the motion displacement test. In this experiment we investigate whether it is possible to shorten the test by reducing stimulus duration whilst maintaining sensitivity to detect glaucoma. **Method:** Frequency of seeing curves were obtained for a line stimulus presented in the temporal field, moving between 2 and 18 min arc displacement, through 5 oscillations, with a stimulus duration of 400, 200 or 100 msec per cycle, for control and glaucomatous eyes. **Results:** The mean test time was 7 min 50 sec for the stimulus duration of 400 msec per cycle. There was a test time saving of 54 sec and 63 sec for the 200 and 100 msec condition. Results to date show little change in threshold for the different durations while continuing to discriminate between groups.
Conclusion: Comparable motion displacement thresholds may be achieved when testing with stimulus durations of 400, 200 or 100msec per cycle. There is a test time advantage when using the shorter stimulus presentations with maintenance of test sensitivity to detect glaucoma for all durations.

This project was supported by IGA, LORS and MRC.

Proceedings of the XIVth International Perimetric Society Meeting
Halifax (NS) Canada
2000

(iii) OPTIMUM NUMBER OF STIMULUS OSCILLATIONS FOR MOTION DISPLACEMENT DETECTION IN GLAUCOMA

GM Verdon-Roe, MC Westcott, AC Viswanathan, FW Fitzke, RA Hitchings

The Institute of Ophthalmology and Moorfields Eye Hospital, London

We are developing a new PC operated test for the detection of Glaucoma using the principal of the motion displacement test. In this experiment we investigate whether it is possible to shorten the test duration by reducing the number of stimulus oscillations whilst maintaining sensitivity to detect glaucoma. **Method:** Frequency of seeing curves were obtained for a line stimulus presented in the temporal field, moving between 2 and 18 min arc displacement, at a duration of 200msec, through one, three or five oscillations, for control and glaucomatous eyes. **Results:** The mean test time was 7 min 47 sec for five oscillations, with a saving of 32 sec and 82 sec for the three and one condition. There was no statistical significant between the threshold measurements of the two groups for three and five oscillations. However, thresholds were significantly higher for one oscillation when compared with three and five ($P < 0.01$). **Conclusion:** Similar motion displacement thresholds may be achieved by testing with three oscillations compared to five, with the advantage of a reduced test duration and maintenance of test sensitivity to detect glaucoma.

This project was supported by IGA, LORS and MRC.

ARVO
The Association for Research in Vision and Ophthalmology
Annual Meeting Fort Lauderdale, Florida
2001

A NEW MULTI-LOCATION MOTION DISPLACEMENT THRESHOLD TEST FOR GLAUCOMA

G M Verdon-Roe [1,3], M C Westcott[2], A C Viswanathan[1,3], D F Garway Heath[1,3], F W Fitzke[1], J Caprioli[2], R A Hitchings[3]

[1] The Institute of Ophthalmology, London. U.K.
[2]Glaucoma Division, Jules Stein Eye Institute, UCLA, Los Angeles, US
[3] Moorfields Eye Hospital. London. U.K.

Background: We have previously reported that motion sensitivity can be affected by the orientation of the stimulus in glaucoma (ARVO 1988). According to this effect, the Motion Displacement Threshold (MDT) is elevated for a line stimulus moving perpendicular to the orientation of the retinal nerve fiber layer (RNFL) compared to parallel. Purpose: To develop a multi-location motion test utilizing this orientation effect, in order to optimize sensitivity to early glaucoma. **Method:** A computer-driven monitor based-test was developed to present moving line stimuli orientated with the direction of the RNFL (to the nearest 45 degrees) at locations corresponding to the Humphrey 24-2. Stimulus line length and minutes of arc displacement were assessed and scaled for eccentricity. 8 Glaucoma Patients (mean age 52, range 25-63 years) with reproducible focal Humphrey Field defects and 8 aged matched controls (mean age 47, range 23-69 years) were tested. For each field location, motion abnormalities were compared against the Humphrey Visual Field Total Deviation (TD) results. **Results:** Within a patient's hemifield, the total number of locations with abnormal motion ranged from 0-19 (median 5) and correlated significantly with the total number of abnormal locations on the TD plot (range 0-22, median 5) $P < 0.05$, $R = 0.6$. All patient hemifields with scotoma on the TD plot had coexisting abnormal motion. The concordance between the extent of motion abnormalities and Humphrey scotoma was good. **Conclusion:** We have developed a novel multi-location motion test using stimuli aligned with the direction of the RNFL. Results so far show promise in detecting established glaucoma and further research will assess its ability to detect the earliest disease.

Supported by The Friends of Moorfields Eye Hospital, The International Glaucoma Association and The Frost Trust.

Proceedings of the XVth International Perimetric Society Meeting
Stratford UK 2002

SPATIAL SUMMATION FOR A SINGLE LINE AND MULTI-LINE MOTION STIMULUS

GM Verdon-Roe[1], DF Garway-Heath[1,2], MC Westcott[2], AC Viswanathan[1], FW Fitzke [2]

The Institute of Ophthalmology[1] & Moorfields Eye Hospital, London[2]

Purpose: To investigate spatial summation for motion displacement of line stimuli as a function of line length, line number and line separation. **Method:** A video display under PC control was used to present horizontal line stimuli of either a single line or triple lines separated by 8, 14, 27 or 54 min arc. 2 experienced normal subjects were tested at -27, 3 eccentricity with peripheral refraction corrected. 5 presentations of each of 7 motion displacements were made between 0-24 min arc. Stimulus presentations consisted of 3 oscillations, duration of 200msec per cycle. Contrast was maintained constant at 84%. Each parameter was tested 3 times, frequency of seeing curves (FOS) were obtained and 50% seen threshold calculated by probit analysis. **Results:** Mean thresholds (min arc) are summarized by chart opposite. **Conclusion:** Equivalent displacement thresholds were found for equivalent lines whether single or distributed amongst 3 shorter lines, indicating spatial summation. This principal may be used to predict motion displacement thresholds when testing within these target dimensions.

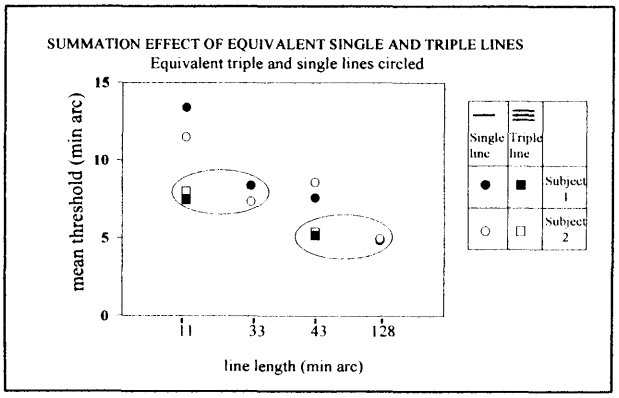

This project was supported by an unrestricted grant from Pharmacia.

The Association for Research in Vision and Ophthalmology
Annual Meeting Fort Lauderdale, Florida
2003

The Effect of Refractive Blur on a Linear Motion Displacement Stimulus

G.M. Verdon-Roe[1], D.F. Garway-Heath[2], F.W. Fitzke[1], A.C. Viswanathan[1], M.C. Westcott[2]. [1]Visual Science, Institute of Ophthalmology, London, United Kingdom; [2]Glaucoma Research Unit, Moorfields Eye Hospital, London, United Kingdom.

Background: we are developing a motion displacement threshold (MDT) test for the diagnosis of early glaucoma using line stimuli moving perpendicular to the orientation of the retinal nerve fiber layer. **Purpose:** to assess the effect of refractive blur on MDT. **Methods:** A video display under PC control was used to present a horizontal line stimulus in the nasal field at -27, 3 degrees at a test distance of 30cm. Contrast was 84%. The right eye of two experienced normal subjects (46 and 30 years) was tested. A central target was fixated and lens strengths of (i) +/- 0,2,4, and 6DSph and (ii) +/- 0,2,4, and 6DCyl at 90/180 degree axis (additional to peripheral refraction determined by retinoscopy under mydriasis) were centered at -27,3 degrees. The line stimulus (lengths 43, 86 or 128 min arc) was programmed to pass through 5 presentations of 7 randomized displacements (0-24 min arc). Stimulus presentation consisted of 3 oscillations, duration 200 msec per cycle. Each parameter was tested 3 times, frequency of seeing (FOS) curves were obtained and 50% seen threshold calculated by probit analysis. **Results:** Mean MDTs [min arc: mean ± standard deviation (range)] were: (a) un-blurred: 5.5± 0.8 (4.9-6.1); 5.1±1.4 (3.8-6.7); 3.5±1.3 (2.6-4.4) (b) blurred DSph: 8.4±2.5 (5.1-14.8); 6.2±2.2(3.1-10.0); 5.9±2.5(1.7-10.9) for 43, 86 and 128 min arc line lengths respectively and (c) blurred DCyl: 5.6±2.1 (3.2-8.7); 6.5±2.4 (3.8-12.6) for 86 min arc line length, 90 and 180 degree axis respectively. Mean min arc change in threshold (blurred-un-blurred) showed a similar pattern for all line lengths: Blurring by +2.0DSph, +4.0DSph and all cylinders produced only small elevation in MDT (< 2 min arc) for both subjects. Increase in MDT was found for +6.0DSph and -2.0DSph (< 5 min arc) and -6.0DSph and -4.0DSph (< 9min arc). **Conclusions:** MDT testing is shown to be robust to the effects of blurring by DCyl. This is of particular interest in the development of the new test with respect to the use of an orientated line stimulus and consideration of peripheral astigmatism, which is reported to physiologically increase with eccentricity (Millodot 1981). The least MDT change is found when using a cylinder orientated at 90 degrees as optically predicted for a horizontal line stimulus. Wear of near spherical correction (with exception of subjects < -4.0DSph) will ensure optimum MDT sensitivity and specificity.

Supported by unrestricted grants from Pharmacia, The Friends of Moorfields and IGA.

The Association for Research in Vision and Ophthalmology
Annual Meeting Fort Lauderdale, Florida
2004

Linear Relationship of Motion Displacement Threshold with Stimulus Energy (calculated as a function of Contrast and Line Length)

G.M. Verdon-Roe[1], A.C. Viswanathan[1,2], M.C. Westcott[3], F.W. Fitzke[1], D.F. Garway-Heath[2]. [1] Visual Science, Institute of Ophthalmology, London, United Kingdom; [2] Moorfields Eye Hospital, London, United Kingdom; [3] St Bartholomew's Hospital, London, United Kingdom.

Purpose: to explore the relationship between motion displacement threshold (MDT) and stimulus energy, calculated as a function of contrast and line length.
Methods: A video display under PC control was used to present a horizontal line stimulus in the nasal field at -27,3 degrees at a test distance of 30cm. The right eye of two experienced normal subjects (47 and 31 years) was tested with peripheral refraction corrected. A central target was fixated and the line stimulus (randomized presentation order of lengths 11, 22, 43, 86 or 128 min arc and contrast 25%, 40%, 55%, 60% or 85%) was programmed to pass through 5 presentations of displacements ranging 0-40 min arc. Stimulus presentation consisted of 3 oscillations of 200 msec per cycle duration. Each parameter was tested 3 times, frequency of seeing (FOS) curves were obtained and 50% seen threshold calculated by probit analysis.
Results: There was a linear correlation of MDT with stimulus energy [stimulus area (min arc^2) x luminance (cd/m^2)] when plotted as a log log function. The slope approximated −1* (-0.93 and -0.94 for each subject).
Conclusions: A linear relationship of MDT with stimulus energy is demonstrated. These results suggest that the stimulus parameters tested lie within the area of linear summation at this peripheral location. This information will be applied to the development of a new multi-location MDT test for the early diagnosis of glaucoma.
Supported by unrestricted grant from Pfizer.

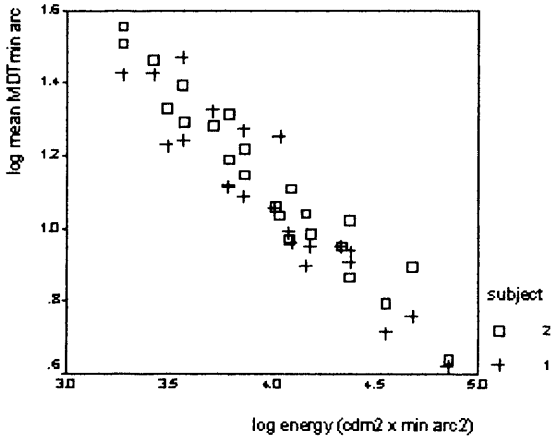

* erratum addressed within text of PhD and IOVS submission 2005.

Submission to IOVS (November 2005)

Exploration of the psychophysics of a motion displacement hyperacuity stimulus for the development of a new test to detect glaucoma.

G.M. Verdon-Roe[1,2], A.C. Viswanathan[1,2], M.C. Westcott[3], F.W. Fitzke[1], D.F. Garway-Heath[1,2]. [1]Visual Science, Institute of Ophthalmology, London, United Kingdom; [2]Moorfields Eye Hospital, London, United Kingdom; [3]St Bartholomew's Hospital, London, United Kingdom

Purpose: to explore the summation properties of a motion displacement hyperacuity stimulus with respect to stimulus area and luminance, with the aim to apply the results to the development of a motion displacement test (MDT) for the detection of early glaucoma.

Methods: A PC-generated line stimulus was presented in the nasal field (-27,3°) with displacements randomized between 0 - 40 min arc. Displacement thresholds (50% seen) were compared for stimuli of equal area but different edge length (orthogonal to the direction of motion). Secondly, MDT thresholds were recorded at five values of Michelson contrast (25% - 84%) for each of five line lengths (11 - 128 min arc). Frequency-of-seeing (FOS) curves were generated and displacement thresholds and interquartile range (IQR, 25% - 75% seen) determined by probit analysis.

Results: Equivalent displacement thresholds were found for stimuli of equal area but differing edge length. Elevations of thresholds and IQR were demonstrated as line length and contrast were reduced. Equivalent displacement thresholds were also found for stimuli of equivalent energy ([stimulus area] * [stimulus luminance – background luminance]), in accordance with Ricco's law. There was a linear relationship (slope –0.5) between log MDT threshold and log stimulus energy.

Conclusions: Stimulus area, rather than edge length, determined displacement thresholds within the experimental conditions tested. MDT thresholds are linearly related to the square root of the total energy of the stimulus. A new law, the 'threshold-energy-displacement' (TED) law, is proposed to apply to MDT summation properties, giving the relationship $T = K \sqrt{E}$ where T = MDT threshold; K= constant; E = stimulus energy.

Supported by an unrestricted grant from Pfizer.

Chapter 14

APPENDIX

A1 INTRODUCTION

Table 14-1. Conversion values for Snellens acuity, cycle/degree and min arc.

METERS	FEET	CYCLE/DEG	MIN ARC
6/6	20/20	30	1
6/12	20/40	15	2
6/18	20/60	9.8	3
6/24	20/80	8	4
6/36	20/100	6	5
6/60	20/200	3	10
2/60	20/600	1	30
1/60	20/1200	0.5	60

PERIPHERAL REFRACTION RESULTS FOR DISTANT VIEWING

Table 14-2. Summary of corrected central and peripheral (-27,3) refraction.

	Central correction	- 25 degrees
Subject 1	-5.0DSph	-2.75/-1.75 x 105°
Subject 2	α/-0.5 x 180°	-0.75/-0.50 x 90°
Subject 3	+0.5	+1.0/-1.25 x 90°

Figure 14-1. Off-axis retinoscopy readings corrected for distance viewing 25 degrees from central fixation.

Dilated tropicamide 1%
N: nasal retina (temporal field) T :temporal retina (nasal field)
I: inferior retina (superior field) S: superior retina (inferior field)

(i) Subject 1 (right eye).
central correction: -5.0 DSph; VA 6/5.

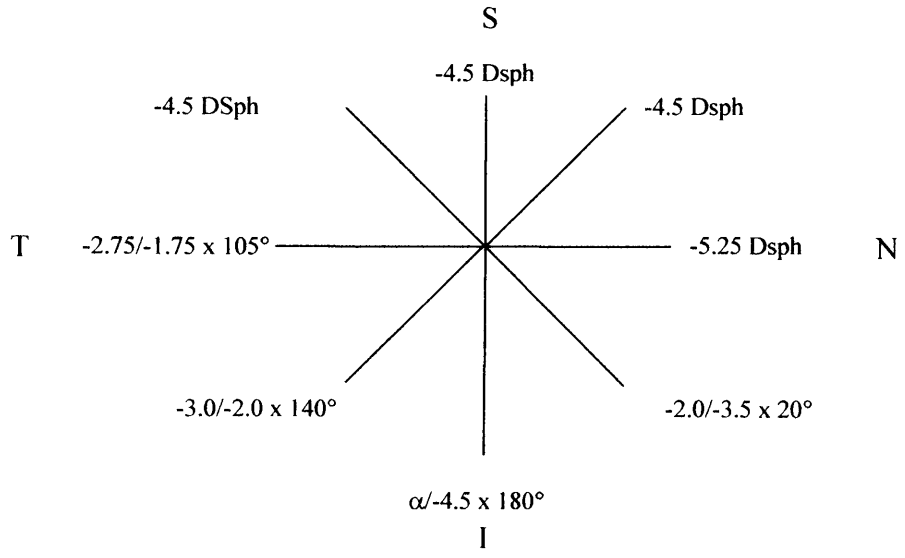

(ii) Subject 2 (right eye).
central correction: α/-0.5 axis 180°; VA 6/5pt.

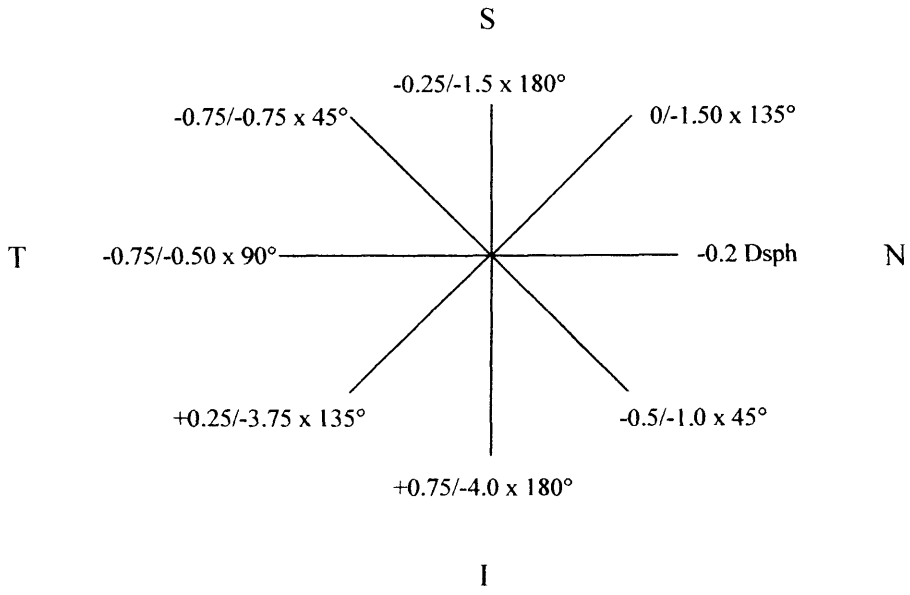

(iii) Subject 3 (right eye).
central correction: +0.75; VA 6/6.

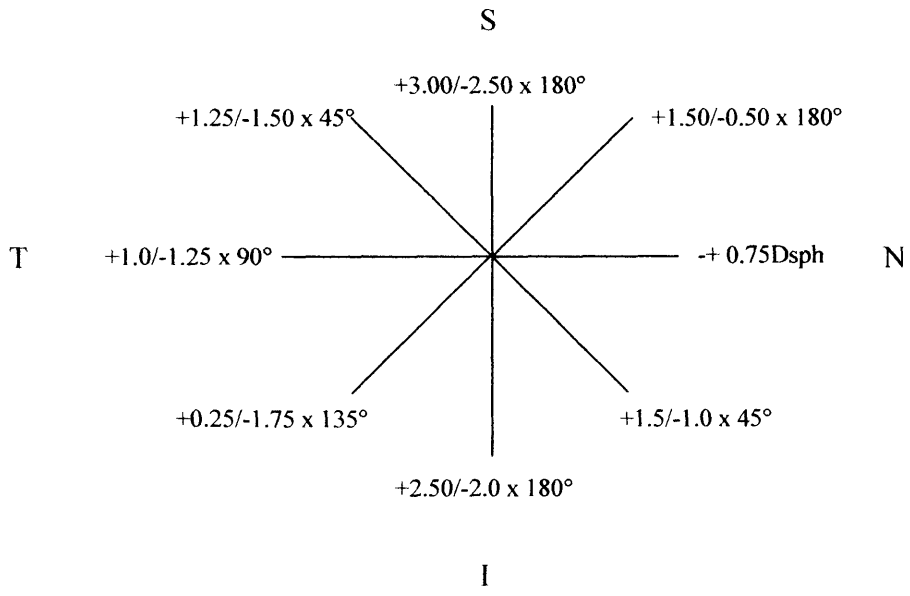

A 5 SPATIAL SUMMATION FOR SINGLE AND MULTI-LINE STIMULI

Table 14-3. Spatial summation for single and multi-line stimuli.

(i) MDT threshold, (range) and standard deviation for single line MDT.

Line length (min arc)	MDT threshold (range) and standard deviation (min arc)
11	12.5 (11.5 - 13.4) ± 1.39
33	7.9 (7.4 - 8.4) ± 0.71
43	8.1 (7.6 - 8.6) ± 0.71
128	4.9 (4.9 - 5.0) ± 0.09

(ii) MDT threshold, (range) and standard deviation (min arc) for 3-line stimuli (line lengths of 11 and 43 min arc for separations of 8, 14,27, and 54 min arc).

	8	14	27	54
11	7.7 (7.1 - 8.3) ± 0.80	8.5 (8.0 - 9.1) ± 0.78	8.0 (7.9 –8.0) ± 0.09	6.9 (6.7 – 6.8) ± 0.07
43	5.4 (5.1 – 5.6) ± 0.33	5.2 (5.0 – 5.3) ± 0.19	5.6 (5.3 –5.9) ± 0.40	5.1 (5.0 –5.1) ± 0.07

Table 14-4. Comparison between merged and unmerged frequency of seeing MDT thresholds for stimuli of equivalent area, but different length-edge.

% contrast	Stimulus (min arc)	Merged FOS curves	Unmerged FOS curves
85%	12x8	5.6 (4.4 - 6.8) ± 0.85	5.6 (4.8 – 6.3) ± 0.60
	24x2	6.0 (4.9 - 7.3) ± 0.91	5.9 (5.3 – 6.9) ± 0.58
	48x2	5.2 (3.6 - 7.2) ± 1.28	5.0 (5.3 – 6.9) ± 1.05
40%	5x8	19.1 (14.1 - 26.0) ± 4.15	19.0 (14.4 – 23.1) ± 3.2
	9x4	20.8 (16.4 - 27.8) ± 3.98	20.3 (15.3 - 22.9) ± 2.68
	18x2	18.7 (14.2 - 22.2) ± 2.89	18.6 (13.9 - 20.8) ± 3.00

MDT threshold, (range) and standard deviation (min arc).

Merged FOS curves: probit analysis done for 3 merged FOS curves for each individual.
Unmerged FOS curves: probit analysis done for each individual FOS curves.

Figure 14-2. Frequency of seeing curves as a function of contrast and line length for individual subjects.

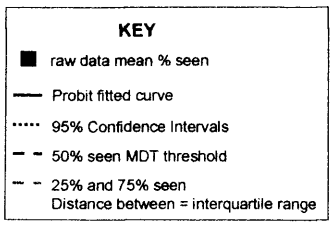

(i) (a) 128 min arc line length subject 1.

(a) 25% contrast

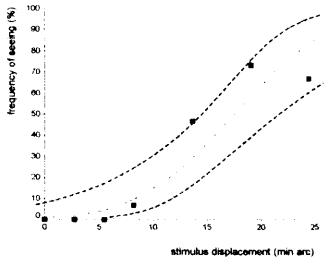

(b) 40% contrast

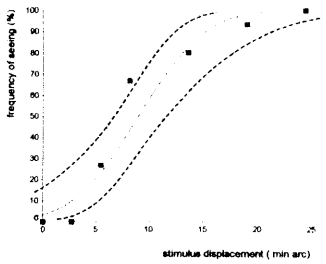

(c) 55% contrast

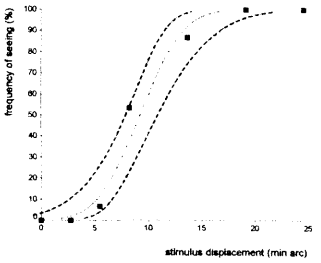

(d) 70% contrast

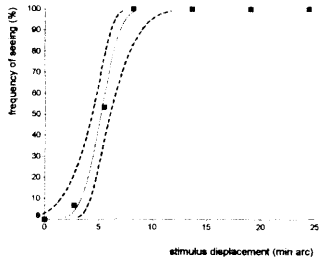

(e) 85% contrast

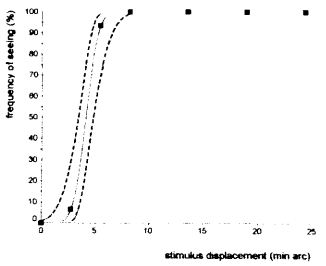

(b) 128 min arc line length Subject 2.

(a) 25% contrast

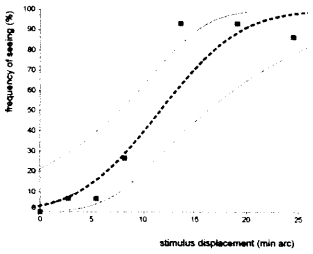

(b) 40% contrast

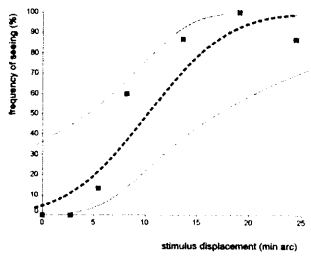

(c) 55% contrast

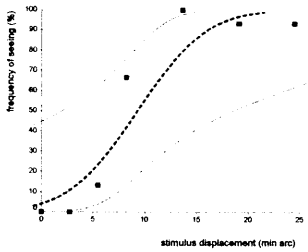

(d) 70% contrast

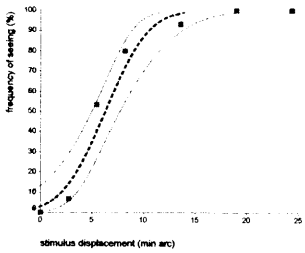

(e) 85% contrast

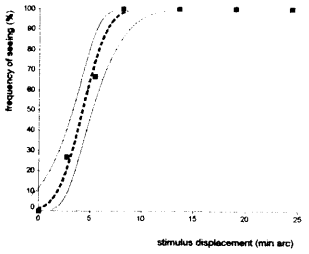

(ii) (a) 86 min arc line length: Subject 1.

(a) 25% contrast

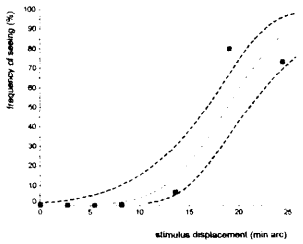

(b) 40% contrast

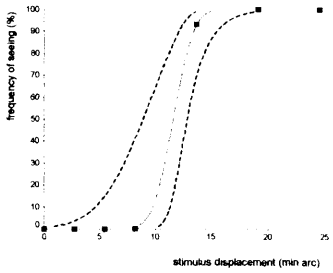

(c) 55% contrast

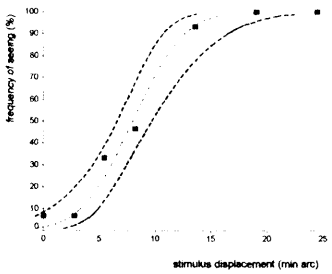

(d) 70% contrast

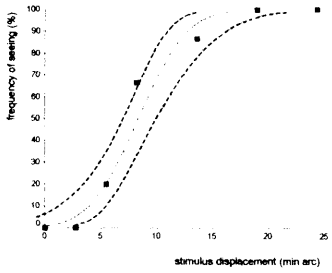

(e) 85% contrast

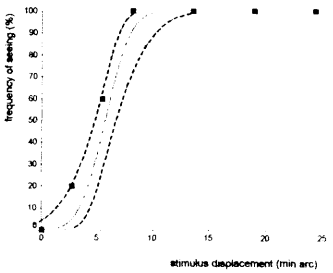

(c) 86 min arc line length: Subject 2.

(a) 25% contrast

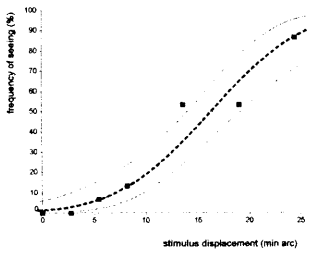

(b) 40% contrast

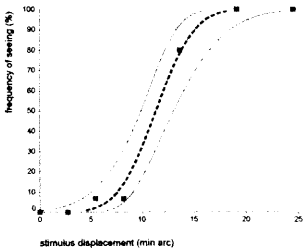

(c) 55% contrast

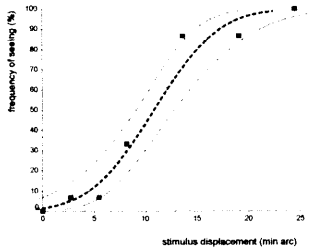

(d) 70% contrast

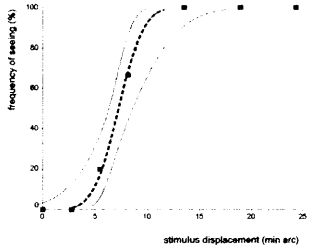

(e) 85% contrast

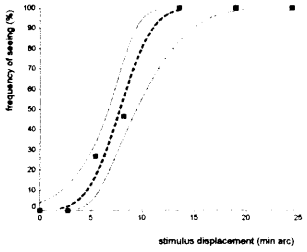

(iii) (a) 43 min arc line length: Subject 1.

(a) 25% contrast

UNSEEN

(b) 40% contrast

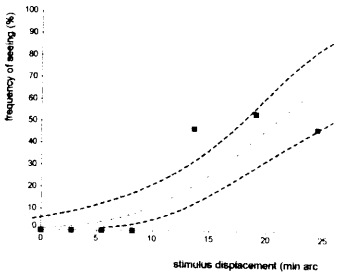

(c) 55% contrast

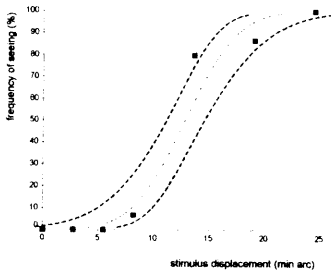

(d) 70% contrast

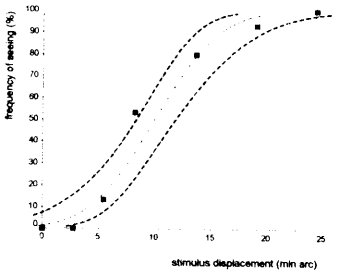

(e) 85% contrast

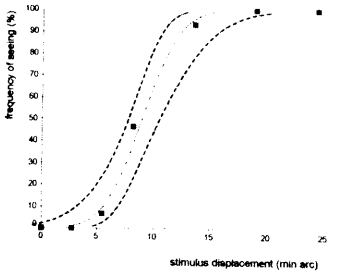

(b) 43 min arc line length: Subject 2.

*** increased upper displacement**

(a) 25% contrast*

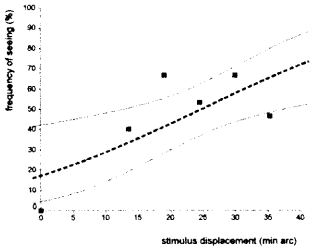

(b) 40% contrast

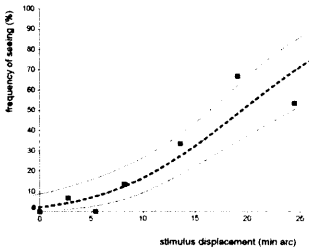

(c) 55% contrast

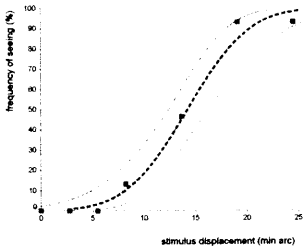

(d) 70% contrast

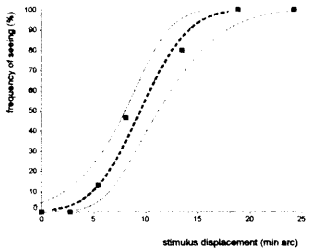

(e) 85% contrast

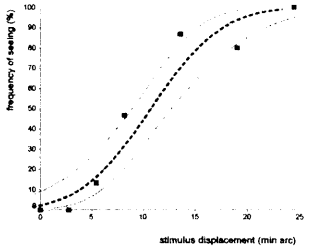

(iv) (a) 22 min arc line length: Subject 1.

*** increased upper displacement**

(a) 25% contrast

UNSEEN

(b) 40% contrast*

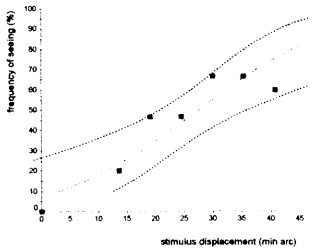

(c) 55% contrast

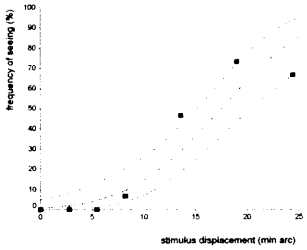

(d) 70% contrast

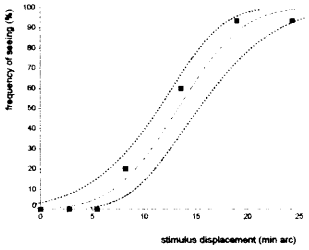

(e) 85% contrast

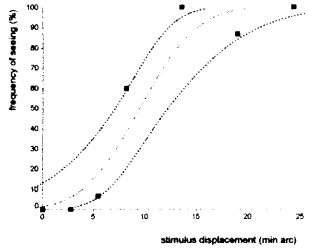

(b) 22 min arc line length: Subject 2.

(a) 25% contrast *

(b) 40% contrast

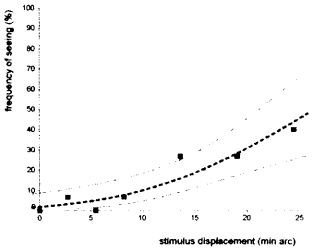

(c) 55% contrast

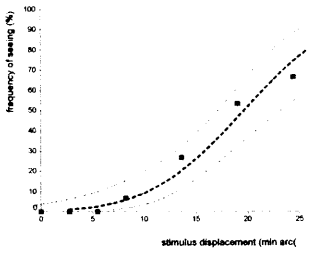

(d) 70% contrast

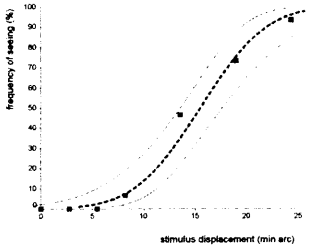

(e) 85% contrast

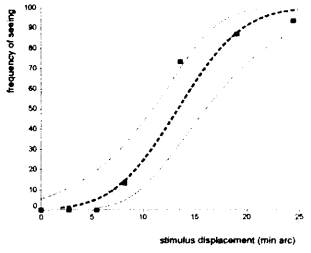

(v) (a) 11 min arc line length: subject 1.

(a) 25% contrast

UNSEEN

(b) 40% contrast

UNSEEN

(c) 55% contrast

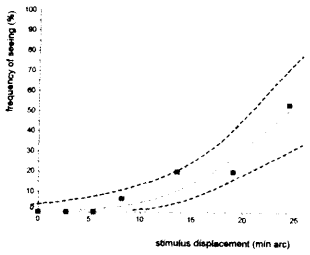

(d) 70% contrast

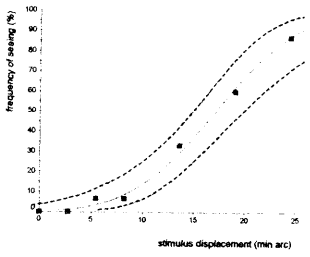

(e) 85% contrast

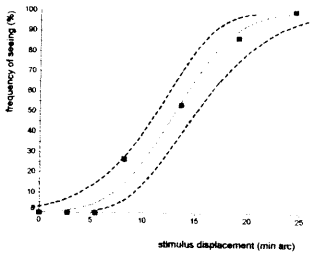

(b) 11 min arc line length: Subject 2.

(a) 25% contrast

UNSEEN

(b) 40% contrast

UNSEEN

(c) 55% contrast

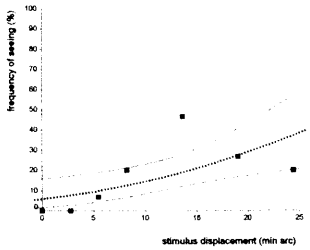

(d) 70% contrast

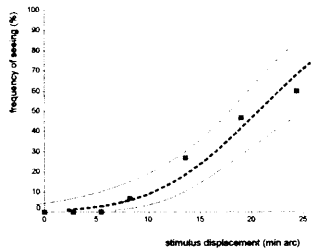

(e) 85% contrast

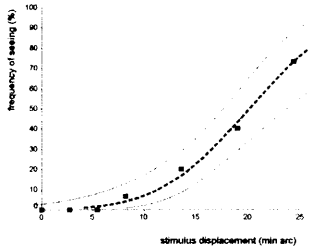

Table 14-5. Summary of MDT thresholds for merged and unmerged frequency of seeing data for line lengths of 11- 128 min arc at 25 - 84 % contrast.

Mean MDT threshold results, (range) and standard deviation (min arc).

(i) Merged frequency of seeing data.

Frequency of seeing curves merged for each individual prior to probit analysis.

	128	86	43	22	11
25%	14.5 (11.6-17.5) ± 4.17	17.6 (16.3-18.8) ± 1.77	24.8** (unseen subject 1)	UNSEEN	UNSEEN
40%	9.6 (9.0-10.2) ± 0.85	11.4 (11.3-11.5) ± 0.14	20.2 (19.5-20.8) ± 0.92	27.0 (26.4-27.5) ± 0.78*	UNSEEN
55%	9.2 (9.2-9.2) ± 0.00	9.4 (8.0-10.8) ± 2.0	13.5 (12.8-14.1) ± 0.92	18.6 (17.5-19.6) ± 1.48	27.6 (24.3-30.8) ± 4.60
70%	5.8 (5.2-6.3) ± 0.78	7.8 (7.3-8.3) ± 0.71	9.8 (9.6-9.9) ± 0.21	14.4 (13.3-15.5) ± 1.56	18.9 (17.1 -20.7) ± 2.55
85%	4.2 (4.1-4.3) ± 0.14	6.8 (5.7-7.8) ± 1.48	9.9 (9.0-10.8) ± 1.27	11.4 (9.5-13.4) ± 2.76	16.6 (13.0 - 20.2) ± 5.09

(ii) Unmerged frequency of seeing data.

Probit analysis done for each individual frequency of seeing curve.

	128	86	43	22	11
25%	14.4 (10.8 - 18.0) ± 5.09	17.7 (16.5 -18.8) ± 1.67	24.8 (15.5 - 33.9) ± 9.2** (unseen subject 1)	UNSEEN	UNSEEN
40%	9.3 (8.9 - 9.7) ± 0.52	11.5 (11.5 - 11.5) ± 0.00	20.2 (19.2 - 21.2) ± 1.44	28.0 (26.7 - 29.2) ± 1.77*	UNSEEN
55%	8.9 (8.9 - 8.9) ± 0.02	9.4 (7.9 - 11.0) ± 2.17	13.2 (12.3 - 14.1) ± 1.23	18.5 (17.5 - 19.6) ± 1.46	29.6 (26.9 - 32.3) ± 3.84
70%	5.7 (5.2 -6.2) ± 0.73	7.7 (7.3 - 8.1) ± 0.54	9.6 (9.3 - 9.8) ± 0.35	14.3 (13.1 - 15.5) ± 1.70	19.3 (17.1- 21.5) ± 3.13
85%	4.3 (4.2 - 4.3) ± 0.12	6.8 (5.7 - 7.8) ± 1.46	9.6 (8.7 - 10.5) ± 1.27	11.0 (9.2 -12.9) ± 2.64	16.8 (13.1 - 20.6 ± 5.3

* increased range of displacement (0-40 min arc) subject 1 only

** increased range of displacement (0-40 min arc) subject 2 only

Figure 14-3. Plots of log mean MDT as a function of log percentage contrast for individual subjects.

(i) subject 1

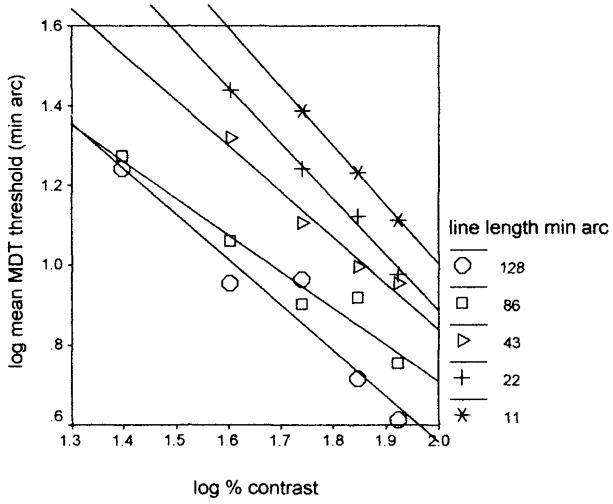

(ii) subject 2

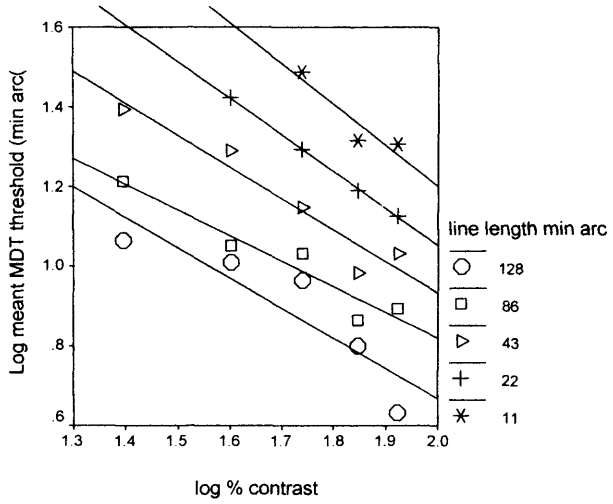

Table 14-6. Slope values of log MDT threshold as a function of log percentage contrast for individual subjects.

Data from figure 14-3.

(i) subject 1

Line Length (min arc)	Slope (95% CI)	R2	P
128	- 1.14 (- 1.49, - 0.79)	0.91	0.008
86	- 0.92 (- 1.15, - 0.68)	0.93	0.005
43	- 1.15 (- 1.44, - 0.86)	0.95	0.017
22	- 1.40 (- 1.55, - 1.25)	0.99	0.003
11	- 1.48 (- 1.50, - 1.45)	1.0	0.006

(ii) subject 2

Line Length (min arc)	Slope (95% CI)	R2	P
128	- 0.76 (- 1.18, - 0.34)	0.81	0.037
86	- 0.65 (- 0.86, - 0.43)	0.92	0.010
43	- 0.80 (- 1.05, - 0.54)	0.92	0.009
22	- 0.92 (- 0.96, - 0.88)	1.00	0.001
11	- 1.03 (- 1.86, - 0.20)	0.85	0.249

Figure 14-4. Plots of log interquartile range as a function of log MDT threshold for individual subjects.

(i) subject 1

(ii) slope 1.23 (95% CI 0.93, 1.53; $R^2 = 0.78$; P: < 0.001).

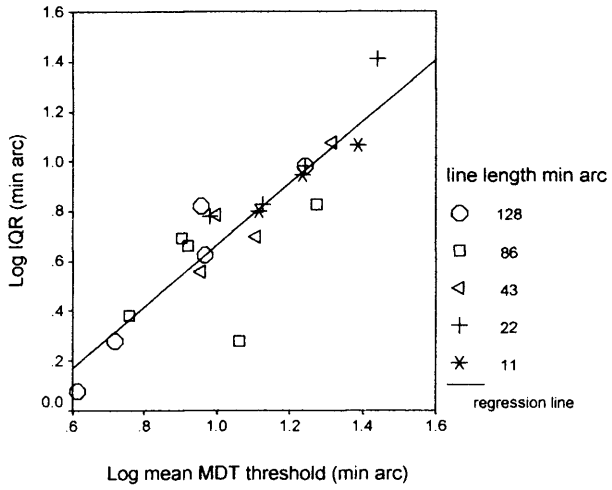

(iii) subject 2

slope – 1.18 (95% CI 0.91, 1.45; $R^2 = 0.79$; P:< 0.001).

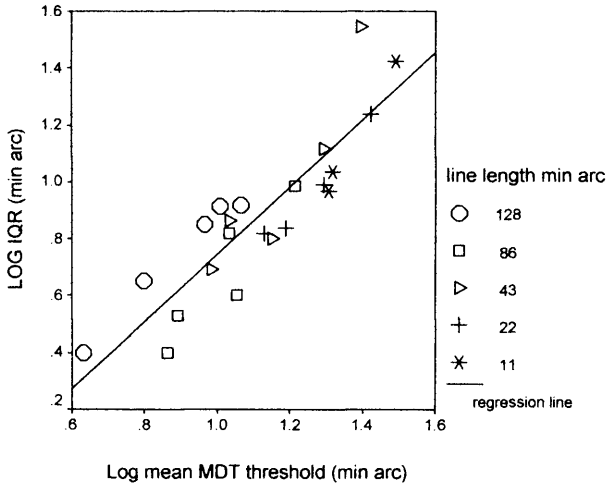

Figure 14-5. Plots of log MDT threshold as a function of log stimulus energy for individual subjects.

Stimulus energy = [stimulus area*(stimulus luminance – background luminance)]

(i) subject 1

slope - 0.46 (95% CI - 0.51, - 0.41; $R^2 = 0.94$; P: < 0.001).

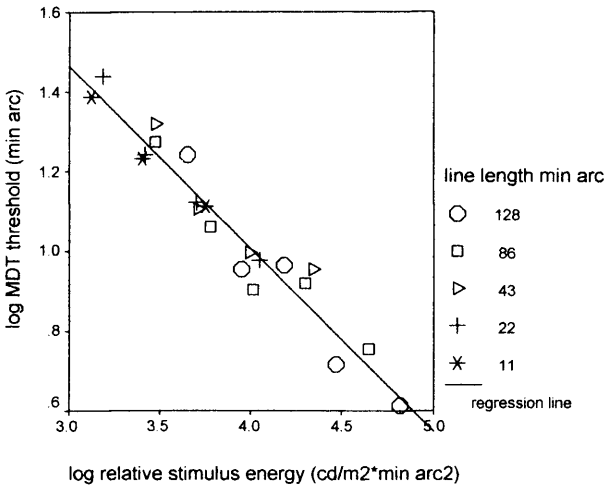

(ii) subject 2

slope - 0.43 (95% CI - 0.36, - 0.49; $R^2 = 0.88$; P: < 0.001).

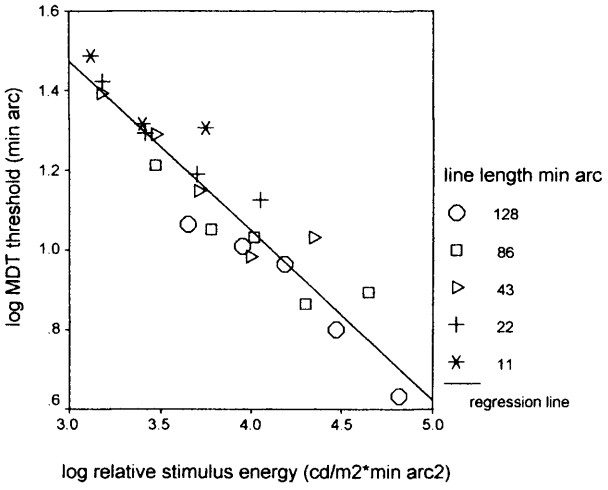

Table 14-7. Selection of staircase parameters by location.

Upper and lower hemi-field locations are matched in pairs
Start position is indicated in bold; DP: Displacement pixels; DMA: Displacement min arc

Location	zone	DP1	DMA1	DP2	DMA2	DP3	DMA3	DP4	DMA4	DP5	DMA5
1;29	6	2	5	3	8	**5**	**14**	7	19	8	22
2;30	5	1	4	2	8	**3**	**13**	4	17	5	21
3;31	3	1	5	2	9	**3**	**14**	4	18		
4;32	2	1	5	2	9	**3**	**14**	4	19		
5;33	1	1	5	**2**	**10**	3	15	4	19		
6;34	1	1	3	2	7	**3**	**10**	4	14	5	17
7;35	2	1	3	2	7	3	10	**4**	**13**	5	17
9;37	5	1	4	2	8	**3**	**13**	4	17	5	21
11;38	5	1	4	2	8	**3**	**12**	4	17	5	21
12;39	4	1	4	2	9	**3**	**13**	4	18		
13,40	3	1	5	2	9	**3**	**14**	4	19		
14,41	2	1	5	2	9	**3**	**13**	4	19		
15,42	2	1	3	2	7	**3**	**10**	4	13	5	17
16,43	3	1	5	2	9	**3**	**14**	4	18		
17,44	4	1	4	2	9	**3**	**13**	4	18		
18,45	5	1	4	2	8	**3**	**12**	4	17	5	21
19,46	5	1	4	2	8	**3**	**13**	4	17	5	21
20,47	4	2	6	3	9	**4**	**13**	5	16	7	22
21,48	3	2	6	3	10	**4**	**13**	5	16	6	19
22,49	3	1	5	2	9	**3**	**14**	4	18	5	23
23,50	4	1	4	2	9	**3**	**13**	4	18	5	22
24,51	5	1	4	2	9	**3**	**13**	4	17	5	21
25,52	5	2	6	3	9	**4**	**12**	6	18	7	20
26,53	5	2	6	3	9	**4**	**12**	6	18	7	21
27,54	5	1	4	2	8	**3**	**13**	4	17	5	21
28,55	5	1	4	2	8	**3**	**12**	4	17	5	21

Table 14-8. Response times at threshold in control (GMVR) by zone.
[mean (range) and standard deviation (msec)]

Zone	Number of Locations	Strategy	response time (msec)
1	4	1	435 (299 - 734) ± 203
		2	498 (300 - 689) ± 190
2	8	1	479 (370 – 725) ± 113
		2	499 (370 – 829) ± 147
3	10	1	415 (310 – 565) ± 98
		2	522 (335 –820) ± 155
4	8	1	500 (354 – 890) ± 189
		2	558 (419 – 771) ± 124
5	20	1	509 (285 –925) ± 181
		2	502 (265 – 815) ± 162
6	2	1	692 (550 –834) ± 201
		2	524 (374 – 674) ± 212

Table 14-9. The effect of attention on MDT threshold results for scattered and clustered locations.

Mean MDT threshold staircase results, (range) and standard deviation (min arc) determined by staircase strategy [- 9.9 (scattered) and - 27,3 (clustered and scattered). A single location is tested at the end of examination in isolation (-27,3) to investigate the effect of fatigue].

Number locations	-9,9 (scattered)	-27, 3 (clustered)	-27,3 (scattered)
1	10.7 (9-14) ± 2.89	5.0 (2.7 – 7.3) ± 3.20	
2	9.0 (9.0 –9.0) ± 0.00	6.8 (4.5 – 9.1) ± 3.21	
6	12.3 (9-14) ± 2.89	6.3 (3.6 – 9.1) ± 3.85	5.0 (4.5 - 5.4) ± 0.64
12	12.3 (9-14) ± 2.89	6.3 (4.5 – 8.2) ± 2.56	6.3 (5.4 – 7.3) ± 1.28
26	12.3 (9-14) ± 2.89	6.3 (5.4 – 7.3) ± 1.28	8.6 (6.4 – 10.9) ± 3.20
52	12.3 (9-14) ± 2.89	8.2 (6.4 – 10.0) ± 2.56	
Repeat 1 (fatigued)		6.8 (5.4 – 8.2) ± 1.92	

Table 14-10. The effect of crowding (adjacent distractors) on MDT threshold.

MDT threshold (location -9,9) determined by probit analysis (50% seen), (range) and standard deviation (min arc).

All locations present	5.3 (4.9 – 6.1) ± 0.69	6.6 (5.5 – 8.9) ± 1.96
Adjacent locations present	4.8 (4.1 – 5.5) ± 0.70	5.6 (4.9 – 7.1) ± 1.27
Adjacent locations absent	4.9 (4.3 – 5.5) ± 0.60	5.2 (4.9 – 5.5) ± 0.30

Table 14-11. Calculation of equivalent pixel elements for horizontal and oblique stimuli (zones 4 and 5).

	Stimulus Length	Pixels @ 255 RGB	Pixels @ 191 RGB	Pixels @ 184 RGB	Total Values Pixel x RGB
Horizontal	42	126	0	0	32130
Oblique	28	84	56	0	32116
Horizontal	40	120	0	0	30600
Oblique	27	81	0	54	30591

Table 14-12. Glaucoma subject response time at threshold for pilot MDT staircase strategies.

Response time: mean (range) msec

Subject	Eye	Strategy	response time (msec)
1	Left	1	622 (395 – 1005)
		2	661 (455 - 1045)
2	Right	2	785 (575 – 1085)
3	Left	3a	686 (490 – 975)
3	Right	1	677 (394 – 984)
		3a	626 (404 - 884)
4	Right	1	675 (379 - 970)
		3b	628 (430 - 850)
5	Left	3b	740 (420 - 1279)

BIBLIOGRAPHY

Adelson, E. H. and J. R. Bergen (1985). Spatiotemporal energy models for the perception of motion. *J Opt Soc Am A.* 2 (2): 284-99.

AGIS (1994). Advanced Glaucoma Intervention Study. 2. Visual field test scoring and reliability. *Ophthalmology.* 101 (8): 1445-55.

Allingham, R. R., M. Loftsdottir, et al. (2001). Pseudoexfoliation syndrome in Icelandic families. *Br J Ophthalmol.* 85 (6): 702-7.

Allingham, R. R., J. L. Wiggs, et al. (1998). Gln368STOP myocilin mutation in families with late-onset primary open-angle glaucoma. *Invest Ophthalmol Vis Sci.* 39 (12): 2288-95.

Anderson, A. J. and C. A. Johnson (2003). Frequency-doubling technology perimetry and optical defocus. *Invest Ophthalmol Vis Sci.* 44 (9): 4147-52.

Anderson, A. J., C. A. Johnson, et al. (2005). Characteristics of the normative database for the Humphrey matrix perimeter. *Invest Ophthalmol Vis Sci.* 46 (4): 1540-8.

Anderson, R. S. (1996). The selective effect of optical defocus on detection and resolution acuity in peripheral vision. *Curr Eye Res.* 15 (3): 351-3.

Anderson, R. S. (2005). The psychophysics of glaucoma: Improving the structure/function relationship. *Prog Retin Eye Res.*

Anderson, R. S., N. Drasdo, et al. (1995). Parvocellular neurons limit motion acuity in human peripheral vision. *Proceedings:Biological Sciences.* 261 (1360): 129-138.

Anderson, R. S. and F. A. Ennis (1999). Foveal and peripheral thresholds for detection and resolution of vanishing optotype tumbling E's. *Vision Res.* 39 (25): 4141-4.

Anderson, R. S., D. R. McDowell, et al. (2001). Effect of localized defocus on detection thresholds for different sized targets in the fovea and periphery. *Acta Ophthalmol Scand.* 79 (1): 60-3.

Anderson, R. S. and C. O'Brien (1997). Psychophysical evidence for a selective loss of M ganglion cells in glaucoma. *Vision Res.* 37 (8): 1079-83.

Anderson, R. S., M. O. Wilkinson, et al. (1992). Psychophysical localization of the human visual streak. *Optom Vis Sci.* 69 (3): 171-4.

Anderson, S. J. and D. C. Burr (1991). Spatial summation properties of directionally selective mechanisms in human vision. *J Opt Soc Am A.* 8 (8): 1330-9.

Ansari, E. A., J. E. Morgan, et al. (2002a). Glaucoma: squaring the psychophysics and neurobiology. *Br J Ophthalmol.* 86 (7): 823-6.

Ansari, E. A., J. E. Morgan, et al. (2002b). Psychophysical characterisation of early functional loss in glaucoma and ocular hypertension. *Br J Ophthalmol.* 86 (10): 1131-5.

Ansari, I., B. C. Chauhan, et al. (2000). Comparison of conventional and pattern discrimination perimetry in a prospective study of glaucoma patients. *Invest Ophthalmol Vis Sci.* 41 (13): 4150-7.

Artes, P. H., D. M. Hutchison, et al. (2005). Threshold and variability properties of matrix frequency-doubling technology and standard automated perimetry in glaucoma. *Invest Ophthalmol Vis Sci.* 46 (7): 2451-7.

Artes, P. H., D. McLeod, et al. (2002). Response time as a discriminator between true- and false-positive responses in suprathreshold perimetry. *Invest Ophthalmol Vis Sci.* 43 (1): 129-32.

Aung, T., L. Ocaka, et al. (2002). A major marker for normal tension glaucoma: association with polymorphisms in the OPA1 gene. *Hum Genet.* 110 (1): 52-6.

Austin, M. W., C. J. O'Brien, et al. (1994). Flicker perimetry using a luminance threshold strategy at frequencies from 5-25 Hz in glaucoma, ocular hypertension and normal controls. *Curr Eye Res.* 13 (10): 717-23.

Baez, K. A., A. I. McNaught, et al. (1995). Motion detection threshold and field progression in normal tension glaucoma. *Br J Ophthalmol.* 79 (2): 125-8.

Baker, C. L., Jr. and O. J. Braddick (1982). The basis of area and dot number effects in random dot motion perception. *Vision Res.* 22 (10): 1253-9.

Baker, C. L., Jr. and O. J. Braddick (1985). Eccentricity-dependent scaling of the limits for short-range apparent motion perception. *Vision Res.* 25 (6): 803-12.

Barlow, H. B. (1953). Summation and inhibition in the frog's retina. *J. Physiol. (Lond).* 119: 69-88.

Barlow, H. B., R. M. Hill, et al. (1964). Retinal Ganglion Cells Responding Selectively to Direction and Speed of Image Motion in the Rabbit. *J Physiol.* 173: 377-407.

Barlow, H. B. and W. R. Levick (1965). The mechanism of directionally selective units in rabbit's retina. *J Physiol.* 178 (3): 477-504.

Barlow, H. B. and W. R. Levick (1969). Three factors limiting the reliable detection of light by retinal ganglion cells of the cat. *J Physiol.* 200 (1): 1-24.

Bell, R. W. and C. O'Brien (1997). Accuracy of referral to a glaucoma clinic. *Ophthalmic Physiol Opt.* 17 (1): 7-11.

Benardete, E. A. and E. Kaplan (1997a). The receptive field of the primate P retinal ganglion cell, I: Linear dynamics. *Vis Neurosci.* 14 (1): 169-85.

Benardete, E. A. and E. Kaplan (1997b). The receptive field of the primate P retinal ganglion cell, II: Nonlinear dynamics. *Vis Neurosci.* 14 (1): 187-205.

Benardete, E. A., E. Kaplan, et al. (1992). Contrast gain control in the primate retina: P cells are not X-like, some M cells are. *Vis Neurosci.* 8 (5): 483-6.

Bengtsson, B. (2000). Reliability of computerized perimetric threshold tests as assessed by reliability indices and threshold reproducibility in patients with suspect and manifest glaucoma. *Acta Ophthalmol Scand.* 78 (5): 519-22.

Bengtsson, B. and A. Heijl (2000). False-negative responses in glaucoma perimetry: indicators of patient performance or test reliability? *Invest Ophthalmol Vis Sci.* 41 (8): 2201-4.

Bengtsson, B. and A. Heijl (2003). Normal intersubject threshold variability and normal limits of the SITA SWAP and full threshold SWAP perimetric programs. *Invest Ophthalmol Vis Sci.* 44 (11): 5029-34.

Bengtsson, B., J. Olsson, et al. (1997). A new generation of algorithms for computerized threshold perimetry , SITA. : *Acta Ophthalmol Scand.* 75: 368-375.

Bennett, A. G. and R. B. Rabbetts (1984). *Clinical Visual Optics*, Butterworths.

Bex, P. J. and S. C. Dakin (2005). Spatial interference among moving targets. *Vision Res.* 45 (11): 1385-98.

Bex, P. J., S. C. Dakin, et al. (2003). The shape and size of crowding for moving targets. *Vision Res.* 43 (27): 2895-904.

Bosworth, C. F., P. A. Sample, et al. (1998). Motion automated perimetry identifies early glaucomatous field defects. *Arch Ophthalmol.* 116 (9): 1153-8.

Bosworth, C. F., P. A. Sample, et al. (1997a). Motion perception thresholds in areas of glaucomatous visual field loss. *Vision Res.* 37 (3): 355-364.

Bosworth, C. F., P. A. Sample, et al. (1997b). Perimetric motion thresholds are elevated in glaucoma suspects and glaucoma patients. *Vision Res.* 37 (14): 1989-97.

Bosworth, C. F., P. A. Sample, et al. (1999). Spatial relationship of motion automated perimetry and optic disc topography in patients with glaucomatous optic neuropathy. *J Glaucoma.* 8 (5): 281-9.

Boulton, J. C. and C. L. Baker, Jr. (1991). Motion detection is dependent on spatial frequency not size. *Vision Res.* 31 (1): 77-87.

Bourne, R. R., K. E. Sorensen, et al. (2001). Glaucoma in East Greenlandic Inuit--a population survey in Ittoqqortoormiit (Scoresbysund). *Acta Ophthalmol Scand.* 79 (5): 462-7.

Bourne, R. R., P. Sukudom, et al. (2003). Prevalence of glaucoma in Thailand: a population based survey in Rom Klao District, Bangkok. *Br J Ophthalmol.* 87 (9): 1069-74.

Braddick, O. (1974). A short-range process in apparent motion. *Vision Res.* 14 (7): 519-27.

Brandt, J. D., J. A. Beiser, et al. (2001). Central corneal thickness in the Ocular Hypertension Treatment Study (OHTS). *Ophthalmology.* 108 (10): 1779-88.

Brdicka, R. (1995). [The human genome--chromosome 15]. *Cas Lek Cesk.* 134 (15): 484-6.

Brown, M. M., G. C. Brown, et al. (2003). Health care economic analyses and value-based medicine. *Surv Ophthalmol.* 48 (2): 204-23.

Brusini, P., F. Miani, et al. (2000). Corneal thickness in glaucoma: an important parameter? *Acta Ophthalmol Scand Suppl.* (232): 41-2.

Bullimore, M. A., J. M. Wood, et al. (1993). Motion perception in glaucoma. *Invest Ophthalmol Vis Sci.* 34 (13): 3526-33.

Burr, D. C. and B. Corsale (2001). Dependency of reaction times to motion onset on luminance and chromatic contrast. *Vision Res.* 41 (8): 1039-48.

Casagrande, V. A. (1994). A third parallel visual pathway to primate area V1. *Trends Neurosci.* 17 (7): 305-10.

Casson, E. J. and C. A. Johnson (1993). Temporal modulation perimetry in glaucoma and ocular hypertension. *Perimetry Update 1992/1993*. R. P. Mills. Amsterdam, Kugler & Ghedini, pp 443-450.

Casson, E. J., C. A. Johnson, et al. (1993a). Temporal modulation perimetry: the effects of aging and eccentricity on sensitivity in normals. *Invest Ophthalmol Vis Sci.* 34 (11): 3096-102.

Casson, E. J., C. A. Johnson, et al. (1993b). Longitudinal comparison of temporal-modulation perimetry with white-on-white and blue-on-yellow perimetry in ocular hypertension and early glaucoma. *J Opt Soc Am A.* 10 (8): 1792-806.

Chaturvedi, N., W.-E. T. Hedley, et al. (1993). Lateral geniculate nucleus in glaucoma. *Am J Ophthalmol.* 116 (2): 182-8.

Chauhan, B. C., P. H. House, et al. (1999). Comparison of conventional and high-pass resolution perimetry in a prospective study of patients with glaucoma and healthy controls. *Arch Ophthalmol.* 117 (1): 24-33.

Chauhan, B. C., R. P. LeBlanc, et al. (1993a). Comparison of high-pass resolution perimetry and pattern discrimination perimetry to conventional perimetry in glaucoma. *Can J Ophthalmol.* 28 (7): 306-11.

Chauhan, B. C., J. D. Tompkins, et al. (1993b). Characteristics of frequency-of-seeing curves in normal subjects, patients with suspected glaucoma, and patients with glaucoma. *Invest Ophthalmol Vis Sci.* 34 (13): 3534-40.

Chawla, D., G. Rees, et al. (1999). The physiological basis of attentional modulation in extrastriate visual areas. *Nat Neurosci.* 2 (7): 671-6.

Chichilnisky, E. J. and R. S. Kalmar (2002). Functional asymmetries in ON and OFF ganglion cells of primate retina. *J Neurosci.* 22 (7): 2737-47.

Coffey, M., A. Reidy, et al. (1993). Prevalence of glaucoma in the west of Ireland. *Br J Ophthalmol.* 77 (1): 17-21.

Copt, R. P., R. Thomas, et al. (1999). Corneal thickness in ocular hypertension, primary open-angle glaucoma, and normal tension glaucoma. *Arch Ophthalmol.* 117 (1): 14-6.

Corbetta, M., F. M. Miezin, et al. (1991). Selective and divided attention during visual discriminations of shape, color, and speed: functional anatomy by positron emission tomography. *J Neurosci.* 11 (8): 2383-402.

Cornsweet, T. N. (1962). The staircase method in psychophysics. *Am J Psychol.* 75: 485-491.

Coronel, M., D. De Abreu, et al. (1999). [Reaction time to dichotic visual stimulation and its relationship to cerebral hemispheric specialization]. *Acta Cient Venez.* 50 (1): 29-33.

Crabb, D. P. and A. C. Viswanathan (2005). Integrated visual fields: a new approach to measuring the binocular field of view and visual disability. *Graefes Arch Clin Exp Ophthalmol.* 243 (3): 210-6.

Crabb, D. P., A. C. Viswanathan, et al. (1998). Simulating binocular visual field status in glaucoma. *Br J Ophthalmol.* 82 (11): 1236-41.

Craig, J. E., P. N. Baird, et al. (2001). Evidence for genetic heterogeneity within eight glaucoma families, with the GLC1A Gln368STOP mutation being an important phenotypic modifier. *Ophthalmology.* 108 (9): 1607-20.

Crick, R. P. and M. W. Tuck (1995). How can we improve the detection of glaucoma? *Bmj.* 310 (6979): 546-7.

Croner, L. J. and E. Kaplan (1995). Receptive fields of P and M ganglion cells across the primate retina. *Vision Res.* 35 (1): 7-24.

Cronly-Dillon, J. R. (1991). *Vision and Visual Dysfunction*, Macmillan Press.

Crook, J. M., B. Lange-Malecki, et al. (1988). Visual resolution of macaque retinal ganglion cells. *J Physiol.* 396: 205-24.

Curcio, C. A. and K. A. Allen (1990). Topography of ganglion cells in human retina. *J Comp Neurol.* 300 (1): 5-25.

Dacey, D. M. (1993). The mosaic of midget ganglion cells in the human retina. *J Neurosci.* 13 (12): 5334-55.

Dacey, D. M. (1994). Physiology, morphology and spatial densities of identified ganglion cell types in primate retina. *Ciba Found Symp.* 184: 12-28.

Dacey, D. M. and S. Brace (1992). A coupled network for parasol but not midget ganglion cells in the primate retina. *Vis Neurosci.* 9 (3-4): 279-90.

Dacey, D. M. and B. B. Lee (1994). The 'blue-on' opponent pathway in primate retina originates from a distinct bistratified ganglion cell type. *Nature.* 367 (6465): 731-5.

Dacey, D. M. and M. R. Petersen (1992). Dendritic field size and morphology of midget and parasol ganglion cells of the human retina. *Proc Natl Acad Sci U S A.* 89 (20): 9666-70.

Damato, B. Multifixation campimetry on-line. http://www.testvision.org/.

Damato, B. and C. Groenewald (2003). Multifixation campimetry on line: a perimeter for the detection of visual field loss using the internet. *Br J Ophthalmol.* 87 (10): 1296-8.

Dandona, L., R. Dandona, et al. (2000a). Angle-closure glaucoma in an urban population in southern India. The Andhra Pradesh eye disease study. *Ophthalmology.* 107 (9): 1710-6.

Dandona, L., R. Dandona, et al. (2000b). Open-angle glaucoma in an urban population in southern India: the Andhra Pradesh eye disease study. *Ophthalmology.* 107 (9): 1702-9.

Dandona, L., A. Hendrickson, et al. (1991). Selective effects of experimental glaucoma on axonal transport by retinal ganglion cells to the dorsal lateral geniculate nucleus. *Invest Ophthalmol Vis Sci.* 32 (5): 1593-9.

Dandona, R., L. Dandona, et al. (2002). Planning low vision services in India : a population-based perspective. *Ophthalmology.* 109 (10): 1871-8.

Dannheim, F. and S. M. Drance (1971). Studies of spatial summation of central retinal areas in normal people of all ages. *Can J Ophthalmol.* 6 (4): 311-9.

Delange, H. (1958). Research into the dynamic nature of the human fovea-cortex systems with intermittent and modulated light. 1. Attentuation characteristics with white and coloured light. *J Opt Soc Am.* 48: 777-784.

Delgado, M. F., N. T. Nguyen, et al. (2002). Automated perimetry: a report by the American Academy of Ophthalmology. *Ophthalmology.* 109 (12): 2362-74.

Derrington, A. M. and P. Lennie (1984). Spatial and temporal contrast sensitivities of neurones in lateral geniculate nucleus of macaque. *J Physiol.* 357: 219-40.

DeYoe, E. A., D. J. Felleman, et al. (1994). Multiple processing streams in occipitotemporal visual cortex. *Nature.* 371 (6493): 151-4.

DeYoe, E. A. and D. C. Van Essen (1988). Concurrent processing streams in monkey visual cortex. *Trends Neurosci.* 11 (5): 219-26.

Drum, B. and R. Bissett (1991). Optimizing dot size and contrast in pattern discrimination perimetry. *Perimetry Update 1990/1.* R. P. Mills and A. Heijl. New York, Kugler and Ghedini, pp 373-380.

Drum, B., M. Severns, et al. (1988). Pattern discrimination and light detection test different types of glaucomatous damage. *Perimetry Update 1988/99.* A. Heijl. Berkeley, Kugler and Ghedini, pp 341-347.

Dunlop, O., R. Bjorklund, et al. (2002). Early psychomotor slowing predicts the development of HIV dementia and autopsy-verified HIV encephalitis. *Acta Neurol Scand.* 105 (4): 270-5.

Elkington, A. R. and H. J. Frank (1991). *Clinical Optics.* Blackwell Scientific Publications.

Ennis, F. A., R. S. Anderson, et al. (1999). Tumbling E resolution perimetry in glaucoma. *Perimetry Update 1998/1999.* M. Wall and J. Wild. The Hague, The Netherlands, Kugler Publications, pp 179-186.

Enroth-Cugell, C. and J. G. Robson (1966). The contrast sensitivity of retinal ganglion cells of the cat. *J. Physiol. (Lond).* 187: 517-552.

Exner, S. (1875). Uber des Sehen von Bewegung und die Theorie des zusammengesetzten Auges. *Sher. Akad. Wiss. Wien. (Math.-nat. Kl., Abt. 3).* 72: 156-190.

Feghali, J. G., X. Bocquet, et al. (1991). Static flicker perimetry in glaucoma and ocular hypertension. *Curr Eye Res.* 10 (3): 205-12.

Felius, J., L. A. de Jong, et al. (1995). Functional characteristics of blue-on-yellow perimetric thresholds in glaucoma. *Invest Ophthalmol Vis Sci.* 36 (8): 1665-74.

Felius, J., W. H. Swanson, et al. (1996). Spatial summation for selected ganglion cell mosaics in patients with glaucoma. *Perimetry Update 1996/1997.* M. Wall and A. Heijl. The Hague, The Netherlands, Kugler Publications, pp 213-221.

Fellman, R. L., J. R. Lynn, et al. (1988). Clinical importance of spatial summation in glaucoma. *Perimetry Update 1988/1989*. A. Heijl, Kugler Publications, The Hague, The Netherlands, pp 313-324.

Fendick, M. G. and N. V. Swindale (1994). Vernier acuity for edges defined by flicker. *Vision Res.* 34 (20): 2717-26.

Ferree, C. E., G. Rand, et al. (1931). Refraction for the peripheral field of vision. *Arch. Ophthalmol.* 5 (5): 717-731.

Fitzke, F. W., D. Poinoosawmy, et al. (1987). Peripheral displacement thresholds in normals, ocular hypertensives and glaucoma. *Perimetry Update 1986/1987*. E. Greve and A. Heijl. The Hague, The Netherlands, Kugler & Ghedini, pp 447-452.

Fitzke, F. W., D. Poinoosawmy, et al. (1989). Peripheral displacement thresholds in glaucoma and ocular hypertension. *Perimetry Update 1988/1989*. A. Heijl. The Hague, The Netherlands, Kugler & Ghedini, pp 399-405.

Fitzke, F. W., D. Poinoosawmy, et al. (1992). *Motion detection thresholds for predicting visual loss in low tension glaucoma suspects*. 4th Congress EGS Amsterdam.

Foley-Fisher, J. A. (1973). The effect of target line length on Vernier acuity in white and blue light. *Vision Res.* 13 (8): 1447-54.

Foster, P. J., J. Baasanhu, et al. (1996). Glaucoma in Mongolia. A population-based survey in Hovsgol province, northern Mongolia. *Arch Ophthalmol.* 114 (10): 1235-41.

Foster, P. J., R. Buhrmann, et al. (2002). The definition and classification of glaucoma in prevalence surveys. *Br J Ophthalmol.* 86 (2): 238-42.

Foster, P. J. and G. J. Johnson (2001). Glaucoma in China: how big is the problem? *Br J Ophthalmol.* 85 (11): 1277-82.

Gardiner, S. K., D. P. Crabb, et al. (2004). Reducing noise in suspected glaucomatous visual fields by using a new spatial filter. *Vision Res.* 44 (8): 839-48.

Garway-Heath, D. F. (2000). MD thesis: Correlation of structural and functional measurements in primary open angle glaucoma (optic disc morphology and psychophysics). University College London.

Garway-Heath, D. F. (2004). Comparison of structural and functional methods - 1. *Glaucoma Diagnosis. Structure and Function*. R. N. Weinreb and E. L. Greve. The Hague, The Netherlands, Kugler, pp 135-143.

Garway-Heath, D. F., J. Caprioli, et al. (2000a). Scaling the hill of vision: the physiological relationship between light sensitivity and ganglion cell numbers. *Invest Ophthalmol Vis Sci.* 41 (7): 1774-82.

Garway-Heath, D. F., G. E. Holder, et al. (2002). Relationship between electrophysiological, psychophysical, and anatomical measurements in glaucoma. *Invest Ophthalmol Vis Sci.* 43 (7): 2213-20.

Garway-Heath, D. F., D. Poinoosawmy, et al. (2000b). Mapping the visual field to the optic disc in normal tension glaucoma eyes. *Ophthalmology.* 107 (10): 1809-15.

Gaudiano, P. (1994). Simulations of X and Y retinal ganglion cell behavior with a nonlinear push-pull model of spatiotemporal retinal processing. *Vision Res.* 34 (13): 1767-84.

Geisler, W. S. (1984). Physical limits of acuity and hyperacuity. *J Opt Soc Am A.* 1 (7): 775-82.

Geisler, W. S. and R. L. Diehl (2002). Bayesian natural selection and the evolution of perceptual systems. *Philos Trans R Soc Lond B Biol Sci.* 357 (1420): 419-48.

Georgeson, M. A. and N. E. Scott-Samuel (1999). Motion contrast: a new metric for direction discrimination. *Vision Res.* 39 (26): 4393-402.

Glezer, V. D. (1965). The receptive fields of the retina. *Vision Res.* 5 (9): 497-525.

Glovinsky, Y., H. A. Quigley, et al. (1993). Foveal ganglion cell loss is size dependent in experimental glaucoma. *: Invest Ophthalmol Vis Sci.* 34 (2): 395-400.

Gonzalez de la Rosa, M. A., J. Rodriguez, et al. (1998). Flicker-TOP perimetry in normals and patients with ocular hypertension and early glaucoma. *Perimetry Update 1998/1999.* M. Wall and J. Wild. The Hague, The Netherlands, Kugler Publications, pp 59-66.

Graham, S. L. and S. M. Drance (1999). Nocturnal hypotension: role in glaucoma progression. *Surv Ophthalmol.* 43 Suppl 1: S10-6.

Graham, S. L., S. M. Drance, et al. (1995). Ambulatory blood pressure monitoring in glaucoma. The nocturnal dip. *Ophthalmology.* 102 (1): 61-9.

Greve, E. L. (1973). Single and multiple stimulus static perimetry in glaucoma; the two phases of perimetry. *In: Henkes (ed). Doc Ophthalmol 36.*

Hafez, A. S., R. L. Bizzarro, et al. (2003). Evaluation of optic nerve head and peripapillary retinal blood flow in glaucoma patients, ocular hypertensives, and normal subjects. *Am J Ophthalmol.* 136 (6): 1022-31.

Harper, R., D. Henson, et al. (2000). Appraising evaluations of screening/diagnostic tests: the importance of the study populations. *Br J Ophthalmol.* 84 (10): 1198-202.

Harwerth, R. S., L. Carter-Dawson, et al. (1999). Ganglion cell losses underlying visual field defects from experimental glaucoma. *Invest Ophthalmol Vis Sci.* 40 (10): 2242-50.

Harwerth, R. S., L. Carter-Dawson, et al. (2004). Neural losses correlated with visual losses in clinical perimetry. *Invest Ophthalmol Vis Sci.* 45 (9): 3152-60.

Harwerth, R. S., M. L. Crawford, et al. (2002). Visual field defects and neural losses from experimental glaucoma. *Prog Retin Eye Res.* 21 (1): 91-125.

Heijl, A. (1985). *The Humphrey Field Analyzer, construction and concepts.* Proceedings of the 6th International Perimetric Society meeting 1984, Junk, Dordrecht.

Heijl, A., M. C. Leske, et al. (2002). Reduction of intraocular pressure and glaucoma progression: results from the Early Manifest Glaucoma Trial. *Arch Ophthalmol.* 120 (10): 1268-79.

Henson, D. B. (1999). Letter to the editor: Referrals to the Glaucoma Clinic of the Royal Infirmary of Edinburgh. *Ophthalmic Physiol Opt.* 19 (6): 518-9.

Henson, D. B. and P. H. Artes (2002). New developments in supra-threshold perimetry. *Ophthalmic Physiol Opt.* 22 (5): 463-8.

Henson, D. B., S. Chaudry, et al. (2000). Response variability in the visual field: comparison of optic neuritis, glaucoma, ocular hypertension, and normal eyes. *Invest Ophthalmol Vis Sci.* 41 (2): 417-21.

Henson, D. B. and B. C. Chauhan (1985). Informational content of visual field location in glaucoma. *Doc Ophthalmol.* 59 (4): 341-52.

Henson, D. B., B. C. Chauhan, et al. (1988). Screening for glaucomatous visual field defects: the relationship between sensitivity, specificity and the number of test locations. *Ophthalmic Physiol Opt.* 8 (2): 123-7.

Henson, D. B. and E. J. Morris (1993). Effect of uncorrected refractive errors upon central visual field testing. *Ophthalmic Physiol Opt.* 13 (4): 339-43.

Henson, D. B., A. F. Spencer, et al. (2003). Community refinement of glaucoma referrals. *Eye.* 17 (1): 21-6.

Hock, H. S., G. W. Balz, et al. (1998). Attentional control of spatial scale: effects on self-organized motion patterns. *Vision Res.* 38 (23): 3743-58.

Horn, F. K., J. B. Jonas, et al. (1997). The full-field flicker test in early diagnosis of chronic open-angle glaucoma. *Am J Ophthalmol.* 123 (3): 313-9.

Jansiewicz, E. M., C. J. Newschaffer, et al. (2004). Impaired habituation in children with attention deficit hyperactivity disorder. *Cogn Behav Neurol.* 17 (1): 1-8.

Joffe, K. M., J. E. Raymond, et al. (1997). Motion coherence perimetry in glaucoma and suspected glaucoma. *Vision Res.* 37 (7): 955-964.

Johnson, B., M. Miao, et al. (1987). Age-related decline of human optic nerve axon populations. *Age.* 81: 5-9.

Johnson, C. A. (1994). Selective versus nonselective losses in glaucoma. *J. Glaucoma.* 3: S32-S44.

Johnson, C. A., A. J. Adams, et al. (1993). Progression of early glaucomatous visual field loss as detected by blue-on-yellow and standard white-on-white automated perimetry. *Arch Ophthalmol.* 111 (5): 651-6.

Johnson, C. A., G. A. Cioffi, et al. (1999). Frequency Doubling Technology Perimetry using a 24-2 stimulus presentation pattern. *Optom Vis Sci.* 76 (8): 571-581.

Johnson, C. A., D. Marshall, et al. (1995). Displacement threshold perimetry in glaucoma using a Macintosh computer system and a 21-inch monitor. *Perimetry Update 1994/1995.* R. Mills and M. Wall. Amsterdam, Kugler Publications, pp 103-110.

Johnson, C. A., D. P. Sample Ph, et al. (2003). Structure and function evaluation (SAFE): II. Comparison of optic disk and visual field characteristics. *Am J Ophthalmol.* 135 (2): 148-54.

Johnson, C. A. and S. J. Samuels (1997). Screening for glaucomatous visual field loss with frequency-doubling perimetry. *Invest Ophthalmol Vis Sci.* 38 (2): 413-25.

Johnson, C. A. and R. P. Scobey (1980). Foveal and peripheral displacement thresholds as a function of stimulus luminance, line length and duration of movement. *Vision Res.* 20 (8): 709-15.

Jonas, J. B., A. M. Schmidt, et al. (1992). Human optic nerve fiber count and optic disc size. *Invest Ophthalmol Vis Sci.* 33 (6): 2012-8.

Junemann, A. G., F. K. Horn, et al. (2000). The full-field temporal contrast sensitivity test for glaucoma: influence of cataract. *Graefes Arch Clin Exp Ophthalmol.* 238 (5): 427-32.

Kandel ER, S. J., Jessell TM (1991). *Principles of Neural Science*. New York, Elsevier.

Kandel ER, S. J., Jessell TM (2000). *Principles of Neural Science*, Elsevier.

Kapadia, M. K., G. Westheimer, et al. (1999). Dynamics of spatial summation in primary visual cortex of alert monkeys. *Proc Natl Acad Sci U S A.* 96 (21): 12073-8.

Kaplan, E. and R. M. Shapley (1986). The primate retina contains two types of ganglion cells, with high and low contrast sensitivity. *Proc Natl Acad Sci U S A.* 83 (8): 2755-7.

Kass, M. A., D. K. Heuer, et al. (2002). The Ocular Hypertension Treatment Study: a randomized trial determines that topical ocular hypotensive medication delays or prevents the onset of primary open-angle glaucoma. *Arch Ophthalmol.* 120 (6): 701-13; discussion 829-30.

Kastner, S. and M. A. Pinsk (2004). Visual attention as a multilevel selection process. *Cogn Affect Behav Neurosci.* 4 (4): 483-500.

Kelly, D. H. (1961). Visual response to time dependent stimuli. *J. Opt. Soc. Am.* 51: 422-429.

Kelly, D. H. (1966). Frequency Doubling in Visual Responses. *J Am Optom Assoc.* 56 (11): 1628-33.

Kim, Y. Y., J. S. Kim, et al. (2001). Effect of cataract extraction on blue-on-yellow visual field. *Am J Ophthalmol.* 132 (2): 217-20.

Klein, B. E., R. Klein, et al. (1992). Prevalence of glaucoma. The Beaver Dam Eye Study. *Ophthalmology.* 99 (10): 1499-504.

Kline, D. W., J. C. Culham, et al. (2001). Aging effects on vernier hyperacuity: a function of oscillation rate but not target contrast. *Optom Vis Sci.* 78 (9): 676-82.

Kuffler, S. W. (1953). Discharge patterns and functional organization of mammalian retina. *J. Neurophysiol.* 16: 37-68.

Kwon, Y. H., H. J. Park, et al. (1998). Test-retest variability of blue-on-yellow perimetry is greater than white-on-white perimetry in normal subjects. *Am J Ophthalmol.* 126 (1): 29-36.

Lachenmayr, B., H. Rothbacher, et al. (1988). Automated Flicker Perimetry versus Quantitative Static perimetry in early glaucoma. *Perimetry Update 1988/99.* A. Heijl. Amsterdam, Kugler and Ghedini, pp 359-368.

Lachenmayr, B. J. (1994). The role of temporal threshold criteria in psychophysical testing in glaucoma. *Curr Opin Ophthalmol.* 5 (2): 58-63.

Lachenmayr, B. J., S. M. Drance, et al. (1991). Light-sense, flicker and resolution perimetry in glaucoma a comparative study. *Graefes Arch Clin Exp Ophthalmol.* 229 (3): 246-51.

Lachenmayr, B. J. and M. Gleissner (1992). Flicker perimetry resists retinal image degradation. *Invest Ophthalmol Vis Sci.* 33 (13): 3539-42.

Lachenmayr, B. J. and P. M. O. Vivell (1993). *Perimetry and its clinical correlations*, Thieme Medical Publishers.

Lachkar, Y. (2003). Angle-closure chronic glaucoma. *J Fr Ophtalmol.* 26 Spec No 2: S49-52.

Lan, Y. W., D. B. Henson, et al. (2003). The correlation between optic nerve head topographic measurements, peripapillary nerve fibre layer thickness, and visual field indices in glaucoma. *Br J Ophthalmol.* 87 (9): 1135-41.

Langley-Hawthorne, C. (2003). *The Cost of Blindness: an analysis of the costs of visual impairment and blindness in the United Kingdom*, Ethical Strategies Ltd.

Lee, B. B., C. Wehrhahn, et al. (1993). Macaque ganglion cell responses to stimuli that elicit hyperacuity in man: detection of small displacements. *J Neurosci.* 13 (3): 1001-9.

Lee, B. B., C. Wehrhahn, et al. (1995). The spatial precision of macaque ganglion cell responses in relation to vernier acuity of human observers. *Vision Res.* 35 (19): 2743-58.

Lee, B. L. and M. R. Wilson (2003). Ocular Hypertension Treatment Study (OHTS) commentary. *Curr Opin Ophthalmol.* 14 (2): 74-7.

Leibowitz, H. W., C. A. Johnson, et al. (1972). Peripheral motion detection and refractive error. *Science.* 177 (55): 1207-8.

Leonova, A., J. Pokorny, et al. (2003). Spatial frequency processing in inferred PC- and MC-pathways. *Vision Res.* 43 (20): 2133-9.

Leske, M. C., A. M. Connell, et al. (1995). Risk factors for open-angle glaucoma. The Barbados Eye Study. *Arch Ophthalmol.* 113 (7): 918-24.

Leske, M. C., A. Heijl, et al. (1999). Early Manifest Glaucoma Trial: design and baseline data. *Ophthalmology.* 106 (11): 2144-53.

Levene, R. Z. (1980). Low tension glaucoma: a critical review and new material. *Surv Ophthalmol.* 24 (6): 621-64.

Levi, D. M., S. A. Klein, et al. (1985). Vernier acuity, crowding and cortical magnification. *Vision Res.* 25 (7): 963-77.

Levi, D. M., P. V. McGraw, et al. (2000). Vernier and contrast discrimination in central and peripheral vision. *Vision Res.* 40 (8): 973-88.

Livingstone, M. and D. Hubel (1988). Segregation of form, color, movement, and depth anatomy, physiology, and perception. *Science.* 240 (4853): 740-9.

Livingstone, M. S. and D. H. Hubel (1987). Psychophysical evidence for separate channels for the perception of form, color, movement, and depth. *J Neurosci.* 7 (11): 3416-68.

Lou, L. (1999). Selective peripheral fading: evidence for inhibitory sensory effect of attention. *Perception.* 28 (4): 519-26.

Lutjen-Drecoll, E. (1999). Functional morphology of the trabecular meshwork in primate eyes. *Prog Retin Eye Res.* 18 (1): 91-119.

MacVeigh, D., D. Whitaker, et al. (1991). Spatial summation determines the contrast response of displacement threshold hyperacuity. *Ophthalmic Physiol Opt.* 11 (1): 76-80.

Maddess, T. and G. H. Henry (1992). Performance of nonlinear visual units in ocular hypertension and glaucoma. *Clin Vis Sci.* 7: 371-83.

Martin, L., P. Wanger, et al. (2003). Concordance of high-pass resolution perimetry and frequency-doubling technology perimetry results in glaucoma: no support for selective ganglion cell damage. *J Glaucoma.* 12 (1): 40-4.

Martin, P. R., A. J. White, et al. (1997). Evidence that blue-on cells are part of the third geniculocortical pathway in primates. *Eur J Neurosci.* 9 (7): 1536-41.

Martinez, G. A., P. A. Sample, et al. (1995). Comparison of high-pass resolution perimetry and standard automated perimetry in glaucoma. *Am J Ophthalmol.* 119 (2): 195-201.

Mather, G. (1987). The dependence of edge displacement thresholds on edge blur, contrast, and displacement distance. *Vision Res.* 27 (9): 1631-7.

Maunsell, J. H., T. A. Nealey, et al. (1990). Magnocellular and parvocellular contributions to responses in the middle temporal visual area (MT) of the macaque monkey. *J Neurosci.* 10 (10): 3323-34.

McIlhagga, W. and A. Paakkonen (2003). Effects of contrast and length on vernier acuity explained with noisy templates. *Vision Res.* 43 (6): 707-16.

McKendrick, A. M., C. A. Johnson, et al. (2002). Elevated vernier acuity thresholds in glaucoma. *Invest Ophthalmol Vis Sci.* 43 (5): 1393-9.

Membrey, L. (2000). *Comparison of the effects of change in the optical media on frequency doubling perimetry, white-on-white perimetry and motion detection perimetry.* European Glaucoma Society Meeting, London.

Membrey, L. and F. W. Fitzke (2000). Effect of lens opacity on white-on-white perimetry, frequency doubling perimetry, and motion detection perimetry. *Perimetry Update 2000/2001.* M. Wall and J. Wild. The Hague, The Netherlands, Kugler Publications, pp 259-266.

Membrey, L., S. Kogure, et al. (1998). A comparison of the effects of neutral density filters and diffusing filters on motion perimetry, white on white perimetry and frequency doubling perimetry. *Perimetry Update 1998/1999.* M. Wall and J. Wild, Kugler Publications, The Hague, The Netherlands, pp 75-83.

Mennemeier, M. S., A. Chatterjee, et al. (1994). Contributions of the parietal and frontal lobes to sustained attention and habituation. *Neuropsychologia.* 32 (6): 703-16.

Menon, A. G., J. F. Gusella, et al. (1990). Progress towards the isolation and characterization of the genes causing neurofibromatosis. *Cancer Surv.* 9 (4): 689-702.

Merigan, W. H., C. E. Byrne, et al. (1991a). Does primate motion perception depend on the magnocellular pathway? *J Neurosci.* 11 (11): 3422-9.

Merigan, W. H., L. M. Katz, et al. (1991b). The effects of parvocellular lateral geniculate lesions on the acuity and contrast sensitivity of macaque monkeys. *J Neurosci.* 11 (4): 994-1001.

Merigan, W. H. and J. H. Maunsell (1993). How parallel are the primate visual pathways? *Annu Rev Neurosci.* 16: 369-402.

Miglior, S., T. Zeyen, et al. (2002). The European glaucoma prevention study design and baseline description of the participants. *Ophthalmology.* 109 (9): 1612-21.

Millodot, M. (1981). Effect of ametropia on peripheral refraction. *Am J Optom Physiol Opt.* 58 (9): 691-5.

Mitchell, P., F. Hourihan, et al. (1999a). The relationship between glaucoma and myopia: the Blue Mountains Eye Study. *Ophthalmology.* 106 (10): 2010-5.

Mitchell, P., A. J. Lee, et al. (2004). Open-angle glaucoma and systemic hypertension: the blue mountains eye study. *J Glaucoma.* 13 (4): 319-26.

Mitchell, P., E. Rochtchina, et al. (2002). Bias in self-reported family history and relationship to glaucoma: the Blue Mountains Eye Study. *Ophthalmic Epidemiol.* 9 (5): 333-45.

Mitchell, P., W. Smith, et al. (1996). Prevalence of open-angle glaucoma in Australia. The Blue Mountains Eye Study. *Ophthalmology.* 103 (10): 1661-9.

Mitchell, P., W. Smith, et al. (1997). Open-angle glaucoma and diabetes: the Blue Mountains eye study, Australia. *Ophthalmology.* 104 (4): 712-8.

Mitchell, P., J. J. Wang, et al. (1999b). The relationship between glaucoma and pseudoexfoliation: the Blue Mountains Eye Study. *Arch Ophthalmol.* 117 (10): 1319-24.

Montaser-Kouhsari, L. and R. Rajimehr (2005). Subliminal attentional modulation in crowding condition. *Vision Res.* 45 (7): 839-44.

Morgan, J. E. (1994). Selective cell death in glaucoma does it really occur? *Br J Ophthalmol.* 78 (11): 875-9.

Morgan, J. E. (2002). Retinal ganglion cell shrinkage in glaucoma. *J Glaucoma.* 11 (4): 365-70.

Morgan, J. E., H. Uchida, et al. (2000). Retinal ganglion cell death in experimental glaucoma. *Br J Ophthalmol.* 84 (3): 303-10.

Morgan, M. J. (1992). Spatial filtering precedes motion detection. *Nature.* 355 (6358): 344-6.

Morgan, M. J. and T. S. Aiba (1985). Vernier acuity predicted from changes in the light distribution of the retinal image. *Spat Vis.* 1 (2): 151-61.

Morgan, M. J., R. Perry, et al. (1997). The spatial limit for motion detection in noise depends on element size, not on spatial frequency. *Vision Res.* 37 (6): 729-36.

Moss, I. D., J. M. Wild, et al. (1995). The influence of age-related cataract on blue-on-yellow perimetry. *Invest Ophthalmol Vis Sci.* 36 (5): 764-73.

Nakayama, K. and C. W. Tyler (1981). Psychophysical isolation of movement sensitivity by removal of familiar position cues. *Vision Res.* 21 (4): 427-33.

Newman, D. K., S. Anwar, et al. (1998). Glaucoma screening by optometrists: positive predictive value of visual field testing. *Eye.* 12 (Pt 6): 921-4.

Nizankowska, M. H. and R. Kaczmarek (2004). Prevalance of open angle glaucoma and ocular hypertension as a risk factor for primary open angle glaucoma in Wroclaw population. Wroclaw Epidemiology Study. *Klin Oczna.* 106 (1-2 Suppl): 147-52.

Nomura, H., F. Ando, et al. (2004). The relationship between intraocular pressure and refractive error adjusting for age and central corneal thickness. *Ophthalmic Physiol Opt.* 24 (1): 41-5.

Ntim-Amponsah, C. T., W. M. Amoaku, et al. (2004). Prevalence of glaucoma in an African population. *Eye.* 18 (5): 491-7.

Olsson, J., B. Bengtsson, et al. (1997). An improved method to estimate frequency of false positive answers in computerized perimetry. *Acta Ophthalmol Copenh.* 75: 181-183.

Olveczky, B. P., S. A. Baccus, et al. (2003). Segregation of object and background motion in the retina. *Nature.* 423 (6938): 401-8.

Pararajasegaram, R. (1999). VISION 2020-the right to sight: from strategies to action. *Am J Ophthalmol.* 128 (3): 359-60.

Parkes, L., J. Lund, et al. (2001). Compulsory averaging of crowded orientation signals in human vision. *Nat Neurosci.* 4 (7): 739-44.

Poinoosawmy, D., F. W. Fitzke, et al. (1992). Discrimination between progression and non-progression visual field loss in low tension glaucoma using MDT. *Perimetry Update 1992/1993.* R. P. Mills, Kugler Publications, pp 109-114.

Pokorny, J. and V. C. Smith (1997). Psychophysical signatures associated with magnocellular and parvocellular pathway contrast gain. *J Opt Soc Am A.* 14 (9): 2477-86.

Post, R. B., R. P. Scobey, et al. (1984). Effects of retinal eccentricity on displacement thresholds for unidirectional and oscillatory stimuli. *Vision Res.* 24 (8): 835-9.

Quigley, H. A. (1996). Number of people with glaucoma worldwide. *Br J Ophthalmol.* 80 (5): 389-93.

Quigley, H. A. and E. M. Addicks (1981). Regional differences in the structure of the lamina cribrosa and their relation to glaucomatous optic nerve damage. *Arch Ophthalmol.* 99 (1): 137-43.

Quigley, H. A., E. M. Addicks, et al. (1982). Optic nerve damage in human glaucoma. III. Quantitative correlation of nerve fiber loss and visual field defect in glaucoma, ischemic neuropathy, papilledema, and toxic neuropathy. *Arch Ophthalmol.* 100 (1): 135-46.

Quigley, H. A., G. R. Dunkelberger, et al. (1988). Chronic human glaucoma causing selectively greater loss of large optic nerve fibers. *Ophthalmology.* 95 (3): 357-63.

Quigley, H. A., G. R. Dunkelberger, et al. (1989). Retinal ganglion cell atrophy correlated with automated perimetry in human eyes with glaucoma. *Am J Ophthalmol.* 107 (5): 453-64.

Quigley, H. A. and R. M. Hohman (1983). Laser energy levels for trabecular meshwork damage in the primate eye. *Invest Ophthalmol Vis Sci.* 24 (9): 1305-7.

Quigley, H. A., R. M. Sanchez, et al. (1987). Chronic glaucoma selectively damages large optic nerve fibers. *Invest Ophthalmol Vis Sci.* 28 (6): 913-20.

Quigley, H. A. and S. Vitale (1997). Models of open-angle glaucoma prevalence and incidence in the United States. *Invest Ophthalmol Vis Sci.* 38 (1): 83-91.

Quigley, H. A., S. K. West, et al. (2001). The prevalence of glaucoma in a population-based study of Hispanic subjects: Proyecto VER. *Arch Ophthalmol.* 119 (12): 1819-26.

Racette, L., M. R. Wilson, et al. (2003). Primary open-angle glaucoma in blacks: a review. *Surv Ophthalmol.* 48 (3): 295-313.

Rainville, S. J., W. L. Makous, et al. (2005). Opponent-motion mechanisms are self-normalizing. *Vision Res.* 45 (9): 1115-27.

Rao, S. M., P. St Aubin-Faubert, et al. (1989). Information processing speed in patients with multiple sclerosis. *J Clin Exp Neuropsychol.* 11 (4): 471-7.

Raymond, J. E. and S. M. Darcangelo (1990). The effect of local luminance contrast on induced motion. *Vision Res.* 30 (5): 751-6.

Reidy, A., D. C. Minassian, et al. (1998). Prevalence of serious eye disease and visual impairment in a north London population: population based, cross sectional study. *Bmj.* 316 (7145): 1643-6.

Rizzo, M., S. W. Anderson, et al. (2000a). Visual attention impairments in Alzheimer's disease. *Neurology.* 54 (10): 1954-9.

Rizzo, M., S. W. Anderson, et al. (2000b). Vision and cognition in Alzheimer's disease. *Neuropsychologia.* 38 (8): 1157-69.

Robson, J. G. (1966). Spatial and temporal contrast sensitivity function of the visual system. *J. Opt. Soc. Am.* 56: 1141-1142.

Robson, J. G. and N. Graham (1981). Probability summation and regional variation in contrast sensitivity across the visual field. *Vision Res.* 21 (3): 409-18.

Rodieck, R. W. (1965). Quantitative analysis of cat retinal ganglion cell response to visual stimuli. *Vision Res.* 5 (11): 583-601.

Rose, A. (1948a). The sensitivity performance of the human eye on an absolute scale. *J Opt Soc Am.* 38: 196-200.

Rose, A. (1948b). Television pickup tubes and problem of vision. *Advances in Electronics.* 1: 131-166.

Ruben, S. and F. Fitzke (1994). Correlation of peripheral displacement thresholds and optic disc parameters in ocular hypertension. *Br J Ophthalmol.* 78 (4): 291-4.

Ruben, S. T., R. A. Hitchings, et al. (1994). Electrophysiology and psychophysics in ocular hypertension and glaucoma: evidence for different pathomechanisms in early glaucoma. *Eye.* 8 ((Pt 5)): 516-20.

Rudnicka, A. R., R. O. Burk, et al. (1998). Magnification characteristics of fundus imaging systems. *Ophthalmology.* 105 (12): 2186-92.

Ruttiger, L. and B. B. Lee (2000). Chromatic and luminance contributions to a hyperacuity task. *Vision Res.* 40 (7): 817-32.

Sample, P. A., D. S. Ahn, et al. (1992). High-pass resolution perimetry in eyes with ocular hypertension and primary open-angle glaucoma. *Am J Ophthalmol.* 113 (3): 309-16.

Sample, P. A., C. F. Bosworth, et al. (2000a). Visual function-specific perimetry for indirect comparison of different ganglion cell populations in glaucoma. *Invest Ophthalmol Vis Sci.* 41 (7): 1783-90.

Sample, P. A., C. F. Bosworth, et al. (2000b). Visual function-specific perimetry for indirect comparison of different ganglion cell populations in glaucoma. *Invest Ophthalmol Vis Sci.* 41 (7): 1783-90.

Sample, P. A., C. F. Bosworth, et al. (1997). Short-wavelength automated perimetry and motion automated perimetry in patients with glaucoma. *Arch Ophthalmol.* 115 (9): 1129-33.

Sample, P. A., C. A. Johnson, et al. (1996). Optimum parameters for short-wavelength automated perimetry. *J Glaucoma.* 5 (6): 375-83.

Sample, P. A., M. E. Madrid, et al. (1994). Evidence for a variety of functional defects in glaucoma suspect eyes. *J. Glaucoma.* 3 (Suppl. 1): S5-S18.

Sample, P. A., G. A. Martinez, et al. (1993). Colour visual fields: a 5 year prospective study in eyes with primary open angle glaucoma. *Perimetry Update 1992/1993.* R. Mills. The Hague, The Netherlands, Kugler Publications, pp 473-476.

Sample, P. A. and R. N. Weinreb (1992). Progressive color visual field loss in glaucoma. *Invest Ophthalmol Vis Sci.* 33 (6): 2068-71.

Sanchez, R. M., G. R. Dunkelberger, et al. (1986). The number and diameter distribution of axons in the monkey optic nerve. *Invest Ophthalmol Vis Sci.* 27 (9): 1342-50.

Saw, S. M., G. Gazzard, et al. (2003). Awareness of glaucoma, and health beliefs of patients suffering primary acute angle closure. *Br J Ophthalmol.* 87 (4): 446-9.

Schein, S. J. and F. M. de Monasterio (1987). Mapping of retinal and geniculate neurons onto striate cortex of macaque. *J Neurosci.* 7 (4): 996-1009.

Schiller, P. H. (1984). The connections of the retinal on and off pathways to the lateral geniculate nucleus of the monkey. *Vision Res.* 24 (9): 923-32.

Schiller, P. H. (1992). The ON and OFF channels of the visual system. *Trends Neurosci.* 15 (3): 86-92.

Schiller, P. H., J. H. Sandell, et al. (1986). Functions of the ON and OFF channels of the visual system. *Nature.* 322 (6082): 824-5.

Schlottmann, P. G., S. De Cilla, et al. (2004). Relationship between visual field sensitivity and retinal nerve fiber layer thickness as measured by scanning laser polarimetry. *Invest Ophthalmol Vis Sci.* 45 (6): 1823-9.

Scholtes, A. M. and M. A. Bouman (1977). Psychophysical experiments on spatial summation at threshold level of the human peripheral retina. *Vision Res.* 17 (7): 867-73.

Scobey, R. P. (1981). Movement sensitivity of retinal ganglion cells in monkey. *Vision Res.* 21 (2): 181-90.

Scobey, R. P. and J. M. Horowitz (1972). The detection of small image displacements by cat retinal ganglion cells. *Vision Res.* 12 (12): 2133-43.

Scobey, R. P. and J. M. Horowitz (1976). Detection of image displacement by phasic cells in peripheral visual fields of the monkey. *Vision Res.* 16 (1): 15-24.

Scobey, R. P. and C. A. Johnson (1981). Psychophysical properties of displacement thresholds for moving targets. *Acta Psychol (Amst).* 48 (1-3): 49-55.

Seah, S. K., P. J. Foster, et al. (1997). Incidence of acute primary angle-closure glaucoma in Singapore. An island-wide survey. *Arch Ophthalmol.* 115 (11): 1436-40.

Shah, S., A. Chatterjee, et al. (1999). Relationship between corneal thickness and measured intraocular pressure in a general ophthalmology clinic. *Ophthalmology.* 106 (11): 2154-60.

Shapley, R., E. Kaplan, et al. (1981). Spatial summation and contrast sensitivity of X and Y cells in the lateral geniculate nucleus of the macaque. *Nature.* 292 (5823): 543-5.

Sheldrick, J. H., C. Ng, et al. (1994). An analysis of referral routes and diagnostic accuracy in cases of suspected glaucoma. *Ophthalmic Epidemiol.* 1 (1): 31-9.

Silverman, S. E., G. L. Trick, et al. (1990). Motion perception is abnormal in primary open-angle glaucoma and ocular hypertension. *Invest Ophthalmol Vis Sci.* 31 (4): 722-9.

Sinclair, J. R., A. L. Jacobs, et al. (2004). Selective ablation of a class of amacrine cells alters spatial processing in the retina. *J Neurosci.* 24 (6): 1459-67.

Snowden, R. J. and O. J. Braddick (1989). The combination of motion signals over time. *Vision Res.* 29 (11): 1621-30.

Soans, F. P., S. J. Khan, et al. (2004). Thinner Central Corneas in Eyes with More Advanced Glaucomatous Cupping - A New Clue to Glaucoma. *Invest Ophth Vis Sci.* 936.

Solomon, S. G., A. J. White, et al. (2002). Extraclassical receptive field properties of parvocellular, magnocellular, and koniocellular cells in the primate lateral geniculate nucleus. *J Neurosci.* 22 (1): 338-49.

Sommer, A. (1989). Intraocular pressure and glaucoma. *Am J Ophthalmol.* 107 (2): 186-8.

Sommer, A. and J. M. Tielsch (1996). Risk factors for open-angle glaucoma: the Barbados Eye Study. *Arch Ophthalmol.* 114 (2): 235.

Sommer, A., J. M. Tielsch, et al. (1991). Racial differences in the cause-specific prevalence of blindness in east Baltimore. *N Engl J Med.* 325 (20): 1412-7.

Spenceley, S. E. and D. B. Henson (1996). Visual field test simulation and error in threshold estimation. *Br J Ophthalmol.* 80 (4): 304-8.

Spry, P. G., D. B. Henson, et al. (2000). Quantitative comparison of static perimetric strategies in early glaucoma: test-retest variability. *J Glaucoma.* 9 (3): 247-53.

Spry, P. G., C. A. Johnson, et al. (2003). Measurement error of visual field tests in glaucoma. *Br J Ophthalmol.* 87 (1): 107-12.

Steinman, B. A., S. B. Steinman, et al. (1997). Transient visual attention is dominated by the magnocellular stream. *Vision Res.* 37 (1): 17-23.

Strasburger, H., L. O. Harvey, Jr., et al. (1991). Contrast thresholds for identification of numeric characters in direct and eccentric view. *Percept Psychophys.* 49 (6): 495-508.

Sun, H., L. Ruttiger, et al. (2004). The spatiotemporal precision of ganglion cell signals: a comparison of physiological and psychophysical performance with moving gratings. *Vision Res.* 44 (1): 19-33.

Swanson, W. H., J. Felius, et al. (2004). Perimetric defects and ganglion cell damage: interpreting linear relations using a two-stage neural model. *Invest Ophthalmol Vis Sci.* 45 (2): 466-72.

Thibos, L. N. (1997). Acuity perimetry and the sampling theory of visual resolution. The Glen Fry Award Lecture.

Thibos, L. N. (1998). Acuity perimetry and the sampling theory of visual resolution. *Optom Vis Sci.* 75 (6): 399-406.

Thibos, L. N., F. E. Cheney, et al. (1987a). Retinal limits to the detection and resolution of gratings. *J Opt Soc Am A.* 4 (8): 1524-9.

Thibos, L. N., D. J. Walsh, et al. (1987b). Vision beyond the resolution limit: aliasing in the periphery. *Vision Res.* 27 (12): 2193-7.

Thylefors, B. and A. D. Negrel (1994). The global impact of glaucoma. *Bull World Health Organ.* 72 (3): 323-6.

Tielsch, J. M., J. Katz, et al. (1995a). Diabetes, intraocular pressure, and primary open-angle glaucoma in the Baltimore Eye Survey. *Ophthalmology.* 102 (1): 48-53.

Tielsch, J. M., J. Katz, et al. (1994). Family history and risk of primary open angle glaucoma. The Baltimore Eye Survey. *Arch Ophthalmol.* 112 (1): 69-73.

Tielsch, J. M., J. Katz, et al. (1995b). Hypertension, perfusion pressure, and primary open-angle glaucoma. A population-based assessment. *Arch Ophthalmol.* 113 (2): 216-21.

Tielsch, J. M., A. Sommer, et al. (1991a). Socioeconomic status and visual impairment among urban Americans. Baltimore Eye Survey Research Group. *Arch Ophthalmol.* 109 (5): 637-41.

Tielsch, J. M., A. Sommer, et al. (1991b). Racial variations in the prevalence of primary open-angle glaucoma. The Baltimore Eye Survey. *Jama.* 266 (3): 369-74.

Tuck, M. W. and R. P. Crick (1991). Efficiency of referral for suspected glaucoma. *Bmj.* 302 (6783): 998-1000.

Tuck, M. W. and R. P. Crick (1997). The cost-effectiveness of various modes of screening for primary open angle glaucoma. *Ophthalmic Epidemiol.* 4 (1): 3-17.

Tucker, A., V. Vinciotti, et al. (2005). A spatio-temporal Bayesian network classifier for understanding visual field deterioration. *Artif Intell Med.* 34 (2): 163-77.

Turpin, A., A. M. McKendrick, et al. (2002a). Development of efficient threshold strategies for frequency doubling technology perimetry using computer simulation. *Invest Ophthalmol Vis Sci.* 43 (2): 322-31.

Turpin, A., A. M. McKendrick, et al. (2002b). Performance of efficient test procedures for frequency-doubling technology perimetry in normal and glaucomatous eyes. *Invest Ophthalmol Vis Sci.* 43 (3): 709-15.

Tyler, C. W. (1981). Specific deficits of flicker sensitivity in glaucoma and ocular hypertension. *Invest Ophthalmol Vis Sci.* 20 (2): 204-12.

Uyama, K., C. Matsumoto, et al. (1993). *Influence of the target size on the sensitivity of the central visual field in patients with early glaucoma*, Kugler Amsterdam/New York.

Vassilev, A., M. S. Mihaylova, et al. (2003). Spatial summation of S-cone ON and OFF signals: effects of retinal eccentricity. *Vision Res.* 43 (27): 2875-84.

Verdon-Roe, G. M., D. F. Garway-Heath, et al. (2002). Spatial summation for single line and multi-line motion stimuli. *Perimetry Update 2002/2003.* M. Wall and D. B. Henson. The Hague, The Netherlands, Kugler, pp 335-340.

Verdon-Roe, G. M., M. C. Westcott, et al. (2000). Optimum number of stimulus oscillations for motion displacement detection in glaucoma. *Perimetry Update 2000/2001.* M. Wall and J. Wild. The Hague, The Netherlands, Kugler Publications, pp 97-102.

Verdon Roe, G. M. (1995). MSc thesis: Evaluation of Moorfields Eye Hospital protocol for the discharge of low risk glaucoma patients and consideration of the role of psychophysical movement and flicker assessment when screening for early glaucoma. London, UCL.

Viswanathan, A. C., R. A. Hitchings, et al. (2004). Commingling analysis of intraocular pressure and glaucoma in an older Australian population. *Ann Hum Genet.* 68 (Pt 5): 489-97.

Viswanathan, A. C., M. C. Westcott, et al. (2000). Validation of a new motion test. *International Perimetric Society Meeting.* Halifax, Canada.

Volbrecht, V. J., E. E. Shrago, et al. (2000). Spatial summation in human cone mechanisms from 0 degrees to 20 degrees in the superior retina. *J Opt Soc Am A Opt Image Sci Vis.* 17 (3): 641-50.

Wachtler, T., C. Wehrhahn, et al. (1996). A simple model of human foveal ganglion cell responses to hyperacuity stimuli. *J Comput Neurosci.* 3 (1): 73-82.

Wall, M., B. Chauhan, et al. (2004). Visual field of high-pass resolution perimetry in normal subjects. *J Glaucoma.* 13 (1): 15-21.

Wall, M., C. S. Jennisch, et al. (1997). Motion perimetry identifies nerve fiber bundlelike defects in ocular hypertension. *Arch Ophthalmol.* 115: 26-33.

Wall, M. and K. M. Ketoff (1995). Random dot motion perimetry in patients with glaucoma and in normal subjects. *Am J Ophthalmol.* 120 (5): 587-96.

Wall, M., R. J. Maw, et al. (1996). The psychometric function and reaction times of automated perimetry in normal and abnormal areas of the visual field in patients with glaucoma. *Invest Ophthalmol Vis Sci.* 37 (5): 878-85.

Wall, M. and E. B. Montgomery (1995). Using motion perimetry to detect visual field defects in patients with idiopathic intracranial hypertension a comparison with conventional automated perimetry. *Neurology.* 45 (6): 1169-75.

Wassle, H., L. Peichl, et al. (1983). A spatial analysis of on- and off-ganglion cells in the cat retina. *Vision Res.* 23 (10): 1151-60.

Watanabe, M. and R. W. Rodieck (1989). Parasol and midget ganglion cells of the primate retina. *J Comp Neurol.* 289 (3): 434-54.

Watkins, R. and T. Buckingham (1992). The influence of stimulus luminance and contrast on hyperacuity thresholds for oscillatory movement. *Ophthalmic Physiol Opt.* 12 (1): 33-7.

Watt, R. J. and M. J. Morgan (1983). The recognition and representation of edge blur: evidence for spatial primitives in human vision. *Vision Res.* 23 (12): 1465-77.

Webb, B. S., C. J. Tinsley, et al. (2002). Feedback from V1 and inhibition from beyond the classical receptive field modulates the responses of neurons in the primate lateral geniculate nucleus. *Vis Neurosci.* 19 (5): 583-92.

Weber, A. J., H. Chen, et al. (2000). Experimental glaucoma and cell size, density, and number in the primate lateral geniculate nucleus. *Invest Ophthalmol Vis Sci.* 41 (6): 1370-9.

Westcott, M. C., F. W. Fitzke, et al. (1999). Characteristics of frequency-of-seeing curves for a motion stimulus in glaucoma eyes, glaucoma suspect eyes, and normal eyes. *Vision Res.* 39 (3): 631-9.

Westcott, M. C., F. W. Fitzke, et al. (1996). Stimulus orientation can affect motion sensitivity in glaucoma. *Perimetry Update 1996/1997.* M. Wall and A. Heijl. The Hague, The Netherlands, Kugler Publications, pp 35-42.

Westcott, M. C., F. W. Fitzke, et al. (1998a). Abnormal motion displacement thresholds are associated with fine scale luminance sensitivity loss in glaucoma. *Vision Res.* 38 (20): 3171-80.

Westcott, M. C., F. W. Fitzke, et al. (2000a). Response time prolongation for a motion stimulus in patients with glaucoma and its relationship with elevation of the motion threshold. *J Glaucoma.* 9 (4): 289-95.

Westcott, M. C., A. I. McNaught, et al. (1997). High spatial resolution automated perimetry in glaucoma. *Br J Ophthalmol.* 81 (6): 452-459.

Westcott, M. C., D. Poinoosawmy, et al. (1998b). Abnormal maximum line displacement sensitivity and frequency-of-seeing curves for a motion stimulus in glaucoma. *Perimetry Update 1998/1999.* M. Wall and J. Wild. The Hague, The Netherlands, Kugler Publications, pp 201-208.

Westcott, M. C., G. M. Verdon-Roe, et al. (2000b). Optimum stimulus duration for motion displacement detection in glaucoma. *Perimetry Update 2000/2001.* M. Wall and J. Wild. The Hague, The Netherlands, Kugler Publications, pp 103-108.

Westheimer, G. (1975). Editorial: Visual acuity and hyperacuity. *Invest Ophthalmol.* 14 (8): 570-2.

Westheimer, G. (1987). Visual acuity and hyperacuity: resolution, localization, form. *Am J Optom Physiol Opt.* 64 (8): 567-74.

Westheimer, G. and G. Hauske (1975). Temporal and spatial interference with vernier acuity. *Vision Res.* 15: 1137-41.

Westheimer, G. and S. P. McKee (1977). Integration regions for visual hyperacuity. *Vision Res.* 17 (1): 89-93.

White, A. J., S. G. Solomon, et al. (2001). Spatial properties of koniocellular cells in the lateral geniculate nucleus of the marmoset Callithrix jacchus. *J Physiol.* 533 (Pt 2): 519-35.

White, A. J., H. Sun, et al. (2002). An examination of physiological mechanisms underlying the frequency-doubling illusion. *Invest Ophthalmol Vis Sci.* 43 (11): 3590-9.

WHO (1999). WHO launches Vision 2020 to combat avoidable blindness. *Public Health Rep.* 114 (3): 210.

Wilson, M. E. (1970). Invariant features of spatial summation with changing locus in the visual field. *J Physiol.* 207 (3): 611-22.

Wilson, M. R. (2002). Progression of visual field loss in untreated glaucoma patients and suspects in St Lucia, West Indies. *Trans Am Ophthalmol Soc.* 100: 365-410.

Wilson, M. R., O. Kosoko, et al. (2002). Progression of visual field loss in untreated glaucoma patients and glaucoma suspects in St. Lucia, West Indies. *Am J Ophthalmol.* 134 (3): 399-405.

Wojciechowski, R., G. L. Trick, et al. (1995). Topography of the age-related decline in motion sensitivity. *Optom Vis Sci.* 72 (2): 67-74.

Woodworth, R. S. and H. Schlosberg (1954). *Experimental Psychology*. New York, Holt.

Wormald, R. (1995). Assessing the prevalence of eye disease in the community. *Eye.* 9 (Pt 6): 674-6.

Wormald, R., S. Fraser, et al. (1997). Time to look again at sight tests. *Bmj.* 314 (7076): 245.

Wormald, R. P., E. Basauri, et al. (1994). The African Caribbean Eye Survey: risk factors for glaucoma in a sample of African Caribbean people living in London. *Eye.* 8 (Pt 3): 315-20.

Wu, J. (1993). MSc thesis: Visual Screening for blinding diseases in the community using computer controlled video perimetry. London, UCL.

Wu, J., M. Coffey, et al. (1998). Impaired motion sensitivity as a predictor of subsequent field loss in glaucoma suspects: the Roscommon Glaucoma Study. *Br J Ophthalmol.* 82 (5): 534-7.

Wu, X., R. Wormald, et al. (1991). Laptop computer perimetry for glaucoma screening. *Invest Ophthalmol Vis Sci.* 32 (4): S810.

Yoshiyama, K. K. and C. A. Johnson (1997). Which method of flicker perimetry is most effective for detection of glaucomatous visual field loss? *Invest Ophthalmol Vis Sci.* 38 (11): 2270-7.

Young, T. (1801). On the mechanism of the eye. *Philos. Trans. R. Soc. Lond. (Biol.).* 91: 23-88.

Zeyen, T. G. and J. Caprioli (1993). Progression of disc and field damage in early glaucoma. *Arch Ophthalmol.* 111 (1): 62-5.

Zhang, Y. and R. C. Reid (2005). Single-neuron responses and neuronal decisions in a vernier task. *Proc Natl Acad Sci U S A.* 102 (9): 3507-12.

Zhou, Y., W. Wang, et al. (1994). Receptive field properties of cat retinal ganglion cells during short-term IOP elevation. *Invest Ophthalmol Vis Sci.* 35 (6): 2758-64.